

**EXPLORATION OF ANTIDIABETIC,  
ANTIOXIDANT AND ANTICANCER POTENTIAL  
OF *ZANTHOXYLUM ARMATUM*, *SARCOCOCCA  
WALLICHII* AND *SARCOCOCCA CORIACEA*  
FROM NEPAL**



**A THESIS SUBMITTED TO THE  
CENTRAL DEPARTMENT OF CHEMISTRY  
INSTITUTE OF SCIENCE AND TECHNOLOGY  
TRIBHUVAN UNIVERSITY  
NEPAL**

**FOR THE AWARD OF  
DOCTOR OF PHILOSOPHY  
IN CHEMISTRY**

**BY  
JANAKI BARAL**

**JANUARY 2024**



**EXPLORATION OF ANTIDIABETIC,  
ANTIOXIDANT AND ANTICANCER POTENTIAL  
OF *ZANTHOXYLUM ARMATUM*, *SARCOCOCCA  
WALLICHII* AND *SARCOCOCCA CORIACEA*  
FROM NEPAL**



**A THESIS SUBMITTED TO THE  
CENTRAL DEPARTMENT OF CHEMISTRY  
INSTITUTE OF SCIENCE AND TECHNOLOGY  
TRIBHUVAN UNIVERSITY  
NEPAL**

**FOR THE AWARD OF  
DOCTOR OF PHILOSOPHY  
IN CHEMISTRY**

**BY  
JANAKI BARAL**

**JANUARY 2024**

## DECLARATION

Thesis entitled “**Exploration of Antidiabetic, Antioxidant and Anticancer Potential of *Zanthoxylum armatum*, *Sarcococca wallichii* and *Sarcococca coriacea* from Nepal**” which is being submitted to the Central Department of Chemistry, Institute of Science and Technology (IoST), Tribhuvan University, Nepal for the award of the degree of Doctor of Philosophy (Ph. D.) is a research work carried out by me under the supervision of Assoc. Prof. Dr. Achyut Adhikari of the Central Department of Chemistry, Tribhuvan University, and co-supervised by Prof. Dr. Mohammad Iqbal Choudhary of H. E. J. Research Institute of Chemistry, University of Karachi, Pakistan. This research is original and has not been submitted earlier in part or full in this or any other form to any university or institute, here or elsewhere, for the award of any degree.

.....

Janaki Baral

## RECOMMENDATION

This is to recommend that **Mrs. Janaki Baral** has carried out research entitled "**Exploration of Antidiabetic, Antioxidant and Anticancer Potential of *Zanthoxylum armatum*, *Sarcococca wallichii* and *Sarcococca coriacea* from Nepal**" for the award of Doctor of Philosophy (Ph.D.) in **Chemistry** under our supervision. To our knowledge, this work has not been submitted for any other degree.

She has fulfilled all the requirements laid down by the Institute of Science and Technology (IoST), Tribhuvan University, Kirtipur for the submission of the thesis for the award of a Ph.D. degree.

.....  
**Achyut Adhikari, Ph.D**

**Supervisor**

**Associate Professor**

Central Department of Chemistry

Tribhuvan University

Kirtipur, Kathmandu, Nepal

.....  
**Mohammad Iqbal Choudhary, Ph. D.**

**Co-supervisor**

**Professor**

HEJ Research Institute of Chemistry

University of Karachi, Karachi,

Pakistan

**JANUARY 2024**

## LETTER OF APPROVAL

Date: 11/01/2024

On the recommendation of **Assoc. Prof. Dr. Achyut Adhikari** and **Prof. Dr. Mohammad Iqbal Choudhary**, this Ph.D. thesis submitted by **Mrs. Janaki Baral**, entitled "**Exploration of Antidiabetic, Antioxidant and Anticancer Potential of *Zanthoxylum armatum*, *Sarcococca wallichii* and *Sarcococca coriacea* from Nepal**" is forwarded by Central Department Research Committee (CDRC) to the Dean, IOST, T.U.

.....

**Jagadeesh Bhattarai, Ph.D.**

Professor,

Head

Central Department of Chemistry

Tribhuvan University

Kirtipur, Kathmandu, Nepal

## ACKNOWLEDGEMENTS

The completion of my Ph.D. research has been a journey that required immense dedication and support from a multitude of individuals, both within the academic realm and beyond. I take this opportunity to express my heartfelt gratitude to all those who played pivotal roles in making my dream a reality. I am truly indebted to the collective time, energy, and effort generously contributed by everyone.

I extend my sincere thanks to my research supervisor, Assoc. Prof. Dr. Achyut Adhikari of the Central Department of Chemistry, Tribhuvan University, and Prof. Dr. M. Iqbal Choudhary, Director of ICCBS, University of Karachi, Karachi, Pakistan. Their keen interest, precious attention, and unwavering encouragement were instrumental throughout my Ph.D. journey.

I would like to express my sincere gratitude to Prof. Dr. Jagadeesh Bhattarai, Head of the Central Department of Chemistry, and Prof. Dr. Ram Chandra Basnyat, Prof. Dr. Megh Raj Pokhrel, former Heads, for providing the necessary opportunities and laboratory facilities for my research. I am equally grateful to Prof. Dr. Kedar Nath Ghimire for his valuable support and guidance. My acknowledgment to the University Grants Commissions, Nepal for supporting my Ph.D. research through the Fellowship Award and Research Support (Award No. PhD/074-075/S&T-6) and the International Foundation of Sciences (IFS) (grant I-1-F-6437-1) in Sweden.

My special thanks are extended to Prof. Dr. Begam Rokeya, for her supervision during my work at Bangladesh University of Health Sciences, ANRAP in the *in-vivo* work of *Zanthoxylum armatum* DC. My gratitude to Dr. Sajan Lal Shayula, Senior Scientist, Nepal Academy of Science and Technology (NAST).

I would like to thank Dr. Baburam Nepali for his assistance in the collection of plant material. I would like to acknowledge all the eminent personalities of the H. E. J. Research Institute of Chemistry, University of Karachi, Pakistan for their continuous encouragement, of bioassay facilities and spectral analysis of isolated compounds. My gratitude to Dr. Hari Devkota Assistant Professor Kumamoto University, Japan for recording  $^1\text{H-NMR}$  spectra of few isolated compounds. Special thanks to Dr. Prabodh Satyal, Aromatic Plant and Research Centre, Lehi, Utah, United States of America for providing GCMS and enantiomeric composition of the essential oil samples of *Zanthoxylum armatum*. I am thankful to Dr. Yub Raj Pokhrel, South Asian University, New Delhi, India for anticancer activities. I would like to acknowledge Mr. Dipak

Kumar Hitan, Department of Customs for the element detection. My gratitude extends to Prof. Dr. Mahesh Nath Parajuli of Kathmandu University for his continuous encouragement.

I express my thanks to the academic, administrative, and laboratory staff of the CDC, Tri-Chandra Multiple Campus, and appreciate the Research Committee of CDC, and the Dean's Office, IoST, TU, Nepal, for enrollment in Ph.D. at CDC and providing a study leave. I am thankful for the support of my research team Md. Tusher Hassan, Md. Hafizur Rahaman, and Md. Asraffuzaman during my in-vivo work in Bangladesh Dr. Usman Sukarat, Nizeria, Dr. Cedric Noulala from Cameroon and Dr. Rukesh Maharjan for their instructions and support throughout my time at ICCBS, H.E.J laboratories. I appreciate Mr. Santosh Basnet and Dr. Madhav Ghimire, CDP, TU, for assisting in molecular simulation. Special thanks to my notable colleagues Dr. Bhoj Raj Poudel and Dr. Ram Lochan Aryal for their continuous encouragement. I appreciate researchers Mr. Dipesh Shrestha and Mr. Prameshwor Sharma and am thankful to my friend Dr. Richa Gupta, Dr. Prakash Chandra Lohani for their help. I am thankful for all my labmates, Dr. Lekhnath Khanal, Dr. Upendra Chaudhary, Mrs. Nirmla Sapkota, Mrs. Ramina Maharjan, Mr. Sanjaya Singh, and Mr. Prakash Gautam, for sharing space, time and energy as needed.

I express my deep appreciation for my dear parents Mr. Narayan Prasad Baral and Late. Mrs. Sita Devi Baral for lifelong nurturing. Their continuous care, encouragement, support, and blessings served as motivating factors in every step of my life. Similarly, I am thankful to my husband, Mr. Suresh Regmi, for his untiring support, care, love, and exemplary management. Special thanks to my energy boosters, daughters Kesika Regmi and Helika Regmi for their countless sacrifices associated with my motherly duties. A very big thanks to my in-laws Mrs. Radha Regmi and Mr. Khemraj Regmi, for their understanding and cooperation in every challenging situation. My very special thanks go to my mother Ganga Devi Baral and my siblings Sangita Baral, Gayatri Baral, Gita Poudel, Shushila Baral, and Sanjaya Baral for their unconditional affection and encouragement. I am indebted to you all.

Last but not least, I am thankful to all those who provided distant blessings and indirect support, serving as motivation throughout my research journey.

Janaki Baral

January, 2024

## शोध सार

यस् विद्यावारीधी सोधकार्यको उद्देश्य वनस्पति *जान्थोक्साइम आर्माटम* डिसि, *सार्कोकोका वालिची स्टाफ* र *सार्कोकोका कोरिएसि हुक* एफ मा रहेका जैविक क्रियाशीलता बिषेसगरी एन्टीडाइबेटीक, एन्टीअक्सीडेन्ट र एन्टीक्यान्सर गुणको खोज गर्नु हो। प्युठान जिल्लाबाट संकलन गरिएको बिज निकालिएको टिमुको दानाबाट मिथानोलिक र इथानोलिक एक्स्ट्रायाक्ट बनाईएको थियो उक्त इथानोलिक एक्स्ट्रायाकलाई बिभिन्न पोलारिटीको रसाइनिक तत्वमा घोलेर बिभाजन गरियो। उक्त बिभाजनबाट बायोएसे निर्देशनमा इथाइलएसिटेट फ्राक्सनको कोलम क्रोम्याटोग्राफी गरी बिभिन्न सात यौगिकहरु प्राप्त भए । ती यौगिकहरु क्रमसः टाम्बुलिन (१), प्रुडोमेस्टिन (२), सिनामिक एसिड (३), सिनामिक एस्टर (४), इसोव्यानिलिक एसिड (५), इसोक्सेटिन (६), र ड्यूकोस्टेरोल (७) रहेका छन् । यी यौगिकहरुको संरचनाहरुलाई मास स्पेक्ट्रोमेट्री र १-डी र २-डी-एनएमआर स्पेक्ट्रोस्कोपी उपकरण द्वारा पत्ता लगाइयो थियो । एक्सट्रायाक्टहरु, भागहरु र प्लाभोनोइड यौगिकहरु १ र २ को उच्च मात्राको कारणले थप जैव गतिविधिहरु, गरिएको थियो । तीन मुख्य व्यापारिक स्थलहरु म्याग्दी, सुर्खेत, र सल्यानबाट संकलन गरिएको टीमुको बिज निकालिएको बोक्राबाट तेल निकाल्नका लागि क्लेभेन्जर उपकरणको प्रयोग गरिएको थियो । सो तेलको जीसीएमएसको माध्यमबाट उद्वेगी यौगिकहरु र एनान्सियोमेरिक संरचना परीक्षण गरिएको थियो। डीपीपीएचद्वारा मापन गरिएको एन्टीऑक्सिडेन्ट एक्टिभिटी, क्रमसः एथानोलिक एक्सट्रायाक्ट आइसि फिटी भ्यालु १७४.००±१.०१ माइक्रोग्राम प्रति मि.लि., मेथानोलिक एक्सट्रायाक्टको आइसि फिपटी भ्यालु १६९.८५ ± ०.२४४ माइक्रोग्राम प्रति मि.लि., इथाइलेसेटेट फ्रायाक्शनको आइसि फिपटी भ्यालु ४२.९४± १ माइक्रोग्राम प्रति मि.लि. तथा यौगिक १ र २ को आइसी फिपटीभ्यालु क्रमस (३२.६५±०.३१, २६.९६ ±०.१९) माइक्रोग्राम प्रति मि.लि. पाईयो । त्यसैगरी, रिएक्टिभ अक्सीजन स्पेसिस (आरओएस) गतिविधिमा एथानोलिक एक्सट्रायाक्ट प्रवल पाईयो, आइसी फिपटी भ्यालु २०.७ ±०.४ माइक्रोग्राम प्रति मि.लि., मेथानोलिक एक्सट्रायाक्टको आइसी फिपटी भ्यालु २७.७ ± ०.७ माइक्रोग्राम प्रति मि.लि., हेक्सेन फ्रायाक्शनको आइसी फिपटी भ्यालु २६.३ ± १.१ माइक्रोग्राम प्रति मि.लि., इथाइलेसेटेट फ्रायाक्शनको आइसी फिपटी भ्यालु १७.८± १.१ माइक्रोग्राम प्रति मि.लि., र सो एक्टीभिटी बढीप्रदर्शन गर्नेहरुमा क्रमस यौगिक १ र २ पाईयो आइसी फिपटी भ्यालु ७.५±०.३ र १.५± ०.३० माइक्रोग्राम प्रति मि.लि. भने स्टैण्डर्ड आइब्रोफेनको आइसी फिपटी भ्यालु ११.२ ± १.९ माइक्रोग्राम प्रति मि.लि. थियो। यौगिकहरु १ र २ को साइक्लोऑक्सीजेनेज २ (सीओएक्स-२) सँगको मोलेकुलर डोकिङ्ग अध्ययनले श्रेष्ठ बाइन्डिङ एफिनिटि पदर्शन गरेकोमा यौगिकहरु १ र २ को बाइन्डिङ ऊर्जा -८.४ र -८.६ किलोक्यालोरिप्रति मोल देखाएको थियो, जवकी आइब्रोफेनको -७.७ किलोक्यालोरी प्रति मोल थियो। ड्रगलाईकलिनेस् र एडमेट बिश्लेषणले पनि यि दुबै यौगिकहरु १ र २ लाई औसधिय तत्वमा सामेल गर्न निर्देशित गरेको थियो। उक्त एक्सट्रायाक्टहरु, हेक्सेन बिभाजन र सिनामिक एसिडले (३) स्तनको क्यान्सर (एमसीएफ-७) बिरुद्ध साइटोटोक्सिक गतिविधि देखाए। एक्सट्रायाक्टहरु, र हेक्सेन बिभाजनले गर्भाशयको क्यान्सर (होला) बिरुद्ध पनि राम्रो गतिविधि देखाए । योग १ र २ ले सिर्स इन्सुलिन सेक्रेसन गतिविधिहरु २०० मिमो र ५० मिमोमा उत्तम प्रेरित गुल्कोज(११-२५) मिमोमा देखाए । यौगिक २

सँग इन्सुलिन सेक्रेसनको मोलेकुलर डोकिङ र सिमुलेसन अध्ययनले उत्कृष्ट स्थिरतासहित बाइन्डिङ गरेको देखायो । प्रसोधन गरिएको तेलको जीसी-एमएस विश्लेषणले लिनालुललाई प्रमुख घटकको रूपमा देखाएको थियो । हेक्सेन भागको सुगंध र अणुहरूले बायो-कीटनाशकको गुण प्रदर्शन गरेको थियो । ऐक्युट बिषमता परीक्षणका परिणामले स्वास्थ्य स्विस आल्बिनो माइसहरूमा शरीरभारको ५६५.६८ मिलीग्राम प्रतिकिलोग्रामको एलडीफिपटी भ्यालु प्रदर्शन गरेको थियो, र हिस्टोपथोलोजिकल अध्ययनले पेनक्रीयाज र कलेजोमा सुजन रहेको तथा कलेजोमा नेक्रोसिस देखाएको थियो । एक्सट्र्याक्टको असर स्वस्थ लड इभान्स मुसामा देखीएन । लड इभान्स डाइबेटिक मुसाहरूमा गरेको इन भिभो अध्ययनले २५ मिग्राप्रतिकिलो, ५० मिग्राप्रतिकिलो मिथानोलिक एक्सट्र्याक्ट र स्ट्यान्डर्ड ग्लिकाजाइडले रक्त ग्ल्युकोजमा क्रमसः कमी गरेको थियो (पि < ०.०४१, पि < ०.०२३, र पि < ०.००३) । २५ मिग्राप्रतिकिलो डोजले हेपाटिक ग्लाइकोजन उच्च परिणाम प्रदर्शन गरेको थियो (पि < ०.०२), जवकी ५० मिग्राप्रतिकिलोले हाइपरलिपिडेमिया र एच.डी.एल.वृद्धिमा प्रमुख भूमिका देखाएको थियो । पूर्वअध्ययनको आधारमा रहेर अनुसन्धान सुचारु गरीएको वनस्पति *सार्कोकोका कोरिएसि हुक* एफ, र *सार्कोकोका वाल्लिची स्टाफ* ले उत्कृष्ट गतिबिधिहरू जस्तै एन्टीडायबेटिक, एन्टीऑक्सीडेन्ट, साइटोटोक्सिक र एन्टीब्याक्टीरियल देखाए। *सार्कोकोक्सा वालिची* स्टाफ डीसिएम भागको कोलम् क्रोमाटोग्राफीद्वारा चार बिभिन्न यौगहरू, एनए-मेथाइलइपिपासस्यामिन डी (८), टारक्सेरोल (९), बेटा-साइटोस्टेरोल (१०), र ओलिएनोलिक एसिड (११) प्रदान गरेको थियो । एस्. कोरिएसि, एस्-ए र एस्- बीएसको पात र डाँठको हाइड्रौ मेथानोइक एक्सट्र्याक्ट र *एस् कोरिएसि* क्लोरोफर्म फ्राक्सन् पिएच् सात र *एस् वालिचिको* डीसीएम् फ्राक्सन् (एस् डबलु डि) लाई बिभिन्न गतिबिधिहरूको मापन गर्दा राम्रो तथा उत्कृष्ट देखियो । खासगरी एस्सि ए ले पाचन प्रकृयाको इन्जायम् अल्फाग्ल्यूकोसिडेज बिरुद्ध आईसि फिपटी भ्यालु ३९.९२ ± २.५२ माइक्रोग्राम प्रति मि.लि. र एल्फाअमाईलेज बिरुद्ध आईसि फिपटी भ्यालु २२४.३ ± १.८७ माइक्रोग्राम प्रति मि.लि. अवरोध देखाए जवकि, एस्डब्लू डीले एल्फाअमाईलेज बिरुद्ध आईसि फिपटी भ्यालु २.११६ ± ०.०५८ माइक्रोग्राम प्रति मि.लि. र स्टान्डरड एकारबोजको आईसि फिपटी भ्यालु ६.१८ ± ०.९७ माइक्रोग्राम प्रति मि.लि. थियो । एन्टीऑक्सीडेन्ट मापनले देखाएको प्रतिफल अनुसार एस्सि ए आईसि फिटि भ्यालु २४.५६ ± ३.३ माइक्रोग्राम प्रति मि.लि एस्सी बिएस आईसि फिपटी भ्यालु २८.९० ± ५.२२ माइक्रोग्राम प्रति मि.लि. र एस्डब्लू डीले आईसि फिपटी भ्यालु ५३.७९ ± २.५० माइक्रोग्राम प्रति मि.लि. मा प्रदर्शन गरेको थियो । स्तनको क्यान्सर (एमसीएफ-७) बिरुद्ध साइटोटोक्सिक अध्ययनले एससी बी भागले आईसि फिपटी भ्यालु ११.५० ± ०.५० माइक्रोग्राम प्रति मि.लि. र तत्कालीन न्यूट्रल क्लोरोफर्म भागले आईसि फिपटी भ्यालु ६८.४२ ± ५ माइक्रोग्राम प्रति मि.लि. प्रदर्शन गरेको थियो । गर्भाशयको क्यान्सर (होला) बिरुद्ध को अनुसन्धानले एससी बीको आईसि फिपटी भ्यालु ३६.३३ ± १० र एससी एनले आईसि फिपटी भ्यालु ८५.५ ± ५ प्रदर्शन गरेको थियो । एस्. बी. ले राम्रो आन्टिबक्टीरियल गतिबिदी देखियो बिशेष गरी बाक्टेरिया *अ एस. औरेअस्, ई. कोली,* र *सल्मोनेल्ला टाइफ्फी* बक्टेरियाहरूमा ।

**शब्दकुञ्जिहरु :** जैविक क्रियाशीलता, रिएक्टिभ अक्सीजन स्पेसिस, टाम्बुलिन, प्रुडोमिस्टीन, अल्फाग्ल्यूकोसिडेज, मोलेकुलर डोकिङ्ग

## ABSTRACT

The present research aims to explore the bioactive potential of extracts, fractions, and selected compounds from the plants' *Zanthoxylum armatum* DC as well as *Sarcococca coriacea* and *Sarcococca wallichii*. The extract of *Z. armatum* fruit pericarp from Pyuthan district was subjected to bioassay-guided isolation, *in vivo* antidiabetic, *in vivo* toxicity studies, and anticancer activities. Bioassay-guided isolation from *Z. armatum* yielded seven compounds: tambulin (**1**), prudomestin (**2**), cinnamic acid (**3**), cinnamic ester (**4**), isovanillic acid (**5**), isoquercetin (**6**), and ducoesterol (**7**). The structures of the compounds were elucidated using mass spectrometry and 1D-and 2D-NMR spectroscopy techniques. Bioactivities including anti-inflammatory, antioxidant, and anticancer properties, were investigated for extracts, fractions, and compounds, particularly focusing on flavonoids **1** and **2** due to their higher yield. Essential oil extraction was carried out using the Clevenger apparatus through hydro-distillation from the fruit pericarp collected from three major commercial sites, and their GCMS analysis was used to examine volatile components and enantiomeric composition. The antioxidant activities, measured using DPPH, showed increasing activities with IC<sub>50</sub> values of ethanolic extract 174.00 ± 1.01, methanolic extract 169.85 ± 0.244, Ethylacetate fraction 42.94 ± 1.19, compound **1** and **2** as 32.65 ± 0.31, 26.96 ± 0.19 µg/mL respectively. Likewise the reactive oxygen species inhibition activities was found potent of ethanolic extract (IC<sub>50</sub>= 20.7 ± 0.4 µg/mL), methanolic extract (IC<sub>50</sub>= 27.7 ± 0.7 µg/mL), hexane fraction (IC<sub>50</sub>= 26.3 ± 1.1 µg/mL), ethyl acetate fraction (IC<sub>50</sub> =17.8 ± 1.1 µg/mL), and compounds **1** and **2** (IC<sub>50</sub>= 7.5 ± 0.3 and 1.5 ± 0.3) µg/mL, respectively as compared to standard ibuprofen (IC<sub>50</sub>= 11.2 ± 1.9 µg/mL). Molecular docking study of compounds **1** and **2** with cyclooxygenase-2 exhibited optimal binding affinity, with binding energies of -8.4 and -8.6 kcal/mol, respectively compared to standard ibuprofen (-7.7 kcal/mol). Drug likeliness and ADMET analyses indicated superior gastrointestinal absorption for compounds **1** and **2** without any discernible toxic effects. Both the extracts', hexane fraction, and cinnamic acid (**3**) possess activity against breast cancer cell line (MCF-7) while extract and hexane fraction were also active against cervical cancer HeLa as measured through MTT assay. Compounds **1** and **2** demonstrated the highest insulin secretion activities at 200 mM and 50 mM, respectively at optimal stimulatory glucose (11-25 mM). Molecular docking and simulation studies of compound **2** with an insulin-secreting target were

performed and found to be binding with excellent stability. The GC-MS analysis of essential oil indicated linalool as the major constituent. The hexane fraction's odorant and olfactory sensory molecules exhibited the qualities of a bio-pesticide. Acute toxicity results showed an LD<sub>50</sub> value of 565.68 mg/kg body weight in the case of healthy Swiss albino mice and the histopathological studies indicated inflammatory changes and polymorphs in the pancreas and kidney, and liver necrosis in higher doses. The extract was nontoxic to healthy Long Evans Rats. *In vivo* antidiabetic studies on Long Evans Rats revealed significant results in lowering blood glucose at (p<0.041, p<0.023, and p<0.003) 25 mg/Kg, 50 mg/Kg, and the standard drug respectively. A dose of 25 mg/Kg significantly (p<0.02) increased hepatic glycogen while 50 mg was significant in hyperlipidemia and in increasing HDL.

Bioassay-guided isolation of *Sarcococca wallichii* Staph. dichloromethane fraction yielded four different compounds N<sub>a</sub>-Methylepipachysamine D (**8**), taraxerol (**9**), beta-sitosterol (**10**), and oleanolic acid (**11**). Hydro-methanoic extract of *S. coriacea* leaf Sc-A, steam Sc-S, and chloroform fraction of *S. wallichii* at pH 7 (Sw-D) were evaluated for various bioassays and found to be good to potent active. Specifically, Sc-A exhibited notable inhibition against digestive enzymes  $\alpha$ -glucosidase (IC<sub>50</sub>= 39.92 ± 2.52 µg/mL) and  $\alpha$ -amylase (IC<sub>50</sub>= 224.3 ± 1.87 µg/mL), while Sw-D inhibited  $\alpha$ -amylase (IC<sub>50</sub>= 2.116 ± 0.058 µg/mL) exceeding the standard acarbose (IC<sub>50</sub>= 6.18 ± 0.97 µg/mL). Furthermore, antioxidant activities were observed in Sc-A (IC<sub>50</sub>= 24.56±3.3 µg/mL), Sc-S (IC<sub>50</sub>= 28.90 ± 5.22 µg/mL) and Sw-D (IC<sub>50</sub>= 53.79 ± 2.50 µg/mL). Cytotoxicity assessment against breast cancer (MCF-7) revealed an (IC<sub>50</sub>= 11.50 ± 0.50 µg/mL) for a basic fraction (Sc-B) of *S. coriacea* while its neutral chloroform fraction (Sc-N) exhibited an (IC<sub>50</sub>=68.42±5 µg/mL). Anticancer activity against cervical cancer (HeLa) was observed for Sc-B (IC<sub>50</sub> =36.33 ± 10) and Sc-N (IC<sub>50</sub> =85.5 ± 5). Sc-B also possesses remarkable antibacterial activities against *S. aureus*, *E. coli*, *Salmonella typhi*.

**Keywords:** *Biological activity, Reactive oxygen species, Tambulin, Prudomestin,  $\alpha$ -glucosidase, Molecular docking*

## LIST OF ACRONYMS AND ABBREVIATIONS

2D	: Two Dimensions
COSY	: Correlation Spectroscopy
DEPT	: Distortionless Enhancement by Polarization Transfer
EIMS	: Electron Impact Mass Spectroscopy
HMBC	: Hetero Multiple Bond Correlation
HMQC	: Heteronuclear Multiple Quantum Coherence
HPLC	: High Pressure Liquid Chromatography
HRMS	: High Resolution Mass Spectroscopy
IC <sub>50</sub>	: Lethal Concentration for 50% Mortality
IR	: Infrared
KBr	: Potassium Bromide
LD <sub>50</sub>	: Lethal Dose for 50% Mortality
LER	: Long-Evans Rat
MeOD	: Deuterated Methanol
MS	: Mass Spectroscopy
R <sub>f</sub>	: Retention Factor
SAM	: Swiss Albino Mice
Sc-A	: <i>Sarcococca coriacea</i> Hook. Leaf Extract
Sc-B	: <i>Sarcococca coriacea</i> Basic Fraction
Sc-N	: <i>Sarcococca coriacea</i> Neutral Fraction
Sc-S	: <i>Sarcococca coriacea</i> Hook. Stem Extract
Sw-D	: <i>Sarcococca wallichii</i> Staph, Dichloromethane Fraction
TLC	: Thin Layer Chromatography
UV	: Ultra Violet
ZaE	: <i>Zanthoxylum armatum</i> Methanolic Extract
MABA	: Microplate Alamar Blue Assay
DPPH	: 2, 2-Diphenyl-1-Picrylhydrazyl
MIC	: Minimum Inhibitory Concentration

## LIST OF SYMBOLS

$\mu\text{g}$	: Microgram
M	: Molarity
M.p.	: Melting point
$m/z$	: Mass/Charge
$M^+$	: Molecular ion
nm	: Nanometer
$p$	: Probability
$R^2$	: Correlation Coefficient
$\alpha$	: Alpha
$\lambda$	: Wavelength
$\mu\text{L}$	: Microliter
$\chi^2$	: Chi Square

## LIST OF TABLES

	Page No.
<b>Table 1:</b> Anticancer agents derived from nature	6
<b>Table 2:</b> Scientific classification of <i>Z. armatum</i>	7
<b>Table 3:</b> Bioactive constituents in <i>Z. armatum</i>	8
<b>Table 4:</b> Scientific classification of <i>S. coriacea</i> and <i>S. wallichii</i>	9
<b>Table 5:</b> Experimental group for extract toxicity	50
<b>Table 6:</b> Experimental group design I for antidiabetic studies	53
<b>Table 7:</b> Grouping and feeding doses per group in experimental design II	54
<b>Table 8:</b> Quantitative yield of extract and fractions of <i>Z. armatum</i>	67
<b>Table 9:</b> <sup>13</sup> C- and <sup>1</sup> H-NMR chemical shift values of tambulin ( <b>1</b> ) (acetone- <i>d</i> <sub>6</sub> , 125 and 500 MHz)	69
<b>Table 10:</b> <sup>13</sup> C- and <sup>1</sup> H-NMR chemical shift values of prudomestin ( <b>2</b> ) (CDCl <sub>3</sub> , 125 and 500 MHz)	71
<b>Table 11:</b> <sup>13</sup> C- and <sup>1</sup> H-NMR chemical shift values of cinnamic acid ( <b>3</b> ) (CDCl <sub>3</sub> , 100 and 400 MHz)	72
<b>Table 12:</b> <sup>13</sup> C- and <sup>1</sup> H-NMR chemical shift values of cinnamic ester ( <b>4</b> ) (CDCl <sub>3</sub> , 100 and 400 MHz)	73
<b>Table 13:</b> <sup>13</sup> C- and <sup>1</sup> H-NMR chemical shift values of isovanillic acid ( <b>5</b> ) (DMSO- <i>d</i> <sub>6</sub> , 150 and 600 MHz)	74
<b>Table 14:</b> Antioxidant activities of extract, fractions, and isolated compounds from <i>Z. armatum</i>	76
<b>Table 15:</b> Anti-inflammatory activities of extract, fractions, and isolated compounds from <i>Z. armatum</i>	77
<b>Table 16:</b> Dose dependent insulin secretion activity of prudomestin	80
<b>Table 17:</b> Anti-cancer activity of crude extract and fractions of <i>Z. armatum</i> against breast cancer (MCF-7)	81
<b>Table 18:</b> Anticancer activity of crude extract and hexane fraction against cervical cancer (HeLa) cell line	82
<b>Table 19:</b> Yields of essential oils	82

<b>Table 20:</b> Chemical profiling of the constituents of the essential oil (% area) from the fruit pericarp of <i>Z. armatum</i> from different commercial sites of Nepal	83
<b>Table 21:</b> Enantiomeric distribution [%(+):%(-)] of compounds in <i>Z. armatum</i> essential oils	85
<b>Table 22:</b> Phytoconstituent identified in the hexane fraction of <i>Z. armatum</i>	89
<b>Table 23:</b> List of major compounds from hexane fraction of <i>Z. armatum</i> DC	92
<b>Table 24:</b> Mortality in Long-Evans rats and Swiss albino mice concerning the feed dose level	102
<b>Table 25:</b> Fasting serum glucose level in different groups of type-II diabetic model rats	106
<b>Table 26:</b> Effects of <i>Z. armatum</i> extracts on TG: HDL & TC: HDL ratio	108
<b>Table 27:</b> ADMET parameters of compounds <b>1</b> and <b>2</b>	114
<b>Table 28:</b> Molinspiration bioactivity of compounds	115
<b>Table 29:</b> IC <sub>50</sub> values of antioxidant, $\alpha$ -glucosidase, and $\alpha$ -amylase inhibition activity of Sc-A, Sc-S and Sw-D	121
<b>Table 30:</b> Comparing the anticancer activity of Sc-B and Sc-N against breast cancer (MCF-7)	122
<b>Table 31:</b> Anticancer activity of Sc-B and Sc-N against cervical (HeLa) cell line	122
<b>Table 32:</b> MIC values of <i>S. coriacea</i> on five different bacterial strain	123
<b>Table 33:</b> <sup>13</sup> C- and <sup>1</sup> H-NMR chemical shift values of taraxerol (CDCl <sub>3</sub> , 100 and 400 MHz)	126

## LIST OF FIGURES

	<b>Page No.</b>
<b>Figure 1:</b> Compounds used in modern medicine based on natural products	5
<b>Figure 2:</b> Photograph of <i>Z. armatum</i> tree i) raw fruits ii) ripe fruits before harvesting	8
<b>Figure 3:</b> Photograph of <i>Sarcococca coriacea</i>	9
<b>Figure 4:</b> Reaction mechanism of DPPH with compounds containing hydroxyl groups	11
<b>Figure 5:</b> Structure of some of the isolated compounds from <i>Z. armatum</i>	24
<b>Figure 6:</b> Structure of some of the isolated compounds from <i>S. wallichii</i>	25
<b>Figure 7:</b> Structure of some of the isolated compounds from <i>S. coriacea</i>	28
<b>Figure 8:</b> Conceptual framework of extraction and fractionation of plant	30
<b>Figure 9:</b> Photograph of (a) <i>Z. armatum</i> tree (b) ripe fruits (c) fruit pericarp before grinding (d) powdered for extract preparation	31
<b>Figure 10:</b> Methodological framework of extraction and fractionation of <i>Z. armatum</i>	32
<b>Figure 11:</b> Scheme of isolation of <i>Z. armatum</i>	36
<b>Figure 12:</b> Scheme of isolation of compounds 1 and 2 from <i>Z. armatum</i>	37
<b>Figure 13:</b> Scheme of isolation of compounds 3, 4, and 5 from <i>Z. armatum</i>	38
<b>Figure 14:</b> Scheme of isolation of compounds 6 and 7 from <i>Z. armatum</i>	38
<b>Figure 15:</b> Mechanism of (DPPH.) to (DPPH: H) antioxidant reaction	42
<b>Figure 16:</b> Methodological framework of extraction and fractionation of <i>S. wallichii</i>	56
<b>Figure 17:</b> Extraction scheme of <i>S. coriacea</i>	57
<b>Figure 18:</b> Scheme of isolation of compound 9, 10 and 11 from <i>S. wallichii</i>	58
<b>Figure 19:</b> Scheme of isolation of compound 8 from <i>S. wallichii</i>	58
<b>Figure 20:</b> Structure elucidation of tambulin (1)	68

<b>Figure 21:</b>	Key HMBC and COSY correlations of tambulin (1)	68
<b>Figure 22:</b>	Structure elucidation of prudomestin (2)	70
<b>Figure 23:</b>	Key HMBC correlations of prudomestin (2)	70
<b>Figure 24:</b>	Structure elucidation of cinnamic acid (3)	72
<b>Figure 25:</b>	Structure elucidation of cinnamic ester (4)	73
<b>Figure 26:</b>	Structure elucidation of isovanillic acid (5)	74
<b>Figure 27:</b>	Structure of isoquercetin (6)	75
<b>Figure 28:</b>	Structure of $\beta$ -sitosterol glycoside (7)	76
<b>Figure 29:</b>	Graphical representation of antioxidant activities of i) quercetin ii) crude ethanolic extract, ethylacetate fraction, tambulin and prudomestin	76
<b>Figure 30:</b>	Graphical representation of antiinflammatory activities of sample and standard	78
<b>Figure 31:</b>	Insulin secreting activity of tambulin (1)	80
<b>Figure 32:</b>	Insulin secretory activity of prudomestin (2)	81
<b>Figure 33:</b>	Structures of major compounds in the essential oil of <i>Z. armatum</i>	85
<b>Figure 34:</b>	Comparative studies on antimicrobial activities of essential oil of <i>Z. armatum</i> from Myagdi, Salyan and Surkhet	87
<b>Figure 35:</b>	GCMS chromatogram showing tR between (I) 7.0 and 31 min (II) 6.0 to 68 min	89
<b>Figure 36:</b>	Structures of major compounds in hexane fraction	91
<b>Figure 37:</b>	Graphical representation of percentage mortality of various insects due to hexane fraction of <i>Z. armatum</i> and standard drug permethrin	93
<b>Figure 38:</b>	Graphical representation of hexane fraction's relative light unit against concentration	94
<b>Figure 39:</b>	Effect of <i>Z. armatum</i> ethanol extract different doses on body weight of normal healthy mice	96

<b>Figure 40:</b>	Effect of <i>Z. armatum</i> ethanol extract different doses treated, on food consumption habit of normal healthy mice	97
<b>Figure 41:</b>	Effect of water habit on SAM treated with <i>Z. armatum</i> extract	98
<b>Figure 42:</b>	Effect of different doses of <i>Z. armatum</i> extract on the relative organ weight of SAM	99
<b>Figure 43:</b>	Effect of different doses of <i>Z. armatum</i> ethanolic extract on the bodyweight of LER	99
<b>Figure 44:</b>	Effect of different doses of <i>Z. armatum</i> ethanoic extract on the food habit of LER	100
<b>Figure 45:</b>	Effect on the water consumption habit	100
<b>Figure 46:</b>	Effect of <i>Z. armatum</i> ethanoic extract on different doses treated LER's relative organ weight	101
<b>Figure 47:</b>	Histopathological images of vital organs liver, pancreas, and kidney of SAM of different groups	104
<b>Figure 48:</b>	Effect of treated groups on the bodyweight of normal and type II diabetic model rats.	106
<b>Figure 49:</b>	Effect of serum TG & cholesterol level (mg/dl) on treated groups of normal and type II diabetic model rats	107
<b>Figure 50:</b>	Effect of serum HDL & LDL level (mg/dl) on treated groups of normal and type II diabetic model rats	108
<b>Figure 51:</b>	Effect of hepatic glycogen level (mg/mL) on treated groups of normal and type II diabetic model rats	109
<b>Figure 52:</b>	Chronic effects of <i>Z.armatum</i> on the SGPT & SGOT on type-2 diabetic model rats	110
<b>Figure 53:</b>	Superimposition of co-crystallized SC-558 ligand (blue) and redocked ligand (red)	114
<b>Figure 54:</b>	2D & 3D interaction of enzyme (1CX2) with a) compound <b>1</b> and b) <b>2</b> c) Ibuprofen	114
<b>Figure 55:</b>	Docking poses and molecular interactions of prudomestin in the binding pocket of SUR of Katp ion channel	116

<b>Figure 56:</b>	RMSD and molecular interaction analysis of MD simulation trajectory	117
<b>Figure 57:</b>	Structure of N <sub>a</sub> -methylepipachysamine D ( <b>8</b> )	124
<b>Figure 58:</b>	ORTEP diagram of N <sub>a</sub> -methylepipachysamine D ( <b>8</b> )	125
<b>Figure 59:</b>	Structure of taraxerol ( <b>9</b> )	126
<b>Figure 60:</b>	Key COSY and HMBC correlations in taraxerol ( <b>9</b> )	126
<b>Figure 61:</b>	Structure of $\beta$ -sitosterol ( <b>10</b> )	127
<b>Figure 62:</b>	Structure of oleanolic acid ( <b>11</b> )	128
<b>Figure 63:</b>	Key HMBC correlations in oleanolic acid ( <b>11</b> )	128

# TABLE OF CONTENTS

	<b>Page No.</b>
Declaration	ii
Recommendation	iii
Letter of Approval	iv
Acknowledgements	v
शोध सार	vi
Abstract	vii
List of Acronyms and Abbreviations	viii
List of Symbols	ix
List of Tables	x
List of Figures	xi
<b>CHAPTER 1</b>	
<b>1. INTRODUCTION</b>	
1.1 Medicinal plants	1
1.2 Importance of natural products	2
1.3 Nature based anticancer agents	6
1.4 Family rutaceae and <i>Zanthoxylum armatum</i>	7
1.5 Family buxaceae and species <i>Sarcococca</i>	9
1.6 Antioxidant activity	10
1.6.1 Functionalities influencing the antioxidant properties	10
1.6.2 Mechanism of DPPH antioxidant	11
1.6.3 Reason behind the change in colour	11
1.7 Reactive oxygen species	11
1.8 Antidiabetic activity	12
1.9 Anticancer activity	14
1.10 Rationale of the study	15
1.11 Objectives	16
1.11.1 General objectives	17
1.11.2 Specific objectives	17
1.12 Delimitation of the studies	18

## CHAPTER 2

### 2. LITERATURE REVIEW

2.1	<i>Zanthoxylum armatum</i>	19
2.2	Bioactivities of <i>Zanthoxylum armatum</i>	20
2.3	Bioactivities of isolated compounds from <i>S. coriacea</i> and <i>S. wallichii</i>	25
2.4	Research gap	29

## CHAPTER 3

### 3. MATERIALS AND METHODS

3.1	Methodological framework	31
3.2	Sample collection and extraction	32
	3.2.1 <i>Zanthoxylum armatum</i>	32
	3.2.2 Sample collection for extraction of essential oil	33
3.3	Materials and equipment	33
3.4	Fractionation of <i>Z. armatum</i> extract	33
	3.4.1 Column chromatography	34
	3.4.2 Column chromatography of ethylacetate fraction	35
	3.4.3 Isolation and purification of compounds from sub-fractions	36
	3.4.5 Compounds isolated from <i>Z. armatum</i>	39
	3.4.5.1 Tambulin (1)	39
	3.4.5.2 Prudomestin (2)	39
	3.4.5.3 Cinnamic acid (3)	40
	3.4.5.4 Cinnamic ester (4)	40
	3.4.5.5 Isovanilic acid (5)	40
	3.4.5.6 Isoquercetin (6)	40
	3.4.5.7 Ducosterol (7)	41
	3.4.6 Element detection of powder of fruit pericarp of <i>Z. armatum</i>	41
3.5	Bioactivities determination	41
	3.5.1 Determination of antioxidant activity using DPPH assay	41
	3.5.2 <i>In-vitro</i> antidiabetic assay	42
	3.5.2.1 Buffer preparation	42
	3.5.2.2 $\alpha$ -Amylase assay	43

3.5.2.3 $\alpha$ - Glucosidase assay	43
3.5.3 <i>In-vitro</i> antifungal bioassay	44
3.5.4 Microplate alamar blue assay	44
3.5.5 Insecticidal activity by contact toxicity method	44
3.5.6 Anti-inflammatory activity	45
3.5.7 Cytotoxic studies	45
3.5.8 Computational molecular modeling	45
3.5.8.1 Molecular docking and ADMET analysis of compounds <b>1</b> and <b>2</b>	46
3.5.8.2 Preparation of protein and ligands	46
3.5.8.3 Protein active site prediction and molecular docking	46
3.5.8.4 Validation of molecular docking	47
3.5.8.5 Drug likeliness and ADMET analysis	47
3.5.8.6 Molecular docking and simulation of compound <b>2</b> for the insulin target	47
3.6 Essential oil from the fruit pericarp of <i>Z. armatum</i>	48
3.6.1 Quantity based extraction of essential oil	48
3.6.2 Gas chromatography-flame ionization detection (GC-FID)	48
3.6.3 Chiral GC-MS	48
3.7 GC-MS of hexane fraction	48
3.8 Pharmacological studies on <i>Z. armatum</i> extract	49
3.8.1 Toxicity studies on <i>Z. armatum</i> extract	49
3.8.2 Animal model preparation	49
3.8.3 Animal grouping and dose preparation	49
3.8.4 Acute oral toxicity studies	50
3.8.5 Parameters of observation	51
3.8.6 Determination of lethal dose of ethanolic extract of <i>Z. armatum</i>	52
3.9 <i>In vivo</i> antidiabetic properties of <i>Z. armatum</i>	52
3.9.1 Animal models	52
3.9.2 Preparation of type II diabetic model rats	52
3.9.3 Formulation of gliclazide and <i>Z. armatum</i> doses	52
3.9.4 Route of administration	53

3.9.5 Experimental design I	53
3.9.6 Experimental design II	53
3.9.7 Collection of blood samples for biochemical analysis	54
3.9.8 Recording of body weight	54
3.9.9 Biochemical analysis	54
3.10 Extraction of <i>S. wallichii</i> and <i>S. coriacea</i>	55
3.11 Extraction of <i>S. coriacea</i> leaf and stem	56
3.12 Column chromatography and compound isolation from <i>S. wallichii</i>	57
3.13 Compounds isolated from <i>S. wallichii</i>	59
3.13.1 N <sub>a</sub> -methylepipachysamine D ( <b>8</b> )	59
3.13.2 Taraxerol ( <b>9</b> )	59
3.13.3 $\beta$ -sitosterol ( <b>10</b> )	60
3.13.4 Oleanolic acid ( <b>11</b> )	60
3.14 Spectroscopic tools and characterization	60
3.14.1 UV-visible spectrometer	60
3.14.2 Mass spectrometry	60
3.14.3 Base Peak	61
3.14.4 Electron impact mass spectrum	61
3.14.5 High resolution electron impact mass spectrum	61
3.14.6 Fast atom bombardment mass spectrum	61
3.15 Nuclear magnetic spectroscopy	61
3.15.1 1D-NMR spectroscopy	61
3.15.2 2D-NMR spectroscopy	61
3.15.3 Heteronuclear multiple bond connectivity	61
3.15.4 Rotating overhauser enhancement spectroscopy	62
3.15.5 Total correlation spectroscopy	62
3.15.6 Heteronuclear multiple quantum coherence	62
3.15.7 Distortionless enhancement by polarization transfer	62
3.15.8 Broad-band (BB) <sup>13</sup> C-NMR spectrum	62
3.15.9 Chemical shift	62

3.15.10 Coupling constant	62
3.16 Infrared spectroscopy	62
3.17 Instruments	62
3.18 Chemical reagents	63
3.19 Preparation of reagents and stock solutions	63
3.20 Preparing staining reagents for the developed TLC plate	64
3.21 Statistical analysis	65
<b>CHAPTER 4</b>	
<b>4. RESULTS AND DISCUSSION</b>	
4.1 Quantitative yield of extract and fractions of <i>Z. armatum</i>	67
4.2. Structural elucidation of isolated compounds from EAF of <i>Z. armatum</i>	67
4.2.1 Structural elucidation of tambulin (1)	67
4.2.2 Structure elucidation of prudomestin (2)	69
4.2.3 Structure elucidation of cinnamic acid (3)	71
4.2.4 Structure elucidation of cinnamic ester (4)	72
4.2.5 Structure elucidation of isovanilic acid (5)	73
4.2.6 Spectra elucidation of isoquercetin (6)	74
4.2.7 Structure elucidation of ducosterol (7)	75
4.3 Applications	76
4.3.1 Antioxidant activities	76
4.3.2 Anti-inflammatory activities	77
4.3.3 Discussion on antioxidant and anti-inflammatory activities	78
4.3.4 <i>In vitro</i> antidiabetic studies of compound 1 and 2	79
4.3.4.1. <i>In vitro</i> $\alpha$ -glucosidase assay	79
4.3.4.2 Insulin secreting activity of tambulin (1)	79
4.3.4.3 Insulin secretory activity of prudometin (2) in mice pancreatic islets	80
4.3.5 Anticancer activities against breast cancer cell line (MCF-7)	81
4.3.6 Anticancer activity of <i>Z. armatum</i> against cervical cancer (HeLa)	81
4.4 Extraction of essential oil and its quantitative yield	82
4.4.1 GCMS of essential oil of <i>Z. armatum</i> and its composition	82

4.4.2 Structures of major compounds	84
4.4.3 Monoterpenoid enantiomeric distribution	85
4.4.4 Enantiomeric distribution	86
4.4.5 Elements detection in the essential oil of <i>Z. armatum</i>	86
4.4.6 Comparative studies on antibacterial activities of essential oil	86
4.4.7 Variation of constituents in oil from different origins	87
4.4.8 Discussion and implications from the study of essential oil	88
4.5 GCMS of hexane fraction (Hexf) of <i>Z. armatum</i>	89
4.5.1 Structures of major compounds in hexane fraction (Hexf)	90
4.5.2 Bioactive constituents in hexane fraction (Hexf)	91
4.5.3 Major compounds of Hexf of <i>Z. armatum</i>	91
4.5.4 Bioactivities on Hexf	92
4.5.4.1 MABA bioassay	92
4.5.4.2 Insecticidal activity	92
4.5.4.3 Antifungal activity	93
4.5.4.4 Anti-inflammatory activity	93
4.5.5 Discussion on the constituents and bioactivity of Hexf of <i>Z. armatum</i>	94
4.6 Pharmacological studies	95
4.6.1 Acute toxicity impact on body weight of Swiss albino mice (SAM)	96
4.6.2 Calculated supply of food and water	96
4.6.3 Food and water habit	97
4.6.3.1 Consumed food	97
4.6.3.2 Consumed water	97
4.6.4 Impact in relative organ weight of SAM	98
4.6.5 Acute toxicity impact of the extract on body weight of Long Evans rats	99
4.6.6 Effect observed on body weight	99
4.6.7 Feeding pattern of Long Evans rats	100
4.6.8 Observation of relative organ weight among the groups (g/100gm)	101
4.6.9 Effect on relative organ weight	101
4.6.10 Mortality observation and determination of LD <sub>50</sub>	102
4.6.11 Histopathological Studies	103

4.6.12 Comparison and discussion about <i>Z. armatum</i> extract toxicity	104
4.7 Antidiabetic Activities of <i>Z. armatum</i> extract on type II LER	105
4.7.1 Dose variant effect of <i>Z. armatum</i> extract on hypoglycemic properties	105
4.7.2 Effect of <i>Z. armatum</i> extract on fasting serum glucose level	106
4.7.3 Effect of <i>Z. armatum</i> extract on lipid profile	107
4.7.4 Effect of <i>Z. armatum</i> methanoic extract on TG: HDL and TC:HDL	108
4.7.5 Effect of <i>Z. armatum</i> extract on liver glycogen level	108
4.7.6 Effect on hepatic enzyme SGPT and SGOT of type II LER	109
4.7.7 Discussion on the effect of antidiabetic properties of methanoic extract of <i>Z. armatum</i>	110
4.7.7.1 Glucose lowering	111
4.7.7.2 Lipid profile	111
4.7.7.3 Hepatoprotective effect	112
4.8 Molecular docking studies on compound <b>1</b> and <b>2</b>	112
4.9 Drug likeliness and ADMET analysis	113
4.10 Computational study of compound <b>2</b> for insulin target	115
4.11 <i>Sarcococca</i> species	120
4.11.1 Bioactivities of <i>S. coriacea</i> and <i>S. wallichii</i>	120
4.11.2 Antioxidant activity	120
4.11.3 <i>In vitro</i> $\alpha$ -glucosidase and $\alpha$ -amylase inhibition activity	120
4.11.4 Comparative studies on the antioxidant and antidiabetic activities	121
4.11.5 Anticancer activities bioassay	121
4.11.6 Anticancerous activities of <i>S. wallichii</i>	121
4.11.7 Anticancer activities of <i>S. coriacea</i> against breast cancer (MCF-7)	122
4.11.8 Anticancer activities of <i>S. coriacea</i> against cervical cancer (HeLa)	122
4.11.9 Antibacterial activities of <i>S. coriacea</i>	122
4.12 Column chromatography	123
4.12.1 Column chromatography and compound isolation from <i>S. wallichii</i>	123
4.12.2 Structure elucidation of isolated compounds	123
4.12.3 Structure elucidation of N <sub>a</sub> -methylepipachysamine D ( <b>8</b> )	124
4.12.3.1 Anticancer activity against breast cancer cell line (MCF-7)	125

4.12.4 Structure elucidation of taraxerol ( <b>9</b> )	125
4.12.5 Structure elucidation of $\beta$ -sitosterol ( <b>10</b> )	127
4.12.6 Structure elucidation of oleanolic acid ( <b>11</b> )	127
<b>CHAPTER 5</b>	
<b>5. CONCLUSIONS AND RECOMMENDATION</b>	129
5.1 Conclusions	129
5.2 Recommendation	132
<b>CHAPTER 6</b>	
<b>6. SUMMARY</b>	133
<b>7. REFERENCES</b>	135
<b>APPENDIX</b>	

# CHAPTER 1

## INTRODUCTION

### 1.1 Medicinal plants

Plant kingdom inherits potential drug candidates that can heal various diseases. Herbal formulation and traditional knowledge about the floral ecosystem particularly in places lacking proper access to medicine play a crucial impact on the health of indigenous people. Such plants served as a boon to humankind through the ages due to various phyto-constituents consumed as food and medicine in traditional treatment (Cragg & Newman, 2013). Several cultures and indigenous tribes are accustomed to nature healing and the trend is still increasing due to the consciousness of people regarding diet, nutraceuticals, and long-term health benefits. Globally around 70,000 plant species are used as medicine (Farnsworth & Soejarto, 2010). The faith and belief of people in natural plants are beyond comparison to the synthetic medicines that take many lives (Duke, 1990). Herbs that grow in the Himalayan region are the major natural resources of Nepal which has been renowned in Ayurveda throughout the Indian subcontinent. Such medicinal plants from Nepal were traded across neighboring countries such as India and Tibet in their crude form (IUCN Nepal, 2000). Philosophically as stated by, the ancient Greek physician Hippocrates 400 BC ago “Let thy food be thy medicine and thy medicine be thy food” is always significant since the food we consume can play a vital role in maintaining good health and well-being. Every food consists of certain elements and nutritional value that can serve as medicine at appropriate doses and may be toxic at higher. Synthetic medications are associated with a huge number of deaths with so-called safe pharmaceutical drugs, over-the-counter drugs. The long-term adverse impact of synthetic medicine has increased people’s belief in herbal medications since there are no documented deaths due to herbal medications. Hence plant-based medicine is considered safe and effective and does not possess any undesirable side effects (Karimi *et al.*, 2015). Modern healthcare recognizes the importance of nutrition in disease prevention and management but medicinal plants with healthy lifestyles help to prevent diseases (Witkamp & Norren, 2018). Plants, particularly those utilized in Ayurveda, have the potential to yield biologically active compounds and serve as the foundation for the development of modified derivatives that exhibit enhanced activity and /or reduced toxicity. Although only a small fraction of flowering plants have been studied thus far, approximately 90 plant

species have already produced around 120 therapeutic agents with known structures. Notable examples of these beneficial plant-derived drugs include vinblastine, vincristine, taxol, podophyllotoxin, camptothecin, digitoxigenin, gitoxigenin, digoxigenin, tubocurarine, morphine, codeine, aspirin, atropine, pilocarpine, capsaicin, allicin, curcumin, artemisinin, and ephedrine. In certain instances, the crude extract of medicinal plants may be utilized directly as medicaments. Conversely, it is of utmost importance to isolate and identify the active components of these plants, as well as elucidate the mechanism of action of these drugs (Joy *et al.*, 1998).

## **1.2 Importance of natural products**

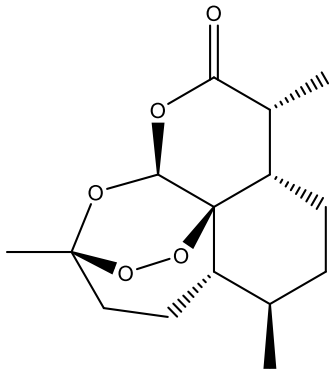
Practicing of natural treatment of any plant parts as medicine requires in-depth knowledge. Documented research based on multiple bioprospecting strategies requires a lengthier process starting from traditional knowledge, practice, and belief. The collection of information is critical in decision making which relies on the clinical and preclinical studies. *In vitro* and *in vivo* analysis on various biological assays of the phytochemical extracts largely supplies the information. Further information also depends on the botanical or pharmacological knowledge of the plant of the indigenous tribe (Sousa *et al.*, 2016). Around 715.1 nature approved small molecules as drugs over the time frame of 1981 till 2019 out of 1394 drugs and 1 out of 63 approved antidiabetic drugs. Similarly, 35 nature-based anticancer drugs were approved from 321 anticancer drugs in total from 1946 to 2019 (Newman & Cragg, 2020).

Modern advancement in medicine equally trusts traditional practice and knowledge. Consuming raw materials from nature is as old as mankind through cooking and choice of food, condiments are majorly influenced by available resources and the connected economic sphere. Likewise, additional preference for certain foods in the community for their particular flavor and impactful medications can be observed to the day (Bottero, 1985). The Romans were in charge of spreading value and expertise and distributing Mediterranean spice and herb plants overall in their empire (Weiss., 2002). Plants with promising potential are still unexplored and in abundance in their wild habitat serving as a storehouse for the ongoing research (Farnsworth & Soejarto, 2010). The interrelationship between natural products, research, pharmaceutical companies, and available commercial medications with lesser side effects and economically accessible to huge masses holds a strong nexus in the global arena. Nearly 80% of people mostly from developing countries rely on herbal medicines due to cultural acceptance and associated lesser economic values few of such major herbal medicines

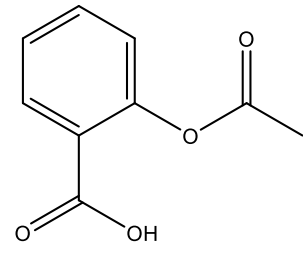
include spices like garlic, ginkgo, saw palmeto, ginseng, and Echinacea (Farnsworth & Norman, 1991). Development of effective anticancer drugs such as paclitaxel and the camptothecin derivatives, topotecan, and irinotecan required 20-30 years of dedicated research (Cragg & Newman, 2005). Notable drugs isolated from plants are arteether, galantamine, nitisinone, and iotropium many of such compounds are in clinical trials such as morphine-6-glucuronide, vinfunine, exatecan, calanolide, etc (Balunas & Kinghorn, 2005). The huge diversity of structural and chemical constituents in nature that have been evolutionarily tuned up to drug-like compounds, contributing as lead drugs in medicines that cannot be matched with any synthetic ones stored as a database of biomolecules (Newman & Cragg, 2012). Over the time frame from around the 1940s to the end of 2014, of the 175 small molecules approved against cancer, 85, or 49%, actually either natural products or their derivatives (Newman & Cragg, 2016). **Figure 1** represents the structures of some of the notable drugs derived from nature such as artemisinin (**12**), aspirin (**13**), cortisone (**14**), diclofenac (**15**), paclitaxel (**16**), quinine (**17**), digitoxin (**18**), amoxicillin (**19**), salbutamol (**20**), piroxicam (**21**).

The exploration of such plant-based medicines is crucial in response to emerging health challenges and adapting to the evolving landscape of diseases. Despite the existence of numerous synthetic drugs for conditions like cancer and diabetes, their high costs and undesirable side effects prompt ongoing efforts to discover more cost-effective and less harmful alternatives. Researchers are increasingly focusing on natural studies, drawn by the accessibility, minimal side effects, and the positive psychological impact of nature-based healing. Nature as a prolific source, continues to be pivotal in the search for innovative drug treatments. With its huge variation in the altitude range a diverse range of ecosystems exists in Nepal. Floral kingdom with 6500 species of flowering plants, 30 gymnosperms, and 450 ferns (Smith *et al.*, 1979). Plant-based therapies are gaining prominence as substitutes for conventional synthetic medications due to their effectiveness, psychological healing attributes, affordability, and simplicity, making them accessible to a larger global population.

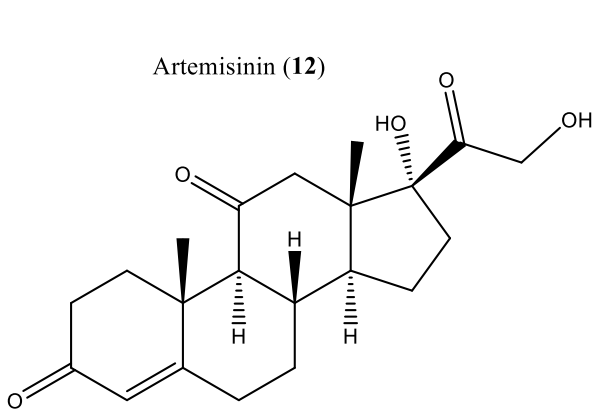
In the realm of cancer and diabetes treatment, herbal remedies derived from nature often stand out as potent anticancer agents, inhibiting tumor formation and irregular cell division. Their appeal lies in the reduced side effects and the psychological comfort they provide to individuals undergoing treatment.



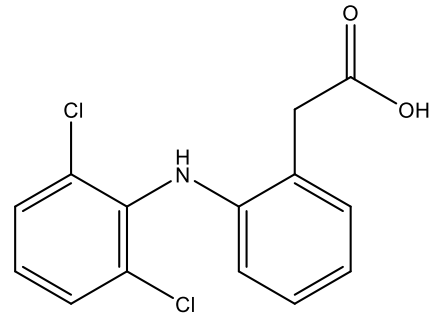
Artemisinin (12)



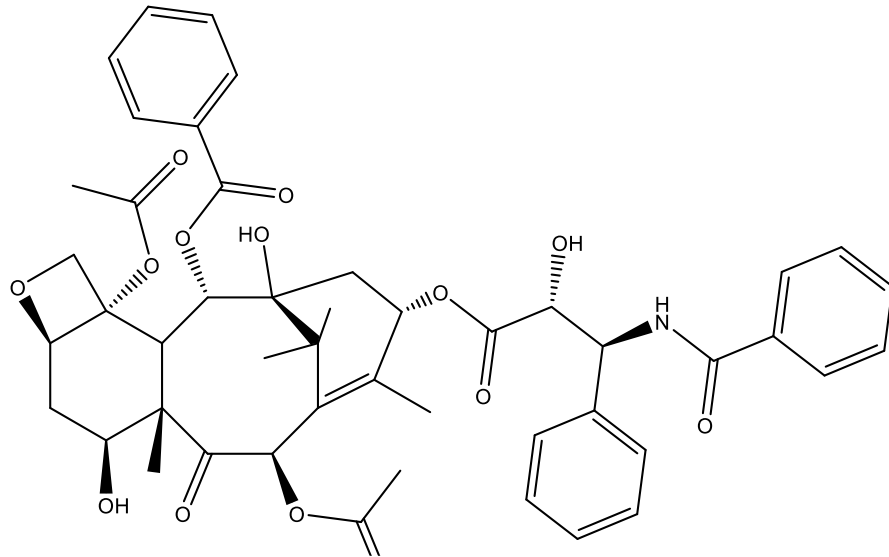
Aspirin (13)



Cortisone (14)



Diclofenac(15)



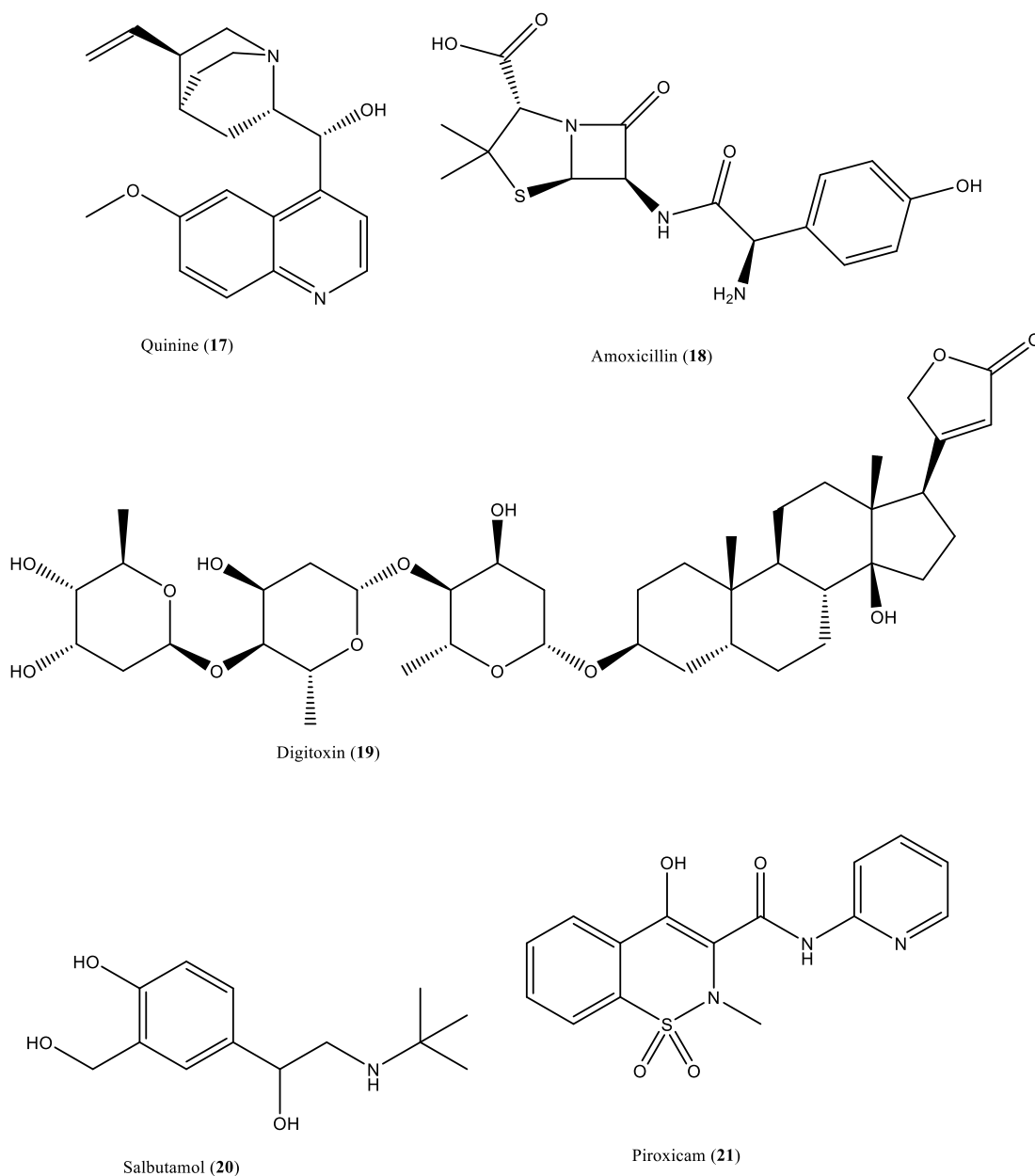


**Figure 1:** Compounds used in modern medicine based on natural products

Nepal, with its diverse topological variation, is endowed with a myriad of unexplored plants, some of which have undergone limited studies. Notable, plants possessing economically significant values such as *Zanthoxylum armatum* DC (*Z. armatum*) commonly called winged prickly-ash in English is popularly known as Timur in Nepali. It is one of the spices in Nepali kitchen. Likewise, an evergreen species *Sarcococca coriacea* and *Sarcococca wallichii* commonly called phitiyephiya remain unexplored in the realm of research. The abundance of various phytoconstituents in these plants has been reported in previous studies. *Z. armatum* inherits different classes of compounds such as polyphenolics, amides, acids, alkaloids with potent anti-

proliferative, anti-mycobacterial, anti-hypoxic, inhibiting growth of cell lines, neuroprotective activities (Nooreen *et al.*, 2019; Siddhanadham *et al.*, 2017; Zhai *et al.*, 2022; Devkota *et al.*, 2013; Ye *et al.*, 2023). Likewise leaves of *S. coriacea* possess cholinesterase inhibitory potent steroidal alkaloids, potent anti-leishmanial activities (Kalauni *et al.*, 2001; Kalauni *et al.*, 2002; Adhikari, 2009) and *S. wallichii* possess anti-inflammatory constituents (Adhikari *et al.*, 2018). Further research on these plants can explore the hidden potential of various prospects.

### 1.3 Nature-based anticancer agents

World Health Organization discusses that cancer is one of the major non-communicable diseases taking the lives of 9.3 million people alone in 2019 (WHO, 2023). Numerous research attempts have been carried out to develop anticancer drugs based on nature. Anticancer agents derived from plant sources at different stages of clinical development are discussed in **Table 1** below.

**Table 1:** Anticancer agents derived from nature

Anticancer agent	Isolated from	Compound activity	Research	Citation
Paclitaxel (Taxol)	Taxane; <i>Taxus brevifolia</i>	Microtubule disruptor; block mitosis; induce apoptosis	Clinical use: Phase I-III clinical trials; early treatment settings, lung breast, ovarian cancer	(Jordan & Wilson, 2004; Che <i>et al.</i> , 2015)
Epipodophyllotoxin	<i>Podophyllum peltatum</i> L; Podophyllotoxin isomer	Pro-apoptotic effects; cell cycle interference	Lymphomas and testicular cancer trials	(Shah <i>et al.</i> , 2013; Shah <i>et al.</i> , 2013)
Pomiferin	<i>Maclura pomifera</i> ; <i>Dereeis Malaccensis</i>	Pro-apoptotic effects; DNA fragmentation; inhibits oxidative damage of DNA; antioxidant activity inhibits histone deacetylases cytotoxicity of cancer cells	Growth inhibition in six human cancer cell lines; ACHN(kidney), NCI-H23 (lung), PC-3 (prostate), MDA-MB-231 (breast), LOX-IMVI(Melanoma), HCT-15 (colon)	(Amin <i>et al.</i> , 2009; Son <i>et al.</i> , 2007)
Sulphoraphane	Isotiocyanate in cruciferous vegetables <i>Brassica</i>	Induces phase 2 detoxification enzymes; inhibits tumour growth in breast cancers, antiproliferate effects	Clinical trials with oral administration of cruciferous vegetable preparation with sulphoraphane	(Pledgie-Tracy <i>et al.</i> , 2007)(Cornblatt <i>et al.</i> , 2007)
Vincristine	<i>Catharanthus roseus</i> G. Don; Vinca alkaloids	Anti-mitotic; microtubule inhibitor; bind to $\beta$ -tubulin; microtubule stabilizers or	Lymphomas, sarcomas and leukaemias; in clinical use ; combination trials	(Amin <i>et al.</i> , 2009; Jordan & Wilson, 2004; Solowey <i>et al.</i> , 2014;

		destabilizers; pro-apoptotic properties and induce cell cycle arrest; anti-tumour activity	Pezzuto <i>et al.</i> ,1997) (Risinger <i>et al.</i> ,2009)
Nblastine	<i>Catharanthus roseus</i> G. Don; Vinca alkaloids	Anti-mitotic;microtubule inhibitor; bind to beta tubulin; microtubule stabilizers or destabilizers; pro apoptotic properties and induce cell cycle arrest; anti tumour activity	Testicular cancer, Hodgkins disease and lymphoma in clinical use ; combination trials (Jordan &Wilson, 2004; Solowey <i>et al.</i> ,2014;Risinger <i>et al.</i> ,2009)
Vinorelbine			Non-small cell lung cancer; single and combination trials : phase I-III (Solowey <i>et al.</i> ,2014;Jordan & Wilson, 2004; Amin <i>et al.</i> , 2009)

#### 1.4 Family Rutaceae and *Zanthoxylum armatum*

Family Rutaceae consists of huge biodiversity in its large family of 160 genera and 1900 species. Most of the species are commercially valued citrus fruits which are linked with topographic distribution (Groppo *et al.*, 2008). *Z. armatum* also called Timur in Nepali is also one of the most economically valued species of the Rutaceae family due to its potent properties. Out of the eight species of *Zanthoxylum* reported from Nepal, five species were accepted taxonomically (Phuyal *et al.*, 2019) notably; *Z. acanthopodium* DC, *Z. niditum* DC, *Z. oxyphyllum* Edgew, *Z. tomentellum* Hook. f., and *Z. armatum* DC. The aromatic plant under this study morphologically grows up to 6m in height with the characteristic flavor and taste which was identified as *Z. armatum* DC. It is also associated with the treatment of certain diseases and disorders (Malla *et al.*, 2014; Phuyal *et al.*, 2019). The scientific classification of *Z. armatum* (Rana & Rawat, 2017) is shown in **Table 2**. The picture of *Z. armatum* plant with unripe at the month of May and ripe fruits at the month of October is presented below in **Figure 2**.

**Table 2:** Scientific classification of *Z. armatum*

Kingdom:	Plantae
Division/Phylum:	Tracheophyta
Class:	Magnoliopsida
Order:	Sapindales
Family:	Rutaceae
Genus:	<i>Zanthoxylum</i>
Species:	<i>armatum</i> DC
Binomial name:	<i>Zanthoxylum armatum</i> DC



**Figure 2:** Photograph of *Z. armatum* tree (i) raw fruits (ii) ripe fruits before harvesting

Different parts of a tree, including leaves, blossoms, barks, fruits, and seeds, have been used to treat illnesses. Its spicy flavor, excellent nutritional content, and numerous medical benefits make it one of the most valued spices in the South Asian region. Some compounds with remarkable activities reported from their non-polar fraction are listed below in **Table 3** with the reported bioactivities. Compound linalool is one of the major constituents reported with diverse activities in addition to palmitic acid, cinnamic acid methyl ester, methyl oleate, trans-13 –octadecenoic acid, palmitoelic acid, and methyl palmitoleate. Studies show these compounds possess wider applications including anticancer, antibacterial, and anti-inflammatory activities.

**Table 3:** Bioactive constituents in *Z. armatum*

Compound	Activities	Citation
Linalool	Antiinflammatory, anticancer, anti hyperlipedemic, antimicrobial, antinoceptive, analgesic, anxiolytic, antidepressive, neuroprotective, anticonvulsant	(Pereira <i>et al.</i> ,2018) (Peana <i>et al.</i> ,2002) (Elisabetsky, 2002)
Palmitic acid	Antiinflammatory	(Aparna <i>et al.</i> ,2012)
Cinnamic acid methyl ester	Anticancer, Antibacterial, Anti-fungal, Neurological disorders	(Ruwezhi & Aderibigbe, 2020)
Methyl oleate	Antifungal	(Lima <i>et al.</i> ,2011)
Trans-13-octadecenoic acid	Human metabolite	
Palmitoelic acid	Antiinflammatory	(Astudillo <i>et al.</i> ,2018)
Methyl palmitoleate	Cytoprotective, anti-inflammatory, antifibrotic	(Product <i>et al.</i> ,n.d.)

### 1.5 Family Buxaceae and species *Sarcococca*

The evergreen Buxaceae family consists of trees and shrubs in its four major genera *Sarcococca*, *Simonsia*, *Pachysandra*, and *Buxus*. These plants have been broadly distributed and used in folk medicine for ages to cure tumors, diarrhea, inflammations, and infections (Kumar *et al.*, 2015). The evergreen buxaceae family has four species of *Sarcococca* across various regions in Nepal, *S. coriacea*, *S. saligna*, *S. hookerina* & *S. wallichii* (Smith *et al.*, 1982). These plants are particularly rich in steroidal alkaloids and the nature of such compounds plays a crucial role. *Sarcococca* species studied here are *S. coriacea* (Hook.F.) also called *Tricera nepalensis* Wall and *S. wallichii* Staph.

**Figure 3** and the taxonomical classification of these plants are presented in **Table 4** below (Rana & Rawat, 2017):

**Table 4:** Scientific classification of *S. coriacea* and *S. wallichii*

Kingdom	Plantae	Plantae
Phylum	Tracheophyta	Tracheophyta
Class	Magnoliopsida	Magnoliopsida
Order	Buxales	Buxales
Family	Buxaceae	Buxaceae
Genus	<i>Sarcococca</i>	<i>Sarcococca</i>
Species	<i>coriacea</i> Hook. F.	<i>wallichii</i> Staph.



**Figure 3:** Photograph of *S. coriacea* plant

## **1.6 Antioxidant activity**

Antioxidants are those substances that inhibit or prevent the oxidation of oxidizable substrates (proteins, carbohydrates, nucleic acids, lipids). These properties include the ability to scavenge free radicals, neutralize reactive oxygen species (ROS), inhibit lipid peroxidation, chelate metal ions, and protect against oxidative damage to biomolecules such as proteins, lipids, and DNA. Antioxidant properties can vary depending on the chemical structure, concentration, and bioavailability of the compound. A very low concentration of an antioxidant is capable of oxidizing an excess amount of substrate. Antioxidants particularly phenolic based on plants are good sources of antioxidants (Soobrattee *et al.*, 2005). The specific technique used for the determination of the antioxidant potencies of certain biological samples is known as assay. Antioxidant assays are thus designed to evaluate the ability of the plant sample/ compound to prevent oxidation of substrates. There are various such assays such as 2,2-diphenyl-1-picrylhydrazyl (DPPH) assay, oxygen radical absorbance capacity (ORAC) assay, ferric reducing antioxidant power (FRAP) assay, and total antioxidant capacity (TAC) assay, etc. Antioxidant activities refer to the effect of antioxidants source on living organisms as observed through a broad range of effects including reducing oxidative stress, inflammation, and cellular damage and promoting overall health and longevity. Such activities can be accessed through *in vitro* as well as *in vivo*. Standard antioxidant quercetin is used in many DPPH assays. Antioxidant activities may include protection against chronic diseases such as cancer, cardiovascular disease, diabetes, neurodegenerative disorders, and aging-related conditions.

### **1.6.1 Functionalities influencing the antioxidant properties**

The inhibitory capacity of any plant reflected as antioxidant properties depends upon the functional moieties and their dominance. Certain phytoconstituents and functionalities such as polyphenolics possess higher antioxidant properties compared to other functional groups due to their replaceable -OH groups. One of the major chemicals used for antioxidant property determination is 2,2-diphenyl-1-picrylhydrazyl assay (DPPH assay).

### **1.6.2 Mechanism of DPPH antioxidant**

Since antioxidants interact with oxidative free radicals. The antioxidant activity of plant extract or sample is measured as it reacts with a methanol solution of stable DPPH radical. Structurally DPPH can accept an electron or a hydrogen radical to become a stable diamagnetic molecule and is oxidized with difficulty and then irreversibly. For

this purpose, DPPH 2, 2-diphenyl-1-picrylhydrazyl a common stable free radical is used for conducting electron spin resonance due to the paramagnetic properties of its odd electron. Because of its odd electron, DPPH shows a strong absorption band at 517 nm in methanol, in which its solution appears a deep violet color. As this electron becomes paired off the absorption vanishes and the resulting decolorization is stoichiometric concerning the number of electrons taken up (Brand-Williams *et al.*, 1995). The schematic reaction is represented as below:

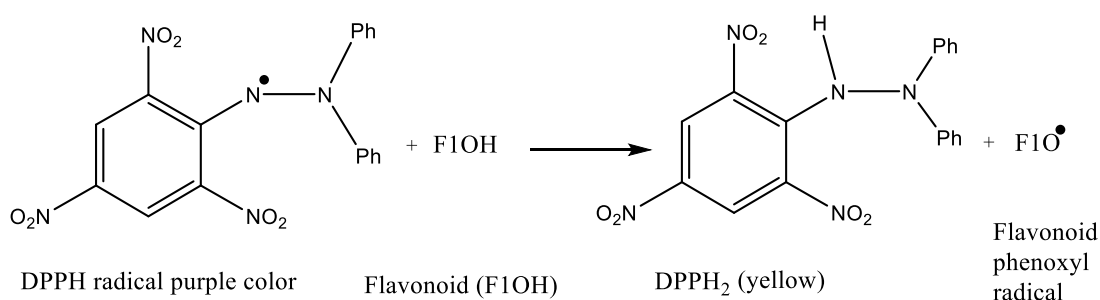
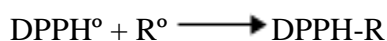


**Figure 4:** Reaction mechanism of DPPH with compounds containing hydroxyl groups

### 1.6.3 Reason behind the change in color

The strong absorption is fortunate because the solubility of DPPH is not great however alcoholic solutions having concentrations of approximately  $5 \times 10^{-4}$  M are nevertheless densely colored. In such low concentrations, the Lambert–Beer Law is obeyed over the useful range of absorption. Its interaction with the compounds having reversibly oxidizable groups DPPH gives results consistent with mechanisms as below (Nature, 1958).

### 1.7 Reactive oxygen species

Reactive oxygen species (ROS) is a group of chemically reactive molecules generated during aerobic respiration as a natural byproduct of normal cellular metabolism that plays a vital role in cell signaling and immune response (Finkel, 2011; Halliwell & Gutteridge, 2015; Sies, 2017; Valko *et al.*, 2007). ROS is necessary for cell stability and kills pathogens while its excess leads to tissue damage through various levels of inflammation. The imbalance between the production and elimination of ROS, results in oxidative stress (Mittal *et al.*, 2014) that damages cells, proteins, lipids, and DNA hence causing various neurodegenerative disorders, cardiovascular diseases, and early aging (Valko *et al.*, 2007). Excess intracellular ROS triggers disorders and

inflammation in old age (Hussain *et al.*, 2016). Neutralizing these ROS to less harmful substances or scavenging to prevent oxidative damage takes place through antioxidants (Gorrini *et al.*, 2013). Oxidative stress is associated with the development and progression of various diseases, including cancer and diabetes. Thus, balance between ROS, stress, inflammation, and antioxidants is necessary to maintain good health. Increased level of ROS amplifies and deteriorate oxidative stress hence aggravating inflammation (Mittal *et al.*, 2014; Gautam *et al.*, 2009). Antioxidants have both endogenous and exogenous defenses in scavenging ROS and its effects. Endogenous deficiency primarily needs enzymatic supplements (Sies, 2015) and pro-oxidants (Halliwell, 2012) which are inaccessible as exogenous sources such as food and vegetables with polyphenols and flavonoids possessing strong immunity regulators, improving inflammation, neurodegeneration, cardiovascular disease and diabetes (Yahfoufi *et al.*, 2018; Guardia *et al.*, 2001). Since flavonoids are non-enzymatic antioxidants and strong XO inhibitors these crucially inhibit the production of ROS functionally (Valko *et al.*, 2007; Orhan & Deniz, 2020). Additionally, polyphenols inhibit enzymes related to pro-inflammation thus decreasing the risk of dementia (Hussain *et al.*, 2016). Hence increased antioxidant supplements through diet activity is quite remarkable (Gorrini *et al.*, 2013).

### **1.8 Antidiabetic activity**

Diabetes mellitus, commonly called type 2 diabetes identified by hyperglycemia is caused due to various degrees of  $\beta$ -cell dysfunction and insulin resistance. Patients with diabetes mellitus are increasing globally with an associated two-fold excess risk of cardiovascular, cerebrovascular, and peripheral artery disease (Kazi & Blonde, 2001; Sarwar *et al.*, 2010). According to the WHO database 2023, diabetic cases globally reached up to 422 million and are still at an increasing rate in low-income countries. Any plant or drug that possesses features and can control high blood glucose levels either through stimulating insulin production, reducing glucose production in the liver, or improving insulin sensitivity are antidiabetic drugs. Synthetic antidiabetic drugs are associated with adverse effects of weight gain, flatulence, and mild anaemia. The feature of synthetic drugs can be their unique mechanism of action in controlling glucose, improving insulin sensitivity, safety, effect on  $\beta$  cells, etc. A search for potent antidiabetic secretagogue from plant origin is in high demand due to low economic value and lesser side effects. The consumed food has a direct impact on blood glucose levels. Indigenous people are fond of consuming wild and cultivated plants to manage

diabetic complications. Generation wise oral transfer of knowledge based on the safety status of plants triggers herbal formulation to people, particularly from developing nations like Nepal. The enzymatic digestion of complex carbohydrates collectively by the role of  $\alpha$ -amylase and  $\alpha$ -glucosidase has been addressed as a potential means of controlling postprandial hyperglycemia by reducing the absorption of glucose from meals (Mccue *et al.*, 2005). Inhibitors of these enzymes help by delaying in breaking mechanism of carbohydrates finally leading to a decrease in the postprandial glucose level in the blood (Kwon *et al.*, 2006). Newmann and Cragg discuss the progress of natural products as a source of new drugs over the time frame of 1981 to 2019 among 63 new chemical entities one of them is based on natural sources (Newman & Cragg, 2020) Various types of research targeting the plant-based inhibitors are on increasing trend against these digestive enzymes  $\alpha$ -amylase and  $\alpha$ -glucosidase as a natural supplement and diet plays pivotal role addressing the concern related to synthetic drugs. Initiation of such research through in-vitro antidiabetic properties of plant extract is expressed by the inhibition of plant sample to the enzymes  $\alpha$ -amylase and  $\alpha$ -glucosidase (Nair *et al.*, 2013). Plants with the highest inhibitory activities against both of these digestive enzymes are rare. Very few natural plants are reported with strong inhibiting capacity to both these enzymes concomitantly (Kazeem *et al.*, 2013). Plants belonging to the buxaceae family are reported to have potent to moderate inhibitory capacity in multiple diseases and need to be researched concerning antidiabetic properties.

Combined disorders with their stress and economic impact are associated with higher mortality (Einarson *et al.*, 2018). The international diabetes federation predicts a probable increase in diabetes would be 7.83 million by the end of 2045 globally from approximately 537 million diabetic adult people in 2021 (Diabetes, 2021). Despite its economic burden for the treatment to low earning people, around 5-10% allocated budget in the health system globally falls under this disorder alone (Gagliardino *et al.*, 2004). Parameters such as low income, multiple complications, and financial burdens force patients to believe and practice traditional treatments, especially in developing countries. Treatment of serious diseases from nature-generated drugs has revolutionized. Remarkable generated drugs from nature are the most antibiotics drugs from microbial products (Wright, 2017). A search for potent antidiabetic secretagogues from edible plant-based resources can serve as an alternative due to their lesser side effects and associated positive psychology. Common drugs such as pycnogenol, acarbose, miglitol, and voglibose are antidiabetic products of natural origin. Galegine

which serves as a significant antidiabetic drug metformin is isolated from the natural plant; *Galega officinalis* (Ríos *et al.*, 2015). Screening many plants for antidiabetic properties *in vitro* results in few ones with inhibiting potentials to both  $\alpha$ -glucosidase and  $\alpha$ -amylase (Baral *et al.*, 2022). Such plants with antidiabetic sources serve as a boon to humankind through diverse mechanisms of drug-like properties. Nature-based extracts and compounds isolated from them are widely studied as antidiabetic drugs both *in vitro* and *in vivo*.

### **1.9 Anticancer activity**

Irregularities in gene functioning and changes in how genes are activated or deactivated resulting in abnormal cells that grow and invade healthy cells in the body are fundamental characteristics of cancer (Jones & Baylin, 2007). A broad term cancer covers 19.3 million new cases and mortality of around 10 million people globally in 2020. The report also diagnosed breast cancer cases with 2.26 million (Ferlay *et al.*, 2021). Cancer is a class of diseases that are characterized by uncontrolled cell proliferation combined with malignant activity and it is the major cause of death globally (Paulmurugan, 2012). According to the International Agency for Research on Cancer's GLOBOCAN series, there were 14.1 million new cases recorded and 8.2 million deaths worldwide in 2012. As with the reported rate of breast cancer (1.67 M), colorectal (1.82 M), and lung cancer (1.36 M), and the leading causes of mortality was stomach cancer (745000 deaths), liver cancer (1.6 M fatalities), and (723000 deaths) (Ferlay *et al.*, 2015). The estimated number of new cases of cancer in 2018 was 18.1 million, with 9.5 million fatalities. Lung cancer is the leading cause of cancer death in men, followed by prostate and stomach cancer, whereas breast cancer is the leading cause of cancer mortality in women, followed by lung and colorectal cancer (Bray *et al.*, 2018). With 24.1 M new cases and 13.0 M deaths anticipated from cancer by 2030, the mortality and morbidity of the disease would likely continue to rise (Sachez *et al.*, 2019). GLOBOCAN 2018, in Nepal, estimated new cancer was 103.7 and the death rate was 77.8 per 100000 population (Shrestha *et al.*, 2020). According to GLOBOCAN, there can be an estimated 4820000 and 2370000 cancer cases in China and the United States, respectively, and 3210000 and 640000 cancer fatalities in 2022 (Xia *et al.*, 2022). Among 247 anticancer drug units around the time frame of 1981 to 2019, 18 units were based on natural products (Newman & Cragg, 2020).

The variation, complexity, and diversity of cancers and the efficacy of any drug unit can vary depending on the type and stage of cancer. The activities of samples as

observed against various cell lines are known as anticancer assay. Anticancer drugs in general inhibit the growth and proliferation of cancer cells. A feature of the drug to be anticancer is selective cytotoxicity but killing cancer cells only is a major challenge. The ability of any anticancer drug to arrest by targeting in multiple phases thus disrupting the cell cycle and uncontrolled cell growth involved in division or inhibiting metastasis. Likewise starving the tumor cells by angiogenesis inhibition or inducing apoptosis programmed cell death. Features of any drug or plant-based formulations or specific units can be highly significant due to lesser side effects on healthy cells. Dietary intake of fruits and vegetables is associated with reducing the risk of many cancerous diseases by double (Ames *et al.*, 1993). Thus, studies that explore plants possessing antioxidants are higher in demand. Some of the nature-based anticancer medicines are paclitaxel, epipodophyllotoxin, pomiferin, sulforaphane, vincristine, vinblastine, flavopiridol, etc.

### **1.10 Rationale of the study**

The global community is very concerned about synthetic drugs and is interested in research on nature-based therapies. Nature's healing potential for various diseases underscores the need to investigate the constituents of plants that support human health through dietary consumption. It is also essential to scrutinize the proper dosage of medicinal plants for efficacy as they can turn toxic at higher doses.

The researcher's prime objective is to find cost-effective solutions to address concerns associated with synthetic medications. Funding towards academic endeavors exploring plant-based therapeutic units that are beneficial to humanity, aiming to alleviate economic burdens and minimize undesirable side effects affecting health. Current treatments for diseases like diabetes, cancer, and disorders associated with antidiabetic, antioxidant, and anticancer medications are capital intensive, possess side effects, and are not easily accessible. Therefore, finding an economically viable, accessible, effective, and sustainable treatment technology is crucial for safeguarding health, resources, and the ecosystem.

Evidence-based studies on natural resources of Nepali origin are of significant importance, considering that farming is the primary occupation for most people in Nepal, and their lifestyle is intricately connected to nature. This study represents a pioneering effort in drug discovery based on potential units derived from plants. Natural product chemistry delves into biodiversity's hidden treasures, leveraging different solvents and technologies, often relying on indigenous practices. Studies on nature-

based antidiabetic plants and the potential insulin secretagogues can largely support diabetic sufferers and help them treat through a nature-based diet. Likewise, nature-based anticancer units can be a boon to the alarming new cases of cancer. Research revealed plants possessing antioxidant properties also possess antidiabetic and anticancer properties. Thus, studies on plants with properties such as antioxidants, antidiabetic, and anticancer properties can be a remarkable leap to humankind. Documented studies on specific flora vary based on plant habitat, and the biodiversity of Nepali origin offers significant benefits due to topological variation, soil composition, and nutrient content. Research on bio-applications could play a vital role in drug discovery. Functional moieties on certain compounds and their potential reactions suggest alternative means to synthetic medications for treating various ailments and disorders. The study aligns with the sustainable development goal “Good health and well-being” recognizing that well-being and good health are interconnected with diet, supplements, and exercise.

### **1.11 Objectives**

The ongoing investigation into nature-based resources holds the potential to unveil medicinal plants, guided by indigenous knowledge and practices. Local communities highly value certain plants regardless of scientific scrutiny, as they have demonstrated outcomes over specific intervals and are readily available in nature. The exploration of these selected plants could contribute to drug discovery by identifying life-saving compounds or molecules with potential activity against emerging viruses and diseases. Nepal, characterized by a vast range of altitude variations, can significantly impact the constituents and yield of these plants. Notably, the chosen plants are of particular interest due to their traditional medicinal use and the limited scientific studies conducted thus far. Despite evaluating the potency of *Zanthoxylum armatum* DC across different geographical locations, there remains a dearth of research on the bioassay-guided isolation of its extract for fractionation and the isolation of compounds with antioxidant, antidiabetic, and anticancer properties especially those originating in Nepal. Existing literature predominantly focuses *Z. armatum* from lower altitudes, while broader studies can reveal compounds with novel activities.

In the case of *Z. armatum*, the main research objectives encompass the assessment of toxicity, antidiabetic studies, and the isolation and characterization of secondary metabolites along with their biological studies. Similarly, a lack of documented studies

on bioactivities, such as antidiabetic, antioxidant, and anticancer properties of *Sarcococca coriacea* (Hook. F.) and *S. wallichii* Staph. prompted the investigation with the belief that these plant species harbor potential bioactive properties that have yet to be explored.

### **1.11.1 General objectives**

Investigation of the antioxidant, antidiabetic, and anticancer potential of *Sarcococca coriacea* (Hook. F.), *Sarcococca wallichii* Staph., and *Zanthoxylum armatum* DC of Nepali origin.

### **1.11.2 Specific objectives**

The specific objectives of the current studies are:

1. Extract preparation, fractionation, isolation, and identification of compounds obtained from *Z. armatum*
2. Bioactivities of *Z. armatum*'s extract, fraction, and compounds along with *in silico* activities of compounds based on their *in vitro* studies
3. Pharmacological studies on toxicity determination of *Z. armatum* extract
4. Determination of hypoglycemic status of type II diabetic rats fed with extract of *Z. armatum*
5. GCMS and bioactivities of hexane fraction of *Z. armatum*
6. Extraction of essential oil of *Z. armatum* from various commercial sites their GCMS and chiral GCMS studies with their comparative antibacterial activities
7. Extract preparation of *S. coriacea* leaf (Sc-A) and stem (Sc-S) and their bioassays
8. Compound isolation from *S. wallichii* their structure elucidation and bioactivities of *S. coriacea* basic fraction (Sc-B), *S. coriacea* neutral fraction (Sc-N), *S. wallichii* DCM fraction (Sw-D)

Interest in these specific plants is due to their various phytoconstituents such as steroidal alkaloids, flavonoids, terpenes, etc with diverse pharmacological activities.

### **1.12 Delimitation of the studies**

This study mainly focuses on extract and fractions of *Z. armatum* while limited studies on *Sarcococca* species. Attempts of isolation of pure compounds and their structure determination were carried out. To the compounds with potent activities observed from *in vitro* activities further *in silico* studies were carried. This research doesn't involve mechanistic studies of isolated compounds or extracts.

## CHAPTER 2

### LITERATURE REVIEW

#### 2.1 *Zanthoxylum armatum*

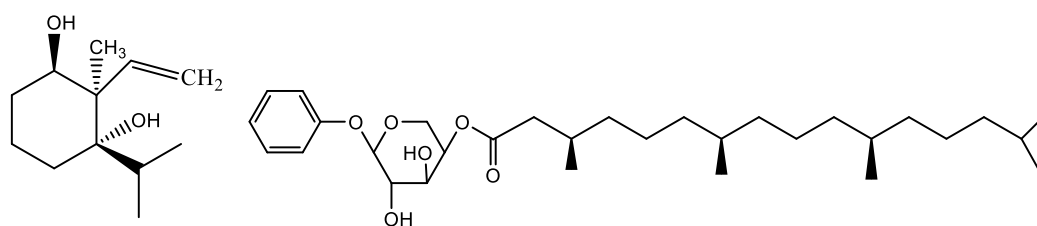
The diverse family rutaceae consists of 160 genera and 1900 species. Most of these are economically valued plants (Groppo *et al.*, 2008). *Z. acanthopodium* DC, *Z. nuditum* DC, *Z. oxyphyllum*, *Z. tomentellum* Hook. f., and *Z. armatum* DC are taxonomically categorized from Nepal (Phuyal *et al.*, 2019). Morphologically *Z. armatum*, is an aromatic tree that grows up to 6 m in height with its branches bearing prickly thorns and small flowers. The fruits are reddish ovoid and split when ripe. It is widely distributed in Nepal from east to west at an elevation of 1000-2500 m in open places and forest areas (Hertog & Wiersum, 2000) besides this plant is also distributed in India, Bhutan, China, Taiwan, Philippines, Malaysia, Pakistan, and Japan at an altitude range of 1300-1500 m (Singh & Singh, 2011). *Z. armatum* is an economically valuable and promising plant of the Rutaceae family commonly called 'Timur' in Nepal. *Z. armatum* DC is also called winged prickly ash. Locals have consumed it for ages as spices in the treatment of various ailments. Due to its high value, it has been consumed by people through the ages in the form of spices and the treatment of various ailments. Its fruit and thorns are also used as fish poison by certain tribes in Nepal (Malla *et al.*, 2014). Properties such as anthelmintic, stomachic, and carminative have increased their uses (Phuyal *et al.*, 2019). The properties of this plant are attributed to the presence of various phytochemicals such as alkaloids, sterols, phenolics, lignins, coumarins, terpenoids, flavonoids, saponins, coumarins, glycosides, benzenoids fatty acids, alkanolic acids, and amino acids working in synergy (Karki *et al.*, 2014; Chopra *et al.*, 1958).

With every emerging disease development and research studies of new drugs depend critically on natural products (Newman & Cragg, 2016). Studies revealed *Z. armatum* from various belts exhibited strong antifungal, cytotoxic, phytotoxic, insecticidal, and anti-leishmanial effects (Alam & Saqib, 2017) in addition to significant antidiabetic and antioxidant properties (Karki *et al.*, 2014). Similar other species like *Z. alatum* possess potent cytotoxic properties in different cell lines due to its lignins (Mukhija *et al.*, 2014), whereas stem bark of *Z. nitidum* inhibits breast cancer cell lines (Yang *et al.*, 2009).

## 2.2 Bioactivities of *Zanthoxylum armatum*

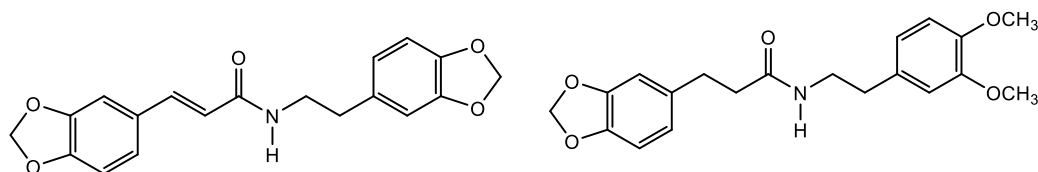
*Zanthoxylum armatum* possesses potent activity which could be attributed to its extensive class of secondary metabolites known as phenols comprised of flavonoids, tannins, hydroxycinnamate esters, alkaloids etc., and structurally related compounds (Grace & Logan, 2000). Some of the chemically identified components isolated from *Z. armatum* are m-methoxy palmityoxy benzene, acetyl phenyl acetate, linoliyl-O-  $\alpha$  – D-xylopyranoside, m-hydroxyphenoxy benzene, palmitic acid along with 2 $\alpha$ -methyl-2 $\beta$ -ethylene-3 $\beta$ -isopropyl-cyclohexan-1 $\beta$ ,3 $\alpha$ -diol (**22**), and phenol-O- $\beta$ -D-arabinopyranosyl-4'-(3", 7", 11", 15"-tetramethyl)-hex-adeacan-1"-oate (**23**) that exhibit notable inhibition of pro-inflammatory cytokines production (Nooreen *et al.*, 2019). Tambulin (**1**), found in *Z. armatum*, has been observed to act as a secretagogue, stimulating insulin secretion (Hameed *et al.*, 2019) as well as a primary vasorelaxant, exerting a direct effect on the vascular smooth muscle through both the cyclic AMP/GMP relaxing pathways (Mushtaq *et al.*, 2019).

A wide range of research conducted on this plant has yielded various compounds. Some of the compounds isolated possessing anti-mycobacterial activities (**24**, **25**) (Siddhanadham *et al.*, 2017) anti-proliferative polyphenolic compounds (**1,2**, **26**, **27**) (Nooreen *et al.*, 2017), isolated lignins (**28**, **29**, **30**, **31**, **32**, **33**, **34**) (Sun *et al.*, 2022; Mukhija *et al.*, 2014) and remarkable lignans from stem bark possessing qualities to protect crops as preservative (**30**, **32**, **35**) (Zhang *et al.*, 2018). A wide range of compounds isolated from the bark of *Z. armatum* are lignins (**30**, **36**). Notable anti-neuroinflammatory agents isolated from the plants include compounds such as trans-ferulic acid (**37**) and methyl ferulate (**38**) (Li *et al.*, 2023). Other isolated compounds are (**39**, **40**, **41**) isobutylhydroxyamides potentially inhibit the growth of NF1-defective tumor cell lines (**42**, **43**, **44**, **45**) (Devkota *et al.*, 2013). In addition notable compounds isolated are armatamide (**46**),  $\alpha$ -amyrins (**51**),  $\beta$ -amyrins (**52**), lupeol (**53**), and  $\beta$ -sitosterol- $\beta$ -D-glucoside(**54**) (Kalia *et al.*, 1999). The twigs of the plant also possess compounds such as eudesmin (**35**) with anti-hypoxic activity (Zhai *et al.*, 2022). Recent studies explored the neuroprotective activities of numerous alkylamides from fruit pericarp (Ye *et al.*, 2023). The characteristic pungent odor, tingling sensation, and numbness associated with various unsaturated fatty acid amides of sanshools in their various forms  $\alpha$ ,  $\beta$ ,  $\gamma$ ,  $\delta$ , and their derivatives (Cheng *et al.*, 2023). Some of the major constituents of *Z. armatum* (**46**, **47**, **48**, **49**, **50**) (Singh & Singh, 2011). The compounds isolated from the plants are presented below in **Figure 5**.



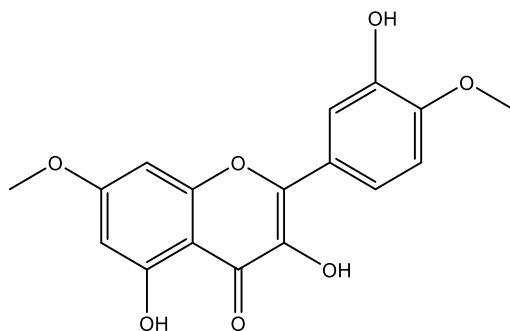
2 $\alpha$ -methyl-2 $\beta$ -ethylene-3 $\beta$ -isopropyl-cyclohexan-1 $\beta$ ,3 $\alpha$ -diol (**22**)

Phenol-O- $\beta$ -D-arabinopyranosyl-4'--(3'',7'',11'',15''-tetramethyl)-hexadecan-1''-oate (**23**)

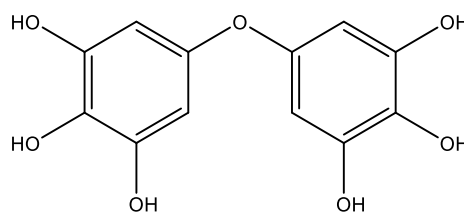


N-(3',4'-Methylene dioxy phenyl ethyl)-3,4-methylene dioxy cinnamoyl amide (**24**)

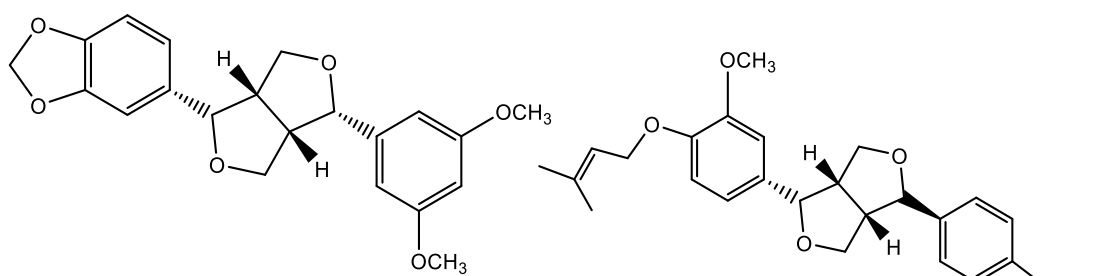
N-(3',4'-dimethoxyphenyl ethyl)-3,4-methylene dioxy dihydro cinnamoyl amide (**25**)



Ombuin (**26**)

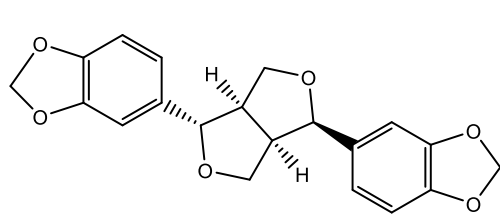


3,4,5,3',4',5'-hexahydroxydiphenyl ether (**27**)

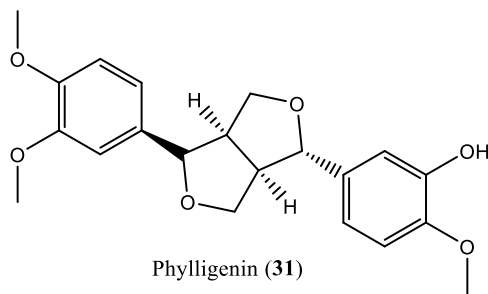


Zanthlignans A (**28**)

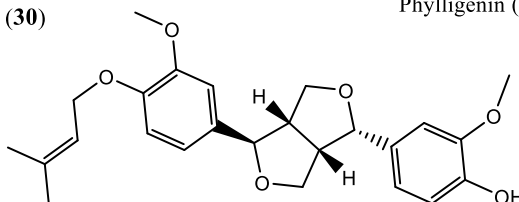
Zanthlignans B (**29**)



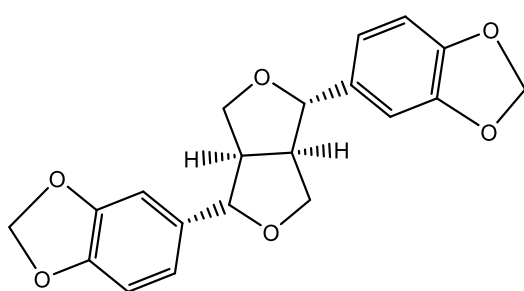
(-)-Asarinin (30)



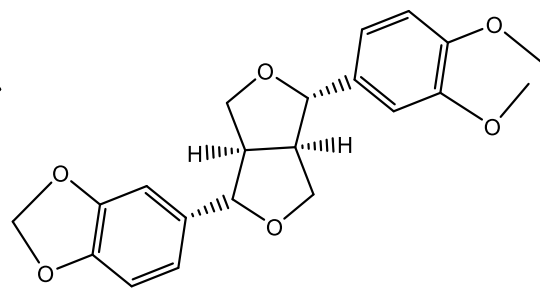
Phylligenin (31)



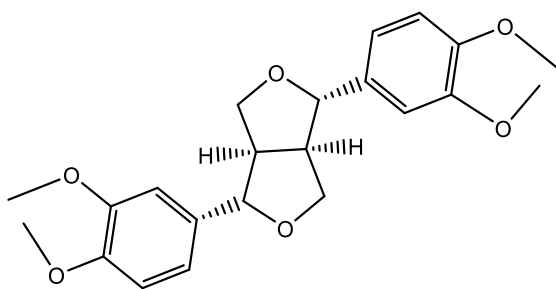
Planispine (32)



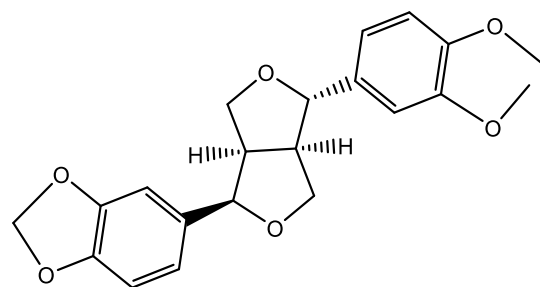
(+) Sesamin (33)



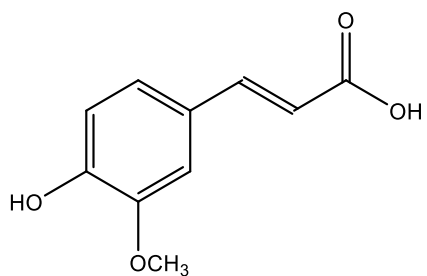
(+) Kobusin (34)



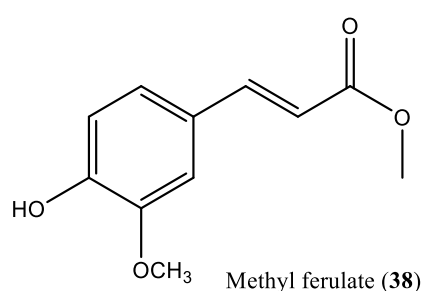
Eudesmin (35)



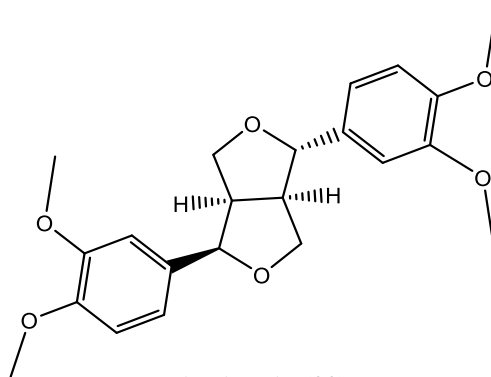
(+) Fargesin (36)



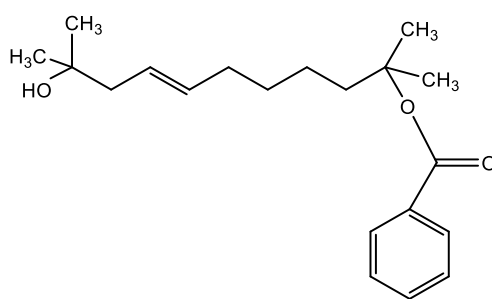
Trans-ferulic acid (37)



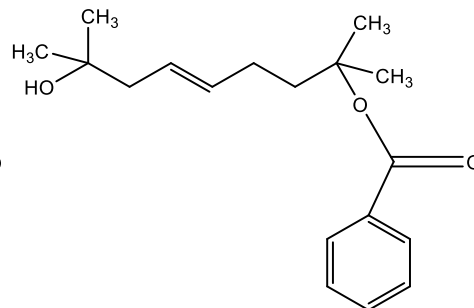
Methyl ferulate (38)



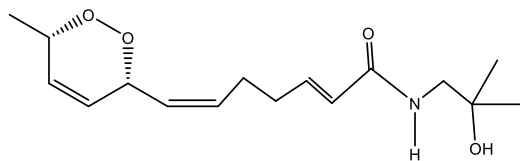
Epleudesmin (39)



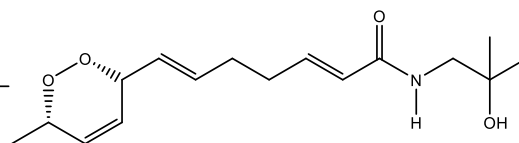
(cis)-2,10-dimethyl-undec-7-en-10-ol-2-oyl benzoate (40)



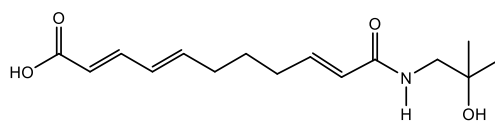
(cis)-2,8-dimethyl-non-5-en-8-ol-2-oyl benzoate (41)



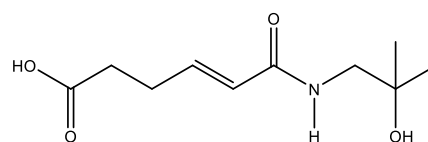
Timuramide A (42)



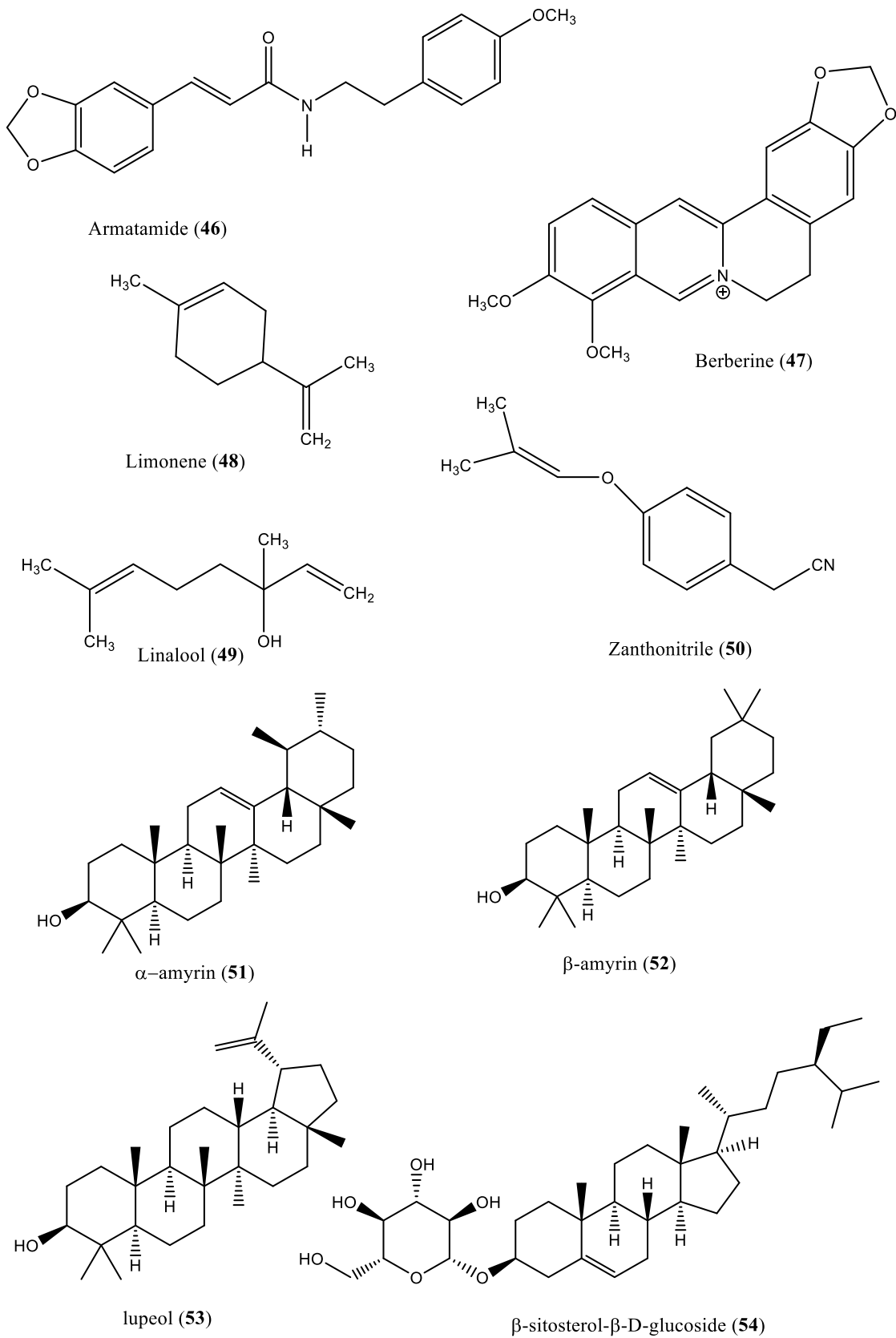
Timuramide B (43)



Timuramide C (44)



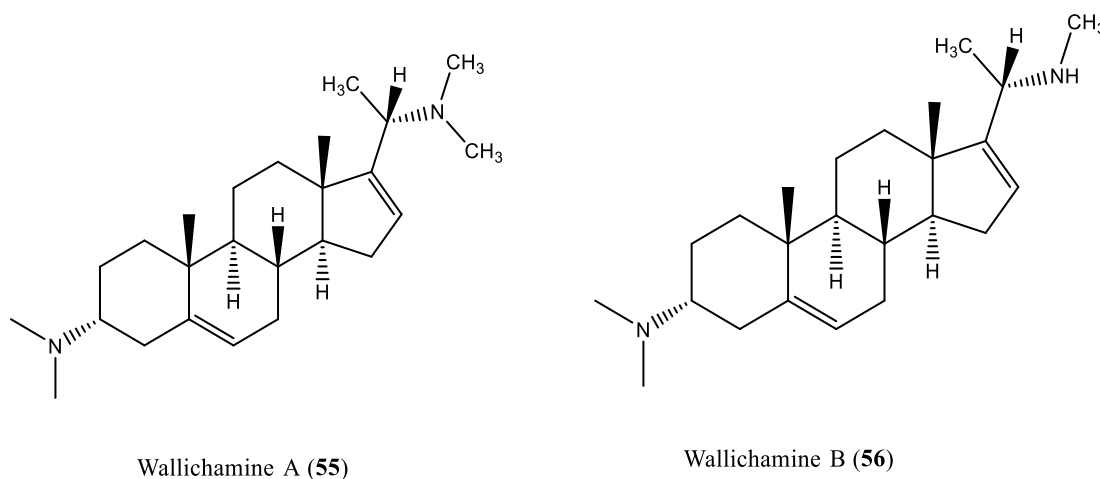
Timuramide D (45)



**Figure 5:** Structure of some of the isolated compounds from *Z. armatum*

### 2.3 Bioactivities of isolated compounds from *S. coriacea* and *S. wallichii*

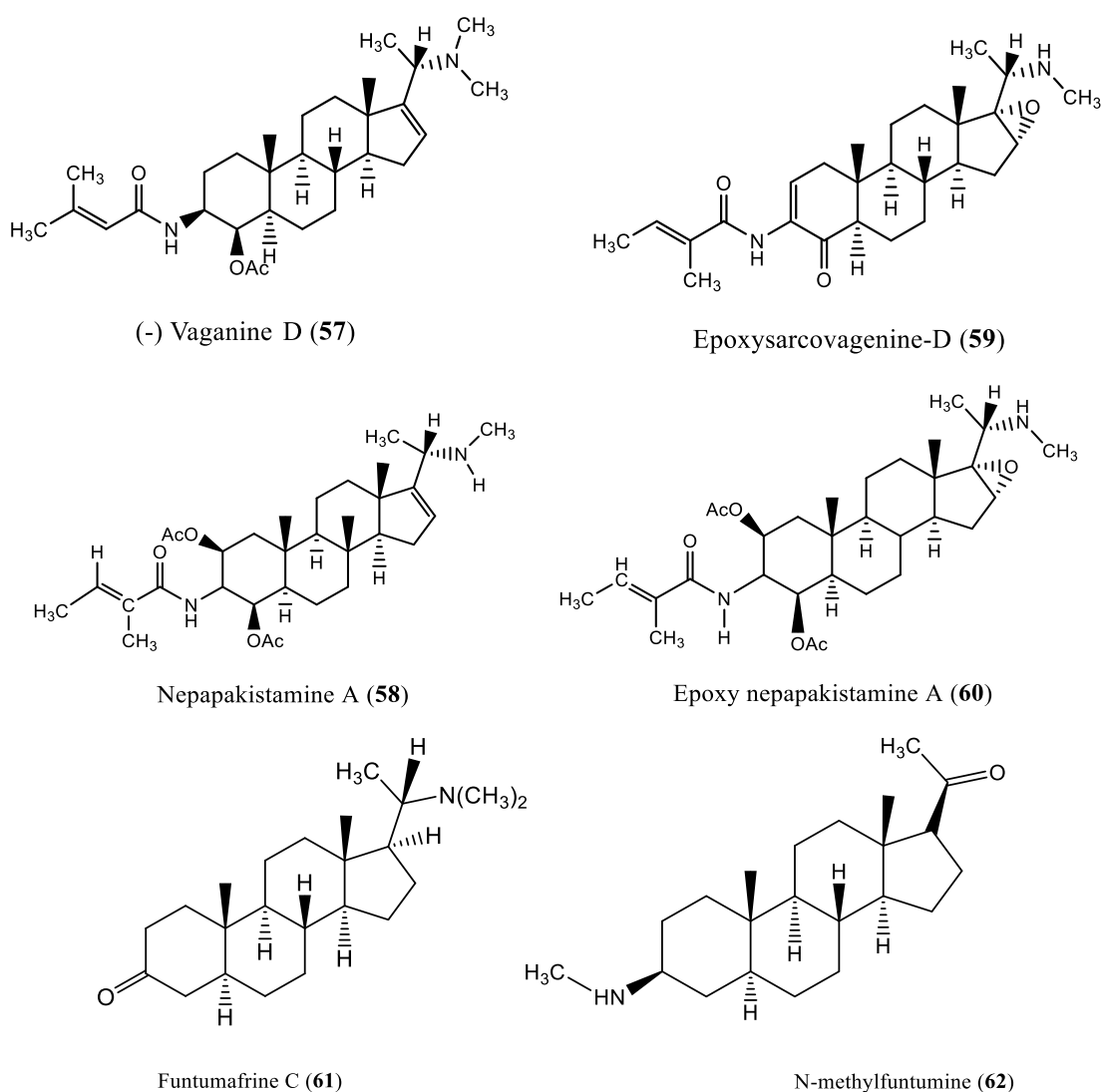
The significance of this genus is evident in numerous research endeavors, where biological activities have been attributed to isolated steroidal alkaloids, specifically pregnane derivatives (Ghulam *et al.*, 2012). N-methylepipachysamine D, Sarcovagine C (**71**), and dictyophlebine (**72**) exhibit dual cholinesterase and antiplasmodial properties (Devkota *et al.*, 2007), displaying significant inhibitory activities. This affluence of research underscores the critical role of this genus and its alkaloid constituents, particularly in the context of their diverse and potent biological effects. Other compounds from *S. hookeriana* possess both cholinesterase and antiplasmodial properties (Devkota *et al.*, 2007) with significant inhibitory activities. Compounds (**55**, **56**) isolated from *S. wallichii* (Adhikari *et al.*, 2015) are detailed in **Figure 6**.

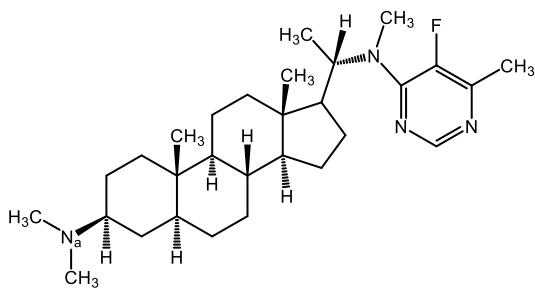


**Figure 6:** Structure of some compounds isolated from *S. wallichii*

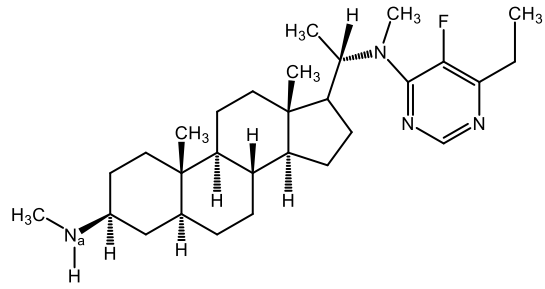
Leaves from *S. coriacea* in Nepal are enriched with potent compounds, including (-)-vaganine D (**57**), (+) nepapakistamine A (**58**), exhibiting cholinesterase inhibitory activities. Other steroidal alkaloids isolated from the leaves namely, epoxysarcovagenine D (**59**), epoxypakistamine -A (**60**), Funtumafrine C (**61**) and N methylfuntumine(**62**), exhibit robust acetylcholinesterase and butyrylcholinesterase inhibition in a concentration- dependent manner (Kalauni *et al.*, 2002). A significant breakthrough in research unfolded with a discovery of a fluorine containing secondary metabolite from *S. coriacea*, introducing a novel class of fluoropyrimidine-substituted alkaloids (**63-70**) alongside numerous steroidal alkaloids possessing potent biological activities (Adhikari, 2009). Additionally isolated compounds encompass alkaloid C (**71**), Na-methylepipachysamine D (**8**), *Iso*-N formylchoenmorphine (**72**), Sarcovagine C (**73**), Sarcovagine D (**74**), N<sub>a</sub>-methylpachysamine A (**75**), dictyophlebine (**76**), 5,6-dihydrosarconidin (**77**), and terminaline (**78**).

The roots of *S. coriacea* exhibit anti-leishmanial activities attributed to steroidal alkaloids such as alkaloid C (**71**) and *Iso-N-formylchonemorphone* (**72**) (Choudhary *et al.*, 2010). The flowers of *S. coriacea* were revealed to contain rare sugar xylitol, alongside other sterols (Rai *et al.*, 2006). These research findings underscore the heightened medicinal value of these species. The impact of this research extends to the local community, where people utilize the bark of *S. coriacea* to alleviate swelling (Sigdel *et al.*, 2013). Moreover, leaves and shoots of *Sarcococca* plants find application in folk medicine for treating rheumatic fever (Kumar *et al.*, 2015). Various parts of this medicinally significant plant, including roots, stem, leaves, bark, and flowers, have been subjects of continuous multidimensional research for years. Some of the compounds isolated (**57**, **58**, **59**, **60**, **61**, **62**) (Kalauni *et al.*, 2001) (Kalauni *et al.*, 2002) and (**63**, **64**, **65**, **66**, **67**, **68**, **69**, **70**) (Adhikari, 2009) from *S. coriacea* are presented in **Figure 7** below.

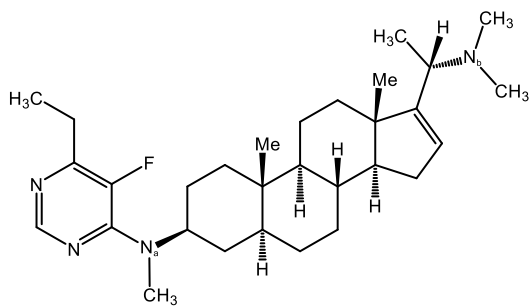




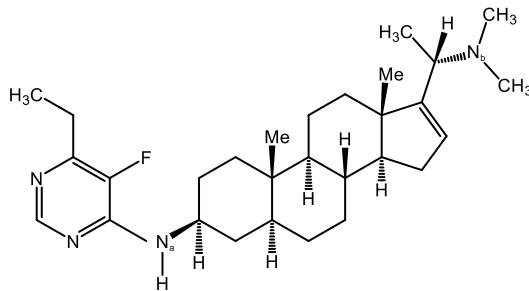
Adhikarimine A (63)



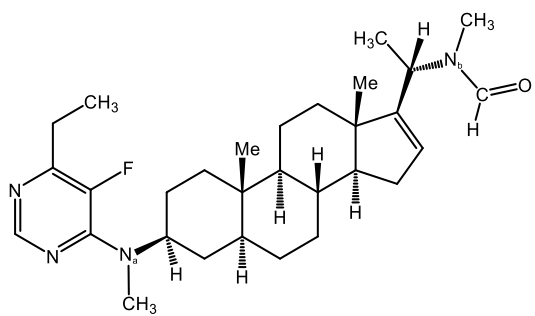
Adhikarimine B (64)



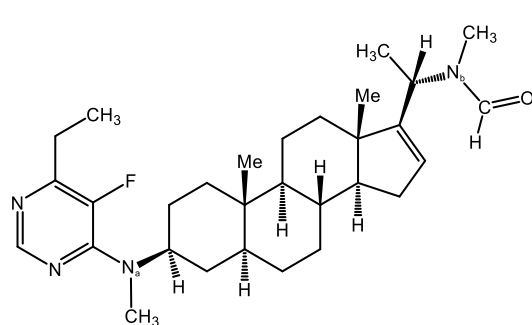
Adhikarimine C (65)



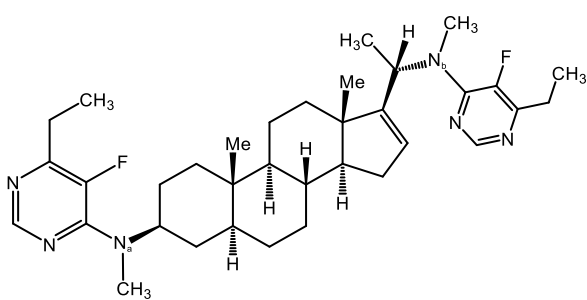
Adhikarimine D (66)



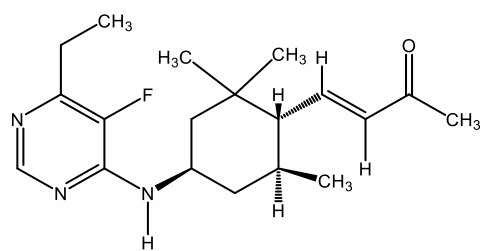
Adhikarimine E (67)



Adhikarimine F (68)



Adhikarimine G (69)



Adhikarione (70)

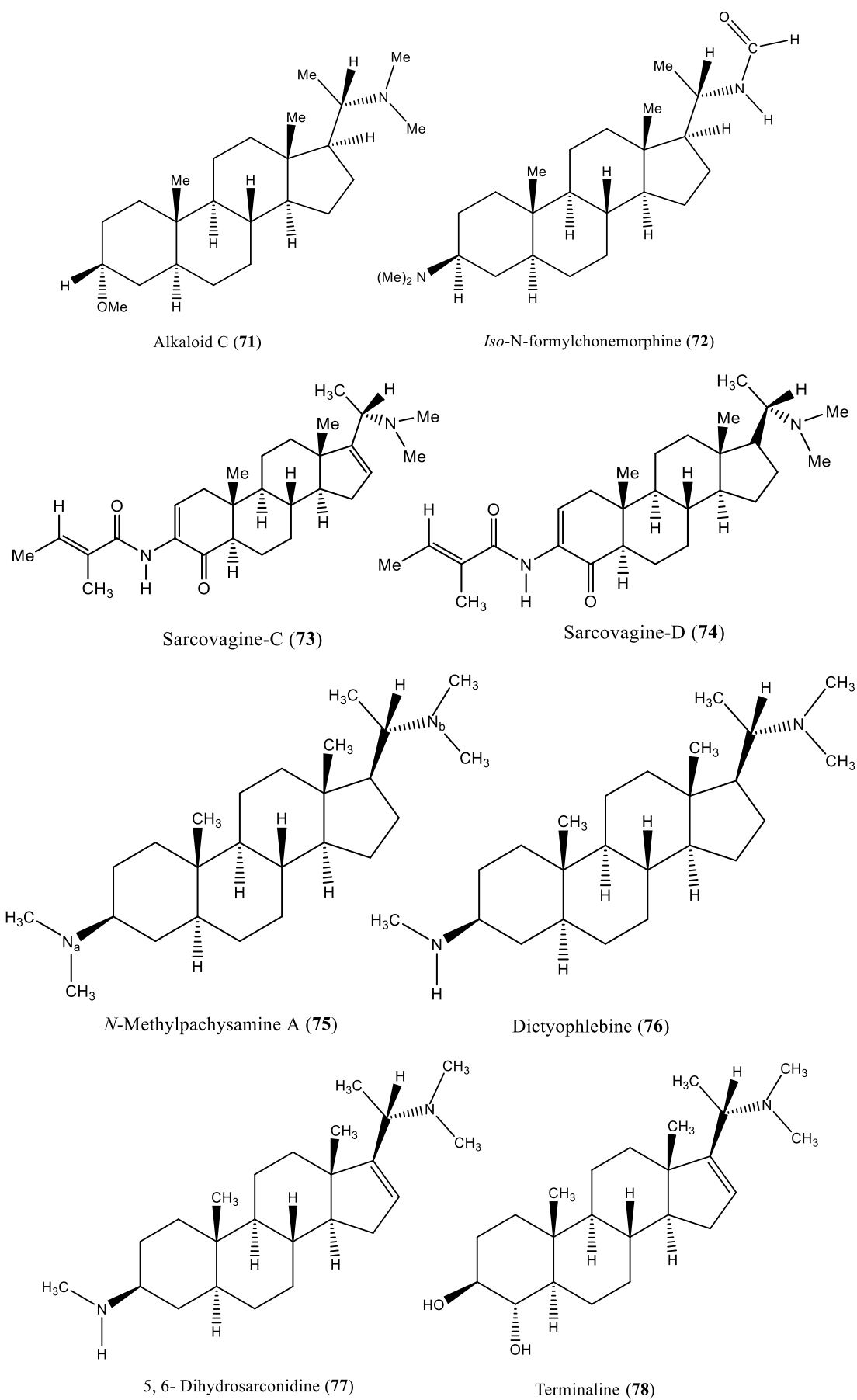


**Figure 7:** Structure of some compounds isolated from *S. coriacea*

## 2.4 Research gap

The literature review has systematically uncovered diverse aspects of research on these plants of interest, such as *Z. armatum*, *S. coriacea*, and *S. wallichii*, along with their isolated compounds. This review predominantly focuses on recent investigations and biological applications associated with these plants. Notably, considerable efforts have been directed towards isolating compounds and elucidating their specific bioactivities. The indigenous treatment practices for various ailments and disorders exhibit variations depending upon topographic nuances and quantitative constituents.

Nature-based therapies not only present cost-effective alternatives but also serve as viable options regarding conventional, costly, and intricate technologies. The challenges associated with synthetic medications, encompassing high costs, limited accessibility, and adverse effects, especially in developing nations like Nepal, underscore the imperative for researchers to delve into nature's reservoir for drug discovery. There exists an urgent necessity for the development of affordable widely accessible, and highly effective nature-based medications.

While numerous researchers have explored plant-based treatments, Ayurvedic medicine has particularly highlighted the potential of *Z. armatum* and its oil in managing inflammatory disorders. Nevertheless, a conspicuous gap exists in specific studies elucidating the antioxidant, antidiabetic, and anticancer properties of *Z. armatum* sourced from higher altitudes. Similarly, evidence-based studies are lacking concerning the bio-potencies of *Sarcococca* species, as per indigenous practices. To the best of our knowledge, there is an absence of research on the antidiabetic, antioxidant, and anticancer properties of these plants within the Nepalese topography. Consequently, our research endeavours aim to address this void by scrutinizing the efficacy of *Z. armatum*, *S. wallichii*, and *S. coriacea* concerning these unexplored properties.

## CHAPTER 3

### MATERIALS AND METHODS

#### 3.1 Methodological framework

Extract preparation, fractionation, and isolation were conducted in the research laboratory of the Central Department of Chemistry, Tribhuvan University, Kathmandu, Nepal, National Academy of Science and Technology (NAST), Lalitpur, Nepal, and University of Karachi, Pakistan. The primary goal of the fractionation of extract was to obtain flavonoid-containing fraction in the case of *Z. armatum*. While isolation of the *S. wallichii* DCM fraction is a continuous work of our research group. **Figure 8** illustrates the methodological framework of extraction and fraction during the study initiated from 80% hydro methanolic/ hydroethanolic solution. However, in the context of *S. coriacea* leaf and stem-only extraction were carried out for bioactivities. A thorough explanation of each procedure is followed on the specific topic.

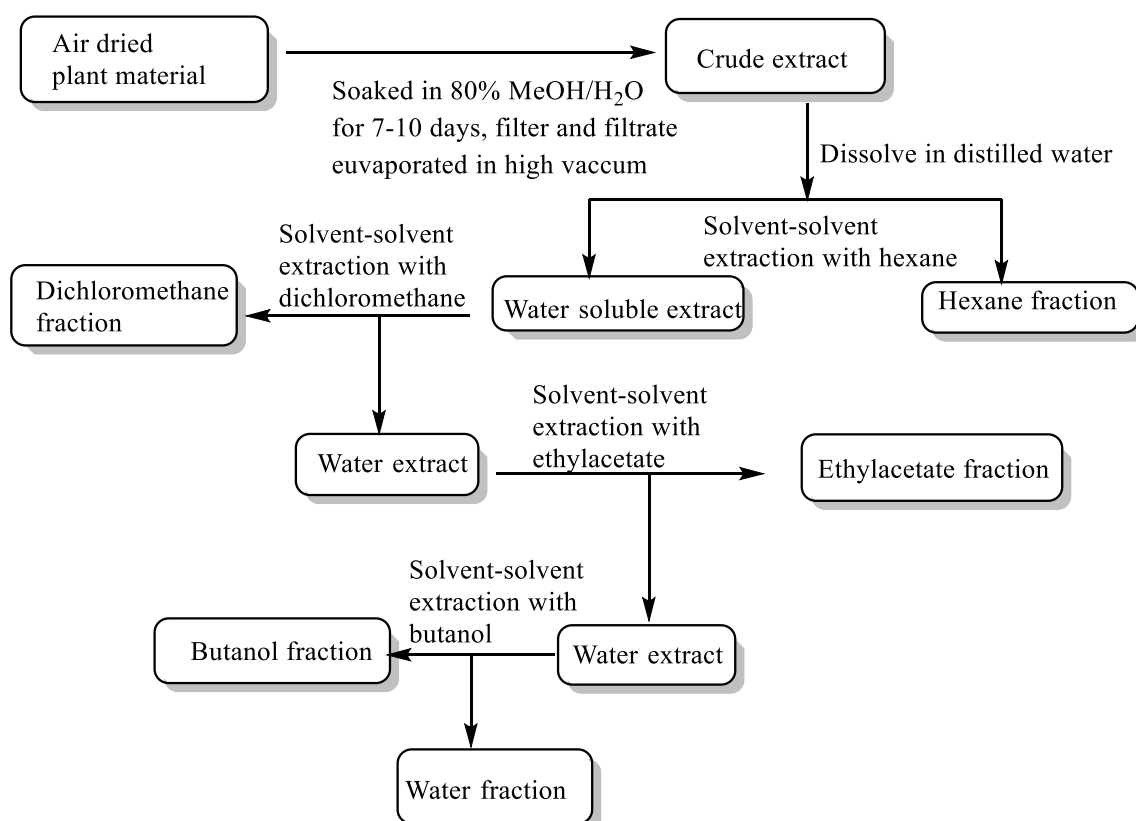


**Figure 8:** Conceptual framework of extraction and fractionation of plant

## 3.2 Sample collection and extraction

### 3.2.1 *Zanthoxylum armatum*

Ripe fruits of *Z. armatum* were collected in October 2018 from the Pyuthan district of Nepal. Botanist Dr. Baburam Nepali assisted in the identification of the plant species in the field during collection. Herbarium authentication was carried out at the Central Department of Botany, Kritipur. The specimen of voucher no TUCH 201016 was collected at Tribhuvan University Central Herbarium (TUCH). Air-dried matured fruits of *Z. armatum* were ground to powder. **Figure 9** represents *Z. armatum* fruit ripe in the plant, harvested, and powdered form. 5 kg of powdered *Z. armatum* was macerated with 7 liters of 80% EtOH: H<sub>2</sub>O at room temperature for 7 days with occasional shaking and the procedure was repeated thrice. The supernatant filtrate was concentrated in a rotary evaporator to obtain a dark viscous semisolid crude extract of 561.04 g. The dried ethanolic extract was dissolved in distilled water for fractionation of its constituents using various organic solvents from hexane (Za-A), ethylacetate (Za-B), and butanol (Za-C). The fractionated solution procedure was concentrated in rotatory evaporator IKA (Werke GmbH & Co. KG, Germany) at 40 °C and dried in the freeze drier (HETOSICC, Heto Lab Equipment, Denmark) at 55 °C.



**Figure 9:** Photograph of (a) *Z. armatum* tree (b) ripe fruits (c) fruit pericarp before grinding (d) powdered fruit pericarp ready for extract preparation

A similar process was adopted for hydromethanolic extract preparation. Extract yield was 9.8% of the dry weight of fruits used. The dried extract was stored in the refrigerator at 4 °C until further use. The methodological framework of the extraction and fractionation step is presented in **Figure 10**.

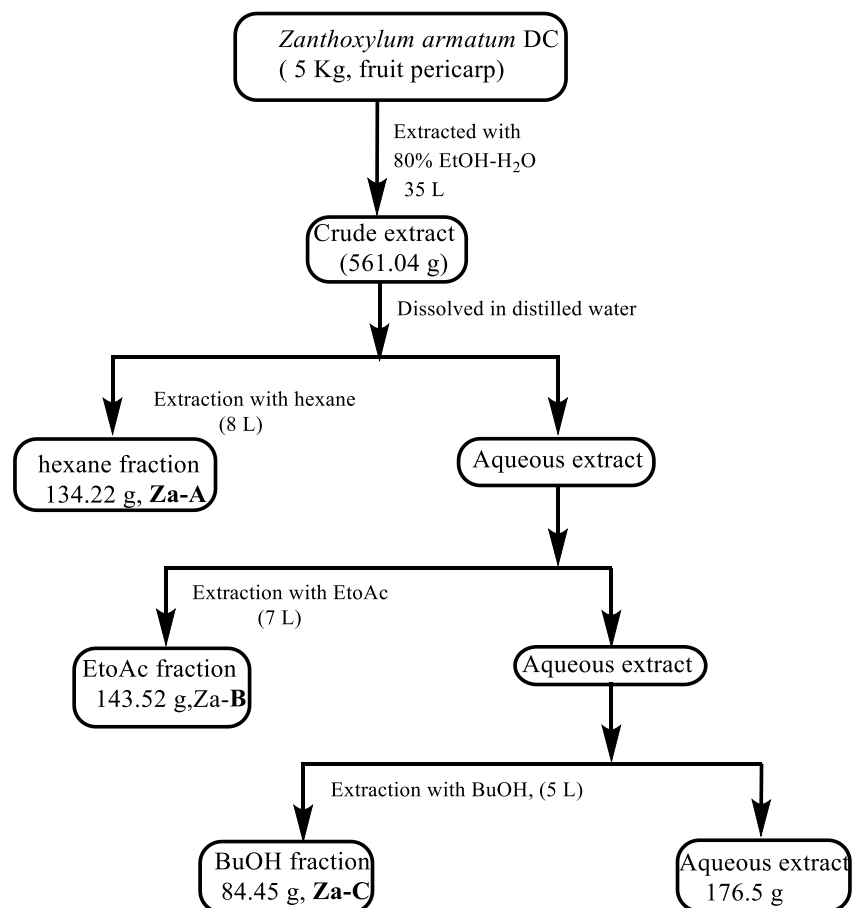


**Figure 10:** Methodological framework of extraction and fractionation of *Z. armatum*

### 3.2.2 Sample collection for extraction of essential oil

For the extraction of essential oil from the matured fruit pericarp, *Z. armatum* were collected from the commercial sites of Salyan (Hertog & Wiersum, 2000) Surkhet and Myagdi district of Nepal.

### 3.3. Materials and equipment

Laboratory-grade organic solvents were used and purchased from E. Merck, Glaxo, and qualigens. 2,2 Diphenyl 1 picrylhydrazyl (DPPH),  $\alpha$ -glucosidase from *Saccharomyces cerevisiae*,  $\alpha$ -amylase from porcine pancreases, 2-Chloro-4-nitrophenyl- $\alpha$ -D-Maltotrioxide (CNPG3) and *p*-Nitrophenyl- $\alpha$ -D-glucopyranoside (PNPG) were purchased from Sigma-Aldrich, Glucose Oxidase (GOD- PAP) and Cholesterol

Oxidase/Peroxidase (CHOD-PAP) were purchased from Randox Laboratories Ltd., UK. Column chromatography (CC) was performed using (60-120, 70-230, and 30-400 mesh size, E. Merk, Darmstadt), and Merck alumina (ASTM mesh 70-230) and LH-Sephadex. Compounds were checked for purity using pre-coated silica gel 0.2 mm analytical thin layer chromatography TLC plates (60, F<sub>254</sub>, E. Merck,). Visualization of TLC plates occurred under ultraviolet light at 254nm for fluorescence quenching spots and at 366 nm for fluorescent spots. Different spraying reagents such as anisaldehyde, sulphuric acid, ferric chloride, Dragendroff reagent, and iodine chamber were employed to stain the compounds on TLC. For spectrophotometry microplate spectrophotometer (Epoch 2, BioTek, Instruments, Inc., USA) was used. Rotatory evaporator IKA (Werke GmbH & Co. KG, Germany) at 40 °C and dried in the freeze drier (HETOSICC, Heto Lab Equipment, Denmark) at 55 °C. The EI-MS spectra were obtained on EI (LR) JEOL MS ROUTE 600H-1, (JEOL, Ltd, Tokyo, Japan). The <sup>1</sup>H-NMR spectra were acquired on AV-400 & 500 instruments (Bruker, Switzerland). Chemical shift values were recorded in ppm( $\delta$ ) relative to CDCl<sub>3</sub>, MeOD, and DMSO and the <sup>1</sup>H NMR data are reported as follows: chemical shift, integration, multiplicity (s = singlet, d = doublet, m = multiplet, dd = doublet of doublet) and coupling constants (Hz). The <sup>1</sup>H-NMR, COSY, HSQC, and HMBC spectra were also taken at 400 & 500 MHz and the coupling constants are estimated in Hertz. The spectroscopic part was recorded at the H. E. J. Research Institute of Chemistry, University of Karachi, Pakistan and Kumamoto University, Japan.

#### **3.4. Fractionation of *Z. armatum* extract**

The fractionation was carried out using liquid-liquid extraction or partition chromatography. In this technique, the sample is dissolved in one solvent, and this solvent is brought into contact with a second, immiscible solvent. The compounds in the sample will distribute themselves between the two immiscible solvents based on their solubility in each. This distribution of compounds between the two solvents is characterized by the partition coefficient ( $K_d$ ). The choice of solvent thus plays a vital role in the fractionation of extract as the nature of solvent and phyto-constituents in the extract determines the distribution of constituents. The nonpolar solvent dissolves nonpolar constituents and vice-versa following the rule of solubility “like dissolves like”. The non-polar hydrocarbons and low polarity compounds are extracted by hexane fraction while the intermediate polar constituents are soluble in ethylacetate fraction. The butanol fraction extracts the more polar compounds and the remaining higher polar

compounds solubilize in water. The hydroethanolic extract of *Z. armatum* was fractionated with solvent in increasing polarity using the separatory funnel. The extract was dissolved with distilled water at first followed by fractionation using lower polarity n-hexane, intermediate polarity ethylacetate and more polar n-butanol and finally the remaining water fraction. Hence choice of solvents, extraction process, separation and finally collection of phases determines the yield of the constituents which can be processed ahead for column chromatography and isolation. The fractionation details of *Z. armatum* extract are presented in scheme **Figure 10**.

### **3.4.1 Column chromatography**

Column chromatography involves separating the constituents of a mixture between two phases, where the solvent acts as the mobile phase, and silica serves as the stationary phase. The distribution coefficient ( $K_d$ ) measures how a compound distributes itself between two immiscible phases the stationary phase (silica gel) and the mobile phase (solvent). Higher  $K_d$  indicates that a compound has a greater affinity for the stationary phase and vice versa however in the case of lower  $K_d$  compound is less retained by the stationary phase, making it more likely to be extracted into the solvent. The selection of a suitable eluent, functioning as the mobile phase, crucially determines the efficacy of the process. The eluent carries the constituents down the column, as the compounds with different  $K_d$  values interact with the stationary phase to varying degrees, they will be eluted at different times. The time and yield in the chromatographic system are influenced by the flow rate and the gradient of elution.

Thus to facilitate the separation of constituents within the extract and isolate the desired compound, column chromatography was employed. The methodology initially started with the careful packing of silica and the extract. The column preparation includes filling it with silica as an adsorbent in slurry form using a nonpolar solvent. To create the slurry for wet packing, silica was preheated in an oven at 120 °C for three hours and soaked in n-hexane overnight. A similar process was applied to the desired extract, using a minimal amount of silica in dry form.

Subsequently, the wet adsorbent was packed into the column first, and the extract was added to the top. The extract was thoroughly mixed, dried, and packed into the column. The column was filled initially with larger mesh size silica gel (mesh size: 60-120), which can allow for a higher flow of the mobile phase through the column leading to faster separation. Above this silica gel slurry, a layer of cotton is placed, and finally,

the fraction/extract is prepared with silica in dry form. Another cotton layer was added to the remaining column space to ensure equal inlet flow, maintaining a smooth internal diameter for the solvent's direct flow and proper liquid distribution in the column. During continuous flow, a final silica layer above the cotton layer was added to act as support and prevent the adsorbent from floating.

The column was initially conditioned by passing pure n-hexane only. The column's stopper controlled the eluent solution's flow rate. Eluent samples at specific intervals (100 mL) were collected in a volumetric flask initially. However, in columns equipped with a fraction collector during purification, 5 mL of eluent at regular intervals were collected using the collector.

Fresh eluents from different collectors were gathered in sets of five, and thin-layer chromatography (TLC) was conducted using a suitable solvent system to assess the similarity or dissimilarity of compounds based on their  $R_f$  values and spots. Gradually increasing the polarity of the gradient solvent system and examining the nature of bands, each unit's TLC profiling was concentrated using a rotary evaporator. Finally, the concentrated eluents were grouped for further purification.

In cases where the eluent system showed no compounds during TLC profiling, the polarity was increased. Eluent tests were conducted to confirm how effectively the particular solvent system eluted various compounds at varying flow rates.

### **3.4.2 Column chromatography of ethylacetate fraction**

For the isolation of compounds thin layer chromatography (TLC) of all the fractions was carried out. Based on the TLC profiling of the fractions the ethylacetate fraction of *Z. armatum* was column chromatographed. This column was packed with a wet slurry of silica as adsorbent as discussed above. The portion of ethylacetate fraction 100 g was homogeneously mixed with silica and dried packed for isolation. It was then loaded into column size (28×5.6 cm) silica gel (230-400 mesh size, Merck, Darmstadt, Germany) with n-hexane: dichloromethane: methanol solvent system as eluent in gradient polarity. Starting from n-hexane (10L), various gradient systems of n-hexane: dichloromethane (1%, 3%, 5%, 7%, 10%, 12%, 15%, 20%, 25%, 30%, 40%, 50%, 50%, 70%, 80%, 90%, 100%) and were finally washed with 1% methanol: dichloromethane up to 5% in the primary column. This yielded 8 major fractions.

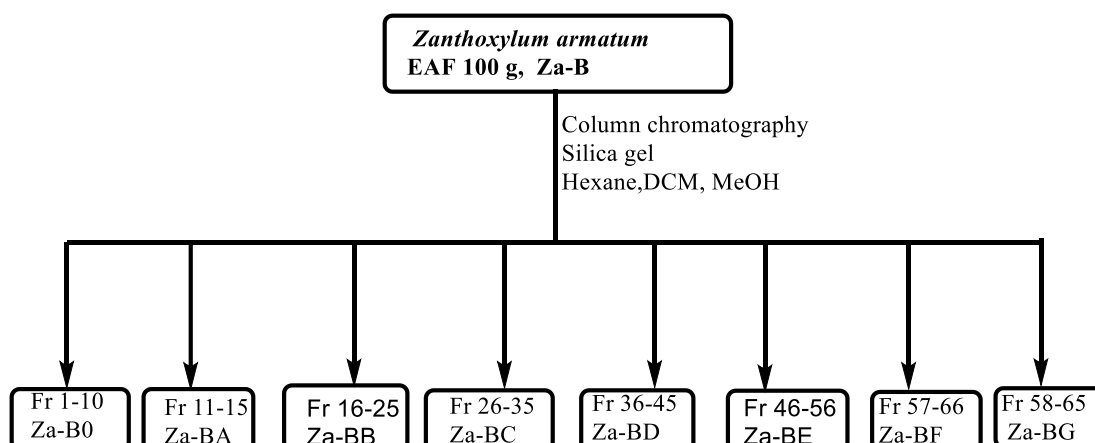


**Figure 11:** Scheme of isolation of *Z. armatum*

### 3.4.3 Isolation and purification of compounds from sub-fractions

The isolation step was initiated based on the TLC profiling of these 8 major fractions on the precoated silica gel sheets (60F 254, E. Merck) detected under UV light at 254 nm and 366 nm for nature and the number of spots. Those fractions having measurable retention factor ( $R_f$ ) as calculated from the formula below of their constituents during TLC were processed for isolation using column chromatography. Column chromatography was conducted on these major fractions (Fr 46-56), Za-BE weighing 20 g, fraction (Fr-11-15), Za-BA weighing 25 g, and fraction (Fr 58-65) Za-BG weighing 20 g.

*Retention factor  $R_f = \text{Distance travelled by the compound} / \text{Distance travelled by the solvent front}$*

- I) Isolation of compounds:** Compounds **1** and **2** were isolated from the fraction (Fr-46-56). The detail of the isolation scheme of compounds **1** and **2** is presented in **Figure 12**.

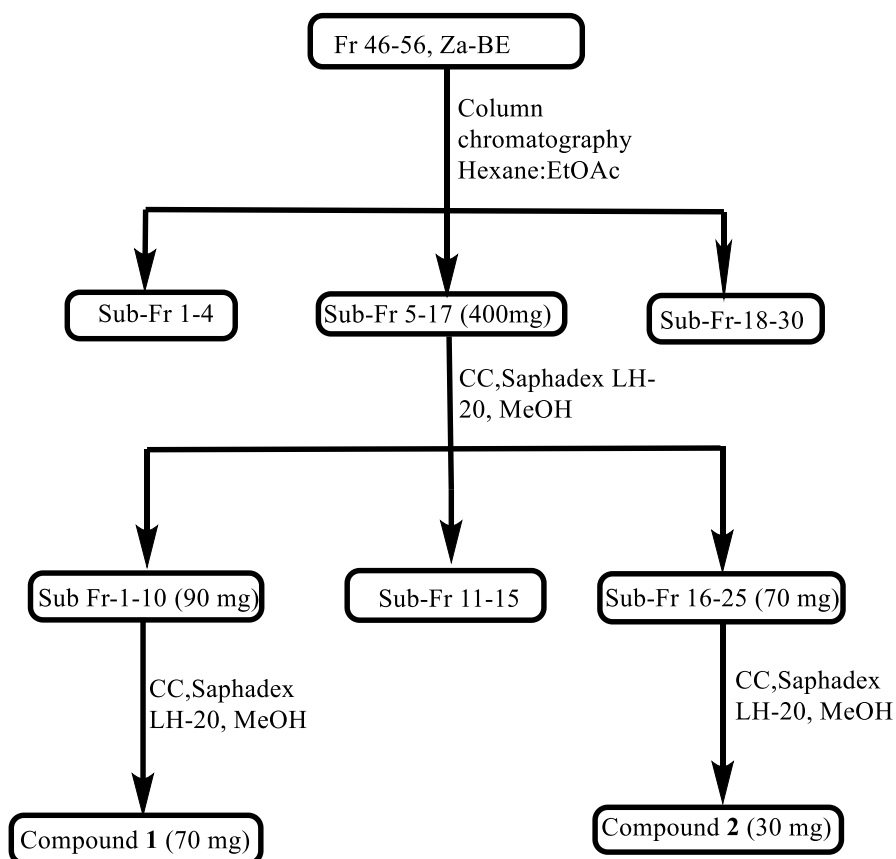
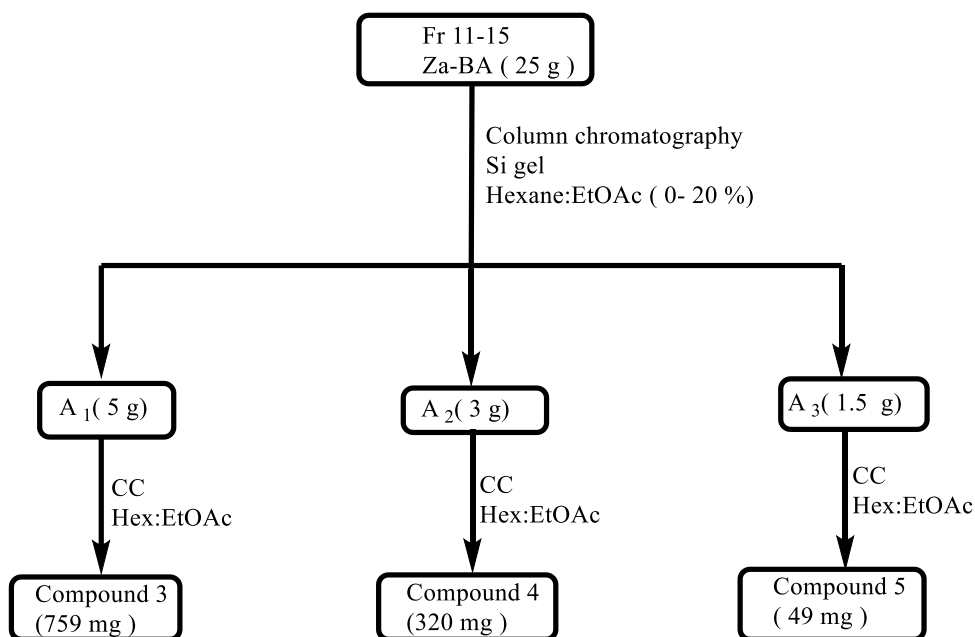


Figure 12: Scheme of isolation of compounds 1 and 2 from *Z. armatum*

- II) **Isolation of compounds 3, 4, and 5:** The fraction (Fr-11-15) with impurities (25 g) was subjected to column chromatography using various gradients of hexane: ethylacetate which leads to three major subfractions A1 (5 g), A 2(3 g), and A 3(1.5 g). These sub-fractions were again subjected to column chromatography that yielded compound 3 (759 mg), compound 4 (320 mg), and compound 5 (49 mg) respectively. The isolation scheme for the compounds 3, 4 and 5 from the Za-BA fraction is presented below in **Figure 13**.



**Figure 13:** Scheme of isolation of compounds **3**, **4**, and **5** from *Z. armatum*

**III) Isolation of compounds 6 and 7:** The polar sub-fraction Za-BG (20 g) on column chromatography yielded sub-fractions G1, G2 and G3. Subfraction G1 (3 g) which on successive CC with ethylacetate and hexane as eluent at 80 % yielded compound **6** (9 mg) and compound **7** (150 mg) in separate columns. **Figure 14** represents the isolation scheme of the compounds.

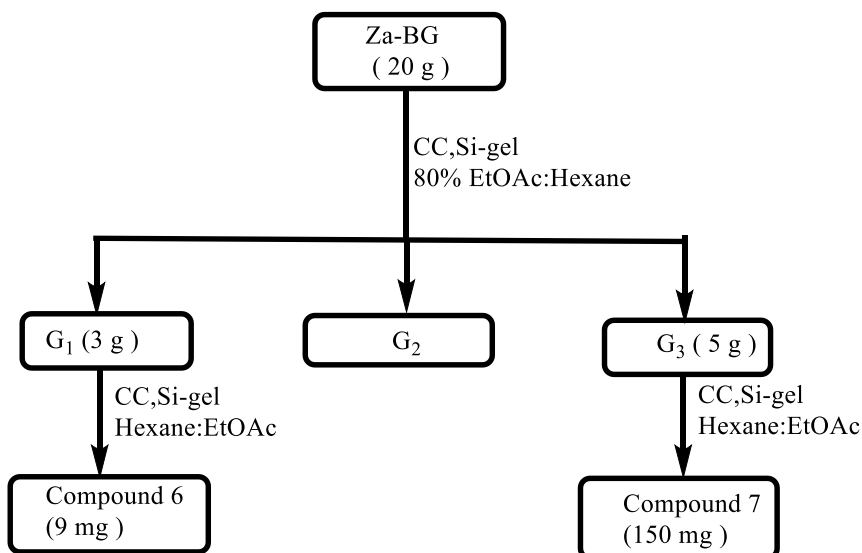


**Figure 14:** Scheme of isolation of compounds **6** and **7** from *Z. armatum*

### 3.4.5 Compounds isolated from *Z. armatum*

#### 3.4.5.1 Tambulin (1)

This compound was obtained from the sub-fraction Za-BE (20 g) eluted at 50% dichloromethane: n-hexane (**Figure 11**) was further subjected to column chromatography hence was loaded into (60×3.5 cm) column and eluted with gradient mobile phase of Ethylacetate: n-hexane (2, 4, 6, 8, 10, 12, 15, 20, 25 %) to obtain 3 sub-fractions based on TLC observation. Slight impurities observed on TLC of sub-fractions 5-17 were removed by passing the sub-fractions of the targeted flavonoid into the Saphadex LH-20 column. Sub fraction 5 obtained from 10% Ethylacetate: n-hexane (400 mg) afforded a semi-pure compound, which on further purification by Sephadex LH-20 column (100×2.5cm) using methanol as an eluent yielded amorphous yellow compound tambulin (**1**) (**Figure 12**). Observed under TLC at  $R_f$ : 0.51 on the solvent system (35% acetone: hexane) this compound appeared as a bright yellow after staining the developed TLC plate with 1% ethanolic solution of aluminium chloride. Quantitative yield of the compound was 70 mg with melting point at 205° C, UV (MeOH) nm: 367, 325, and 273 nm, IR(CHCl<sub>3</sub>): 3327 (OH), 1651 (aromatic), and 1556 (olefinic) cm<sup>-1</sup>, HREI MS  $m/z$ : [M<sup>+</sup>] at  $m/z$ 344.0906 (Calcd for C<sub>18</sub>H<sub>16</sub>O<sub>7</sub> = 344.0896); NMR. Details are presented in **Table 9**.

#### 3.4.5.2 Prudomestin (2)

This yellow crystalline compound was isolated from the sub-fraction Za-BE (20 g) eluted at 50% dichloromethane: n-hexane (**Figure 11**) and was further subjected to column chromatography similar to tambulin (**1**). Slight impurities observed on TLC of sub-fractions 5-17 were removed by passing the sub-fractions of the targeted flavonoid into the Saphadex LH-20 column. The subfraction (Fr-16-25) that yielded (70 mg) on further passing through the Sephadex LH-20 column (100×2.5cm) using methanol as an eluent yielded yellow-coloured compound **2** (prudomestin) (**Figure 12**). This compound was observed under TLC at  $R_f$ : 0.41 on the solvent system (35% acetone: hexane) as a bright yellow after staining the developed TLC plate with 1% ethanolic solution of aluminium chloride. The quantitative yield of the compound was 30 mg with a melting point of 209 °C. The compound quantitatively yields 30 mg. MW: 330.29 g/mol, MF: C<sub>17</sub>H<sub>14</sub>O<sub>7</sub>, UV (MeOH) nm: 367, 325, and 273 nm, IR (CHCl<sub>3</sub>): 3327 (OH), 1651 (aromatic), and 1556 (olefinic) cm<sup>-1</sup>, EI MS  $m/z$ : [M<sup>+</sup>] at  $m/z$  330.09(Calcd. for C<sub>17</sub>H<sub>14</sub>O<sub>7</sub> = 330.29), NMR details is presented on **Table 10**.

#### 3.4.5.3 Cinnamic acid (3)

This compound was isolated from the sub-fraction Za-BG (25 g) eluted at 15 % dichloromethane: n-hexane (**Figure 10**) which was further subjected to column chromatography and loaded into (60×3.5 cm) column and eluted with gradient mobile phase of Ethylacetate: n Hexane to obtain 3 sub-fractions A<sub>1</sub>, A<sub>2</sub> and A<sub>3</sub>. Sub fraction A<sub>1</sub> (5g) were column chromatographed (**Figure 13**) using eluent as hexane Ethylacetate which afforded needle-shaped white-coloured crystalline compound 3 (759 mg) at R<sub>f</sub>: 0.51 at 10% Ethylacetate: hexane. This compound is only visible in UV. The melting point of the compound was observed at 132 °C. The tabulated NMR is presented in **Table 11**.

#### 3.4.5.4 Cinnamic ester (4)

This compound was isolated from the sub-fraction Za-BA (20 g) eluted at 65% dichloromethane: n-hexane (**Figure 10**) of the ethylacetate fraction of *Z. armatum*. This sub-fraction was further subjected to column chromatography and hence was loaded into (60×3.5 cm) column and eluted with gradient mobile phase of ethylacetate: n-hexane to obtain 3 sub-fractions A<sub>1</sub>, A<sub>2</sub> and A<sub>3</sub>. Sub fraction A<sub>2</sub> (3g) was column chromatographed (**Figure 12**) using eluent as hexane Ethylacetate which afforded bright white crystals (320 mg) TLC visible in UV only at R<sub>f</sub>: 0.51 at 30 % ethylacetate: hexane. The observed melting point was 35 °C. Molecular formula: C<sub>10</sub>H<sub>10</sub>O<sub>2</sub>, Molecular mass: 162.07. **Table 12** presents the details of NMR.

#### 3.4.5.5 Isovanillic acid (5)

This compound is isolated from the sub-fraction Za-BG (20 g) eluted at 65% dichloromethane: n-hexane (**Figure 10**) and was further subjected to column chromatography hence was loaded into (60×3.5 cm) column and eluted with gradient mobile phase of ethylacetate: n-hexane to obtain 3 sub-fractions A<sub>1</sub>, A<sub>2</sub> and A<sub>3</sub>. Sub fraction A<sub>3</sub> (1.5 g) were column chromatographed (**Figure 13**) using eluent as hexane: ethylacetate which afforded compound 5 (49 mg) at R<sub>f</sub>: 0.52 at 30% ethylacetate: hexane. It appeared as slightly brownish needle-shaped crystals with a melting point of 250 °C. Molecular formula: C<sub>8</sub>H<sub>8</sub>O<sub>4</sub>, Molecular mass: 168.04.

#### 3.4.5.6 Isoquercetin (6)

This compound is isolated from the sub-fraction Za-BG (20 g) eluted at 65% dichloromethane: n-hexane (**Figure 10**). This sub-fraction was further subjected to column chromatography and hence was loaded into (60×3.5 cm) column and eluted with gradient mobile phase of ethylacetate: n-hexane to obtain 3 sub-fractions G<sub>1</sub>, G<sub>2</sub>

and G<sub>3</sub>. Sub fraction G<sub>1</sub> (3 g) were column chromatographed (**Figure 13**) using eluent as hexane Ethylacetate which afforded compound 6 (9 mg) at R<sub>f</sub>: 0.61 ethylacetate: hexane: MeOH (3:2:0.5 ml). The dark yellow-coloured compound is slightly soluble in DMSO, Ethylacetate and methanol when warmed. Its melting point was observed at 226°C. Molecular Formula: C<sub>21</sub>H<sub>20</sub>O<sub>11</sub>, Molecular mass: 448.01.

#### 3.4.5.7 Ducosterol (7)

The sub-fraction Za-BG (20 g) eluted at 65% dichloromethane: n-hexane (**Figure 10**) was further subjected to column chromatography and hence was loaded into (60×3.5 cm) column and eluted with gradient mobile phase of ethylacetate: n-hexane to obtain three sub-fractions G<sub>1</sub>, G<sub>2</sub> and G<sub>3</sub>. Sub fraction G<sub>3</sub> (5 g) was column chromatographed (**Figure 13**) using eluent as hexane-ethyl acetate which afforded compound 7 (150 mg) at 60 % ethylacetate: hexane. This white-coloured compound was soluble in pyridine observed under TLC at R<sub>f</sub>: 0.41 on the solvent system (35% acetone: hexane) and stains under sulphuric acid. Molecular formula: C<sub>35</sub>H<sub>60</sub>O<sub>6</sub>, Molecular weight: 576.86

#### 3.4.6 Element detection of fruit pericarp powder of *Z. armatum*

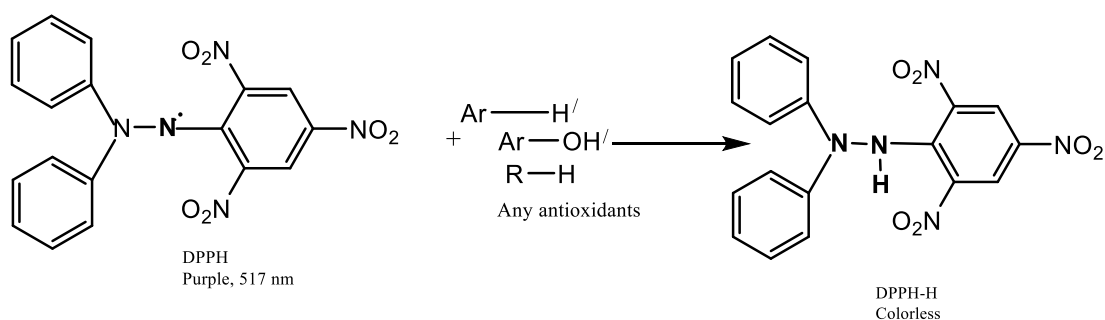
An energy dispersive X-ray fluorescence spectrometer microanalysis technique for elemental analysis was used to determine the metals in the sample under study (Khoddami *et al.*, 2013). For the determination of metals and their toxicity, EDX were carried in the powdered fruit pericarps' and the essential oil of *Z. armatum*. (Instrument: EDX-8000, Shimadzu, Department of Customs, Nepal). EDX qualitatively and quantitatively analyses the sample either in powder or in liquid state without destruction.

### 3.5 Bioactivities determination

#### 3.5.1 Determination of antioxidant activity using DPPH assay

Any plant sample possessing an antioxidant agent changes the purple color of DPPH to colourless at 517 nm as represented in **Figure 15** below.





$$\% \text{ Inhibition} = ((A_{\text{control}} - A_{\text{sample}}) / A_{\text{control}}) * 100\%$$

*A* is the absorbance

**Figure 15:** Mechanism of (DPPH.) to (DPPH: H) antioxidant reaction

For the determination of DPPH activity 0.1mM DPPH solution was prepared by dissolving 3.9 mg DPPH in 100 mL methanol in a volumetric flask wrapped with foil paper and kept in dark and standard quercetin solution was prepared in various concentrations from the stock of 1mg/mL of quercetin in methanol. Serial dilutions of quercetin were prepared ranging from 200, 100, 50, 25 and 12.5  $\mu\text{g/mL}$ . Likewise, plant samples from stock 50 mg/mL (50% DMSO) were diluted serially from 1000, 500, 250, 125 and 62.5  $\mu\text{g/mL}$ . The slightly modified protocol from (Mensor *et al.*, 2001) was used for the determination of antioxidant activity using a 96-well plate from a colourimetric method. 20  $\mu\text{g/mL}$  of quercetin was used as positive control and 50% DMSO was used as a negative control. The positive control quercetin, negative control DMSO and plant samples (100  $\mu\text{L}$ ) were loaded in 96 well plates in triplicate. Then 100  $\mu\text{L}$  of DPPH reagent was added to each well. After initial reading, the well plate was incubated for 30 minutes and absorbance was taken at 517 nm. The change in colour of the DPPH solution is reflected due to the scavenging ability of the sample. The capability to scavenge DPPH radical was calculated by using the following equation:

$$\% \text{ Inhibition} = ((A_{\text{control}} - A_{\text{sample}}) / A_{\text{control}}) * 100\%$$

where, *A* is the absorbance

### 3.5.2 *In vitro* antidiabetic assay

#### 3.5.2.1 Buffer preparation

Phosphate buffer due to its high solubility in water and high buffering capacity was used in the experiment. The buffer was adjusted to pH 6.8 at a concentration of 0.1M using 80 mL of deionized water in a container. 1.312 g of sodium phosphate dibasic heptahydrate and 704.3 mg of sodium phosphate monobasic monohydrate were added

to the container and stirred. The solution was adjusted to pH 6.8 using HCl or NaOH to a final volume of 100ml and stored for in-vitro antidiabetic assays (AAT Bioquest, 2022). Further adjustments were made to the prepared concentration on need as per the protocol followed in specific experiments.

### 3.5.2.2 $\alpha$ -Amylase assay

For *in vitro* antidiabetic properties of the plants under study  $\alpha$ -amylase inhibition activities were carried out following the protocol (Khadayat *et al.*, 2020). For this phosphate buffer, 50% DMSO, Substrate CNPG3 and an enzyme of 1.5 U/mL were used. Plant samples of 50 mg/mL were prepared in 50% DMSO and diluted to 500  $\mu$ g/mL. For  $\alpha$ -amylase inhibition activity phosphate buffer of pH 6.8.0 prepared above was used. 80 $\mu$ l  $\alpha$ -amylase at 1.5 units/mL final concentration of enzyme with various concentrations of plants sample and 100  $\mu$ l of substrate CNPG3 (0.5mM) at final concentration prepared in phosphate buffer were used. All the experiments were performed in triplicate with a final volume of 200  $\mu$ l using 50% DMSO as negative control and acarbose as positive control. The change in absorbance by the release of p-nitroaniline was monitored by using a microplate reader (Epoch 2, BioTek, Instruments, Inc., USA). For calculating  $\alpha$ -amylase inhibition activity following formulas were used:

$$\% \text{ inhibition} = \left( \frac{A_{\text{control}} - A_{\text{sample}}}{A_{\text{control}}} \right) \times 100$$

Where  $A_{\text{control}}$  &  $A_{\text{sample}}$  is the absorbance of the control (DMSO) and sample.

### 3.5.2.3 $\alpha$ - Glucosidase assay

For the glucosidase inhibition activity of the plant samples were prepared from the stock solution of 50 mg/mL to obtain 500  $\mu$ g/mL which was then serially diluted. A phosphate buffer of pH 6.8 prepared was used in the experiment.

The  $\alpha$ -glucosidase activity of plant extracts was calculated by the method described by (Fouotsa *et al.*, 2012) with slight modification. Different concentrations of 20  $\mu$ L plant sample were mixed with 20  $\mu$ L enzyme (0.2 U/mL) and 120  $\mu$ L of phosphate buffer solution (pH 6.8) and pre-incubated at 37 °C for 15 minutes. Then 40  $\mu$ L of 0.7 mM of substrate PNPG was added. Finally, after 30 minutes the  $\alpha$ -glucosidase activity was determined by measuring the p-nitrophenyl released from the hydrolysis of p-Nitrophenyl  $\alpha$ -D glucopyranoside at 405 nm. Acarbose was used as a positive control and 30% DMSO as a negative control. All the experiments were performed in triplicate

in a final volume of 200  $\mu$ L, using a microplate reader. The percentage of  $\alpha$ -glucosidase activity was calculated by the following formula.

$$\% \text{ inhibition} = \left( \frac{A_{\text{control}} - A_{\text{sample}}}{A_{\text{control}}} \right) \times 100$$

Where  $A_{\text{control}}$  and  $A_{\text{sample}}$  represents the absorbance of the control (DMSO) and sample.

### **3.5.3 In-vitro antifungal bioassay**

*In vitro*, antifungal bioassay was performed with minor changes on predesigned protocol (Ayatollahi *et al.*, 2010) with a concentration of sample as 3000 $\mu$ g/mL of DMSO with an incubation time of 7 days and temperature of 27°C. Seven different fungi used were *Trichophyton rubrum*, *Candida albicans*, *Aspergillus niger*, *Microsporum canis*, *Fusarium lini*, *Candida glabrata* and *Aspergillus fumigatus*. The standard drugs used with minimum inhibitory concentration Miconazole (*MIC*; 70  $\mu$ g/mL), Miconazole (*MIC*: 110), Amphotericin B (*MIC*: 20), Miconazole (*MIC*: 98.4), Miconazole (*MIC*: 73.25), Miconazole (*MIC*: 110.8), Amphotericin B (*MIC*: 100) recorded for particular fungus.

### **3.5.4 Microplate alamar blue assay (MABA)**

For antimicrobial activity, Alamarblue assay is used in which resazurin dye is used. Resazurin is a blue, non-fluorescent compound that is reduced to resorufin, a pink and highly fluorescent compound, in the presence of metabolically active cells. This color change and fluorescence shift can be quantitatively measured, making the assay useful for evaluating antimicrobial activity, as it can indicate the metabolic activity and viability of cells in response to antimicrobial agents. Five different bacteria were used for this assay *Escherichia coli* (ATCC 25922), *Bacillus subtilis* (ATCC 23857), *Staphylococcus aureus* (NCTC 6571), *Pseudomonas aeruginosa* (ATCC 10145) and *Salmonella typhi* (ATCC 14028). Standard drug Ofloxacin of 10 mg at a concentration of 100  $\mu$ g/mL was used. The amount of extract used was 60 mg at 3000  $\mu$ g/mL concentration. Further dilution was carried out based on the primary screening result for calculating MIC values.

### **3.5.5 Insecticidal activity by contact toxicity method**

The insecticidal activity of the hexane fraction extracted from *Z. armatum* was observed using the contact toxicity method following the predesigned protocol (Atta-ur Rahman *et al.*, 2001) against three insect species: *Tribolium castaneum*, *Sitophilus oryzae*, and *Rhyzopertha dominica*. The hexane fraction was applied at a concentration of 2038.20

$\mu\text{g}/\text{cm}^2$ . As a reference, the standard drug permethrin exhibited 100% activity against the tested insects at the concentration of  $239.50 \mu\text{g}/\text{cm}^2$ .

### **3.5.6 Anti-inflammatory activity**

The anti-inflammatory activity was tested by the luminol-enhanced chemiluminescence assay as described by Helfand (Helfand *et al.*, 1982). In short, 25  $\mu\text{L}$  of diluted whole blood HBSS++ (Hanks Balanced Salt Solution, containing calcium chloride and magnesium chloride) [Sigma, St. Louis, USA] was mixed with 25  $\mu\text{L}$  of three different concentrations of compounds each in the triplicate and was incubated. HBSS++ and cells were added to the control wells, but no compounds were added. The experiment was carried out in a white half-area 96 well-plate [Costar, NY, USA], which was incubated for 15 minutes at  $37^\circ\text{C}$  in the thermostat chamber of a luminometer [Labsystems, Helsinki, Finland]. After incubation, 25  $\mu\text{L}$  of serum opsonized zymosan (SOZ) [Fluka, Buchs, Switzerland] and 25  $\mu\text{L}$  of luminol [Research Organics, Cleveland, OH, USA], an intracellular reactive oxygen species detecting probe, were added to each well except blank wells (containing just HBSS++). A luminometer was used to measure the amount of ROS in terms of relative light units (RLU).

### **3.5.7 Cytotoxic studies**

The standard MTT (3-[4, 5-dimethylthiazole-2-yl]-2, 5-diphenyl-tetrazolium bromide) colorimetric assay was used to assess compound cytotoxicity in 96-well flat-bottomed microplates (Mitra *et al.*, 2016). HeLa cells (Cervical Cancer) were cultured in  $75 \text{ cm}^3$  flasks in Minimum Essential Medium Eagle, supplemented with 5% foetal bovine serum (FBS), 100 IU/mL penicillin, and 100 g/mL streptomycin, and kept in a 5%  $\text{CO}_2$  incubator at  $37^\circ\text{C}$ . Cells that were exponentially growing were harvested, counted with a haemocytometer, and diluted with a specific medium. Cell culture was prepared at a concentration of  $6 \times 10^4$  cells/mL and introduced (100  $\mu\text{L}$ /well) into 96-well plates. After overnight incubation, the medium was removed and 200  $\mu\text{L}$  of fresh medium with varying concentrations of compounds (1-30  $\mu\text{M}$ ) was added. After 48 hrs, 200  $\mu\text{L}$  MTT (0.5 mg/mL) was added to each well and incubated further for 4 hrs. Afterwards, 100  $\mu\text{L}$  of DMSO was added to each well. The absorbance at 570 nm of a microplate reader (Spectra Max Plus, Molecular Devices, CA, USA) was used to calculate the extent of MTT reduction to formazan within cells. The cytotoxicity was measured as the concentration that inhibited HeLa cell growth by 50% ( $\text{IC}_{50}$ ). The percent inhibition was calculated by using the following formula:

$\% \text{ Inhibition} = 100 - ((\text{mean of O.D of test compound} - \text{mean of O.D of negative control}) / (\text{mean of O.D of positive control} - \text{mean of O.D of negative control})) * 100$

The results (% inhibition) were processed by using Soft- Max Pro software (Molecular Device, USA)

### **3.5.8 Computational molecular modeling**

This study is carried out for the interactions and behavior of molecules at the atomic and molecular levels. Molecular docking focuses on predicting the preferred orientation of one molecule to a second when bound together, while simulation studies the dynamic simulation of molecular systems over time. Together these methods provide valuable insights into the structure, function, and interactions of these biomolecules. Thus, the isolated flavonoids were further studied for their additional parameters using molecular docking. Further to ensure the safety of a candidate drug its effectiveness and favorable pharmacokinetic profile for therapeutic use analysis of properties such as absorption, distribution, metabolism, excretion, and toxicity (ADMET) were carried out of compounds **1** and **2** for ROS inhibition. Likewise, molecular docking and simulation studies of compound **2** for the insulin target were carried out in the central department of chemistry and physics.

#### **3.5.8.1 Molecular docking and ADMET analysis of (1) and (2)**

#### **3.5.8.2 Preparation of protein and ligands**

The three-dimensional structure of Cyclooxygenase-2 (prostaglandin synthase-2) complexed with a selective inhibitor SC-558 (PDBID: 1CX2) was retrieved from the protein data bank (PDB) (<https://www.rcsb.org/>) in .pdb format. The protein was prepared using chimeraX and autodocktools-1.5.6. All the co-crystallized ligands, non-standard residues, and water molecules were removed from the protein. In addition, the polar hydrogens and Kollman charges were added to it and saved in .pdbqt format for molecular docking. The ligands were prepared using Avogadro and autodocktools-1.5.6. The 3D structures of **1** and **2** and the standard ibuprofen were downloaded from PubChem (<https://pubchem.ncbi.nlm.nih.gov/>) in .sdf format. The downloaded ligands in .sdf format were first converted to .pdb format using Avogadro after optimizing geometry. Then, they were converted into .pdbqt format.

#### **3.5.8.3 Protein active site prediction and molecular docking**

The active binding site of the downloaded protein was predicted using the biovia discovery studio. After determining the perfect binding site of the enzyme, a grid box

was set to  $20 \times 20 \times 20$  with spacing  $0.375 \text{ \AA}$  and the center set to  $x = 25.720$ ,  $y = 28.054$ , and  $z = 7.827$ . All the target proteins, ligands, and grid box center data were saved as a configuration.txt file. Lastly, molecular docking was performed using autodock vina (Trott & Olson, 2010). In the context of bioactive compounds, the conformation of the ligand with the lowest affinity was considered the most stable conformation. Biovia Discovery Studio was used to analyze the result.

#### **3.5.8.4 Validation of molecular docking**

The molecular docking protocol was validated by isolating the SC-558 ligand from the protein (1CX2) and redocking in the same position. The lowest energy pose on redocking was chosen to superimpose the previous bind position of the ligand, and its root mean square deviation (RMSD) was calculated.

#### **3.5.8.5 Drug likeness and ADMET analysis**

The compounds were subjected to the drug-likeness test. Lipinski's rule of 5 (RO5), Ghose, Veber, Egan, and Muegge's rules were applied to test the drug-likeness of the compounds (Egan *et al.*, 2000; Ghose *et al.*, 1999; Lipinski *et al.*, 2012; Muegge *et al.*, 2001; Veber *et al.*, 2002). The drug-likeness was tested using SwissADME, and pkCSM web server (Daina *et al.*, 2017; Pires *et al.*, 2015). Additionally, molinspiration webserver was used to determine the enzyme inhibitor mol inspiration bioactivity score.

#### **3.5.8.6 Molecular docking and simulation of compound 2 for the insulin target**

Molecular docking and molecular dynamics modelling were done with SUR of the pancreatic ATP-sensitive potassium channel to understand the molecular behavior of prandomestin (Hawkins *et. al*, 2010). Using Schrödinger's Maestro's 2D sketcher, the ligand structures were sketched and transformed into a low-energy 3D state (Schrödinger Release, 2023). The ligand structures were prepared using Open Eye Scientific Software, where the Omega module was used to generate possible conformers (Hawkins *et. al*, 2010). The structure of the pancreatic ATP-sensitive potassium channel along with SUR (PDB: 6JB1) was obtained from the RCSB protein data repository and was prepared using Open Eye Scientific's Spruce module (Ding *et al*, 2019). Our goal was to dock ligand on the SUR subunit. Therefore, only the H chain of the SUR of the Katp channel was used for molecular modeling. A receptor was made by integrating the co-crystallized ligand, and it was docked using Fred from Open Eye Scientific Software (Mc Gann, 2011).

To study the molecular dynamics behavior of the protein-ligand complex, a 500 ns molecular dynamics simulation was performed using Academic Desmond 2019

(Bowers *et. al*, 2006). By default, under orthorhombic periodic boundary conditions with a buffer region of 10 Å, the molecular system was solvated using the explicit solvation model (SPC). To neutralize the system, Na<sup>+</sup> and Cl<sup>-</sup> ions were used in the system builder. By doing a short-duration simulation and minimization, the system was made more relaxed. In the NPT ensemble, to maintain the temperature and pressure at 300 K and 1.01325 bar, the Noose-Hoover thermostat method and the Martyna-Tobias-Klien barostat method were employed, respectively. In the dynamics study of bonded, near, and far bonded interactions, a multiple-time step RESPA integrator was used.

### **3.6 Essential oil from the fruit pericarp of *Z. armatum***

#### **3.6.1 Quantity-based extraction of essential oil**

The matured fruits of the plants were collected from the commercial sites of Salyan Surkhet and Myagdi. Fruits weighing 250 g were hydro-distilled for three hours in the Clevenger apparatus.

#### **3.6.2 Gas chromatography-flame ionization detection (GC-FID)**

Thus, obtained essential oils of the fruit pericarp of *Z. armatum* were analyzed through Gas chromatography-flame ionization detection with a previously reported methodology by Lawson *et al.*, 2021 with similar operating conditions for GC-MS using Shimadzu GC 2010 with flame ionization detector, and column ZB-5GC. Raw peak areas were used for the determination of percentage composition without standardization.

#### **3.6.3 Chiral GC-MS**

Determination of chiral GC-MS was followed with a Shimadzu GCMS-QP2010S instrument, and a Restek B-Dex 325 column of length 30 m, diameter of 0.25 mm, and film thickness of 0.25 µm) at the temperature setting of injector and detector at 240 °C. Helium is a carrier gas with a column head pressure of 53.8 kPa and a flow rate of 1.00 mL/min. The oven temperature program for gas chromatography was set as 50 °C initially, with a hold time of 5 min, and the ramp rate increased 1.0 °C/min to 100 °C, then increased 2.0 °C/min to 220 °C. Injection parameters were 0.3 µl, 5% essential oil in dichloromethane (split mode, 24:1). Comparing the retention times with authentic samples from Sigma-Aldrich (Milwaukee, WI, USA) distribution of enantiomers was calculated.

### **3.7 GC-MS of hexane fraction**

Characterization of the n-hexane fraction of *Z. armatum* obtained from hydroethanolic extract was carried out using the triple Quadrupole Acquisition method using Agilent

technologies 7000 GC-MS triple quadrupole system (MS-7000, GC 7890A) and a ZEBRONZB-5HT column of dimension 30m× 320 μm×0.25 μm at 400 °C. In Front SS inlet He was used and vacuum outlet. The oven was equilibrated for 5 minutes, at 60 °C, with a run time of 72 minutes and a temperature program of 8 °C/min increased to 240 °C for 20 minutes and then increased to 300 °C at a rate of 15 °C/minute for 5 minutes. The volume of the injected sample was 1.5 μL.

### **3.8 Pharmacological studies on *Z. armatum* extract**

For pharmacological studies, two different animal species were used. Healthy Long Evans Rats and Swiss Albino mice for toxicity studies. Further, after dose fixation studies comparative dose variant studies were carried out on type II diabetic model rats prepared.

#### **3.8.1. Toxicity studies on *Z. armatum* extract**

##### **3.8.2 Animal model preparation**

This study used adult Long Evans Rats weighing (170-220) g and Swiss Albino Mice 40 g. The animals were bred at the Bangladesh University of Health Science animal house in Dhaka, Bangladesh, where they were kept at a constant room temperature of 22°C, with humidity of 40-70%, and a natural 12-hour day-night cycle. The experiment was carried out following the Bangladesh Association for Laboratory Animal Science's ethical guidelines.

Animals with similar metabolic properties and consecutive effects serve as models in the research of toxicity in drug discovery. Mostly rodents such as mice and rats are involved in such studies since they reflect diverse information with associated complications (Chatzigeorgiou *et al.*, 2009). Both LER and SAM were used as model animals for extract toxicity in this study as they share similar metabolic and signaling pathways with the humans, referring to suitable generalization (Iannaccone & Jacob, 2009). In general, an adult LER ranges its body weight around (191-270) g and SAM around (30-49) g. Housing includes a constant temperature of (22 ± 1 °C) on a 12-hour light/dark cycle with free access to water and nutritionally supplied with typical commercial food pellets in calculated amounts. The investigation was according to the guide for the care and use of laboratory animals (1996) followed by ARRIVE guidelines for reporting animal research during manuscript preparation (Kilkenny *et al.*, 2010). All these experimental parameters were according to the guidelines prescribed.

### 3.8.3 Animal grouping and dose preparation

Acute toxicity studies of the hydroethanolic extract of *Z. armatum* were performed based on ARRIVE guidelines (OECD, 2002) with slight modifications in two different animal species. Thirty healthy Swiss Albino Mice and thirty Long Evans Rats were used for the study **Table 5** below. The single dose of hydroethanolic extract of *Z. armatum* fruit pericarp was fed orally following the dose fixation method in geometric ratio starting from 200 mg/kg bdwt, 400 mg/kg bdwt, 800 mg/kg bdwt, 1600 mg/kg bdwt to 3200 mg/kg bdwt on both animal species SAM and LER. The observations every 10 minutes for the first 3 hours include changes in behavior, signs of toxicity, and immediate mortality. Later on, hourly observations, and during the feeding period until 14 days were carried. Changes in body weight, feeding habits, and vital organs observation by histopathology for any toxic impressions were major experimental parameters. For the species in which mortality was observed half lethal dose (LD<sub>50</sub>) was calculated using Lorke's method. Grouping of SAM and LER five in each group was done. The grouping of SAM and LER with their calculated dose for feeding is presented in **Table 5** below.

**Table 5:** Experimental groups for extract toxicity

Groups	Swiss Albino Mice	Long Evans Rats
(I)Water control	n=5 (M)	n=5 (M)
(II)200 mg	n=5 (M)	n=5 (M)
(III)400 mg	n=5 (M)	n=5 (M)
(IV)800 mg	n=5 (F)	n=5 (F)
(V)1600 mg	n=5 (F)	n=5 (F)
(VI)3200 mg	n=5 (F)	n=5 (F)

### 3.8.4 Acute oral toxicity study

Models utilized for administering test substances, whether chemically induced, drug-induced, metal-induced, radiation-induced, or genetic, constitute the fundamental aspects of hepatotoxicity (Bhakuni *et al.*, 2016). The present study adhered to the ARRIVE guidelines with slight modifications and involved both male and female rats and mice. A total of 15 female and 15 male rats and mice were included in the study. Before grouping, an initial body weight was recorded for each animal, with five animals assigned to each of the six groups (I to VI). A week was dedicated to acclimating the animals to the environmental conditions. Grouping was based on the same sex to avoid complications related to pregnancy. The animals were provided with the calculated

amounts of normal food and water supply. The feeding dose of the ethanoic extract was prepared by dissolving the predetermined amount of extract per kg in 10 mL of water, administered after an overnight fast.

Observations were conducted individually during the initial four hours of feeding to identify critical symptoms of toxicity and mortality. Subsequent observations were made twice daily in the morning and evening during the days of food and water supply. Physical observations included monitoring behavioural changes, clinical signs of toxicity, delayed mortality, and specific parameters such as fur condition, mucus production, vomiting, respiratory depression, piloerection, sedentary and lethargic behaviour, food and water consumption habits, socializing behaviour, coma, and seizures.

On the 13<sup>th</sup> day of the experiment, both rats and mice were fasted overnight and then euthanized using halothane. Blood samples were collected through heart puncture. Organ-to-body weight changes were considered important indicators in toxicity studies (Michael *et al.*, 2007). Vital organs such as the heart, lungs, kidneys, pancreas, and spleen were dissected, defatted, observed macroscopically for visible abnormalities and lesions, weighed to obtain absolute organ weight, and finally preserved in a 10% formalin solution for histopathological observations. Changes observed during the experiment were calculated for those recorded, as organ weight serves as a reliable parameter in toxicity studies (Michael *et al.*, 2007).

The relative organ weight of all vital organs was calculated using the equation below: Weight on the 13<sup>th</sup> day final weight (Fw) and initial weight (Iw).

$$\text{Body weight (\%)} = (Fw - Iw / Iw) \times 100$$

$$\text{Relative organ weight (\%)} = (\text{Organ weight} / Fw \text{ rat/mice on sacrifice day}) \times 100$$

$$\text{Food consumed (gm)} = (\text{Calculated food supplied} - \text{leftovers after 24hours}) \text{ gm}$$

$$\text{Water consumed (mL)} = (\text{Calculated water supplied} - \text{remaining after 24 hours})$$

$$\text{Consumption pattern} = (\text{Food consumed by particular group} - \text{food consumed by control})$$

$$\text{Water consumption pattern} = (\text{Water consumed by particular group} - \text{water consumed by control})$$

### **3.8.5 Parameters of observations**

For the evaluation of the toxic effects of crude hydroethanolic extract *Z. armatum* following parameters of normal Swiss Albino Mice and Long Evans Rats were observed:

- Change in body weight
- Food intake and water intake
- Relative Organ Weight
- Histopathological observation of vital organ

### **3.8.6 Determination of lethal dose of hydro-ethanoic extract of *Z. armatum***

After monitoring both animal models for two weeks, the toxicity of the extract as observed in the lethality of the species was assessed for the calculation of the Lethal Dose (LD<sub>50</sub>) based on the formula suggested by Lorke (Lorke, 1983) as outlined below:

$$LD_{50} = \sqrt{D_0 \times D_{100}}$$

D<sub>0</sub> = Highest dose that gave no mortality

D<sub>100</sub> = Lowest dose that produces mortality within 24 hours of drug administration

### **3.9 *In vivo* antidiabetic properties of *Z. armatum***

#### **3.9.1 Animal models**

Adult long Evans rats of type II diabetic model (T2DM) were used for the antidiabetic study of plant extract. On average, all the diabetic rats weighing 170-220 g were used in this study.

#### **3.9.2 Preparation of type II diabetic model rats**

A single intraperitoneal injection of streptozotocin (STZ) in citrate buffer (pH 4.5) at a dose of 90 mg/kg body weight into rat pups (48 hrs old, average weight 7 gm) simulated for preparing type II diabetic model rats. After three months of STZ injection, rats' blood glucose levels were measured using an oral glucose tolerance test (OGTT). At fasting, rats with blood glucose levels of 7.00 mmol/L and higher were chosen for the study of the effect of hydroethanolic extract of *Z. armatum*. The rats were fed a standard laboratory pellet diet and given free access to water. Wheat (40%), wheat bran (20%), rice polishings (5%), fish meal (10%), oil cake (10%), gram (3.9%), pulses (3.9%), milk (3.8%), soyabean oil (1.5%), molasses (0.95%) and salt (0.95%) were all included in the standard rat pallet.

#### **3.9.3 Formulation of gliclazide and *Z. armatum* doses**

The standard drug gliclazide was used as a positive control in this study. Gliclazide was prepared and administered orally at a dose of 20 mg per 5 mL of solvent (Water + a few drops of 1N Sodium Hydroxide)/kg body weight of T2DM rat models. To assess the antidiabetic activity, the hydroethanolic extract of *Z. armatum* was administered orally to rats for 4 weeks at a dose of 1.25 g/kg body weight. However, as all the rats fed with

the extract died within the first week the experiment design Ist was changed to determine the toxicity of the extract and to progress the research with a different dose.

### 3.9.4 Route of administration

Standard drug gliclazide was administered orally to Type 2 diabetic model rats at a dose of 20 mg/5 mL/kg body weight for the pharmacological studies and extract of 1.25 g/kg body weight as per the protocol determined in the first chronic experiment. The second set of the protocol used the extract with 25 mg/kg (ZaE1) bodyweight and 50 mg/kg (ZaE2) bodyweight, distilled water was fed to the control groups.

### 3.9.5 Experimental Design I

A total of 24 (Normal and type 2 diabetic model) rats were used in this 28-day chronic experimental period with each group containing six rats. **Table 6** below illustrates the grouping and feeding doses in each classified group.

**Table 6:** Experimental groups design Ist for antidiabetic studies

Categories	Feeding
Group I	Normal water control [10mL/kg]
Group II	Type II water control [10mL/kg]
Group III	Type II glicazide control [20mg/5mL] water+fewdrops of 1N NaOH/kg bdwt
Group IV	<i>Z. armatum</i> 1.25g/kg bdwt.

The experimental design I couldn't be completed as designed. The lethality was observed in the type II model rats during the initial week of the feed dose. Different symptoms such as altered locomotor activity due to difficulty in coordinating movements, and neurological symptoms such as tremors, seizures, ataxia, wheezing, and labored breathing with decreased consumption of food and water were observed after the feeding of extract of calculated doses on the type II model rats.

### 3.9.6 Experimental Design II

To elucidate the hypoglycemic effect after toxicity studies of the chronic experiment in diabetic model rats on the final doses 25 mg/kg body weight (ZaE1) and 50 mg/kg body weight (ZaE2) on STZ-induced type 2 diabetic model rats, an investigation was carried out on groups of thirty Long Evans Rats for 28 days period. Sulfonylureas drug gliclazide was used as standard.

The experimental groups consist of five categories with six rats in each group. Group first of non-diabetic water control and other all groups were diabetic models selected randomly for four different groups. Group I non-diabetic water control (NWC), group II diabetic water control (DWC), group III gliclazide treated (GT), group IV extract dose of ZaE1, and group V extract dose of ZaE2 are depicted in **Table 7** below.

**Table 7:** Grouping and feeding doses per group in experimental design II

Grouping	Feeding doses
NWC (n=6)	Normal water control group, water administered [10 mL/kg]
DWC (n=6)	Type II diabetic model rats water control group, water administered [10 mL/kg]
GT (n=6)	Type II diabetic model rats positive control gliclazide treated group administered [20 mg per 5 mL of solvent (Water +few drops of 1N Sodium Hydroxide )/kg body weight]
ZaE1 (n=6)	<i>Z. armatum</i> treated group (25 mg/kg body weight)
ZaE2 (n=6)	<i>Z. armatum</i> treated group (50 mg/kg body weight)

### 3.9.7 Collection of blood samples for biochemical analysis

Blood samples were obtained from rats that had undergone a 12-hour fast a day before the start of the experiment, utilizing tail-tip amputation under diethyl ether anesthesia. Blood collection occurred four times at 30-minute intervals. To facilitate vasodilation, the tail was briefly immersed in warm water (approximately 40 °C) for 30-40 seconds before amputation. Careful extraction of 0.2 mL of blood from the tail tip was performed and deposited into a microcentrifuge tube to prevent hemolysis.

On the 28th day, following the decapitation of the animals, blood was collected from their hearts through cardiac puncture. The collected blood samples underwent centrifugation at 2500 rpm for 15 minutes, and the resulting serum was carefully separated into additional microcentrifuge tubes for subsequent biochemical analysis. A volume of 100 µl of serum was then frozen at -20 °C until the time of analysis.

### 3.9.8 Recording of body weight

All the rats were maintained under identical environmental conditions with access to sufficient food and water *ad libitum* throughout the experimental period. Different groups of rats were fed with their respective treatment and the body weights of each rat were measured weekly.

### 3.9.9 Biochemical analysis

For the evaluation of anti- diabetic effects of *Z. armatum* the following parameters of type 2 diabetic model rats were measured:

- Serum glucose was measured by glucose oxidase (GOD-PAP) method using a micro-plate reader (Bio-Tec, ELISA).
- Serum total cholesterol by enzymatic colorimetric (Cholesterol Oxidase/Peroxidase. CHOD-PAP) method (Randox Laboratories Ltd., UK), using autoanalyzer, AutoLab.
- Serum triglyceride (TG) by enzymatic colorimetric (GPO-PAP) method (Randox Laboratories Ltd., UK) using autoanalyzer, AutoLab.
- Measurement of glycogen from rat liver by (standard Method) Anthrone-sulphuric acid method.
- Serum insulin by Rat Insulin enzyme-linked immunosorbent assay (ELISA) method. (Crystal Chem Inc., USA).

### **3.10 Extraction of *S. wallichii* and *S. coriacea***

Aerial part of *S. wallichii* Staph. Were collected from Dhampus (Kaski, Nepal) and identified at the Central Department of Botany, Tribhuvan University, Kirtipur, Kathmandu, Nepal. A voucher specimen (No: SW-06) was deposited in the same department. The methodological framework for the extraction of *S. wallichii* is presented below in **Figure 16**. A similar scheme of extraction and fractionation was carried out for the *S. coriacea* roots, the basic and the neutral fractions **Sc-B** and **Sc-N** of this fractionation part were accessed for various bioactivities as the continuation of the previous research activity of the team.

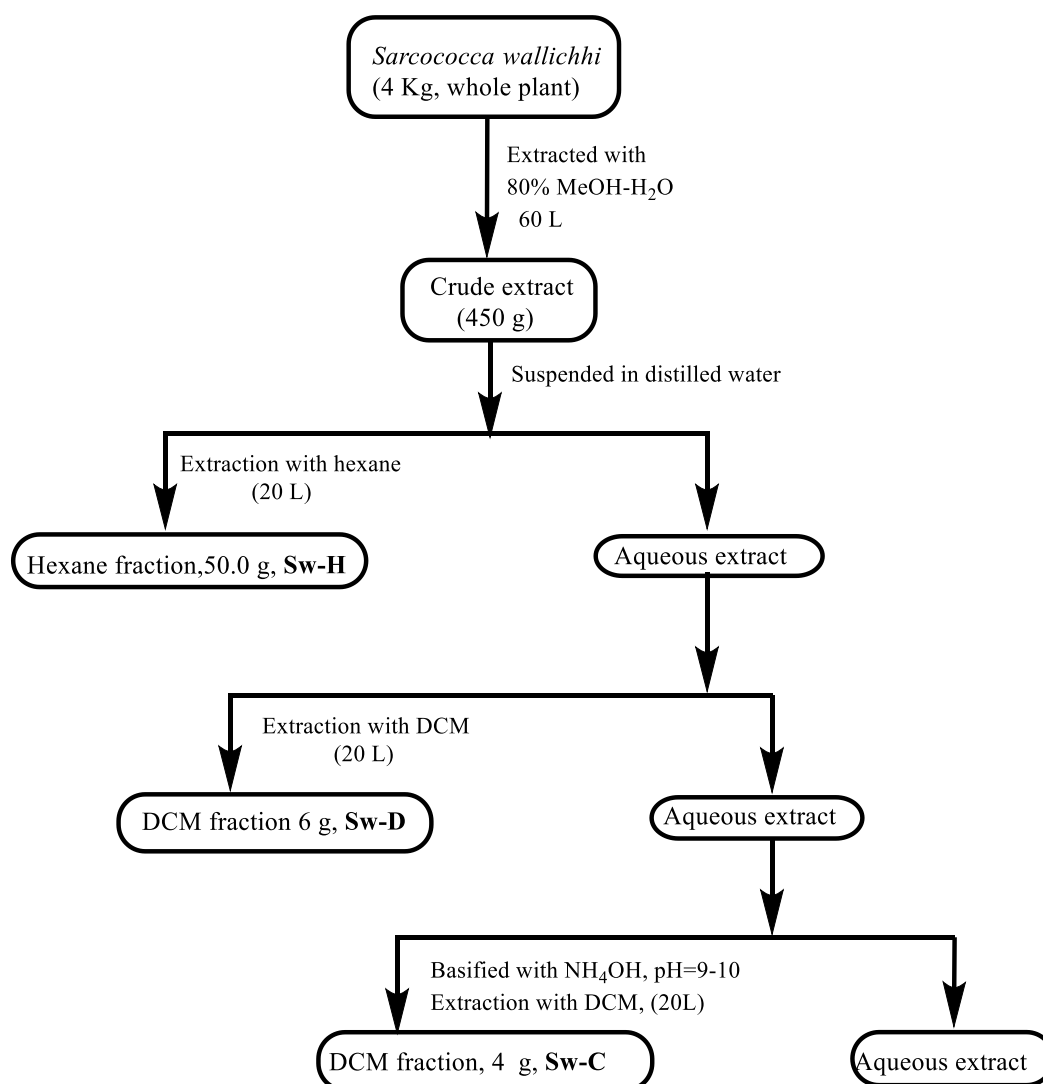


**Figure 16:** Methodological framework of extraction and fractionation of *S. wallichii*

### 3.11 Extraction of *S. coriacea* leaf and stem

*S. coriacea* aerial part was collected from Kathmandu district, Kritipur Municipality, Champadevi-4, and verified as *S. coriacea* (Hook F.) at National Herbarium & Plant Laboratories (KATH) voucher no: JB (100). Air-dried, whole plants (3 kg) of *S. coriacea* were separated into leaves and stems manually. The aerial part of the stem and leaves of 3 kg was separated into 2 kg of leaf and 1kg of the stem which was extracted with 80% methanol/water (8 L) to obtain 156 g of leaf extract and 59 g of stem extract. The concentrated extract is preserved under 4°C for biological activities. The methodological procedure for the extraction scheme is presented below in **Figure 17**.

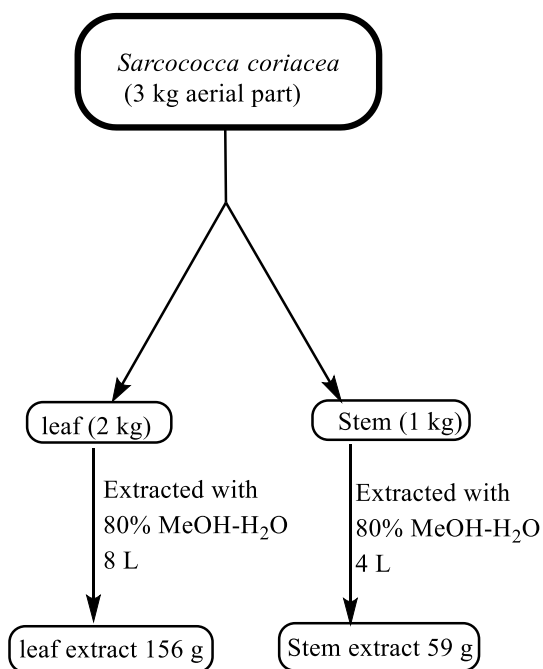


**Figure 17:** Extraction scheme of *S. coriacea*

### 3.12 Column chromatography and compound isolation from *S. wallichii* staph.

Hydromethanolic extract 80% of 450 g was defatted using hexane that yielded 50.0 g coded as Sw-H. To obtain the neutral fraction aqueous layer was then re-extracted with dichloromethane that yielded 6 g coded as Sw-D. Some portion of this neutral fraction (Sw-D) of *S. wallichii* 4 g were column chromatographed using silica gel, as eluent hexane and acetone with a drop of diethyl amine. Various sub-fractions were recovered at the first column using up to 10 % acetone: hexane with few drops of diethylamine. The probable sub-fractions were again column chromatographed which yielded compounds **(8)**, **(9)** and **(10)** in measurable quantities. Likewise, fraction 57-66 (350 mg) yielded 3 sub-fractions A1, A2, and A3. The sub-fraction A2 was chromatographed using neutral alumina which yielded a compound **11** (15 mg). The staining reagents used for developed plates of TLC were dragendroff, sulphuric acid and anisaldehyde.

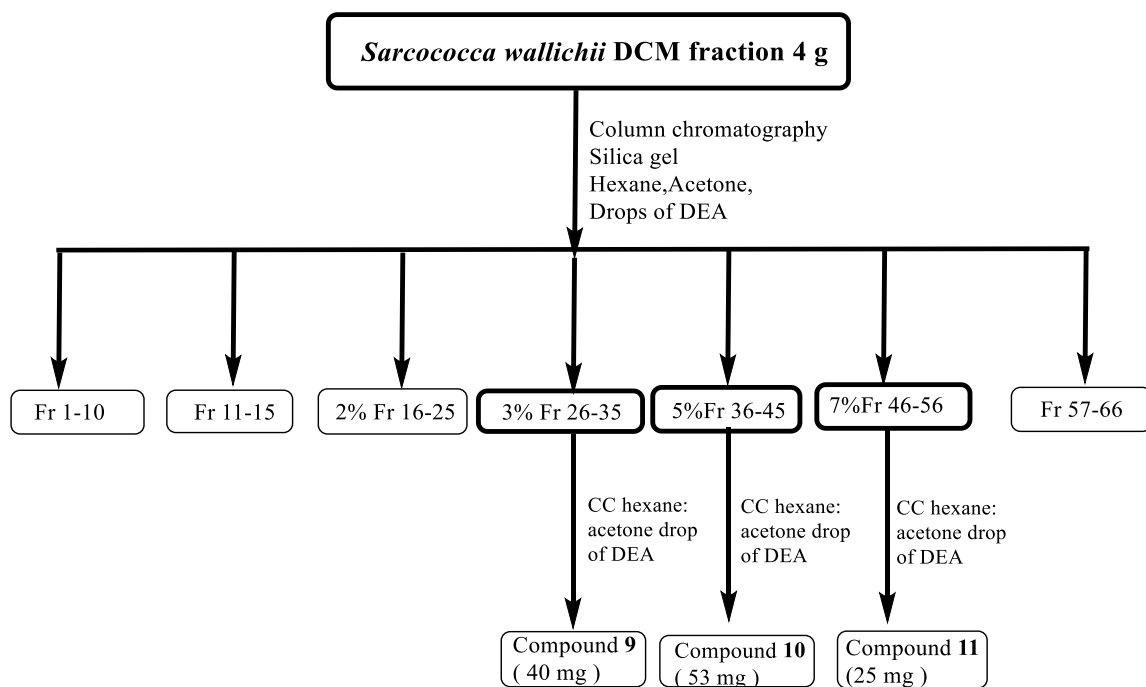


**Figure 18:** Scheme of isolation of compounds **9**, **10**, and **11** from *S. wallichii*

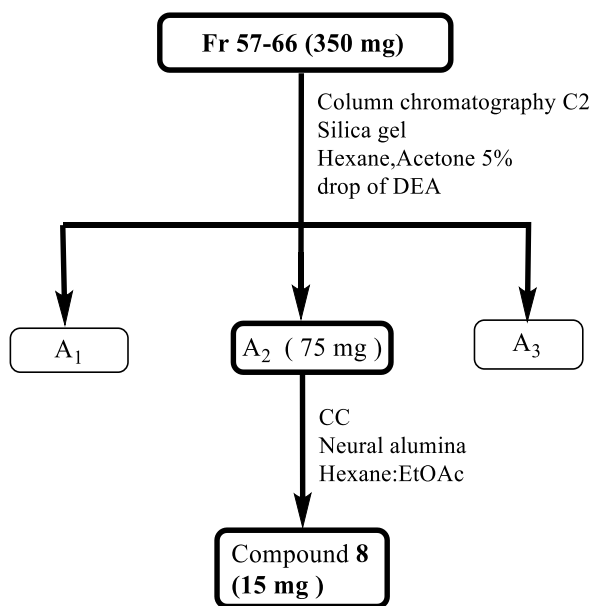


**Figure 19:** Scheme of isolation of compound **8** from *S. wallichii*

### 3.13 Compounds isolated from *S. wallichii*

#### 3.13.1 N<sub>a</sub>-methylepipachysamine D (8)

The sub-fraction (Fr-57-66) 1.5 g eluted at 5% hexane: acetone (**Figure 19**) was further subjected to column chromatography hence was loaded into (60×3.5 cm) column and eluted with gradient mobile phase of hexane: acetone with few drops of diethylamine (2, 4, 10 %) to obtain three sub-fractions A<sub>1</sub>, A<sub>2</sub>, and A<sub>3</sub> based on TLC observation. Subfraction A<sub>2</sub> was column chromatographed using neutral alumina as adsorbent with solvent system hexane: ethylacetate. Compound 8 was yielded which was visible at UV at R<sub>f</sub> 0.53, eluent on TLC (4 mL MeOH 0.5 mL acetic acid: drop of water). It was stained by Dragendroff reagent. The quantitative yield for the compound was 15 mg. The EI MS showed the M<sup>+</sup> at *m/z* 464, base peak at *m/z* 72, and other fragment peaks at *m/z* 105, and 136. The <sup>1</sup>H-NMR spectrum exhibited the occurrence of two up-field singlets at δ 0.67 and 0.78 assigned for C-18 and C-19 angular methyl's, separately. A doublet at δ 1.18 (*J*<sub>21, 20</sub> = 6.5 Hz) was due to C-21 methyl protons. The NMe<sub>2</sub> protons have appeared at δ 2.26. Two broad multiplets at δ 3.43 and 4.43 were attributed to H-20 and H-3 protons, respectively. The N-Me protons also appeared as a singlet at δ 2.58. The downfield signals between δ 7.24 -7.36 were allocated to the aromatic protons. The broad-band decoupled (BB) <sup>13</sup>C-NMR spectra of the compound presented resonances for 31 carbons. The structure of the compound was further established by using 2D-NMR (HMQC, COSY, HMBC). The crystal of the compound was studied using the X-ray diffractometer, the Bruker D8 Venture, with a Photon 100 detector using Cu K $\alpha$  radiation. SAINT program was used for data collection and reduction and 3D molecular structure representation was generated using ORTEP-3 (Malik *et al.*, 2021). Characterization of the isolated compound was carried out at H.E.J. research institute of Chemistry, ICCBS, University of Karachi, Pakistan.

#### 3.13.2 Taraxerol (9)

Compound **9** was obtained as a white amorphous from the 3% Fr(26- 35) acetone /hexane (**Figure 18**) under silica gel as adsorbent under column chromatography which was again column chromatographed to obtain 40 mg. The compound was UV inactive but appeared as a single black spot at R<sub>f</sub>: 0.70 after spraying with ceric sulphate. The solvent system used for TLC was 0.7 mL acetone: 4 mL hexane and 2 mL ethylacetate: 4 mL hexane. The melting point was observed at 285 °C. EIMS spectrum showed M<sup>+</sup> at *m/z* 426, and other fragment peaks at *m/z* 411, 302, 287, 204, and 135. The details of NMR is presented on **Table 33**.

### 3.13.3 $\beta$ -sitosterol (10)

This compound 10 was obtained as a white crystalline compound after purification. Obtained from the 5% Fr (36- 45) (**Figure 18**) acetone/hexane under silica gel column chromatography. The sub-fraction was again column chromatographed to obtain 53 mg. This compound was UV inactive but appears as a single black spot at  $R_f$ : 0.50 after spraying with ceric sulphate. The solvent system used for TLC was 0.5 mL acetone: 3 mL hexane. The melting point was observed at 135 °C. EIMS spectrum showed  $M^+$  at  $m/z$  414, and other fragment peaks at  $m/z$  414, 396, 381, 329, 303, 289, 273, 255, and 231. The compound gave a positive test for steroids (both positive tests for Salkowskis and Liberman- Buchard). The chemical shift values of NMR match with previously reported compounds in literature (Patra *et al.*, 2010).

### 3.13.4 Oleanolic acid (11)

This compound 11 was isolated as a white amorphous form from 7% (Fr-46-56), (**Figure 18**) of *S. wallichii*. On repeated column chromatography UV invisible 25 mg of the compound was obtained. The compound was spotted as a single spot at  $R_f$ : 0.52 on staining with sulfuric acid on the solvent system: 2 mL ethyl acetate: 4 mL hexane and soluble in chloroform. Its melting point was observed at 309 °C. The EIMS of this compound displayed an  $M^+$  peak at  $m/z$  456 and major fragments peak at  $m/z$  248 (96%) and 203 (100%), indicating the oleanolic acid-type skeleton.

## 3.14 Spectroscopic tools and characterization

The isolated compounds were characterized by using spectroscopic tools like mass, NMR, HRMS, and UV-Vis.

### 3.14.1 UV-visible spectrophotometer

Using a UV-Vis spectrophotometer (UV-2450 Shimadzu, Japan) at a suitable range of 190-400 nm and 400-800 nm the chromophoric absorption in molecules was determined.

### 3.14.2 Mass spectrometry

For mass spectrometry, EI-MS spectra were obtained on EI (LR) JEOL MS ROUTE 600H-1, (JEOL, Ltd, Tokyo, Japan). The EI-MS spectrum displays molecular ion peak which gives general information about the molecular formula of the compound. The presence of molecular ion peak with key mass fragmentation suggests probable structure. Mass spectra were collected in the preferred solvent of choice depending on the solubility  $CDCl_3$ , MeOD, and DMSO at room temperature at the University of Karachi, Pakistan.

### **3.14.3 Base peak**

In the mass spectrum, the most intense peak is referred to as a base peak and is used as the standard to measure the intensities of other ion peaks.

### **3.14.4 Electron impact mass spectrum**

The method of electron impact mass spectrometry entails subjecting molecules to an electron beam (typically 70 eV) to generate ions.

### **3.14.5 High-resolution electron impact mass spectrum**

High-resolution electron impact mass spectrum furnishes precise elemental composition details via exact mass measurements. Typically, a double-focusing mass spectrometer is employed for this purpose.

### **3.14.6 Fast atom bombardment mass spectrum**

Fast atom bombardment mass spectrometry, a gentle ionization technique in mass spectrometry, serves to confirm the molecular ion of a compound as either a positive or negative ion.

## **3.15 Nuclear magnetic spectroscopy**

### **3.15.1 1D-NMR spectroscopy**

<sup>1</sup>H-NMR spectra were acquired on AV-400 instruments (Bruker, Switzerland). Proton-NMR (<sup>1</sup>H-NMR) spectroscopy presents a one-dimensional spectrum, offering insights into the electronic surroundings of the protons (<sup>1</sup>H) within the molecule. The <sup>1</sup>D-NMR was done in the preferred solvent of choice depending on the solubility CDCl<sub>3</sub>, MeOD, and DMSO at room temperature on 400 & 500 MHz at the University of Karachi, Pakistan.

### **3.15.2 2D-NMR spectroscopy**

2D-NMR Spectra HMBC, HSQC, COSY, NOESY, ROESY, and TOCSY are used in confirming the final structure of the compound.

### **3.15.3 Heteronuclear multiple bond connectivity**

In this HMBC experiment, a two-dimensional technique operates inversely to identify distant, heteronuclear interactions between carbons and protons (typically <sup>1</sup>J<sub>C-H</sub>, <sup>2</sup>J<sub>C-H</sub>, <sup>3</sup>J<sub>C-H</sub>).

#### **3.15.4 Rotating overhauser enhancement spectroscopy**

It determines molecular confirmation and stereochemistry by analyzing the spatial proximity of protons, facilitating an exchange of transverse magnetization between the interacting nuclei.

#### **3.15.5 Total correlation spectroscopy**

TOCSY is used to identify long-range  $^1\text{H}/^1\text{H}$  correlations within a spin system.

#### **3.15.6 Heteronuclear multiple quantum coherence**

Heteronuclear multiple quantum coherence known as HMQC spectroscopy reveals single bond  $^1\text{H}/^{13}\text{C}$  shift correlations.

#### **3.15.7 Distortionless enhancement by polarization transfer**

DEPT, a  $^{13}\text{C}$ -NMR experiment, enhances carbon signal intensities and distinguishes the multiplicities of carbon atoms, distinguishing between  $\text{CH}_3$ ,  $\text{CH}_2$ , and  $\text{CH}$  signals.

#### **3.15.8 Broad-band $^{13}\text{C}$ -NMR spectrum**

This fully decoupled broad band  $^{13}\text{C}$ -NMR spectrum (BB) exhibits each magnetically distinct carbon as a singlet.

#### **3.15.9 Chemical shift**

Chemical shift, expressed symbolically by  $\delta$  in values of ppm denotes the variance between the nucleus's precise frequency and the carrier frequency, characterizing different molecular environments. Chemical shift thus corresponds to the difference between the precision frequency of the nucleus and the carrier frequency.

#### **3.15.10 Coupling constant**

In  $^1\text{H}$ -NMR spectra, proton's signals are split into multiplets, doublets, triplets and etc due to chemically nonequivalent protons on the same or adjacent carbon atoms. The coupling constant " $J$ " independent of the magnetic field strength, expressed as cycles/second or Hz reflects molecular stereochemistry and decreases with factors such as increased bond distance between coupled protons.  $J$  can be positive or negative.

### **3.16 Infrared spectroscopy**

Infrared radiation alters molecules' vibrational and rotational motions, facilitating the detection of functional groups within the  $400\text{-}4000\text{ cm}^{-1}$  range.

### **3.17 Instruments**

- GC-MS: Shimadzu GC 2010, column ZB-5GC
- Chiral GC-MS: Shimadzu GCMS-QP2010S instrument, Restek B-Dex 325 column (length 30 m, diameter 0.25 mm, thickness 0.25  $\mu\text{m}$ )

- Thermostat chamber luminometer: Labsystems, Helsinki, Finland
- Microplate reader (Epoch2, BiotTek, Instruments, Inc, USA)
- Element detection: EDX-8000, Shimadzu
- Rotatory Evaporator IKA(Werke GmbH & Co. KG, Germany)
- Freeze drier (HETOSICC, Heto Lab Equipment, Denmark)

### 3.18 Chemical reagents

- Laboratory-grade organic solvents were used and purchased from E. Merck, Glaxo, Qualigens
- 2,2 Diphenyl 1 picrylhydrazyl (DPPH),  $\alpha$ -glucosidase from *Saccharomyces cerevisiae*
- $\alpha$ -amylase from porcine pancreases, 2-Chloro-4-nitrophenyl- $\alpha$ -D- Maltotrioside (CNPG3) and *p*-Nitrophenyl- $\alpha$ -D- glucopyranoside (PNPG) were purchased from Sigma-Aldrich
- Serum glucose was measured by glucose oxidase (GOD-PAP), cholesterol oxidase/peroxidase (CHOD-PAP), Randox laboratories ltd, UK
- Serum total cholesterol by enzymatic colourimetric (cholesterol oxidase/ peroxidase, CHOD-PAP) method (Randox laboratories ltd., UK), using autoanalyzer, autolab.
- Serum triglyceride (TG) by enzymatic colourimetric (GPO-PAP) method (Randox laboratories ltd., UK) using autoanalyzer, autolab.
- Measurement of glycogen from rat liver by (standard Method) Anthrone-sulphuric acid method.
- Serum insulin by Rat Insulin enzyme-linked immunosorbent assay (ELISA) method. (Crystal Chem Inc., USA).
- Thin Layer Chromatography (TLC) plate Kieselgel (60 F<sub>254</sub>.E. Merck)
- Silica gel (230-400 mesh size, Merck, Dramstat, Germany.
- Buffer tablets of pH 4, 7 and 9.2, (AR grade, Qualigens Fine Chemicals, India)
- Solvents: hexane, dichloromethane, ethylacetate, butanol, acetone, methanol, ethanol, diethylamine (AR grade, Qualigens fine chemicals, India)
- Potassium dihydrogen phosphate, KH<sub>2</sub>PO<sub>4</sub> (AR grade, Sigma aldrich, India)
- Sodium hydroxide (NaOH) (AR grade, Qualigens fine chemicals, India)
- Sodium nitrate (NaNO<sub>3</sub>) (AR grade, Qualigens fine chemicals, India)

### 3.19 Preparation of reagents and stock solutions

Most of the chemicals were of the analytical reagent (AR) grade and were utilized without further purification. All aqueous solutions were made with deionized (DI)

water. Followings chemical reagents were used in the experiments for the preparation of stock solution:

- **pH adjustment solution:** 0.1 N HCl and NaOH solutions were used to adjust the pH. portable pH meter (Thermo scientific orion star A221, India) was used to measure pH.
- **Buffer solutions:** By dissolving the appropriate buffer tablets in 100 mL of DI water, buffer solutions of pH 4, 7, and 6.8 were prepared.
- A stock solution of 30% DMSO was made by dissolving 30 mL DMSO in 70 mL DI water.
- A stock solution of 50% DMSO was prepared by dissolving 1:1 DMSO in DI water.
- A stock solution of various gradient solvent systems was prepared depending on the isolation procedure.

### **3.20 Preparing staining reagents for the developed TLC Plate**

- **Visible or UV light**

In some cases, spot is visible when it absorbs visible light very strongly and in many cases, TLC UV lamps generally help in spotting some compounds. However many compounds can be visible in staining agents as follows.

- **Iodine vapor chamber**

In a jar with lit nearly half a spoon of iodine crystals are added and covered with silica gel. The iodine vapour on the jar acts as a staining reagent on the developed plates.

- **Acidic vanillin**

To 10 g of vanillin, 250 mL of acidic ethanol prepared by adding 2.5 mL conc sulfuric acid is poured and stirred.

- **Basic KMnO<sub>4</sub>**

1% aqueous NaOH is mixed into a solution prepared from 1.5 g of KMNO<sub>4</sub> and 10 g of potassium carbonate in 200 mL water and stirred. The compound present in TLC shows up as a yellow spot remaining portion purple.

- **Cerium ammonium sulphate**

In 100 mL water, 5 g of ammonium molybdate and 1g of cerium sulfate was dissolved. Finally 10mL of conc. H<sub>2</sub>SO<sub>4</sub> was added and stirred.

- **Preparation of aluminium chloride as staining reagent**

A 1% ethanolic solution of aluminium chloride was prepared for the flavonoids. After staining and drying of the TLC plates flavonoids were detected as yellow fluorescence in long wavelength UV light (360 nm).

- **Preparation of anisaldehyde for tlc staining**

Solutions freshly prepared 0.5 mL of p-anisaldehyde in 50 mL glacial acetic acid and 1 mL 97 % sulfuric acid. The TLC plates were heated to 105 °C until maximum visualization of spot brightened due to water vapour. Alternatively, 200 mL of ethanol in 4 mL of anisaldehyde is dissolved into the solution of 3 mL of glacial acetic acid. To this solution, 10 mL of concentrated sulfuric acid is added.

- **Dragendroff's reagent:**

The spray reagent was prepared by the following methods: solution A was prepared by dissolving 0.85 g bismuth nitrate [ $\text{Bi}(\text{NO}_3)_2 \cdot 5\text{H}_2\text{O}$ ] in acetic acid and water (10 mL + 40 mL). Solution B was prepared by dissolving 8 g potassium iodide in 20 mL water. Solutions A and B were mixed in equal volumes and stored in the dark as a stock solution. The final spray reagent was prepared by mixing 1 mL stock solution with 2 mL acetic acid and 10 mL water.

### **3.21 Statistical analysis**

Statistical package for social sciences (SPSS, version 16, Chicago, IL, USA) was used to perform statistical analysis (IBMnc, 2007). Results were expressed as mean  $\pm$  SD. Statistical evaluation of data was performed using a one-way analysis of variance (ANOVA) and paired t-test. The level of significance was considered at  $p < 0.05$  in animal model studies. All investigations were accomplished in triplicate and the findings were represented as the mean  $\pm$  standard deviation. Data were analyzed using excel at first and graph pad prism version 8.4.3 for  $\text{IC}_{50}$  calculation.

## **CHAPTER 4**

### **4. RESULTS AND DISCUSSION**

#### **PART ONE**

*Zanthoxylum armatum* DC

#### 4.1 Quantitative yield of extract and fractions of *Zanthoxylum armatum*

Air-dried 5 kg of matured fruits of *Z. armatum* were ground to powder and macerated with 9 litres of 80% EtOH: H<sub>2</sub>O at room temperature for 7 days with occasional shaking and the procedure was repeated thrice. The same step was repeated for 80% MeOH: H<sub>2</sub>O to prepare methanoic extract. The supernatant filtrate was concentrated in a rotary evaporator to obtain a dark viscous semisolid crude extract of 561.04 g. The average yield was 98.04 g/Kg of methanoic extract and 112.07 g/Kg of ethanolic extract. The crude ethanolic extract was dissolved in distilled water and then partitioned with solvents of increasing polarity. n-hexane used for partition yielded 134.22 g, 143.52 g of ethyl acetate, 84.45 g of n-BuOH and 176.5 g of water-insoluble fraction g of residue was obtained as depicted in **Table 8**.

**Table 8:** Quantitative yield of extracts and fractions of *Z. armatum* ethanolic extract

Extracts/fractions	Quantity
Crude Ethanol	561.04 g /5kg
n-Hexane fraction	134.22 g
Ethylacetate fraction	143.52 g
Butanol Fraction	84.54 g
Aqueous fraction	176.05 g

#### 4.2 Structure elucidation of isolated compounds from *Z. armatum* EAF

##### 4.2.1 Structure elucidation of tambulin (1)

Compound **1** was obtained as a yellow powder. The EI-MS spectrum of compound **1** showed molecular ion [M<sup>+</sup>] at  $m/z$  344, and base peak at  $m/z$  329. The molecular formula C<sub>18</sub>H<sub>16</sub>O<sub>7</sub> was determined from the HREI-MS spectrum which showed [M<sup>+</sup>] at  $m/z$  344.0906 (Calcd for C<sub>18</sub>H<sub>16</sub>O<sub>7</sub> = 344.0896), and <sup>13</sup>C-NMR (BB and DEPT) spectra. The IR spectrum displayed absorptions at 3327 (OH), 1651 (aromatic), and 1556 (olefinic) cm<sup>-1</sup>. The UV spectrum showed absorptions at 367, 325, and 273 nm. The <sup>1</sup>H-NMR spectrum exhibited resonances for three singlets at  $\delta$  3.98, 3.89, and 3.90 were attributed to protons of methoxy groups attached to C-4', C-7 and C-8, respectively. A downfield singlet resonated at  $\delta$  6.51 was ascribed to H-6. Similarly, two downfield ortho coupled doublets at  $\delta$  7.14 d ( $J_{3',2'/5'}$ ,  $\delta$  = 9.0 Hz) and 8.28 d ( $J_{2',3'/6'}$ ,  $\delta$  = 9.0 Hz), were assigned to H-3'/H-5' and H-2'/H-6' respectively. Two exchangeable protons appeared at  $\delta$  11.58 and 6.55 due to hydroxyl protons attached to C-5 and C-3,

respectively. The  $^{13}\text{C}$ -NMR spectra (Broad-band decoupled and DEPT) displayed the resonances for all eighteen carbons including three methyls, five methine and ten quaternary carbons. The structure of the compound was further confirmed from 2D-NMR spectra (COSY, HSQC, HMBC and NOESY). The position of hydroxyl and methoxy groups was assigned with the help of the HMBC correlations. The HMBC between protons and carbons resonated at  $\delta$  3.98 and  $\delta$  162.2 (C-4'), 3.90 and  $\delta$  130.3 (C-8), and 3.89 and 160.0 (C-7) indicated the position of methoxy groups in the compound. Structure elucidation of tambulin (**1**) is represented with their corresponding  $^1\text{H}$ -NMR and  $^{13}\text{C}$ - chemical shift values in **Figure 20**. The key HMBC and COSY correlations in compound **1** are shown in **Figure 21**. Details of  $^{13}\text{C}$ - and  $^1\text{H}$ -NMR Chemical shift values of tambulin (**1**) (acetone- $d_6$ , 125 and 500 MHz are presented in **Table 9** below. All the spectra of the compounds were closely similar to previously reported compound (Horie *et. al*, 1998).

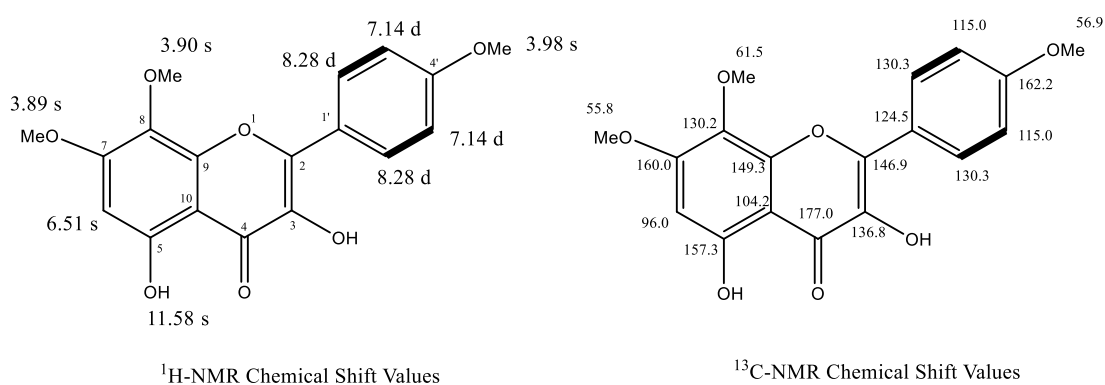


**Figure 20:**  $^1\text{H}$ - and  $^{13}\text{C}$ -NMR chemical shift values of tambulin (**1**)

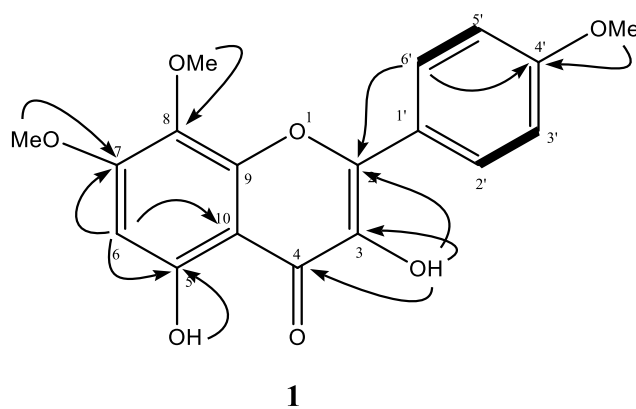


**Figure 21:** Key HMBC (→) and COSY (▬) correlations of **1**

**Table 9:**  $^{13}\text{C}$ -and  $^1\text{H}$ -NMR chemical shift values of tambulin (**1**) (acetone- $d_6$ , 125 and 500 MHz)

C. No.	$\delta_{\text{C}}$	$\delta_{\text{H}}$ (J, Hz)
1	-	-
2	146.9	-
3	136.8	-
4	177.0	-
5	157.3	-
6	96.0	6.51 s
7	160.0	-
8	130.2	-
9	149.3	-
10	104.2	-
1'	124.5	-
2'	130.3	8.28 d (9.0 Hz)
3'	115.0	7.14 d (9.0 Hz)
4'	162.2	-
5'	115.0	7.14 d (9.0 Hz)
6'	130.3	8.28 d (9.0 Hz)
C-7/OCH <sub>3</sub>	55.8	3.89 s
C-4'/OCH <sub>3</sub>	56.9	3.98 s
C-8/OCH <sub>3</sub>	61.5	3.90 s
C-5/OH	-	11.58 s

#### 4.2.2 Structure elucidation of prudemestine (**2**)

Compound **2** was obtained as a yellow powder. The EI-MS spectrum of compound **2** showed molecular ion  $[\text{M}^+]$  at  $m/z$  330, and base peak at  $m/z$  315. The molecular formula  $\text{C}_{17}\text{H}_{14}\text{O}_7$ , was determined from HREI- MS spectrum which showed  $[\text{M}^+]$  at  $m/z$  330.0746 (Calcd for  $\text{C}_{17}\text{H}_{14}\text{O}_7 = 344.0740$ ). The IR spectrum displayed absorptions at 3327 (OH), 1651 (aromatic), and 1556 (olefinic)  $\text{cm}^{-1}$ . The UV spectrum showed absorptions at 367, 325, and 273 nm. The  $^1\text{H}$ -NMR spectrum exhibited resonances for two singlets at  $\delta$  3.88, and 4.02 were attributed to protons of methoxy groups attached to C-4', and C-8, respectively. A downfield singlet resonated at  $\delta$  6.42 was ascribed to H-6. Similarly, two downfield ortho coupled doublets at  $\delta$  7.04 d ( $J_{3',2'/5',6'} = 9.0$  Hz) and 8.18 d ( $J_{2',3'/6',5'} = 9.0$  Hz), were assigned to H-3'/H-5' and H-2'/H-6' respectively. Three

exchangeable protons appeared at  $\delta$  11.54, 6.60 and 6.29 due to hydroxyl protons attached to C-5, C-3, and C-7, respectively. The structure of the compound was further confirmed from 2D-NMR spectra (COSY, HSQC, HMBC and NOESY). The position of hydroxyl and methoxy groups was assigned with the help of the HMBC correlations. The HMBC correlations between protons and carbons resonated at  $\delta$  3.88 and  $\delta$  161.2 (C-4'), and 4.02 and 127.6 (C-8) indicated the position of methoxy groups in the compound. Structure elucidation of prudomestin (**2**) is represented with their corresponding  $^1\text{H-NMR}$  and  $^{13}\text{C-}$  chemical shift values in **Figure 22**. The key HMBC correlations in compound **2** are shown in **Figure 23**. Details of  $^{13}\text{C-}$  and  $^1\text{H-NMR}$  chemical shift values of prudomestin (**2**) ( $\text{CDCl}_3$ , 125 and 500 MHz) are presented in **Table 10** below.

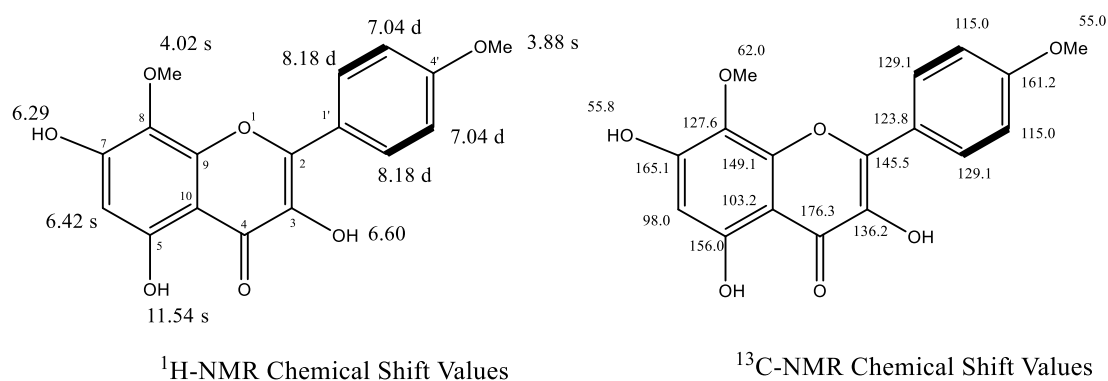


**Figure 22:**  $^1\text{H-}$  and  $^{13}\text{C-NMR}$  chemical shift values of prudomestin (**2**)

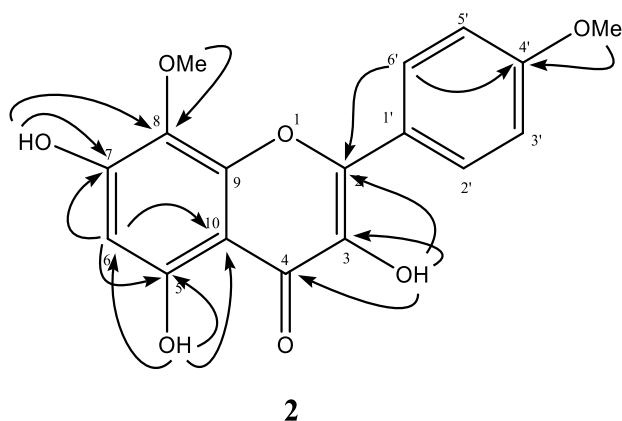


**Figure 23 :** Key HMBC ( $\longleftrightarrow$ ) correlations of **2**

**Table 10:** <sup>13</sup>C- and <sup>1</sup>H-NMR chemical shift values of prudomestin (**2**) (CDCl<sub>3</sub>, 125 and 500 MHz)

C. No.	δ <sub>C</sub>	δ <sub>H</sub> (J, Hz)
1	-	-
2	145.5	-
3	136.2	-
4	176.3	-
5	156.0	-
6	98.0	6.42 s
7	165.1	-
8	127.6	-
9	149.1	-
10	103.2	-
1'	123.8	-
2'	129.1	8.18 d (9.0 Hz)
3'	115.0	7.04 d (9.0 Hz)
4'	161.2	-
5'	115.0	7.04 d (9.0 Hz)
6'	129.1	8.18 d (9.0 Hz)
C-7/OH	-	6.29 s
C-4'/OCH <sub>3</sub>	55.0	3.88 s
C-8/OCH <sub>3</sub>	62.0	4.02 s
C-5/OH	-	11.54 s
C-3/OH	-	6.60 s

#### 4.2.3 Structure elucidation of cinnamic acid (**3**)

Cinnamic acid was isolated from ethylacetate fraction using the first column: dichloromethane: n-hexane 30%. During the first column, it was isolated as an impure compound which is then purified using various solvents. In TLC it was reflected as a single spot at R<sub>f</sub> 0.41 with solvent system acetone: n-hexane (3:7) Only UV visible: 254 nm spotted blue, yield 759 mg.

The EIMS of the compound showed M<sup>+</sup> at *m/z* 148 and M<sup>+</sup>-H peak at *m/z* 147. The <sup>1</sup>H-NMR spectrum of the compound displayed signals for trans-olefinic protons at δ 6.44 (H-2) and 7.78 (H-3). While signals of five protons appeared at the aromatic range from δ 7.40 to 7.54. The <sup>13</sup>C-NMR spectra (**Table 11**) showed a peak for a conjugated acid carbonyl carbon at δ 172s.1. All the spectra confirmed that the structure of the

compound is cinnamic acid. Structure elucidation of cinnamic acid (**3**) is represented with their corresponding  $^1\text{H-NMR}$  and  $^{13}\text{C}$ - chemical shift values in **Figure 24**.

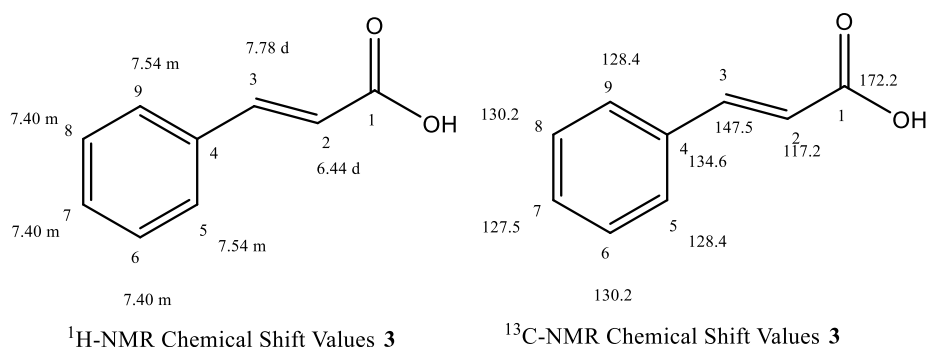


**Figure 24:**  $^1\text{H}$ - and  $^{13}\text{C}$ -NMR chemical shift values of cinnamic acid (**3**)

**Table 11:**  $^{13}\text{C}$ - and  $^1\text{H}$ -NMR chemical shift values of cinnamic acid (**3**) ( $\text{CDCl}_3$ , 100 and 400 MHz)

C. No.	$\delta\text{C}$	$\delta\text{H}$ (J, Hz)
1	172.1	-
2	117.2	6.44 d (16 Hz)
3	147.5	7.78 d (16 Hz)
4	134.6	-
5	128.4	7.54 m
6	130.2	7.40 m
7	127.5	7.40 m
8	130.2	7.40 m
9	128.4	7.54 m

#### 4.2.4 Structure elucidation of cinnamic ester (**4**)

The EIMS of the compound showed  $\text{M}^+$  at  $m/z$ 162 and  $\text{M}^+\text{-OMe}$  peak at  $m/z$  131. The  $^1\text{H-NMR}$  spectrum of the compound displayed signals for trans olefinic protons at  $\delta$  6.45 (H-2) and 7.70 (H-3). While signals of five protons were appeared at aromatic range from  $\delta$  7.39 to 7.53. A singlet at  $\delta$  3.81 indicated the presence of methoxy group in the compound. The  $^{13}\text{C-NMR}$  spectra (**Table-12**) showed peak for a conjugated ester carbonyl carbon at  $\delta$  167.1. All the spectra confirmed that the structure of the compound is cinnamic ester. Structure elucidation of cinnamic ester (**4**) is represented with their corresponding  $^1\text{H-NMR}$  and  $^{13}\text{C}$ - chemical shift values in **Figure 25**.

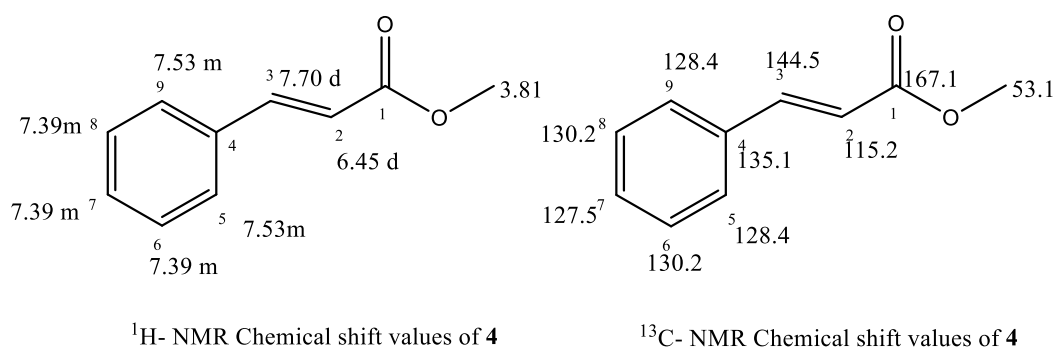


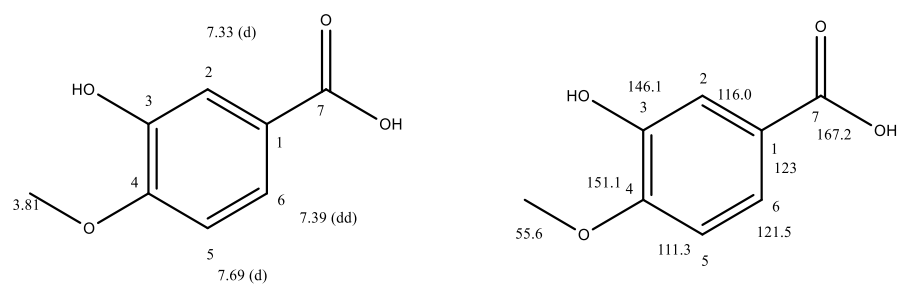
**Figure 25:** <sup>1</sup>H- and <sup>13</sup>C-NMR chemical shift values of cinnamic ester (**4**)

**Table 12:** <sup>13</sup>C- and <sup>1</sup>H-NMR chemical shift values of cinnamic ester (**4**) (CDCl<sub>3</sub>, 100 and 400 MHz)

C. No.	$\delta$ C	$\delta$ H (J, Hz)
1	167.1	-
2	115.2	6.45 d (16 Hz)
3	144.5	7.70 d (16 Hz)
4	135.1	-
5	128.4	7.53 m
6	130.2	7.39 m
7	127.5	7.39 m
8	130.2	7.39 m
9	128.4	7.53 m
OCH <sub>3</sub>	53.1	3.81

#### 4.2.5 Structure elucidation of isovanillic acid (**5**)

The EIMS of the compound showed M<sup>+</sup> at *m/z* 168 and M<sup>+</sup>-H peak at *m/z* 167. The <sup>1</sup>H-NMR spectrum of the compound displayed signals on the aromatic region (**Table-13**)  $\delta$  7.33 (H-2), 6.97 (H-5), and 7.39 (H-6). A singlet at  $\delta$  3.81 indicated the presence of a methoxy group in the compound. The <sup>13</sup>C-NMR spectra (**Table-13**) showed a peak for a conjugated acid carbonyl carbon at  $\delta$  167.2. The position of the methoxy group was confirmed using HMBC correlation. All the spectra confirmed that the structure of the compound is isovanillic acid. Structure elucidation of isovanillic acid (**5**) is represented with their corresponding <sup>1</sup>H-NMR and <sup>13</sup>C- chemical shift values in **Figure 26**.



<sup>1</sup>H-NMR chemical shift values of **5**

<sup>13</sup>C- NMR chemical shift values of **5**

**Figure 26:** <sup>1</sup>H- and <sup>13</sup>C-NMR chemical shift values of isovanillic acid (**5**)

**Table 13:** <sup>13</sup>C- and <sup>1</sup>H-NMR chemical shift values of isovanillic acid (**5**) (DMSO-d<sub>6</sub>, 150 and 600 MHz)

C. No.	$\delta$ C	$\delta$ H (J, Hz)
1	123	-
2	116.0	7.33 d (2.0)
3	146.1	-
4	151.1	-
5	111.3	6.97 d (9.0)
6	121.5	7.39 dd (9.0, 2.0)
7	167.2	-
OCH <sub>3</sub>	55.6	3.81

#### 4.2.6 Structure elucidation of isoquercetin (**6**)

The EI-MS of the compound showed a peak for only the aglycone part at  $m/z$  286. The <sup>1</sup>H-NMR spectrum of the compound exhibited an ABX system at  $\delta$  7.82 (1H, d,  $J=2.4$  Hz, H-2'), 7.57 (1H, dd,  $J=8.5$  and 2.4 Hz, H-6') and 6.86 (1H, d,  $J=8.5$  Hz, H-5'). Two meta-coupled signals at  $\delta$  6.20 and 6.40, d,  $J=2.1$  Hz respectively were due to for H-6 and H-8 protons. A doublet at  $\delta$  5.16 (H-1'', d,  $J=7.6$  Hz) was attributed to an anomeric proton of sugar and suggested a glycosidic  $\beta$ -linkage. Six signals at  $\delta$  3.44-3.94 were assigned to H-2'' to H-6'' protons. The position of sugar was assigned with the help of HMBC spectrum which displayed the correlation of H-1'' ( $\delta$  5.16) to C-3 ( $\delta$  136.4). The Structure of the compounds was finally confirmed using 2D-NMR techniques. All the spectroscopic data of the compound was matched with the previously reported compound isoquercetin (El-Sayed *et al.*, 2010). The structure of isoquercetin (**6**) is represented in **Figure 27**.

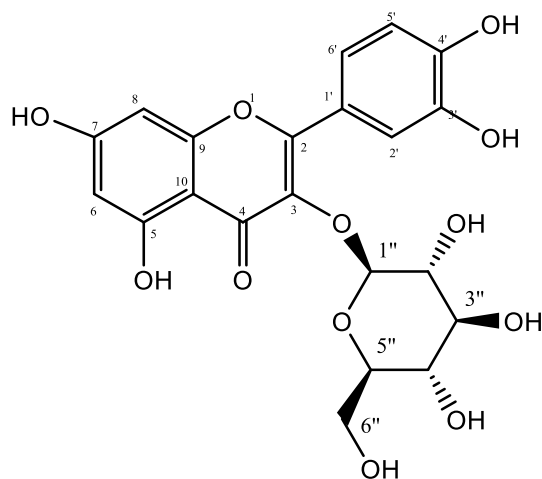


**Figure 27:** Structure of isoquercetin (6)

#### 4.2.7 Structure elucidation of daucosterol (7)

The EI-MS of the compound displayed a peak for the aglycone part at  $m/z$  414 and 396. The  $^1\text{H-NMR}$  spectrum of the compound displayed a peak at  $\delta$  5.34 br s was assigned to H-6. Another doublet at  $\delta$  5.03 (d,  $J = 7.6$  Hz), was ascribed to the anomeric proton of glucose (H-1').

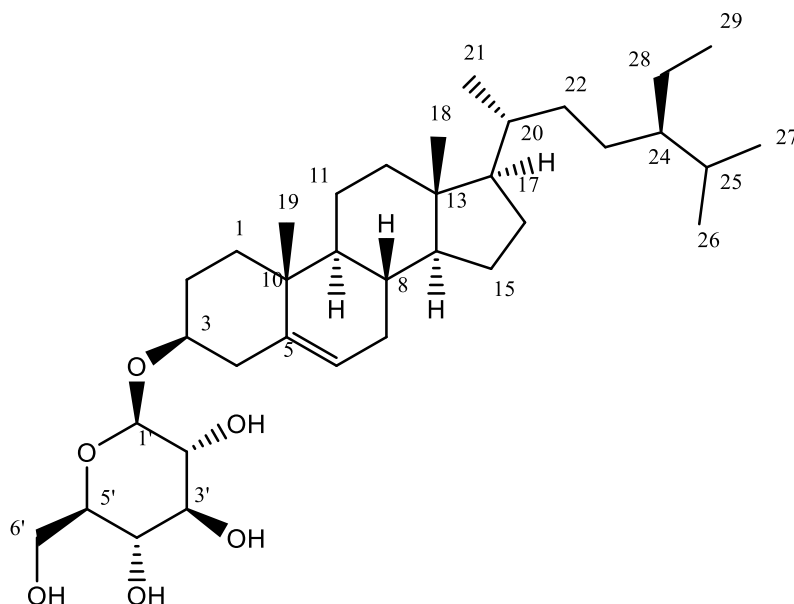


**Figure 28:** Structure of  $\beta$ -sitosterol glycoside (7)

A signal at  $\delta$  4.53 m, was attributed to H-3. The other six signals at  $\delta$  3.91 to 4.40 were due to protons of the sugar moiety. All the spectra of the compounds were closely similar to previously reported compounds (Lee *et al.*, 2011). The structure of daucosterol (7) is represented in **Figure 28**.

### 4.3 Applications

#### 4.3.1 Antioxidant activities

The antioxidant values of the extract, fractions, and pure compounds were determined. Only those samples inhibiting  $\geq 50\%$  at this concentration were further diluted for the calculation of the  $IC_{50}$  value. The calculated values of the samples and the standard are presented in **Table 14** and their graphical representation is in **Figure 29**.

**Table 14:** Antioxidant activities of extract, fractions, and some isolated compounds from *Z. armatum*

Sample	$IC_{50}$ ( $\mu\text{g}/\text{mL}$ )
Crude ethanolic extract	$174 \pm 1.01$
Crude methanolic extract	$169.85 \pm 0.244$
Hexane fraction	NC
Ethylacetate fraction	$42.94 \pm 1.19$
Tambulin	$32.65 \pm 0.31$
Prudomestin	$26.96 \pm 0.19$
Quercetin	$1.17 \pm 0.35$

Data are expressed as  $IC_{50} \pm$  Standard Error Mean (SEM) of three independent assays NC: Not Calculated.

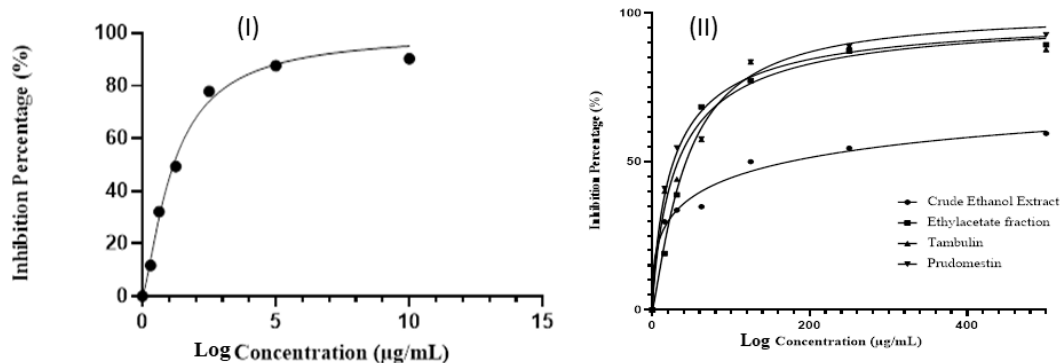


**Figure 29:** Graphical representation of antioxidant activities of i) quercetin ii) crude ethanolic extract, ethylacetate fraction, tambulin and prudomestin

The antioxidant potential resulted in decreasing order as prudumestin>tambulin>ethylacetate fraction>ethanolic extract and lowest on hexane fraction. The lower value of antioxidants in the case of hexane fraction could be due to associated compounds and its solvent effect possessing lower polarity. Since phenolic compounds are stronger proton donors like tocopherols, flavonoids and organic acids as coumaric acids etc this phenolic content is correlated with antioxidant property (Sarker *et al.*, 2007; Juan & Chou, 2010). The higher potency of prudomestin could be accounted for due to the

polyphenolic component in it. Likewise, the same holds for tambulin which exhibits similar properties. Such as the -OH and -OCH<sub>3</sub> substituents in the aromatic rings of these polyphenolics are responsible for relatively higher potency. Ethylacetate fraction which can hold a mixture of flavonoids and other such compounds revealed its higher potency than its analogue. The higher antioxidant potency of the isolated compounds strongly suggests fruit of *Z. armatum* is one of the natural antioxidants that could restrict the undesired oxidation process. Hence regular consumption of *Z. armatum* as a valued species and condiment proves to be beneficial.

#### 4.3.2 Anti-inflammatory activity

All samples were screened at the concentration of 50 µg/mL at first. Only those samples inhibiting ≥50% at this concentration were further diluted for the calculation of the IC<sub>50</sub> value. However, in the case of pure isolated compounds activities were performed at 25 µg/mL. Crude ethanolic extract that possesses 85.5% inhibition was fractionated in increasing polarity to obtain hexane and ethylacetate fractions. The ethyl acetate fraction possesses higher inhibition with an IC<sub>50</sub> value of 17.8±1.1 µg/mL whereas the hexane fraction possesses the lowest value of IC<sub>50</sub> at 26.3 ± 1.1 µg/mL. Thus ethylacetate fractions were column chromatographed to obtain various compounds among which the flavonoids exhibited remarkable potency. Tambulin (**1**) revealed significant anti-inflammatory activity with an IC<sub>50</sub> value of 7.5 ± 0.3 µg/mL whereas prudomestin (**2**) reflected its inhibition activity with the lowest value as IC<sub>50</sub> 1.5 ± 0.3 µg/mL. The IC<sub>50</sub> value for the standard drug ibuprofen was found to be 11.2 ± 1.9 µg/mL. The IC<sub>50</sub> values of all samples are presented in **Table 15** and graphically represented in **Figure 30**.

**Table 15:** Anti-inflammatory activities of extract, fractions, and some isolated compounds from *Z. armatum*

Sample	Concentration	Inhibition Percentage (%)	IC <sub>50</sub> (µg/mL)
Methanolic extract	50	66.2	27.7 ± 0.7
Ethanolic extract	50	85.5	20.7 ± 0.4
Hexane fraction	50	79.4	26.3 ± 1.1
Ethylacetate fraction	50	79.6	17.8 ± 1.1
Tambulin	25	72.5	7.5 ± 0.3
Prudomestin	25	97.2	1.5 ± 0.3
Ibuprofen	25	73.2	11.2 ± 1.9

*Data are expressed as IC<sub>50</sub> ± Standard Error Mean (SEM) of three independent assays*

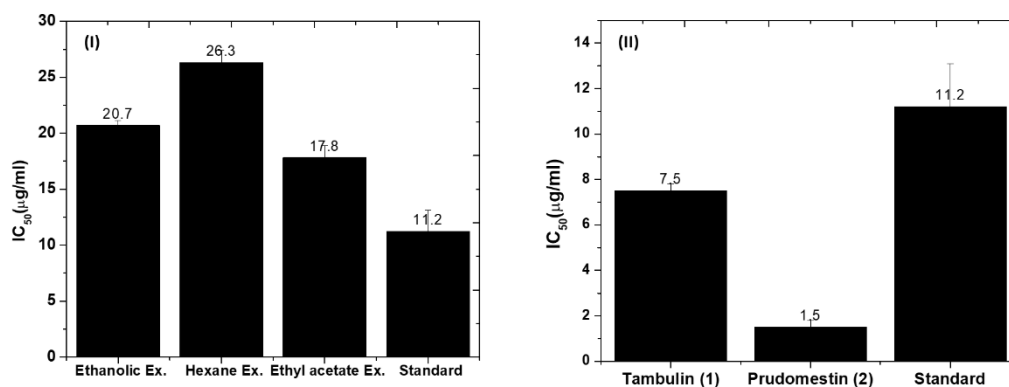


**Figure 30:** (I-II): Graphical representation of IC<sub>50</sub> ± Standard error of mean (SEM) values of ROS inhibition activities of sample versus standard of three independent tests of each sample

#### 4.3.3 Discussion on antioxidant and anti-inflammatory properties

The synergetic effect of phytoconstituents in its ethylacetate fraction revealed stronger antioxidant and anti-inflammatory potency which is reflected in its polyphenolic compounds' flavonoids. Potent antioxidant activity possessed by extract may be attributed to its extensive class of secondary metabolites known as phenols comprised of flavonoids, tannins, hydroxycinnamate esters, and the structurally related compounds (Grace & Logan, 2000) and the isolated compounds under the same category. However, slightly lower activities of hexane fraction could be attributed to the presence of non-polar compounds, fatty acids, and their oxides in predominance. Particular chelating properties of polyphenolic structure in the flavonoids and the like with -OH, -OCH<sub>3</sub> substituents assist in exchange scavenging free radicals and chelate with transition metals could contribute to higher antioxidant abilities in natural plants (Arora *et al.*, 2000). Tambulin with a greater number of -OCH<sub>3</sub> substituents possesses lower antioxidant properties than prudomestine possessing a higher number of -OH groups. Likewise, previous *in vivo* studies in mice also revealed ethyl acetate fraction of *Z. armatum* with anti-inflammatory activity (Hertog & Wiersum, 2000) and ethanolic extract exhibiting potent anti-inflammatory activities (Bhatt & Upadhyaya, 2010). Recent studies on its essential oil found to show anti-inflammatory activity (Dhami *et al.*, 2019) since indigenous people use twigs of the plant as toothbrushes popularly for curing inflamed gums and to treat toothache in different countries (Ahmed *et al.*, 2004; Abbasi *et al.*, 2013; Kanwal *et al.*, 2015). One of the key constituent's tambulin also recorded multiple benefits as a secretagogue in stimulating insulin secretion, vasorexalant, and as an antiproliferative, antiageing, and Parkinson's disease (Hameed *et al.*, 2019, Mushtaq *et al.*, 2019, Nooreen *et al.*, 2017; Pandey *et al.*,

2019). Tambulin and prudomestin both are potent polyphenolic compounds isolated from the fruit of *Z. armatum* of Nepali origin that support traditional consumption during inflammation.

#### **4.3.4 *In Vitro* antidiabetic studies of compound 1 and 2**

##### **4.3.4.1 *In vitro* $\alpha$ -glucosidase activity**

Alpha-glucosidase is involved in breaking down starch and disaccharides into glucose that is absorbable directly. *In vitro*  $\alpha$ -glucosidase inhibition activities values of tambulin (**1**), prudomestin (**2**), and cinnamic acid (**3**) were (  $IC_{50}= 39.31 \pm 1.8$ ), ( $IC_{50}= 17.5 \pm 1.41$ ), and ( $IC_{50}= 226.8 \pm 1.5$ ) respectively. The  $IC_{50}$  value of the standard acarbose used was  $IC_{50}= (5.66 \pm 0.8)$ .

##### **4.3.4.2 Insulin secreting activity of tambulin (1)**

For the insulin secretory mechanism(s) of tambulin (**1**) particularly in glucose-dependent, KATP- and  $Ca^{2+}$  channels dependent, and cAMP-PKA pathways was carried. Mice islets and MIN6 cells were incubated with tambulin in the presence of pharmacological agonists/antagonists and the secreted insulin was measured using a mouse insulin ELISA kit. The intracellular cAMP was measured by an acetylation cAMP ELISA kit. Tambulin (**2**) (200  $\mu$ M) showed potent insulin secretory activity only at stimulatory glucose (11–25 mM) concentrations; however, no change in insulin release was observed at basal glucose both in mice islets and MIN6 cells. Hence tambulin (**1**) enhances insulin secretion through a pathway that doesn't involve KATP channels but it relies on calcium ions and a process that amplifies the signaling involved in insulin release. Calcium ions play a crucial role in this pathway adding the amplification of insulin secretion triggered by glucose. Hence such a role of tambulin can boost the release of insulin in response to glucose by utilizing a  $Ca^{2+}$ -dependant amplifying pathway that doesn't rely on KATP channels. **Figure 31** presents the insulin secretory activity of the compound.

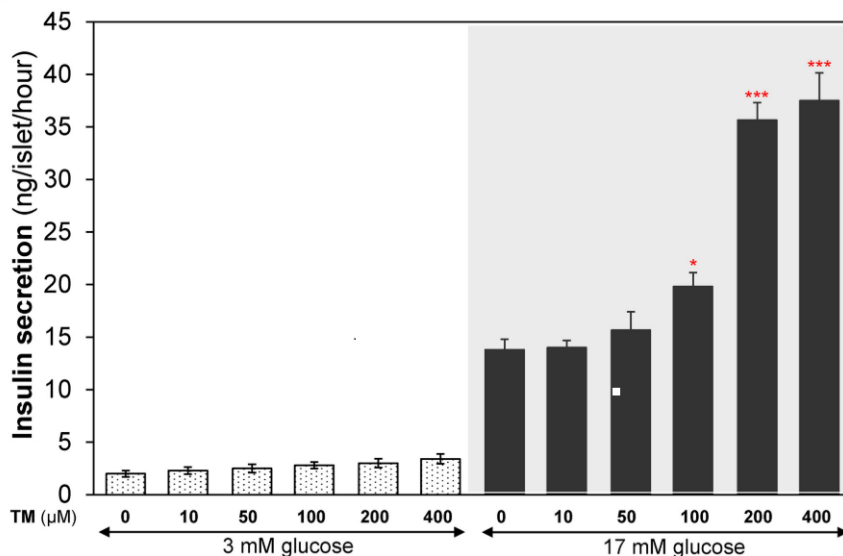


**Figure 31:** Insulin secreting activity of tambulin (1)

#### 4.3.4.3 Insulin secretary activity of prudomestin (2) in mice pancreatic islets

Prudomestin (2) was tested for insulin secretion potential in mice pancreatic islets. Fresh islets were isolated by the collagenase digestion method, as described previously (Hafiz *et al.*, 2015). On completion of pre-incubation for 1 hr at 37 °C, islets of similar size in groups of two were treated with different concentrations (10- 200 mM) of the compound in stimulatory glucose conditions. On completion of post-incubation for 45 minutes at 37 °C, the supernatant was collected for insulin estimation using an Ultra-Sensitive Mouse Insulin ELISA kit. It is observed that prudomestin (2) enhanced insulin secretion activity at all tested doses. The optimal insulin secretion activity was found at 50mM concentration of compound 2. The preliminary data of our experiments are as shown below in **Table 16** and diagrammatically in **Figure 32**.

**Table 16:** Dose dependent insulin secretion activity of prudomestin (2)

Code	Dose	Insulin secretion	Remarks
Control	17mM glucose	18.34	Reference ctrl
Prudomestin	10 micromoles	31.3	Moderate
Prudomestin	50 micromoles	55.2	Potent
Prudomestin	100 micromoles	52.1	Potent
Prudomestin	200 micromoles	40.4	Moderate
Tolbutamide (TB)	200 micromoles	28.9	Standard drug

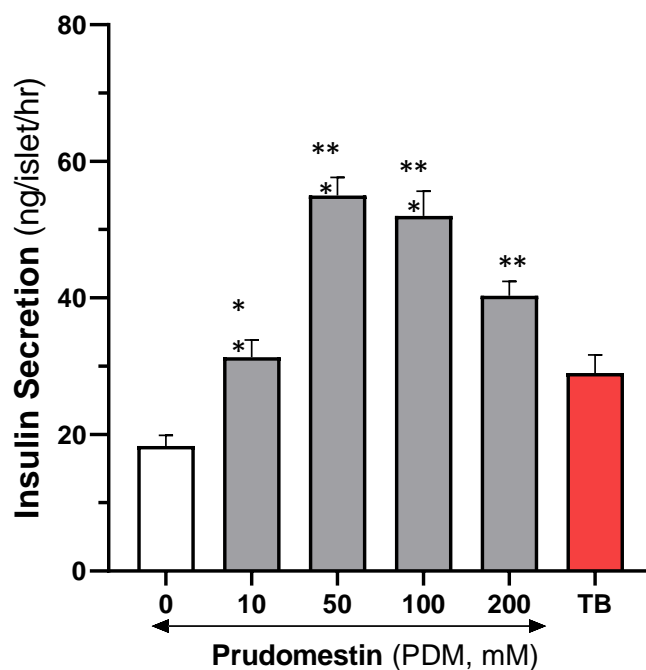


**Figure 32:** Insulin secretory activity of prudomestin (2)

Data was represented as Mean  $\pm$  SD. TB – Tolbutamide, a standard drug. The graph represents the optimal insulin secretion of prudomestin is at 50mM.

#### 4.3.5 Anticancer activities against breast cancer cell line (MCF-7)

Anticancer activities of *Z. armatum* methanolic, ethanolic extract and hexane fractions expressed activity against breast cancer (MCF-7) cell line. Since all the samples showed activity against breast cancer at the highest concentration (400  $\mu$ g/mL) therefore observation was conducted in lower concentrations (200, 100, 50 and 25  $\mu$ g/mL) which revealed potency of these different samples as expressed through their half minimum inhibitory concentration ( $IC_{50}$ ) at varying range. **Table 17** below represents the  $IC_{50}$  values.

**Table 17:** Anti-cancer activity of *Z. armatum* against breast cancer (MCF-7)

Sample	$IC_{50}$ ( $\mu$ g/mL)
Za MeOH	74.51 $\pm$ 5
Za EtOH	54.62 $\pm$ 5
ZaHex	73.03 $\pm$ 5
Cinnamic acid (3)	85 $\pm$ 2
Doxorubicin	0.9 $\pm$ 0.14

The result showed that ethanolic extract possesses stronger activity against MCF-7 cell lines among the studied samples.

#### 4.3.6 Anticancer activity of *Z. armatum* against cervical cancer (HeLa) cell line

Anticancer activity of the extracts and fractions of *Z. armatum* was evaluated against the cervical cancer (HeLa) cell line. At the highest tested concentration of 400 µg/mL, significant inhibition was observed, whereas concentration lower than this exhibited less than 20% inhibition. Notably, both the crude methanolic extract and hexane fractions demonstrated activity against cervical cancer (HeLa) cell line as presented in **Table 18** below.

**Table 18:** Anticancer activity of *Z. armatum*'s extract and fractions against cervical cancer (HeLa)

Sample	IC <sub>50</sub> (µg/mL)
Za MeOH	66.17 ± 10
Za EtOH	-
ZaHex	85.81 ± 2

None of the fractions and compounds of *Z. armatum* exhibited anticancer activity against the 3T3 cell line. In contrast, the extracts showed significant anticancer activity against breast cancer cell lines, with effects observed even at the lowest concentration tested.

#### 4.4 Extraction of essential oil and its quantitative yield

The matured fruits of the plants were collected from the commercial sites of Salyan (Hertog & Wiresum, 2000) Surkhet and Myagdi. These fruits 250 g were subjected to hydro-distillation for three hours using the Clevenger apparatus. The yield of oil from different sites is presented in **Table 19**.

**Table 19:** Yields of essential oil

Site of collection	Dry plant mass	Essential oil color	Percent yield (v/w)
Salyan	250 g	Transparent	3.5
Surkhet	250 g	Transparent	3.4
Myagdi	250 g	Transparent	4

*ZaSI, ZaSII and ZaM all were collected at the same period from their site of collection.*

#### 4.4.1 GCMS of essential oil of *Z. armatum* and its composition

GCMS of *Z. armatum* Salyan origin (ZaSI), *Z. armatum* of Surkhet (ZaSII) and *Z. armatum* of Myagdi (ZaM) all revealed 60 different constituents at various retention times. Compositionwise GCMS of the essential oil from the fruits of *Z. armatum* revealed a predominant constituent of Linalool; 58.32%, 58.45%, and 80.37% in ZaSI, ZaSII and ZaM respectively. Limonene consists of 16.67%, 11.2%, and 3.65% in ZaSI,

ZaSII, and ZaM respectively. A quantitative remarkable difference was observed in oil from ZaM. *Trans*-methyl cinnamate occupies 8.22%, 14.61% and 9.55% at ZaSI, ZaSII, and ZaM respectively. A quantitatively higher amount was observed in ZaSII. Additionally, the content of  $\beta$ -Phellenderene is similar 1.71%, 1.91%, and 1.23 % respectively. *Cis*, and *trans* linalool oxide are relatively lower in the case of ZaM with only 0.5% whereas both these constituents are >1% in both ZaSI and ZaSII respectively. The chemical compositions of the constituents are depicted in a compiled form in **Table 20** below.

**Table 20:** Chemical profiling of the constituents of the essential oil (% area) from the fruit pericarp of *Z. armatum* from different commercial sites in Nepal

Compound	ZaSI	ZaSII	ZaM
Styrene	0.01	-	-
$\alpha$ -Thujene	0.12	0.11	0.05
$\alpha$ -Pinene	0.2	0.18	0.04
Benzaldehyde	0.16	0.18	0.03
Sabinene	0.99	1.04	0.53
$\beta$ -Pinene	0.19	0.17	0.04
6-Methyl-5-hepten-2-one	-	-	0.01
Myrcene	1.53	1.64	0.51
$\delta$ -2-Carene	0.05	0.04	-
para-Mentha-1(7),8-diene	0.03	-	-
para-Cymene	0.73	0.74	0.17
Limonene	16.67	11.2	3.65
$\beta$ -Phellandrene	1.71	1.91	1.23
<i>cis</i> -Linalool oxide (furanoid)	1.66	1.37	0.5
<i>trans</i> -Linalool oxide (furanoid)	1.42	1.16	0.5
Perillene	0.03	-	-
Linalool	58.31	58.45	80.37
Hotrienol	0.01	-	-
Linalool derivative	0.12	0.1	-
endo-Fenchol	0.05	0.04	-
<i>trans</i> -para-Mentha-2,8-dien-1-ol	0.09	0.06	0.01
<i>cis</i> -para-Menth-2-en-1-ol	0.21	0.04	0.04
<i>cis</i> -Limonene oxide	0.09	0.07	-
<i>cis</i> -para-Mentha-2,8-dien-1-ol	0.12	0.1	-
<i>trans</i> -para-Menth-2-en-1-ol	0.15	0.14	0.04
Citronellal	-	-	0.03
Lavandulol	0.02	-	-
Unidentified	0.03	-	-
<i>trans</i> -Isocitral	0.11	0.15	-
para-1,8-Menthadien-4-ol	0.09	0.04	-
Terpinen-4-ol	1.34	1.09	0.25
Cryptone	1.4	1.05	0.36
<i>cis</i> -Hexenyl butyrate	0.45	0.38	-

3-Cis-Hexenyl butyrate	-	-	0.1
$\alpha$ -Terpineol	0.44	0.38	0.18
Methyl chavicol	0.1	0.08	0.03
Dihydro carveol	0.05	-	-
Unidentified	0.07	-	-
Cumin aldehyde	0.15	0.11	0.03
Carvone	0.19	0.11	0.02
Linalyl acetate	0.04	0.04	0.01
Piperitone	0.33	-	0.17
Methyl citronellate	0.03	0.02	0.01
Phellandral	0.32	0.18	0.04
$\alpha$ -Terpinen-7-al	0.04	0.03	0.01
neo-Dihydro carveol acetate	0.06	0.04	-
Limonene hydroperoxide	0.06	0.04	-
Hydroxy cryptone	0.03	0.05	0.01
Oxo-para-menth-1-en-7-al	0.07	0.07	-
Unidentified	0.06	-	-
Terpenediol	0.47	0.53	0.23
Limonene hydroperoxide	0.04	0.04	-
<i>trans</i> -Methyl cinnamate	8.22	14.61	9.55
Unidentified	0.03	-	-
Unidentified	0.03	-	-
$\beta$ -Caryophyllene	0.06	0.05	0.14
Unidentified	0.17	-	-
Unidentified	0.25	-	-
Caryophyllene oxide	0.2	0.18	0.12
Humulene epoxide II	-	-	0.01
$\gamma$ -Cadinene	-	-	0.01
$\alpha$ -Muurolol	-	-	0.01
Methyl palmitoleate	0.14	0.22	0.12
Methyl palmitate	0	0.06	0.03
Cyclhexadecanolide	-	-	0.06
Unidentified	0.09	0.09	0.03
Unidentified	0.06	0.04	0.01
<i>cis</i> -9-Tricosene	0.08	0.05	-

#### 4.4.2 Structures of major compounds

Structures of some of the remarkable compounds present in the essential oil of *Z. armatum* as observed in GC-MS profile are presented in **Figure 33** below:

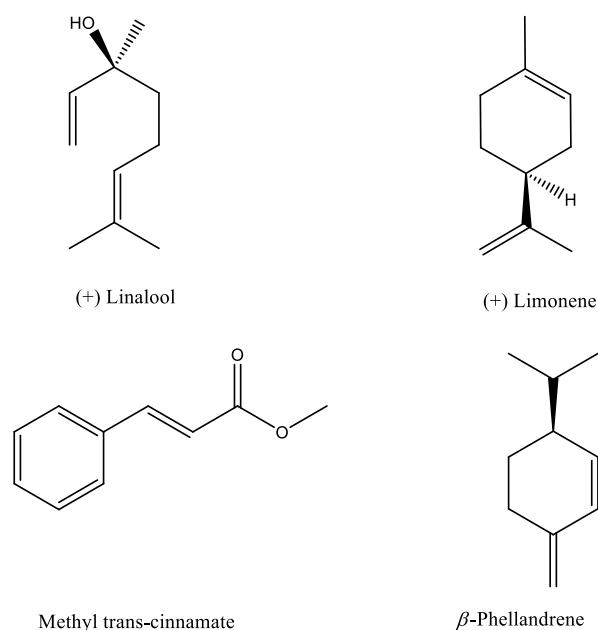


**Figure 33:** Structures of major compounds in the essential oil of *Z. armatum*

#### 4.4.3 Monoterpenoid enantiomeric distribution

Among 25 chiral compounds identified, the chiral GCMS revealed 13 compounds with their enantiomeric distribution as depicted in **Table 21** below. Linalool in its *d* or (+) form is the dominant constituent of essential oil from all three sites. An almost racemic mixture of limonene in all oil in general whereas (-)  $\beta$ -phellandrene and other enantiomeric components were dominantly in levorotatory forms as the majority in all the samples.

**Table 21:** Enantiomeric distribution [%(+): %(-)] of compounds in *Z. armatum* essential oils

Compounds	ZaSI	ZaSII	ZaM
$\alpha$ -Thujene	5.38:94.62	7.13:92.87	4.87:95.13
$\alpha$ -Pinene	13.64:86.36	13.74:86.26	21.01:78.99
Sabinene	7.73:92.27	7.73:92.27	8.68:91.32
$\beta$ -Pinene	7.63:92.37	6.69:93.31	9.15:90.85
Limonene	56.62:43.38	54.92:45.08	56.74:43.26
$\beta$ -Phellandrene	0.29:99.71	0.31:99.69	0.2:99.8
cis-Linalool oxide	19.79:80.21	16.09:83.91	21.11:78.89
trans-Linalool oxide	9.34:90.66	10.14:89.86	7.88:92.12
Linalool	92.59:7.41	93.11:6.89	93.13:6.87
Terpinen-4-ol	27.13:72.87	28.16:71.84	28.08:71.92
$\alpha$ -Terpineol	41.96:58.04	40.87: 59.13	41.54:58.46
Piperitone	21.81:78.19	21.5:78.5	18.9:81.1
$\beta$ -Caryophyllene	0:100	0:100	0:100

#### 4.4.4 Enantiomeric distribution

(+) Linalool is one of the predominant constituents in all the samples along with Limonene whereas all other compounds were dextrorotatory in nature. Enantiomeric distribution of the trace elements present as  $\alpha$ -Thujene,  $\alpha$ -Pinene,  $\beta$ -Pinene and Sabinene revealed more of their dextrorotatory distribution than the laevorotatory ones. Among all the thirteen constituents in their various enantiomeric distributions,  $\beta$ -Caryophyllene is the only constituent that is dextrorotatory.

#### 4.4.5 Elements detection in the essential oil of *Z. armatum*

The elements detected in *Z. armatum* oil (EDX-8000) quantitatively revealed the presence of S (0.438%) and Cu (0.003%) only, with abundant hydrocarbons (99.559%). The presence of Sulphur in a mixture of volatile-natured compounds imparts its characteristic pungent order (Depree *et al.*, 1998) in addition to dominant olfactory receptors (Cicchetti *et al.*, 2017), ethyl *cis*-cinnamate and methyl *trans*-cinnamate. The dominance of methyl *trans*-cinnamate possessing characteristic flavour imparts tartness in spices and condiments for pickles and vegetables.

#### 4.4.6 Comparative studies on antibacterial activities of essential oil

The essential oil obtained from the fruit of *Z. armatum* was moderately active against the bacteria tested compared to ciprofloxacin. **Figure 34** illustrates the potency of the samples in inhibiting bacterial growth. Notably, the essential oils extracted from *Z. armatum* fruit pericarp from Myagdi (ZaM) displayed the highest zone of inhibition (ZOI) against *Escherichia coli* (22 mm) and a moderate effect against *Klebsiella pneumonia* (19 mm), while no activity was observed against the gram-positive *Staphylococcus aureus*. *Z. armatum* essential oils demonstrated significant ZOI against gram-negative bacteria (G) in contrast to gram positive ones. This finding contradicts previous studies that highlighted an impact on gram-positive bacteria (Burt, 2004). The traditional use of *Z. armatum* twigs by indigenous people for oral care, including teeth brushing, alleviating toothaches, soothing inflamed gums, and treating wounds and cuts, may be attributed to its antimicrobial properties.

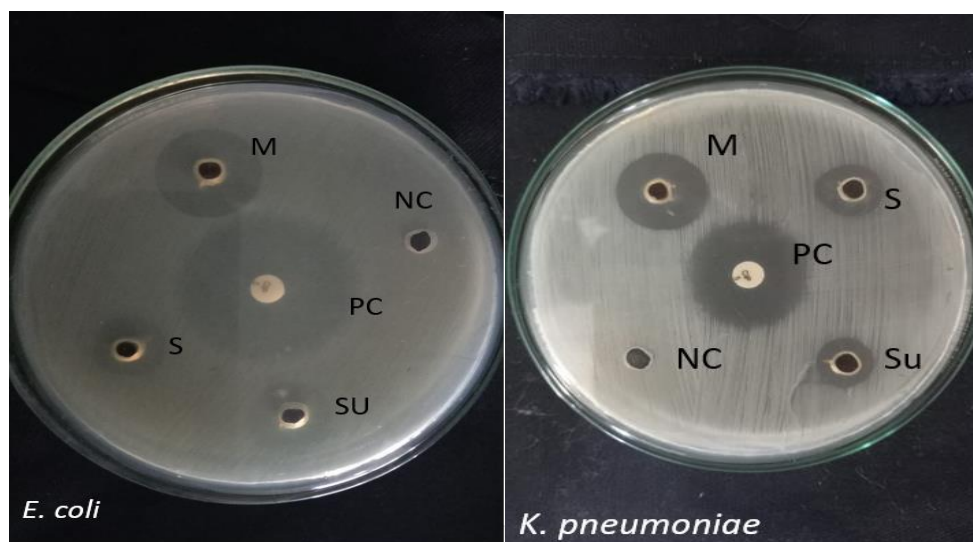


**Figure 34:** Antibacterial activities of essential oil of *Z. armatum* from Myagdi, Salyan and Surkhet

#### 4.4.7 Variation of constituents in oil from different origins

The components of the essential oil of *Z. armatum* from various sites as shown in Table 3 reflected the same qualitative content with slight differences in quantity and (+) linalool being one of the abundant compounds in all samples. This plant economically supports the livelihood of many farmers being a major financial contributor in Myagdi (Neupane *et al.*, 2023). Nationally 90% of its essential oil from various parts of Nepal is exported while only 10% holds the local market (Nepal, 2013). Present study revealed *Z. armatum* from Myagdi with its highest content of linalool (80.37%) breaking its previous record (74.12%) (Phuyal *et al.*, 2020) such variation could be due to differences in collection timing, maturity of the sample, and specific part of the plant and topographical variation (Burt, 2004). The research explored essential oil from the bark of *Z. armatum* with  $\alpha$ -pinene in dominance (Dhami *et al.*, 2019). Our study revealed the enantiomeric composition of chiral components of (-) nature with almost racemic distribution of Limonene whereas the essential oil of *Z. armatum* from Pakistan (Waheed *et al.*, 2011) did not possess limonene. Biologically potent activities of this oil constituent in synergy possess larvicidal activity against mosquito vectors (Tiwary *et al.*, 2007) whereas antibacterial potency and reduction of plasma triglyceride (Jun *et al.*, 2014) of the oils of *Z. armatum* are particularly associated with the (+) linalool (Kamatou & Viljoen, 2008). Topological variation in oil constituent of its fruit is observed with abundance of 3-borneol and isobornyl acetate but not limonene (Waheed *et al.*, 2011) in the plant of Pakistan origin, whereas leaves extracted essential oil of *Z. armatum* belonging to India, possess bornyl acetate abundantly with fewer percentages

of limonene and linalool (Negi *et al.*, 2012) likewise major constituents of its bark reveal  $\alpha$ -pinene and 2-undecanone (Dhami *et al.*, 2019). The nature of constituent variation and the length of the fatty acid chain are detrimental to the biological properties. The olfactory response associated with cis and trans isomers of some constituents also possess drastic variations in cholesterol metabolism (Woollett & Dietschy, 1994). Some more biologically potent activities of the essential oil of this plant are significant anti-inflammatory, analgesic (Bisht *et al.*, 2014) as well and antifungal (Li *et al.*, 2021) these potent properties of the plant are mainly due to its major volatile natured constituent as linalool and limonene as its. Essential oil particularly from plants of the Rutaceae family is claimed to possess qualitative improvement in lipid profile. Despite all these facts that essential oil possesses diverse activities, however, few notable undesirable consequences of the essential oil of *Z. armatum* were observed as it raised the level of urea in animal models (Liaqat *et al.*, 2018). Besides some plants possessing essential oils such as *M. longifolia* are toxic (Odeyemi *et al.*, 2009) in nature. These qualitative properties of numerous plants possessing essential oil outweigh the limitations thus continuous research exploring their potential in a wider dimension is the demand of time that can add value to existing knowledge, belief, and indigenous practice. Since nature-based medications are associated with the positive psychology of healing, cost-effective and accessible to many people.

#### **4.4.8 Discussion and implications from the study of its essential oil**

The result of this study provides important information for academics, investors in industrial sectors, and stakeholders for boosting the economy of farmers. These types of flavor/fragrances have no boundaries hence their therapeutic applications serve as important drugs. This study particularly focused on determining constituents of essential oil based on GC/MS, their enantiomers, and the antimicrobial activity of essential oil. Based on our study, essential oil from the fruit of *Z. armatum* possesses a predominance of linalool from all commercial sites with slight differences in other constituents. The dominance of a particular compound largely determines the bioactivity of the sample under study. Studies focusing on the activity of a particular constituent could add value to existing knowledge and applications. The differences observed in antimicrobial properties revealed through the zone of inhibition from various sites is one of the potential parts of this study. However, further research based on *In-vivo* studies and mechanism studies is needed to justify the exact microbial mode

of action. Likewise, future researchers could explore probable reasons behind remarkable differences in the constituent of *Z. armatum* based on topography and their toxicological studies.

#### 4.5. GC-MS of hexane fraction (Hexf) of *Z. armatum*

Gas chromatography coupled with mass spectrometry is a direct and quick analytical approach. It operates with high separation efficiency flexibility and selectivity with mass sensitivity in detection (Koek *et al.*, 2011). Identification of volatile matters generally includes long and short-chain polyunsaturated fatty acids, hydrocarbons, esters, alcohols etc. The GC-MS chromatogram of the hexane fraction indicating total ion concentration is shown in **Figure 35** below whereas **Table 22** consists of the compounds identified from each constituent's mass spectral fragmentation pattern from head to tail. The sample mainly consists of hydrocarbons, polyunsaturated fatty acids, long and short-chain hydrocarbons, terpenoids and esters. The aromatic flavour of the fruit was found to be a mixture of esters and various compounds.

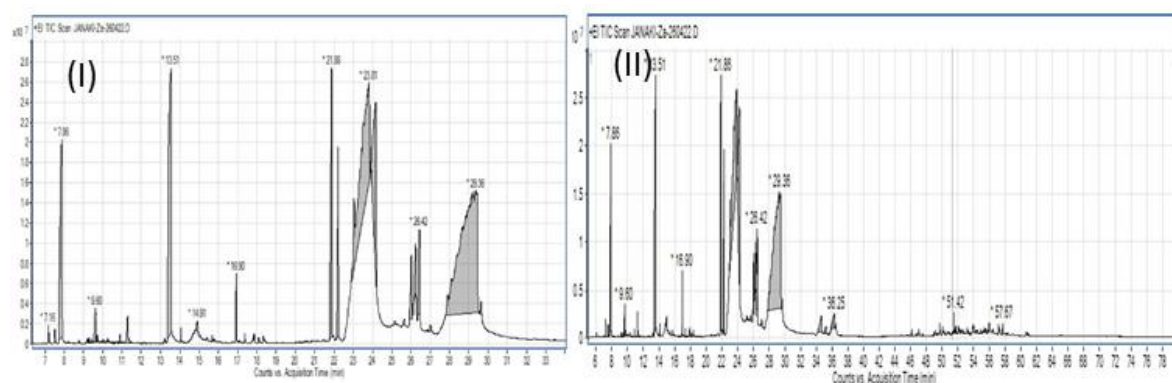


**Figure 35:** GCMS chromatogram showing tR between (I) 7.0 and 31 min (II) 6.0 and 68 min

**Table 22:** Phytoconstituent identified in the hexane fraction of *Z. armatum*

SN	t <sub>R</sub> (min.)	Compound	Compound nature	Peak area
1	5.96	Bicyclo[3.1.1]hept-3-en-2-one, 4,6,6-trimethyl-	4,6,6- 2-Pinen-4-one	0.04
2	7.16	2Furanmethanol,5ethanyltetrahydro- $\alpha,\alpha,5$ -trimethyl-cis-	cis-Linalool Oxide	0.16
3	7.49	$\alpha$ -methyl- $\alpha$ [4-methyl-3pentrnyl]oxiranemethanol		0.16
4	7.86	1,6-Octadien-3-ol,3,7,dimethyl-	$\beta$ -Linalool	6.77
5	9.4	3-Cyclohexen-1-ol, 4-methyl-1-(methylethyl)-	p-Menth-1-en-4-ol	0.03

6	9.6	3,7-octadione-2,6-diol,2,6-dimethyl	1,5-Octadiene-3,7-diol,3,7-dimethyl-	1.72
7	13.51	2-propenoic acid,3 phenylmethylester	Methyl cinnamate	11.08
8	14.06	Bicyclo[7.2.0]undec-4-ene,4,11,11-trimethyl-8-methylene-[IR-(1R*,4Z,9S*)]	1,4,11,11-Trimethyl-8-methylenebicyclo[7.2.0]undec-4-ene	0.12
9	14.89	2-Propenic acid, 3-phenyl	Cinnamic acid	0.22
10	16.9	Caryophyllene oxide	$\beta$ -Caryophyllene oxide	0.61
11	21.85	Methylhexadec-9-enoate		5.58
12	22.2	Hexadecanoic acid, methylester	Palmitic acid, methyl ester	2.77
13	23.8	<i>Cis</i> -9 hexadecenoicacid	Palmitoleic acid	18.66
14	24.2	n-hexadecanoic acid	Palmitic acid	7.5
15	26	9-octadecenoicacid( <i>Z</i> )-methylester	Oleic acid, methyl ester	2.93
16	27.85- 29.46	9,12-Octadecadienoic acid ( <i>Z</i> , <i>Z</i> -)	Linoleic acid	1.78
17	29.36	<i>Trans</i> -13-Octadecenoic acid		36.08
18	29.63- 36.25	Icosapent	$\omega$ -3 Marine Triglycerides	3.28
19	51.42	Isopulegol acetate	Isopulegyl acetate	0.37
20	57.67	$\beta$ -Amyrin	Olean-12-en-3-ol, (3 $\beta$ )-	0.14

#### 4.5.1 Structures of major compounds in hexane fraction (Hexf)

The structure of some compounds of hexane fraction *Z. armatum* is presented in **Figure 36** below.

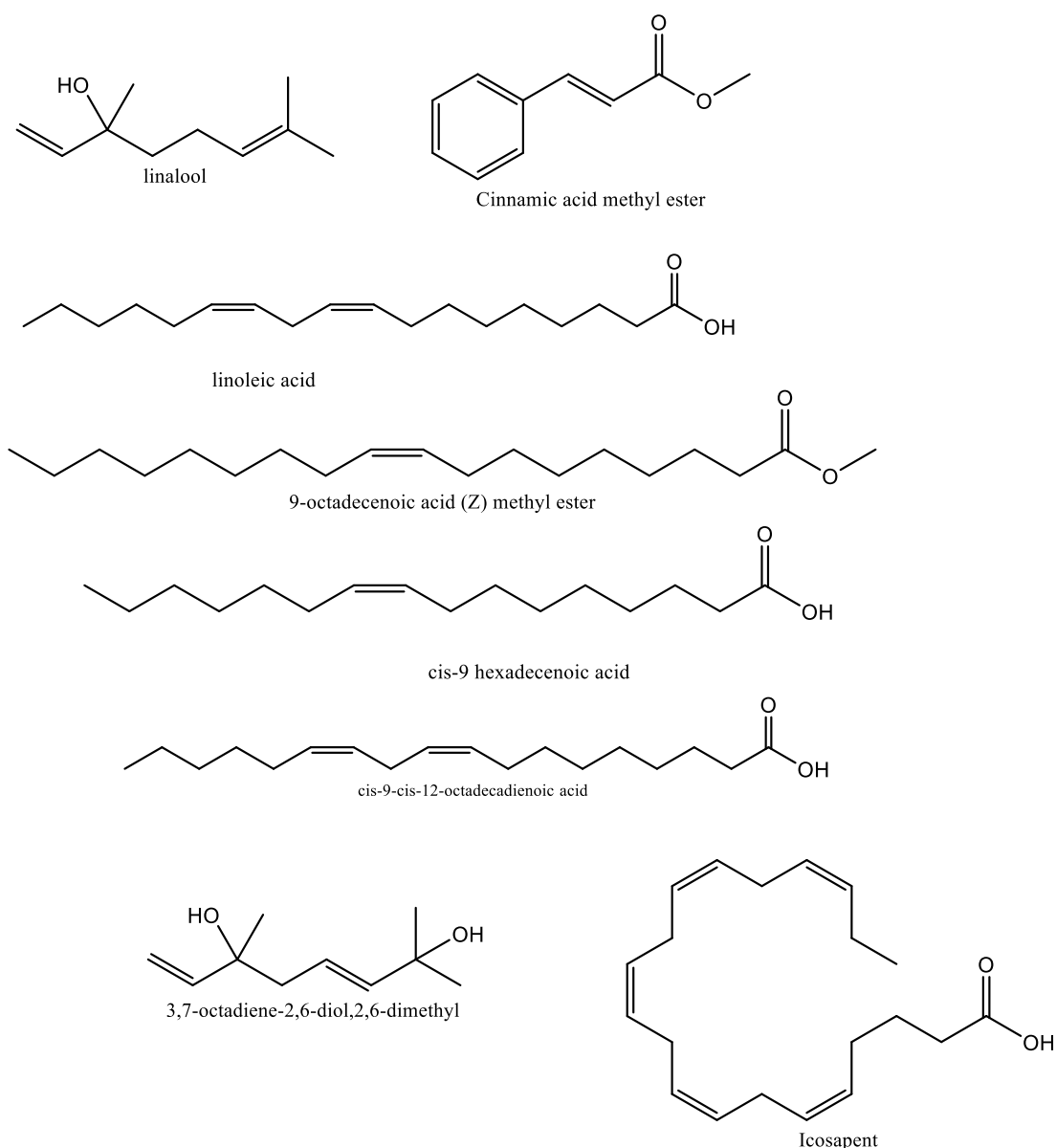


**Figure 36:** Structures of major compounds in hexane fraction

#### 4.5.2 Bioactive constituents in hexane fraction (Hexf)

Among the twenty compounds identified from the hexane fraction linalool is one of the major constituents reported with diverse activities along with palmitic acid, cinnamic acid methyl ester, methyl oleate, trans-13 –octadecenoic acid, palmitoelic acid and methyl palmitoleate. Studies show these compounds as anticancer, antibacterial, anti-inflammatory along with diverse applications.

#### 4.5.3 Major compounds of Hexf of *Z. armatum*

Predominant compounds with area percentages above 10% are presented in **Table 23** below with their name/nature, molecular weight, molecular formula, and NIST matching as observed from GC-MS.

**Table 23:** List of major compounds from hexane fraction of *Z. armatum*

Peak no	Retention time	Area %	Compound name/nature	MF/Mwt	NIST matching
7	13.51	11.08	2-propenoicacid,3 phenylmethylester(Methyl cinnamate)	C <sub>10</sub> H <sub>10</sub> O <sub>2</sub> 162	229225
13	23.81	18.66	Cis-9-hexadecenoicacid (Palmitoleic acid)	C <sub>16</sub> H <sub>30</sub> O <sub>2</sub> 254	333195
18	29.36	36.08	Trans-13-Octadecenoic acid	C <sub>18</sub> H <sub>34</sub> O <sub>2</sub> 282	333615

NB: MF: Molecular Formula, Mwt: Molecular weight

#### 4.5.4 Bioactivities on Hexf

##### 4.5.4.1 Microplate Alamar blue assay

The preliminary screening of antibacterial assay of hexane fraction revealed good percentage inhibition against *S. aureus* (65.25%) and *B. subtilis* (67.27%) only but no activity against *Escherichia coli* ATCC 25922, *Pseudomonas aeruginosa* ATCC 10145, and *Salmonella typhi* ATCC 14028. The standard drug ofloxacin possesses 91.23%. The inhibition against particular bacteria could be related to the major constituents of hexane fraction possessing a hydrophobic nature which makes it easier during partition with the lipids in the cell membrane of bacteria thus making it more permeable by disrupting the cell membrane leading to changes in cytoplasm, and leakage of critical molecules eventually causing the death of the bacterial cells (Chouhan *et al.*, 2017).

##### 4.5.4.2 Insecticidal activity

The insecticidal activity was observed using the contact toxicity method in three types of insects namely *Tribolium castaneum*, *Sitophilus oryzae*, *Rhyzopertha dominica*. The hexane fraction used for the activity was 2038.20 µg/cm<sup>2</sup> whereas the standard insecticidal drug Permethrin used was 239.5 µg/cm<sup>2</sup>. Insecticidal activity revealed hexane fractions as highly active. The percentage mortality of these insects observed was 100% against *Rhyzopertha dominica* and moderately active against *Tribolium castaneum* at 60% and *Sitophilus oryzae* at 50%. The hexane fraction of *Z. armatum* was active against *Tribolium castaneum* and *Sitophilus oryzae* but the highest activity was similar to the standard drug; in the case of *Rhyzopertha dominica* could be accounted due to the presence of acyclic monoterpenoids like linalool. **Figure 37** below

illustrates the efficacy of hexane fraction equivalent to the standard drug in the case of *Rhyzopertha dominica* along with other insects used during insecticidal activity by contact toxicity method.

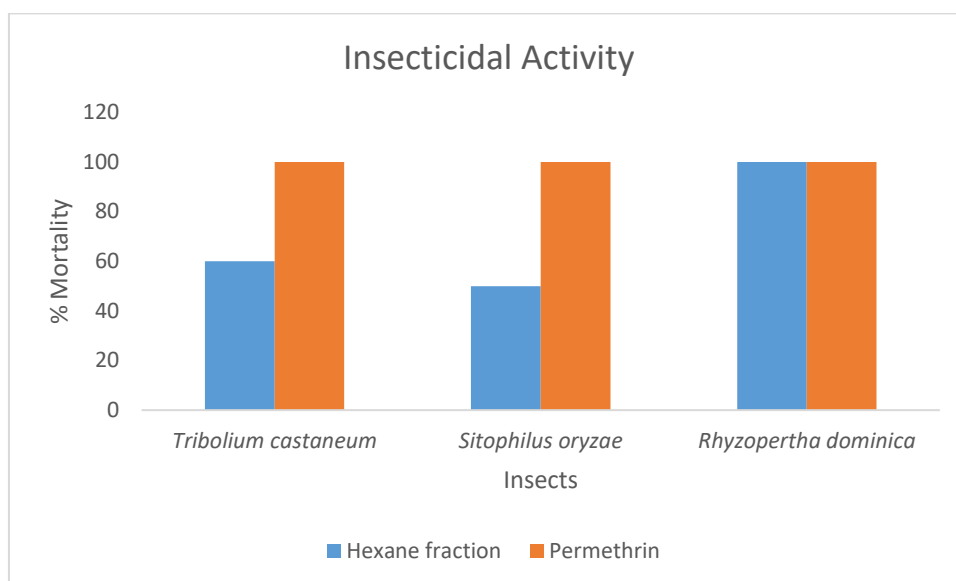


**Figure 37:** Graphical representation of percentage mortality of various insects due to hexane fraction of *Z. armatum* and standard drug permethrin

#### 4.5.4.3 Antifungal activity

*In vitro* antifungal bioassay was performed with a concentration of sample as 3000 µg/mL of DMSO with an incubation time of 7 days and temperature of 27°C. Among seven different fungus; *Trichophyton rubrum*, *Candida albicans*, *Aspergillus niger*, *Microsporiumcanis*, *Fusarium lini*, *Candida glabarata* and *Aspergillus fumigatus*. The hexane fraction was significant against *Fusarium lini* with linear growth of 15 mm, and inhibition of 85%. Standard drug Miconazole inhibited at 100% at 73.25 µg/mL as its minimum inhibitory concentration. Particular antifungal properties of *F. lini* might be due to terpenes in this fraction(Paduch *et al.*, 2007).

#### 4.5.4.4 Anti-inflammatory activity

Inflammation is a non-specific immune response that occurs after physical injury with primary symptoms as changes in blood flow, cellular metabolism and related. This disorder in some conditions leads to chronic inflammatory disease (Ferrero-Miliani *et al.*, 2007) amplifying stress in chronic condition cases disturbing the quality and productivity of life with huge financial loss (De Cássia Da Silveira *et al.*, 2013). For the anti-inflammatory activity determination 1mg of hexane fraction was used with the standard as Ibuprofen. The percentage inhibition of Ibuprofen at 25 µg/mL was (73.2 ±

1.4) % with the inhibitory capacity  $IC_{50} = 11.2 \pm 1.9 \mu\text{g/mL}$ . Likewise, the hexane fraction at  $10 \mu\text{g/mL}$  concentration inhibited 79.4% revealing potency  $IC_{50} = 11.2 \pm 1.9 \mu\text{g/mL}$ . The potency of this fraction against reactive oxygen species (ROS) might be due to the well-known anti-inflammatory compounds such as terpenes and sesquiterpenes. Studies show the use of terpenes as a skin penetration booster medium in the case of various inflammatory diseases probably supports the potency of hexane fraction (Paduch *et al.*, 2007). **Figure 38** represents the anti-inflammatory activities of hexane fraction at various concentrations and standard drug ibuprofen used.

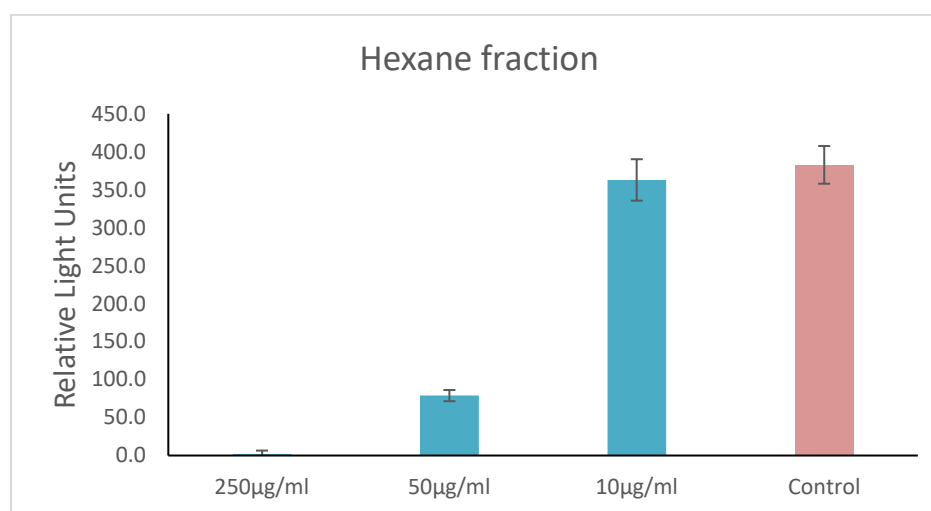


**Figure 38:** Graphical representation of hexane fraction's relative light unit against concentration

#### 4.5.5 Discussion on the bioactivity of Hexf of *Z. armatum*

This analysis of non-polar constituents using GC-MS revealed the prevalence of polyunsaturated fatty acids, their oxygenated derivatives, and terpenes. Quantitative GC-MS identified 20 phytoconstituents. The major bioactive compounds identified were 2-propenoic acid, and 3-phenylmethylester consisting of 11.08 percent of the area. Similarly, *cis*-9-Hexadecenoic acid consists of 18.66 and the largest percentage of compound 36.08 are *trans*-13-octadecenoic acid. These environmentally friendly, degradable, non-toxic bioactive compounds contribute to insecticidal and antimicrobial properties, making them potential bio-pesticides (Nefzi & Ben, 2016).

The higher mortality observed in tested insects with the n-hexane fraction is attributed to the presence of the mono-terpenoids and their unique properties. The strong order of fruits is linked to various esters and a mix of aromatic compounds. The potent properties of its volatile oil including insecticidal effects can be attributed to compounds like linalool, limonene, and lignin (Singh & Singh, 2011).

GC-MS studies of the hexane extract obtained through hot soxhlet revealed 36 phytoconstituents, with 2-hydroxy cyclopentadecanone as a major one (Kayat *et al.*, 2016) as the plant was collected from the Dhorpatan Hunting Reserve area of Nepal. Variation in GC-MS results may be influenced by the solvent, temperature, and extraction site. Compounds like unsaturated fatty acids are crucial for the early stage of neurodevelopment (Decsi *et al.*, 2002; Das, 2006). Polyunsaturated fatty acids due to their flexibility and conformational states are more significant than saturated fatty acids, as the liver prefers to convert them to ketone bodies rather than to other atherogenic lipoproteins (Beynen *et al.*, 1985; Wassall & Stillwell, 2009).

Dietary supplementation of *Z. armatum*, rich in polyunsaturated fatty acids holds practical significance. Polyunsaturated fatty acids have been employed in treating atherosclerosis and inhibiting thrombosis (Goodnight *et al.*, 1982). Together with hyperlipidemia and statin medication, they aid in lowering triglyceride levels (Zuliani *et al.*, 2009). Considering the impact of dietary saturated fatty acids on inflammation and raising low-density lipoprotein (LDL) cholesterol levels the intake of polyunsaturated fatty acids from *Z. armatum*, a plant-based source, is crucial for improving lipid profiles (Woollett & Dietschy, 1994; Poledne, 2013).

The hexane fraction's potent insecticidal, antifungal, and antimicrobial properties designate it as a potential bio-pesticide. Its specific insecticidal activity against *Rhyzopertha dominica* strongly suggests the hexane fraction of *Z. armatum* as a promising biopesticide. Thus, collective efficacy of the hexane fraction in various biological applications, including insecticidal, antibacterial, antifungal, and anti-inflammation is attributed to the presence of hydrophobic volatile organic compounds to some extent.

#### **4.6 Pharmacological studies**

The pharmacological studies include the toxicity of *Z. armatum* extract and its antidiabetic studies using animal models. In the case of extract toxicity studies two species of adult healthy animal models were used one Swiss albino mice and the other Long Evans rats were used to gather a more comprehensive understanding of the effects of various treatments. The antidiabetic studies involve only type II diabetic model Long Evans Rats. The impact of extract toxicity in LER and SAM and the anti-diabetic properties of the extract on LER are presented below.

#### 4.6.1 Acute toxicity impact on body weight of Swiss Albino Mice (SAM)

All the mice in different experimental groups were weighed at the start of the experiment, which was the initial weight. Every third day weights were taken for all groups. Finally, the weight was taken at last. The difference was recorded as a change in body weight as represented in **Figure 39**. This toxicity study on Swiss albino mice resulted in a very slight decrease in body weight on their 13<sup>th</sup> day 200 mg treated group decreased by 3%, 400 mg/kg/10 mL and 800 mg/kg/10 mL both groups decreased by 5% on the same case the water control group also decreased its weight by 8% from their baseline value. However, no significant changes were observed compared to the control group.

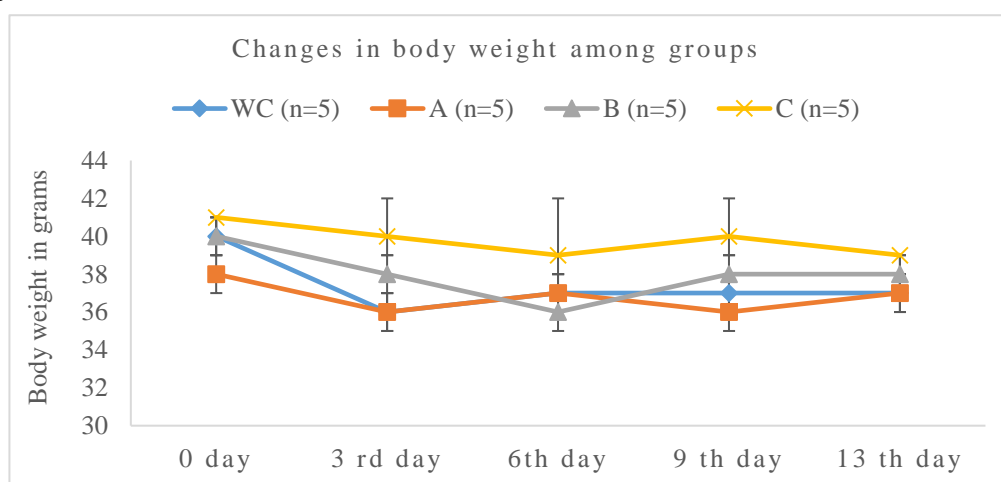


**Figure 39:** Effect of *Z. armatum* ethanol extract different doses treated, on the body weight of normal healthy mice. Group WC, A, B, and C represent water control, 200 mg, 400 mg, and 800 mg treated group mice respectively. Data presented as mean  $\pm$  standard deviation ( $M \pm SD$ ). Statistical comparison between groups was performed using a paired sample t-test.

There was no statistical difference in the mean body weight of mice between the treated and control groups from the initial to final time of the study period ( $p > 0.05$ ).

#### 4.6.2 Calculated supply of food and water

Regular observation of the feeding pattern of food and water was recorded during feeding time at 9:00 am. The water consumed/water intake was recorded as the difference in supplied volume with remaining water in the feeding bottle within 24-hour periods. The calculated amount of water provided was 10 mL for each species using a measuring cylinder in the feeding bottle with stainless steel nozzles. Similarly, food intake was also measured by providing the calculated amount of food 7.5 g/100 g/10 mL. Food consumption was measured by weighing the remaining amount of food

in the container after 24 hours from the amount supplied in grams. The predesigned cage for food supply served as food containers.

### 4.6.3 Food and water habit

Not any significant effect was observed on the food consumption habit of the mice but water consumption for the group of 400 mg and 800 mg treated groups dramatically decreased by 54% and 36% respectively.

#### 4.6.3.1 Consumed food

Consumption of food in the first three days in decreasing trend of all the extract feed groups in comparison to the control group then the intake was gradually increased to the 13<sup>th</sup> day. Dose group B had a remarkable change in food habits increased at first with a steep decrease on the 9<sup>th</sup> day and finally adjusted equal to the control group. Group doses A and C have also a change in food patterns where higher doses have higher consumption and vice-versa concerning the control group. **Figure 40** represents the food consumed by different groups during the study period.

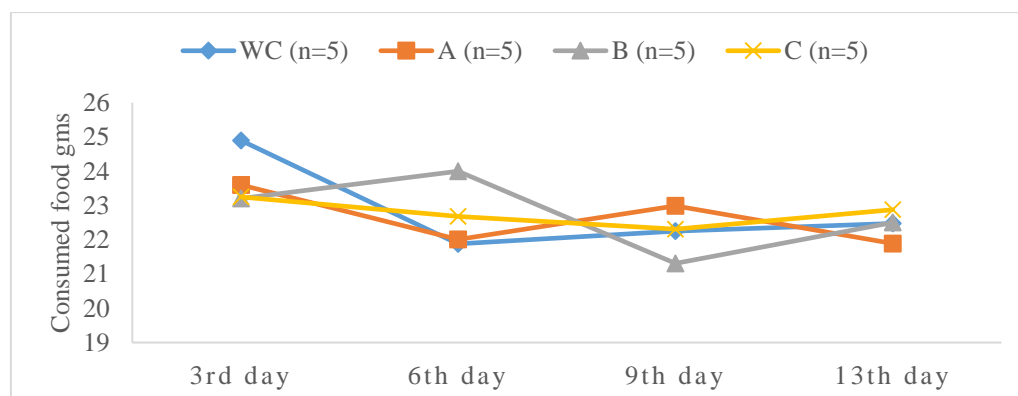


**Figure 40:** Effect of *Z. armatum* ethanol extract in different doses treated, on food consumption habits of normal healthy mice. Group WC, A, B, and C represent water control, 200 mg, 400 mg, and 800 mg treated group mice respectively. Data presented as mean  $\pm$  standard deviation ( $M \pm SD$ ). Statistical comparison between groups was performed using paired sample t-test

#### 4.6.3.2 Consumed water

Water consumption in this research can be generalized as a lower dose consuming a higher volume of water than the control while there was a remarkable reduction of water consumption in the case of higher doses. Dose feed group B had the least water intake on the final day which was reduced to less than half the required amount to their body weight. Water consumption is more significant in all the groups with lower doses consuming higher volume while intermediate doses consumed the least as represented

in **Figure 41**. The decrease in water consumption could be due to the impact of the extract.

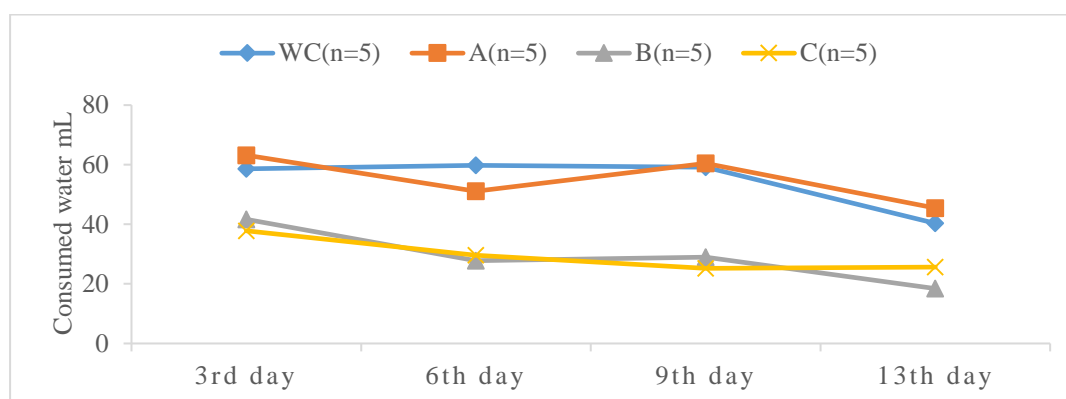


**Figure 41:** Effect of water habit on the SAM treated with *Z. armatum* ethanoic extract on different doses. Group WC, A, B and C represent water control, 200 mg, 400 mg and 800 mg treated group mice respectively. Data presented as mean  $\pm$  standard deviation ( $M \pm SD$ ). Statistical comparison between groups was performed using a paired sample t-test

#### 4.6.4 Impact on relative organ weight of Swiss Albino Mice

The relative organ weight has a slight effect: The Liver of 200 mg and 400 mg treated group decreased by 15% whereas the liver of 800 mg treated group decreased by 20% from the baseline value compared with the water control group. No effect was observed on the relative weight of the heart, kidney, and spleen but changes were observed in the pancreas of the 800 mg treated group which decreased by 25%. Significant changes were observed in the case of the liver ( $p=0.005$ ,  $0.005$ , and  $0.003$ ) in groups A, B, and C in comparison with the control group. Changes observed in the case of the pancreas were ( $p=0.572$ ) in group C with the control group. Similarly, significant changes were observed among treated dose pancreas ( $p=0.059$ ,  $p=0.062$ ) among dose A against dose C and dose B against dose C. However, no significant changes were observed in the relative organ weight of the heart, kidney, and spleen among the groups. **Figure 42** depicts the extract's effect on the relative organ weight of SAM.

The changes in the liver were significant as there was a gradual decrease in extract-treated groups compared to water control. Likewise, a decrease in relative organ weight of the pancreas of survived mice of higher doses further supports a piece of general information that there is an adverse effect of the extract on mice fed with a dose level equivalent to or higher than 800 mg/kg body weight.

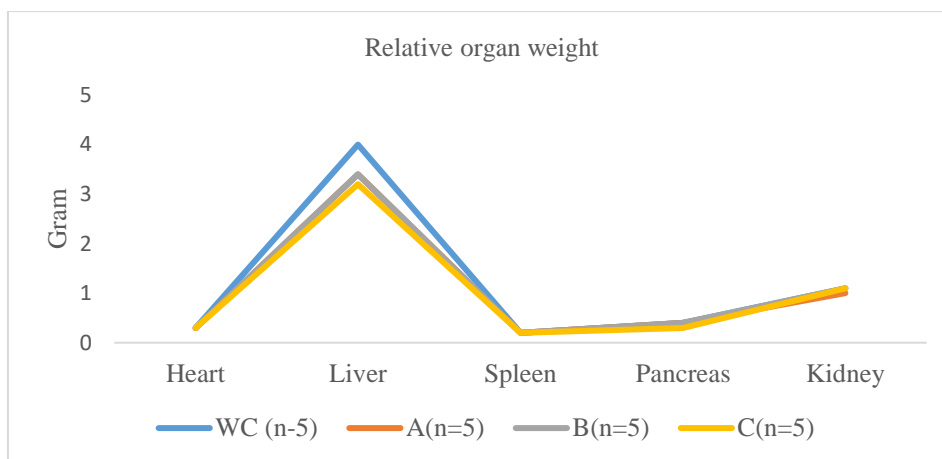


**Figure 42:** Effect of different doses of *Z. armatum* ethanolic extract on the relative organ weight of SAM on group WC, A, B and C.

WC, A, B and C represents water control, 200 mg, 400 mg and 800 mg treated group mice respectively. Data presented as mean  $\pm$  standard deviation ( $M \pm SD$ ). Statistical comparison between groups was performed using one-way ANOVA.

#### 4.6.5 Acute toxicity impact of the extract on body weight of Long Evans Rats(LER)

##### 4.6.6 Effect observed on body weight

A slight increment in body weight was observed on the 13<sup>th</sup> day of all groups including the control as well. The group treated with 400 mg had increased their weight by 25% whereas the 1600 mg and 3200 mg group had 21% and 14% increments in their body weight from their baseline value. The group treated with 200 mg and 800 mg did not affect their body weight as presented in **Figure 43**. Group B and Group D have a significant increase in body weight ( $p=0.052$ ) and ( $p=0.043$ ) compared to Group A having a stable body weight. It concludes that there is an overall increase in body weight to all extract feed groups on the last day of the experiment however more fluctuations were observed in the case of least feed dose.

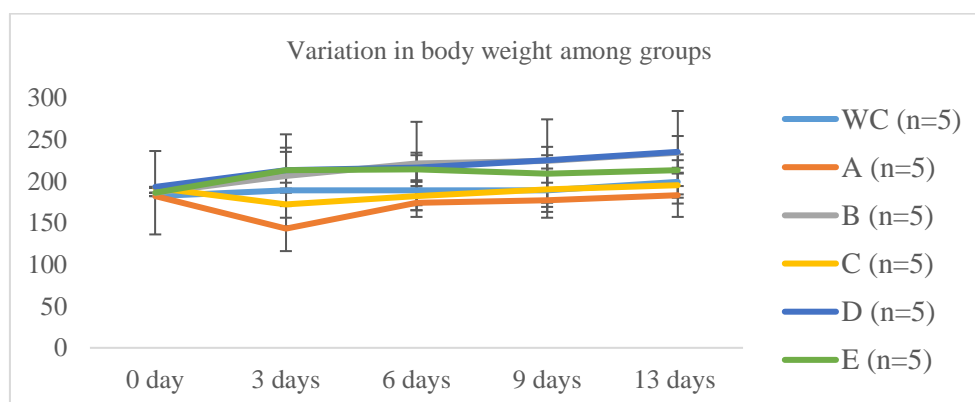


**Figure 43:** Effect of different doses of *Z. armatum* ethanolic extract, on the body weight of LER on groups WC, A, B, C, D, and E

Group WC, A, B, C, D, and E represent water control, 200 mg, 400 mg, 800 mg, 1600 mg, and 3200 mg/kg dose treated group rats respectively. Data presented as mean  $\pm$  standard deviation ( $M \pm SD$ ). Statistical comparison between groups was performed using one-way ANOVA.

#### 4.6.7 Feeding pattern of Long Evans Rats

Rats possess a good sense of communication skills with their members especially in regards to food as they are neophobic as well in comparison to their wild varieties. (Wishaw I, 2005). In the case of food consumption, there was an increment in their food intake since the third day in all groups except the group treated with 800 mg which had a decrease in food consumption habit by 44%. But in the case of water consumption, there was a decrease in the first week followed by an increment in the last week in the case of all the groups. **Figure 44** graphically represents the effect of different doses of *Z. armatum* ethanolic extract, on the food habit, and **Figure 45** represents the effect on the water consumption habit of normal healthy LER.

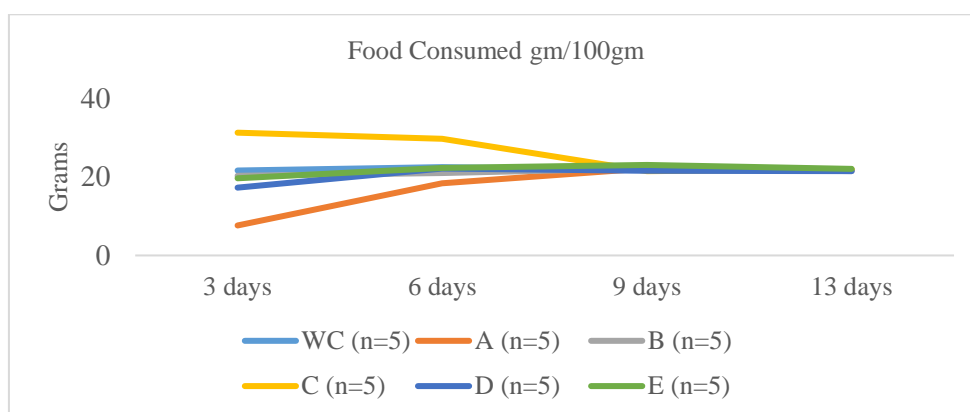


**Figure 44:** Effect of different doses of *Z. armatum* ethanolic extract, on the food habit of normal healthy LER. Group WC, A, B, C, D, and E represent water control, 200 mg, 400 mg, 800 mg, 1600 mg, and 3200 mg/kg dose treated group rats respectively. Data represented as mean

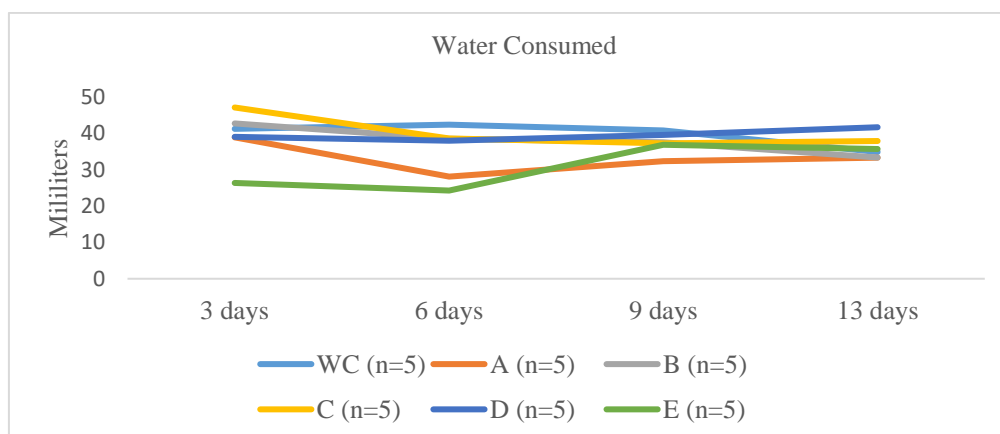


**Figure 45:** Effect of *Z. armatum* ethanol extract in different doses treated, on the water consumption of normal healthy rats Group WC, A, B, C, D, and E represents water control, 200 mg, 400 mg, 800 mg, 1600 mg, and 3200 mg/kg dose treated group rats respectively. Data represented as mean

#### 4.6.8 Observation of relative organ weight among the groups (g/100gm)

At the end of the experiment sacrifice of the live rats was carried out to observe the effect on relative organ weight. The graphical representation of the effect of *Z. armatum* ethanoic extract on different doses of treated LERs' relative organ weight is represented in **Figure 46**.

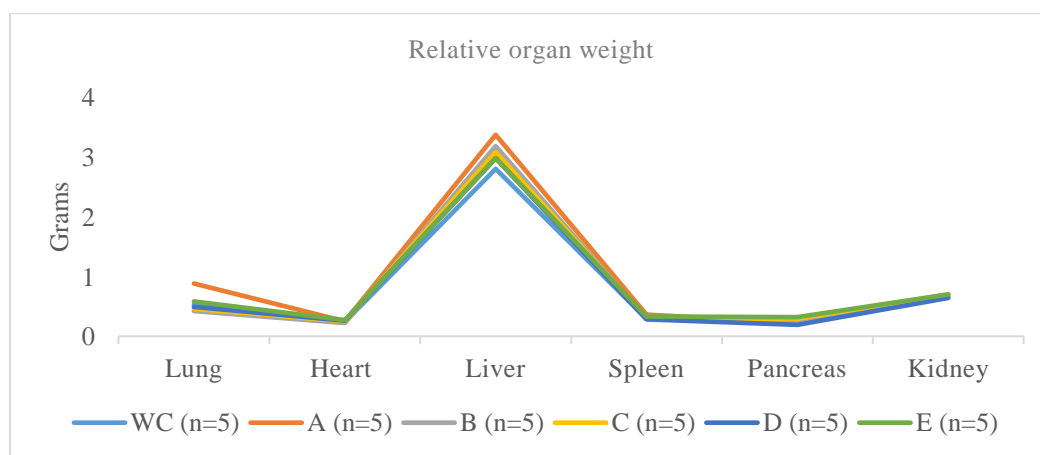


**Figure 46:** Effect of *Z. armatum* ethanoic extract on different doses of treated LERs' relative organ weight

Group WC, A, B, C, D, and E represent water control, 200 mg, 400 mg, 800 mg, 1600 mg, and 3200 mg/kg dose treated group rats respectively. Data presented as mean  $\pm$  standard deviation ( $M \pm SD$ ). Statistical comparison between groups was performed using one-way ANOVA

#### 4.6.9 Effect on relative organ weight

The organ weight was taken after defatting them in normal saline immediately after sacrifice on the final day after the completion of the toxicity test on the 14<sup>th</sup> day. Observation shows a slight effect on comparison with the water control group.

**Lungs:** The group treated with 200 mg and 3200 mg had an incremental effect on their lungs by 66% and 9% respectively whereas there was a decrease in the lung weight of 400 mg, 800 mg, and 1600 mg treated group by 21%, 14%, and 8% respectively.

**Heart:** The 200 mg treated group had an increment in heart weight by 4%, whereas the 400 mg group had decreased their heart weight by 9%, the 800 mg group increased by 4%, the 1600 mg increased by 8%, and the 3200 mg increased by 12% respectively from the baseline value compared with the water control group.

**Liver:** The liver; one of the largest organs is responsible for the metabolism process of intake of food and drug so a healthy liver resembles a healthy animal model. Any disease in the liver is life-threatening as health is associated with different autoimmune disorders such as viral infection, toxic chemical or food intake, and changing feeding habits (Bhakuni *et al.*, 2016). So, the status of a healthy liver is determined by

biochemical markers where pathological changes can be observed by the increase in hormones such as SGOT and SGPT. In this research study the least dose-treated group had a 20% increment in relative liver weight, the 400 mg group had a 13% increment, the 800 mg had a 10% increment, and the 1600 mg and 3200 mg group had 6% increment in their relative weight of liver.

**Spleen:** No such significant effect was observed on the relative weight of the spleen in the group treated with 400 mg and 800 mg whereas there was an increase of 24% in the group with 200 mg and a 13% increase in the group of 3200 mg.

**Pancreas:** The group treated with 200 mg and 400 mg had decreased in their relative weight by 22%, no significant effect was observed in the group treated with 800 mg, a 33% decrease was observed in the 1600 mg treated group, and 13% increase on group treated with 3200 mg.

**Kidney:** There was no significant effect on the relative weight of the kidney in all the treated groups.

#### 4.6.10 Mortality observation and determination of LD<sub>50</sub>

Lethal dose calculation depends on two consecutive doses occurring mortality. In this, study there is mortality in the case of mice fed with doses 800, 1600, and 3200 mg respectively whereas there is mortality observed on the dose feed day at dose level 1600 mg and no mortality in other groups. **Table 24.** Below is the mortality in mice and rats concerning the feed dose.

**Table 24:** Mortality in Long Evans rats and Swiss albino mice with respect to the feed dose level

Group	Dose mg/kg/bodyweight	Mortality mice	Mortality rats
A	200	0/5	0/5
B	400	0/5	0/5
C	800	2/5	0/5
D	1600	5/5	1/5
E	3200	5/5	0/5
WC	Control	0/5	0/5

As the effect was observed to the extent of lethality in the case of Swiss albino mice, so determination of lethal dose 50 seems fundamental to progress the research. LD<sub>50</sub> is calculated (Lorke, 1983) formula as:

$$LD_{50} = \sqrt{D_0 \times D_{100}}$$

$D_0$  = Highest dose that gave no mortality,  $D_{100}$  = Lowest dose that produced mortality within 24 hours of drug administration. During our acute toxicity, immediate toxicity observation resulted in no mortality for the feed dose of 200 mg and 400 mg/kg bd. wt. treated group mice while 2 mice were died immediately that were fed with a dose of 800 mg, whereas all mice of 1600 and 3200 mg treated groups died within a few minutes of feed. Since  $D_0=400$  mg,  $D_{100}= 800$  mg. So, the calculated  $LD_{50}$  value is 565.68 mg for the Swiss Albino Mice.

#### **4.6.11 Histopathological studies**

The histopathological studies on samples of the sacrificed Swiss albino mice revealed the normal condition of the liver, pancreas, and kidney in the case of the 200 mg feed group. The higher the doses higher the inflammatory changes and polymorphs were observed in the liver. Similarly, degenerative changes and necrosis were observed in the case of the pancreas with a normal kidney on the group feed with 400 mg. Likewise, the group feed with the dose of 800 mg possesses inflammatory changes and polymorphs in the liver. Inflammatory changes and polymorphs were higher in the case of the pancreas of this group. Remarkable inflammatory changes and necrosis were observed in the kidney in this group. However slight necrosis in the liver, inflammatory changes, and polymorphs in the case of the pancreas and kidney were observed in the control group as well suggesting such conditions to be normal in the experimental models under study. The photomicrographs in **Figure 47** represent the images of vital organs liver, pancreas, and kidney of SAM of 200 mg, 400 mg, 800 mg, and water control group.

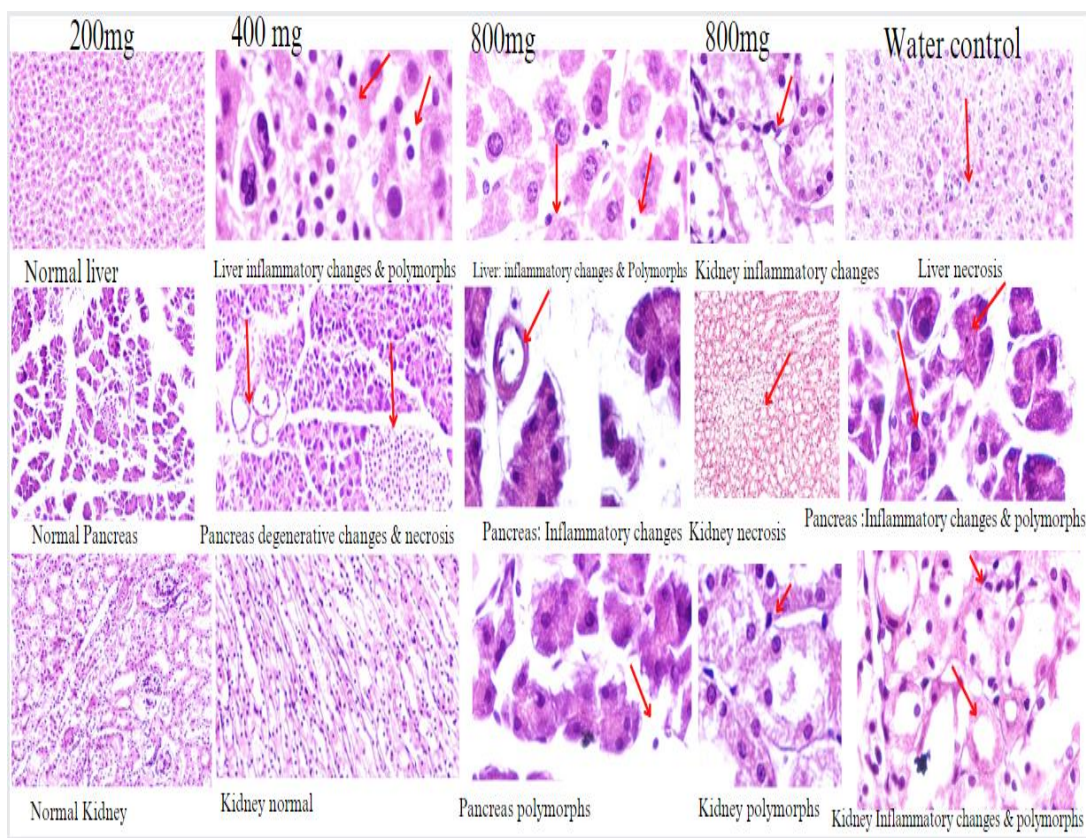


**Figure 47:** Histopathological images of vital organs liver, pancreas, and kidney of SAM of 200 mg, 400 mg, 800 mg, and water control group

#### 4.6.12 Comparison and discussion about *Z. armatum* extract toxicity

Toxicity studies on rodents as well as non-rodents have many significant associations with human toxicities that finally assist in many pharmaceutical benefits (Olson *et al.*, 2000). This acute toxicity study revealed vital organs such as the liver, pancreas, and kidney through histopathological observation to be unsafe at higher levels. Generally, toxicity involves a higher dose of extract/test material for determining acute toxicity and basic toxicological research parameters like serum biochemical observation focus on liver damage in preclinical toxicity (Ramaiah, 2007). Though the excess level of elements causes toxicity however plants do require a trace amount of some metal to maintain metabolism (Nagajyoti *et al.*, 2010). Elemental analysis of *Z. armatum* fruit dominantly consists of K and Ca whereas S, Fe, Si, Cl, Mn, Zn, Cu, Ti, Rb, and Br were in traces and were free from toxic levels of heavy metals. Similar to previous studies fruit possesses elements like K, Na, Zn, Fe, Cu, Mn, and additionally Ni, Cr elements in decreasing order. Elements like Zn, Mn, and Cr thus justify to hypoglycemic potential of this plant (Ibrar *et al.*, 2015). Present geometric ratio of toxicity used (200-3200) mg/kg bdtw of extract for oral feeding. Study revealed 400 mg/kg did not caused

any mortality or visible signs of toxicity in Swiss Albino mice till 14 days. Survival of all Long Evans rats suggests LD<sub>50</sub> is predictably higher than 3200 mg/kg body weight. Initially, the extract at 1.25 gm/kg/10 mL resulted in lethality in rats of type II models. Hence this research is analogous to studies on the compound tambulin from the same plant that worked exclusively at higher glucose concentrations; but not at basal ones(Hameed *et al.*, 2019). The present result of the LD<sub>50</sub> value of 565.68 mg/kg body weight applies only in the case of healthy Swiss albino mice. The decrease in body weight of all the mice at the end of the study period contradicts that from similar studies reported on this plant-based in Pakistan. The study revealed that diabetes-induced mice fed with an oral dose of 500 mg/kg showed a decrease in body weight and an increase in normal ones(Alam *et al.*, 2018). Further, the single dose level up to 3200 mg/kg body weight to healthy Long Evans rats resulted in no such recordable changes like the normal ones with slight fluctuations in between.

#### **4.7 Antidiabetic activities of *Z. armatum* extract on type II Long Evans rats**

##### **4.7.1 Dose variant effect of *Z. armatum* extract on hypoglycemic properties of type II model Long Evans Rats**

During the experimental period, the body weight of different groups was recorded as depicted in **Figure 48**. Initial body weight (g) were [201 ± 7.4, 191 ± 16, 192 ± 16.9, 270 ± 20, 191 ± 19.8] (Mean ± SD) of NWC, DWC, GT, ZaE1 and ZaE2 treated groups respectively. At the end of the experiment, slight increments in the body weight were recorded in each group as: 215 ± 3.0 (↑6%), 206 ± 28.4 (↑7%), 206 ± 26.4 (↑7%), 284 ± 25 (↑5%), 208 ± 31.9 (↑8%) respectively. However, no significant changes were observed in their body weight when compared with their corresponding baseline values. During the period of study, all experimental rats increased their body weight by 5-8% gradually.

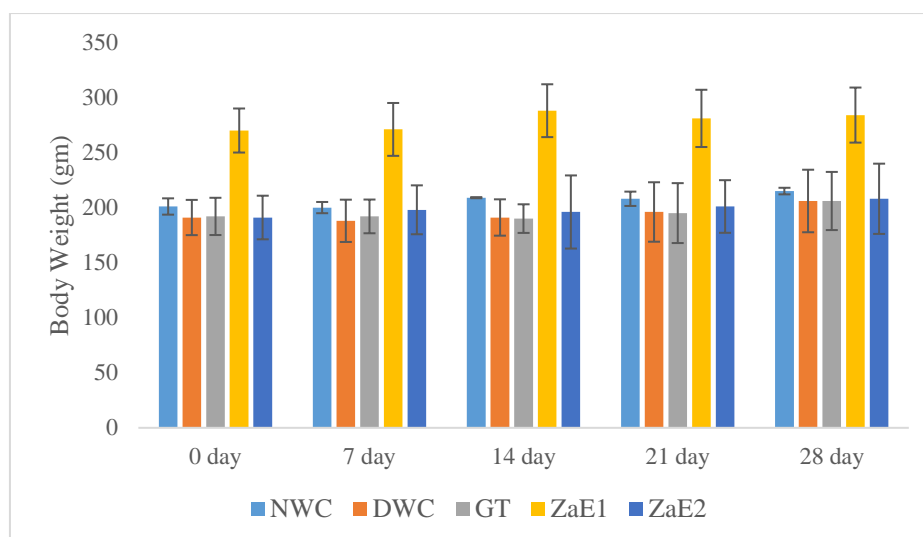


**Figure 48:** Effect of treated groups on the body weight of normal and type II diabetic model rats. Data presented as mean  $\pm$  standard deviation ( $M \pm SD$ ). Statistical comparison between groups was performed using a paired sample t-test.

#### 4.7.2 Effect of *Z. armatum* extract on fasting serum glucose level

Chronic effects of *Z. armatum* on serum glucose levels of different treated experimental groups measured were presented below in **Table 25**. Decreases in the baseline Fasting Serum Glucose (FSG) levels were observed after 28 days of consecutive oral feeding of ZaE1 and ZaE2, [ $6.30 \pm 0.77$  ( $\downarrow 20\%$ ), and  $5.54 \pm 0.42$  ( $\downarrow 27\%$ )] respectively. Significant changes in FSG were observed ( $p < 0.02$ ,  $p < 0.04$ ) in both doses compared to their baseline values. Statistical significance of ZaE2 over DWC was observed ( $p < 0.02$ ). Similarly, positive control group GT signifies ( $p < 0.003$ ) to its baseline value. This FSG level indicates the potency of the extract as an excellent source of anti-diabetic properties.

**Table 25:** Fasting serum glucose level in different groups of type-II diabetic model rats

Groups	Fasting serum glucose level (mmol/L)	
	0 day (100%)	28day
NWC (n=6)	$6.44 \pm 0.43$	$6.74 \pm 1.06$ (104%)
DWC(n=6)	$8.17 \pm 2.70$	$8.32 \pm 1.89$ (101%)
GT(n=6)	$8.67 \pm 0.30$	$6.95 \pm 1.20$ (80%)
ZaE1(n=6)	$7.84 \pm 1.63$	$6.30 \pm 0.77$ (80%)**
ZaE2(n=6)	$7.52 \pm 1.49$	$5.54 \pm 0.42$ (73%)* $\psi$

Data presented as mean  $\pm$  standard deviation ( $M \pm SD$ ). Statistical comparison between groups was performed using one-way ANOVA and paired sample t-test. \* $p < 0.04$  (0 vs 28 days), \*\* $p < 0.02$  (0 vs 28 day),  $\psi p < 0.02$  (ZaE2 vs DWC).

### 4.7.3 Effect of *Z. armatum* extract on lipid profile

The impact of extracts treated was observed on lipid profile as depicted below in **Figure 49** and **Figure 50**. Changes observed in triglyceride level of NWC, DWC, GT, ZaE1 and ZaE2 treated groups were [(68.68±5.36) & (74.22±0.19) (↑8%)], [(70.30±4.11)&(73.61±10.39)(↑3%)], [(75.98±3.13) & (70.14±9.72) (↓8%)], [(170.22±2.92) & (86.71±6.71) (↓50%)], [(112.91±6.82) & (84.14± 5.03) (↓26%)] respectively. Statistically significant changes were observed in ZaE1 and ZaE2 ( $p<0.001$ ,  $p<0.001$ ). Similarly changes observed in total cholesterol level were [(59.60±8.23) & (63.57±5.97) (↑6%)], [(55.70±8.76) & (63.74±4.41) (↑14%)], [(72.27±6.37) & (63.52±4.41) (↓13%)], [(62.75±4.99) & (59.16±4.4) (↓6%)], [(83.97±2.60) & (66.19±1.65) (↓22%)] in the respective groups. Changes observed in HDL level were [(27.05±3.32)& (25.68±1.07)(↓6%)], [(28.04±5.67)&(25.78±0.87) (↓9%)], [(27.58±2.00) &(33.25±3.97)( ↑20%)], [(21.52±1.21) & (23.02±0.68)(↑6%)],[ (26.33±3.18)&(30.02±4.12)(↑14%)] respectively. Corresponding changes and reduction on LDL observed were [(17.19±2.40) & (19.55±2.72) (↑15%)], [(13.17±3.61) & (15.26±6.69) (↑15%)], [(23.80±2.84) & (14.46±2.76) (↓40%)], [(15.33±1.66) & (10.53±1.30) (↓32%)], [(29.11±2.72) & (24.53±2.02) (↓16%)]. HDL cholesterol level increased significantly ( $p<0.02$ ) in ZaE2 corresponding to its baseline value. Similar positive impacts were observed with more significant changes ( $p<0.01$ ) compared to ZaE1. LDL cholesterol levels were significantly ( $p<0.01$ ,  $p<0.004$ ) reduced in both doses when compared to corresponding baseline values.

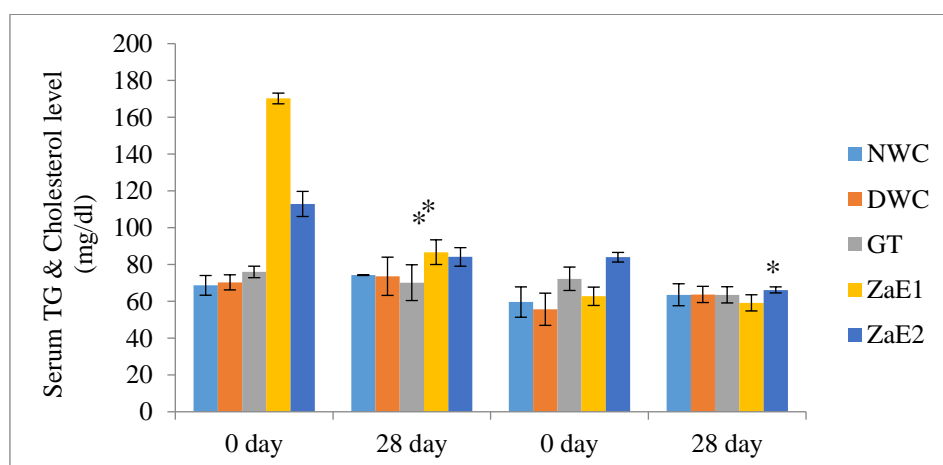


**Figure 49:** Effect of Serum TG & Cholesterol level (mg/dl) on treated groups of normal and type II diabetic model rats. Data presented as mean ± standard deviation (M ± SD). Statistical comparison between groups was performed using one-way ANOVA and paired sample t-test. \* $p<0.001$ .

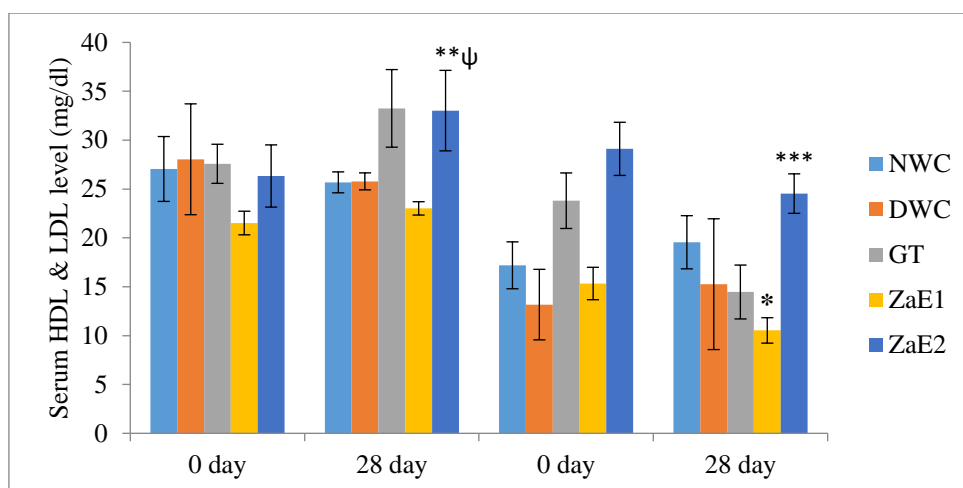


**Figure 50:** Effect of Serum HDL & LDL level (mg/dl) on treated groups of normal and type II diabetic model rats. Data presented as mean  $\pm$  standard deviation ( $M \pm SD$ ). Statistical comparison between groups was performed using one-way ANOVA and paired sample t-test. \* $p < 0.001$ .

#### 4.7.4 Effect of *Z. armatum* methanol extract on TG: HDL and TC: HDL

The ratio of Triglycerides: High-Density Lipoprotein (HDL) ratio and Total cholesterol: HDL ratio level is demonstrated in **Table 26**. On the final day of the experimental period, TG: HDL ratio was significantly ( $p < 0.001$  &  $p < 0.007$ ) and reduced in both doses treated groups. Moreover, TC: HDL level was statistically significant ( $p < 0.001$  &  $p < 0.001$ ) represented by a decrease in both doses treated groups compared to the corresponding initial ones.

**Table 26:** Effects of *Z. armatum* extracts on TG : HDL & TC : HDL ratio

Group	TG : HDL		TC : HDL	
	0 day	28 day	0 day	28 day
NWC	2.56 $\pm$ 0.27	2.89 $\pm$ 0.12	2.23 $\pm$ 0.45	2.48 $\pm$ 0.28
DWC	2.68 $\pm$ 0.55	2.91 $\pm$ 0.41	2.00 $\pm$ 0.16	2.47 $\pm$ 0.19
GT	2.76 $\pm$ 0.23	2.14 $\pm$ 0.41	2.62 $\pm$ 0.23	1.92 $\pm$ 0.20
ZaE1	7.92 $\pm$ 0.42	3.77 $\pm$ 0.35**	2.91 $\pm$ 0.18	2.57 $\pm$ 0.18**
ZaE2	4.32 $\pm$ 0.436	2.34 $\pm$ 1.17*	3.21 $\pm$ 0.30	2.23 $\pm$ 0.25**

Data presented as mean  $\pm$  standard deviation ( $M \pm SD$ ). Statistical comparison between groups was performed using a paired sample t-test. \* $p < 0.001$ , \*\* $p < 0.007$  (0 day vs 28<sup>th</sup> days).

#### 4.7.5 Effect of *Z. armatum* extract on liver glycogen level

The chronic effect of *Z. armatum* extracts on hepatic glycogen content of type 2 diabetic model rats was presented in **Figure 51**. After 28<sup>th</sup> days of regular feeding of *Z. armatum* hepatic glycogen content was measured. At the end of the experiments, the hepatic glycogen content of NWC, DWC, GT, ZaE1, and ZaE2 treated groups were (15.92  $\pm$

0.84),  $(14.03 \pm 4.02)$ ,  $21.89 \pm 1.41$ ,  $16.17 \pm 1.13$ ,  $19.01 \pm 0.90$  respectively. Positive control-treated group gliclazide showed a 56% increase hepatic glycogen levels compared to the DWC. ZaE1 treatment also significantly increased hepatic glycogen content compared to the gliclazide group ( $p < 0.02$ ). ZaE2 treated group showed a 35% increase in hepatic glycogen content compared to the DWC group, with a p-value of 0.06, indicating a trend towards significance.

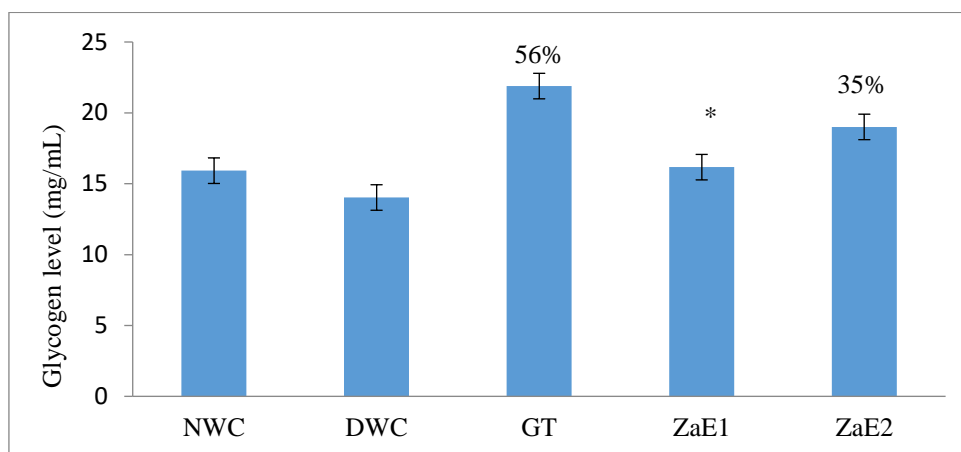


**Figure 51:** Effect of Hepatic Glycogen level (mg/mL) on treated groups of normal and type II diabetic model rats. Data presented as mean  $\pm$  standard deviation ( $M \pm SD$ ). Statistical comparison between groups was performed using a paired sample t-test.

#### 4.7.6 Effect on hepatic enzyme SGPT and SGOT of type II LER

The liver is the largest organ involved in the metabolism of all food and drugs. Hence diseases related to the liver are life-threatening. Health status is reflected through the biomarkers that can be assayed in biological fluids and observed as pathological changes. (Bhakuni *et al.*, 2016). Conditions like necrosis, steatosis, cholestasis, and vascular disorders arise due to various peripheral proteins released in response to cellular damage causing hepatotoxicity. Enzymes such as SGOT/ALT and SGPT/AST are cytosolic markers of liver injury indicated by pathological changes in enzymes reflecting hepatic impairment can also be caused by their food intake (Amacher, 2002). SGOT/ALT is found in the liver and other vital organs such as the heart, brain, kidney and in muscle that supports producing proteins and is also helpful for detecting acute and chronic hepatic injury but not its severity (Dufour *et al.*, 2000). Injury in any such cases to any tissue can cause an increase of these enzymes in blood level (Bhakuni *et al.*, 2016). The present study after the causative treatment shows that SGPT levels were increased in all groups as depicted in the figure. Despite the rise in level in all

experimental models the level rise of the group treated with extracts ZaE1 and ZaE2 is significantly lower. Enzyme SGPT plays an important role in amino acid metabolism and gluconeogenesis. It is also one of the reliable biomarkers of hepatotoxicity(Bhakuni *et al.*, 2016).

The result indicates the SGOT level of the 0-day value of treated rats with its 28<sup>th</sup> as an increment in all groups graphically represented in **Figure 52**. However, in comparing doses, ZaE1 and ZaE2 SGOT values of the treated group were lower than the standard drug-treated and control group. This observation reflects that the extract-treated group has a relatively lowering impact on hepatic enzymes SGPT and SGOT than the control ones, indicating the extract's efficacy.

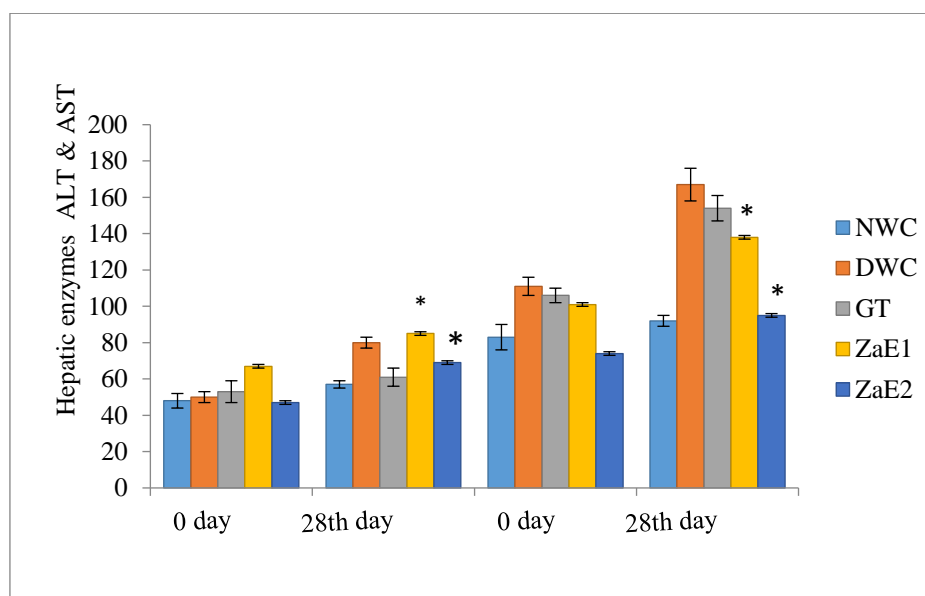


**Figure 52:** Chronic effects of *Z. armatum* on the SGPT & SGOT on type-2 diabetic model rats

In general ALT/SGOT is released in every group increased levels of liver enzymes were observed finally even in the positive control ones. However, a lower level in the case of extract feed in comparison to the GT-treated group signifies the importance of extract as hepatoprotective. The extract feed group reflects better than the group treated with positive control in the enzyme levels of SGOT especially ZaE2 in comparison. Similarly, the case of AGPT/AST levels was also similar to GT. Compared to DWC, the level of AST in extract feed ZaE1 and ZaE2 were lower which is also significant. When comparing ZaE1 and ZaE2 combined effects were observed in both groups significantly.

#### **4.7.7 Discussion on the effect of antidiabetic properties of methanolic extract of *Z. armatum***

*Z. armatum* is one of the highly valued natural plants of interest not only to local people but also to researchers as well. Research on the same species of various topography has variations in results. The present study on *Z. armatum* of Nepali origin has proven the minimum dose level of extract feed, i.e., 25 mg/kg b.w, and 50 mg/kg b.w in the animal models with significant effects as an antidiabetic property. Similar research reported on higher doses on mice and rat were 200mg/kg b.w., 250 mg/kg b.w., 400 mg/kg b.w, 500 mg/kg b.w and above on bark, leaf, and fruit of *Z. armatum* from India and Pakistan origin were proven to be good antidiabetic doses (Karki *et al.*, 2014; Rynjah *et al.*; 2018; Alam *et al.*; 2018).

##### **4.7.7.1 Glucose lowering**

Reduction in blood glucose of the extract feed group ZaE1 and ZaE2 proves its effectiveness as equal to and more than the standard drug gliclazide. The feed group of ZaE1 has a similar value of serum glucose level in comparison to the GT-treated group. ZaE2 is more effective in lowering blood glucose than ZaE1 and even more effective than the standard drug GT. Significant improvement in blood glucose levels by the treatment of extracts doses ZaE2 ( $P < 0.041$ ) was observed. A reduction in serum glucose level by more than 25% was observed in this group. On comparing both groups, diabetic water control with ZaE2, the impact observed was significant ( $P < 0.021$ ). The gradual pattern of decrease in blood glucose of extract-treated groups was similar to standard drug-treated ones. This potency of *Z. armatum* extract indicates it's one of the hypoglycemic properties probably through multiple biological pathways simultaneously.

##### **4.7.7.2 Lipid profile**

Lipid profile conveys an important message in the case of in-vivo diabetic models depending on their type of feed. The significant difference in total cholesterol and triglyceride levels was observed in groups ZaE1 and ZaE2 and were compared with other groups NWC, DWC, and GT. Triglyceride decreased by 50% in the case of ZaE1 and in the case of ZaE2 it decreased nearly by 25% indicating the effectiveness in extract and relative significance ( $p < 0.001$  and  $p < 0.001$ ) on its 0 day to 28<sup>th</sup> days value in the same group. The lowering of cholesterol by *Z. armatum* was more pronounced by dose ZaE2 than its corresponding lower dose ( $p < 0.001$ ). Extract with ZaE2 is more

significant ( $p < 0.001$ ) than standard drug ( $p < 0.051$ ). Thus, a combined effect of lowering cholesterol and triglycerides of the extract-treated group in the case of lipid profile signifies the potency of this plant. The high-density lipoprotein (HDL) is one of the strongest indicators of a lipid profile that lowers the risk of coronary heart disease. HDL of the ZaE1 feed group slightly increased, whereas ZaE2 was more prominent ( $p < 0.025$ ) in comparison to the standard drug ( $p < 0.046$ ). Another supporting parameter for the extract on improving serum lipid profile is the decrease in LDL values. LDL values of ZaE1 have a similar impact as that of standard drugs whereas ZaE2 decreases by 16% ( $p < 0.004$ ). Comparing both the doses concerning high-density lipoprotein profile ZaE2 is more effective in treating the diabetic model rats among groups revealing its significance ( $p < 0.014$ ). These improvements in the lipid profile of diabetic model rats also signify the importance of the fruits of *Z. armatum*. The treatment of ZaE1 and ZaE2 extract significantly lowered the levels of total cholesterol, and low-density lipoprotein and ironically increased essential high-density lipoprotein collectively supports plant to be one of the medicinal plants to treat hyperlipidemia.

#### **4.7.7.3 Hepatoprotective effect**

Hepatoprotective studies in animal models generally involve studies in chemical biomarkers and histopathological slides of liver tissue. Impact on liver glycogen and changes in serum markers SGOT and SGPT with the minimum dose level of ZaE1 and ZaE2 were observed. Both doses were proven to be effective in comparison to diabetic water control and satisfactory in comparison to the standard drug-treated group. The impact could be accredited to the various phytochemicals and their synergetic effect. Previous research claimed hepatoprotective activity of its leaves in ccl4 induced hepatotoxicity in rats. Such rats were fed with defatted leaves of *Z. armatum* extract at the dose level of 500mg/kg which resulted in a significant decrease in liver enzymes such as SGOT and SGPT as well as liver inflammation (Verma & Khosa, 2010). Another study on ethanoic extract of the same plant at dose levels 100, 200, and 400mg/kg proved significant protective effects against hepatotoxicity induced by ccl4 were indicated by a proportionate increase in levels of antioxidant enzymes such as superoxide dismutase, catalase, and glutathione (Ranawat *et al.*, 2010). The present study claims both ZaE1 and ZaE2 as the minimum dose of in-vivo studies so far on fruits of *Z. armatum* with efficacy as a hepatoprotective plant.

#### 4.8 Molecular docking studies on compounds 1 and 2 with 1CX-2

The Autodock vina was used to perform molecular docking. The protocol was validated by re-docking the extracted compound (SC-558) from 1CX2 to its same position. The overlay of the conformer of the SC-558 before and after docking is pictured in **Figure 53**, and its RMSD value was found to be  $< 2 \text{ \AA}$ . Compounds **1** and **2** and the standard anti-inflammatory ibuprofen were docked into the binding cavity of COX-2. Compound **1** reported perfect binding to the active site of COX-2 with a binding affinity of  $-8.4 \text{ kcal/mol}$  as compared to the standard ibuprofen's affinity of  $-7.7 \text{ kcal/mol}$ . The binding was supported by the hydrogen bonding between HIS388 and ASN382 to the oxygen atom of **1**. Some pi-interactions further assisted the binding with LEU390, ALA199, LEU391, HIS214, HIS386, and HIS207. **Figure 54 (a)** depicts the 2D diagram of the interaction of tambulin and amino acid residues. Binding affinity for **2** was found to be  $-8.6 \text{ kcal/mol}$ , as compared to the ibuprofen's affinity of  $-7.7 \text{ kcal/mol}$ . HIS388, ASN382, and TYR385 form hydrogen bonds with oxygen and hydrogen atoms of the **2**. At the same time, a couple of pi-interactions were observed with HIS386, HIS 207, ALA 199, and LEU 390. The 2D and 3D representation of the binding interaction of enzyme (1CX2) with **1**, **2** and ibuprofen is shown in **Figure 54**.

#### 4.9 Drug-likeness and ADMET analysis

The isolated compounds **1** and **2** have molecular weights of  $344.32 \text{ g/mol}$  and  $330.29 \text{ g/mol}$ , respectively, and a topological polar surface area (TPSA) of  $98.36 \text{ \AA}^2$  and  $109.36 \text{ \AA}^2$ , which is an acceptable criterion for being a drug candidate as suggested by Lipinski's rule of five. Both compounds did not violate any rules for drug-likeness, as suggested by Lipinski, Ghose, Veber, Egan, and Muegge, with both compounds having a bioavailability score of 0.55. Inhibition of these cytochromes enzymes is the main mechanism that causes pharmacokinetic drug-drug interactions (Wang *et al.* 2015; Hakkola *et al.* 2020). As the Swiss ADME web server predicted, **1** and **2** were foreseen to inhibit enzymes CYP12, CYP2C9, CYP2D6, and CYP3A4. In addition, it also indicated that both compounds are non-inhibitors of the enzyme CYP2C19. Both compounds have high gastrointestinal absorption. Compounds **1** and **2** tested for no blood-brain barrier penetration levels, which means both compounds would not have CNS negative effects. Moreover, compounds are necessary to test for toxicity. Both **1** and **2** were also found to have no AMES toxicity, skin sensitization, and hepatotoxicity, as predicted by the pkCSM web server. The ADMET properties of compounds **1** and **2**

are presented in **Table 27**, and the mol-inspiration enzyme inhibition score in **Table 28**. This table displays activities with a specific focus on enzyme inhibition by compounds 1 & 2 since the *in-silico* studies were carried out after the compounds' potent activities were observed in *in vitro*. Both studies contribute differently to a comprehensive understanding of compounds and their properties in designing a drug candidate.

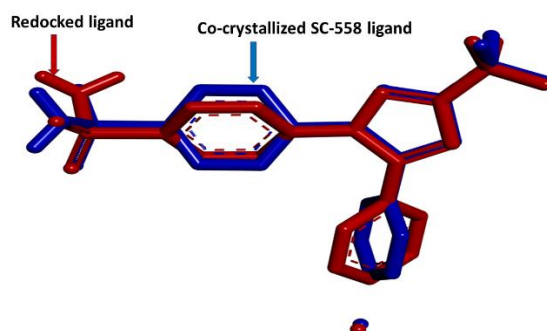


**Figure 53:** Superimposition of co-crystallized SC-558 ligand (blue) and redocked ligand (red)

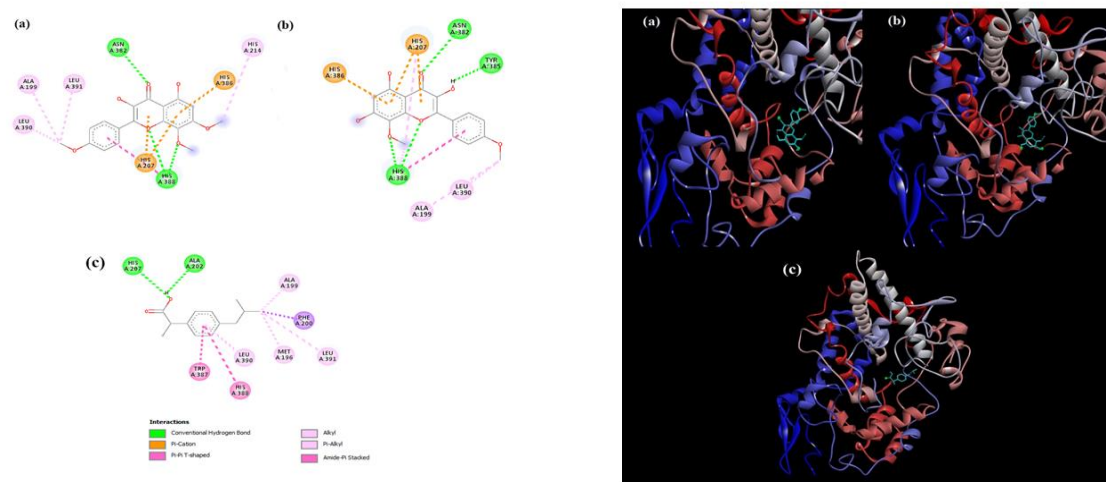


**Figure 54:** 2D & 3D interaction of enzyme (1CX2) with a) compound 1 and b) 2 c) ibuprofen

**Table 27:** ADMET parameters of compounds 1 and 2

Properties	Tambulin (1)	Prudomestin (2)
Molecular Weight (g/mol)	344.32	330.29
Topological Polar Surface Area (TPSA)	98.36 Å <sup>2</sup>	109.36 Å <sup>2</sup>
Water Solubility	Moderately soluble	Moderately soluble

Gastrointestinal (GI) absorption	High	High
BBB permeant	No	No
CYP1A2 inhibitor	Yes	Yes
CYP2C19 inhibitor	No	No
CYP2C9 inhibitor	Yes	Yes
CYP2D6 inhibitor	Yes	Yes
CYP3A4 inhibitor	Yes	Yes
AMES toxicity	No	No
Hepatotoxicity	No	No
Skin sensitization	No	No
Drug-likeness	Yes	Yes
(Lipinski, Ghose, Veer, Egan, Muegge)		

**Table 28:** Molinspiration bioactivity score of compounds

Compounds	Enzyme inhibitor (molinspiration bioactivity score)
<b>1</b>	0.17
<b>2</b>	0.20

#### 4.10 Computational study of compound 2 for insulin target

According to research, insulin secretagogues bind to the SUR subunit, preventing the dimerization of the SUR subunit's NBD1 and NBD2 chains and the opening of the Kir6 pore. This leads to depolarization of pancreatic  $\beta$  cells, activation of the voltage-gated calcium channel, and subsequent release of insulin. Therefore, in this study, we also docked molecules in the SUR subunit of this Katp ion channel complex [**Figure 55 a**, **Figure 55 b**]. The estimated docking scores for prandomest in and tolbutamide were -9.30 kcal/mol and -10.01 kcal/mol, respectively. The docking revealed that the amino acids ARG1246, ARG1300, ASN1293, ASN1296, GLU1249, GLU1253, LEU1149, LEU373, THR588, TRP1297, TYR1294, and TYR377 were present in the prandomest in binding site [**Figure 55 c**, **Figure 55 d**]. In the binding score of prandomest in, hydrogen bonding contribution was found to be -5.19 kcal/mol. We hypothesize that non-covalent bonding with SUR's binding site residues may be the cause of prandomest in's ability to inhibit SUR.

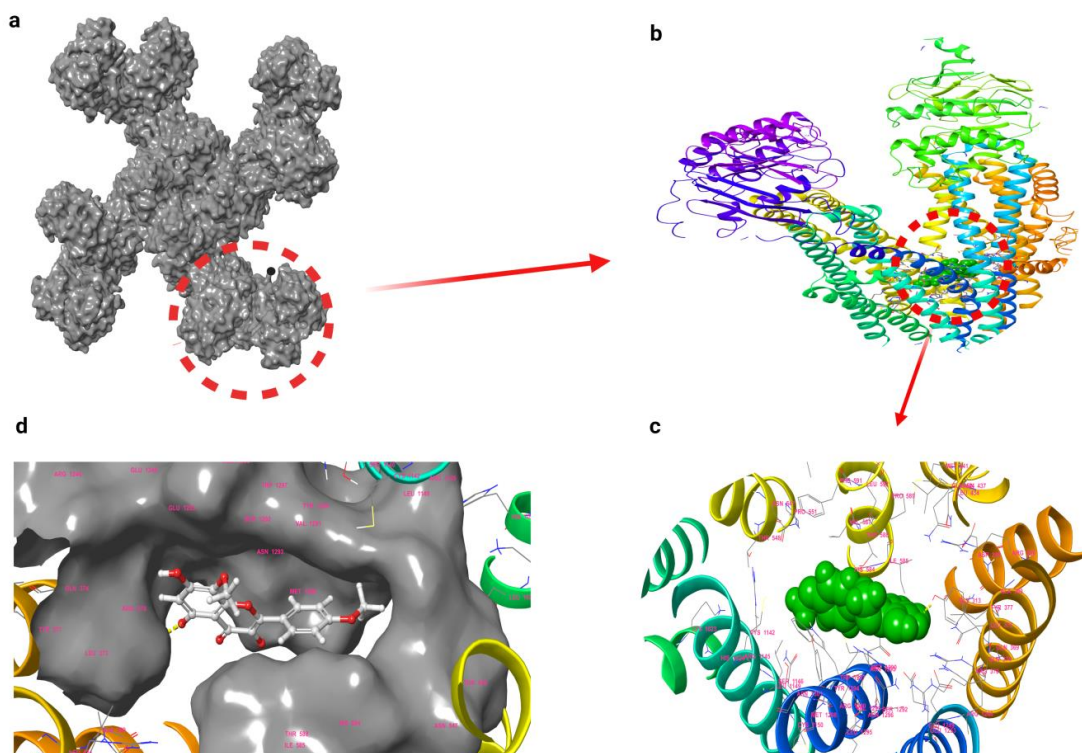


**Figure 55:** Docking poses and molecular interactions of prudomestine (2) in the binding pocket of SUR of Katp ion channel: (a) Katp ion channel with SUR subunit (b) 3D molecular diagram of SUR with prudomestine (2) (Side View). Prudomestine (2) is represented in CPK and SUR is represented in the cartoon. (c) 3D molecular diagram of SUR with prudomestine (2) (Top View). Prudomestine (2) is represented in CPK and SUR is represented in the cartoon. (d) 3D molecular diagram of SUR with prudomestine (2) (Top View). Prudomestine (2) is represented in ball and stick, and SUR is represented in the surface and cartoon.

Molecular docking predicts the binding mode between a protein and a ligand. It cannot, however, foresee the molecule's stability and dynamic behavior during the binding process. To investigate the stability of the hit, protein prudomestine complexes were subjected to a 500 ns, 1000 frame molecular dynamics simulation. The molecular dynamics simulation predicted that prudomestine would be comparatively more stable with SUR than tolbutamide. The backbone of SUR in the prudomestine complex was deviated by 6.5 Å. After a sharp initial deviation to 5 Å, it nearly stabilized. Throughout the simulation, prudomestine deviated around 0.5 Å (tolbutamide = 1 Å) in its alignment with itself and approximately 5 Å (tolbutamide = 6 Å) in its alignment with the protein (**Figure 56a**). As a result, prudomestine's stability with SUR may be comparable, as indicated by the aforementioned comparative deviations.

A minimum of 10 protein-ligand interactions, of which at least few were significant,

were observed between SUR and tolbutamide as well as SUR and prudomestine throughout the simulation (**Figure 56b**, **Figure 56c**). Prudomestine interacted with ARG370, ASN1293, and ARG1300 via multiple hydrogen bonds over most of the simulated duration (**Figure 56b**, **Figure 56d**). Whereas, tolbutamide interacted with residues (ARG306, ARG370, TYR377, ASN437, and GLU1249) for most of the simulation period via multiple hydrogen bonding (**Figure 56c**, **Figure 56e**).

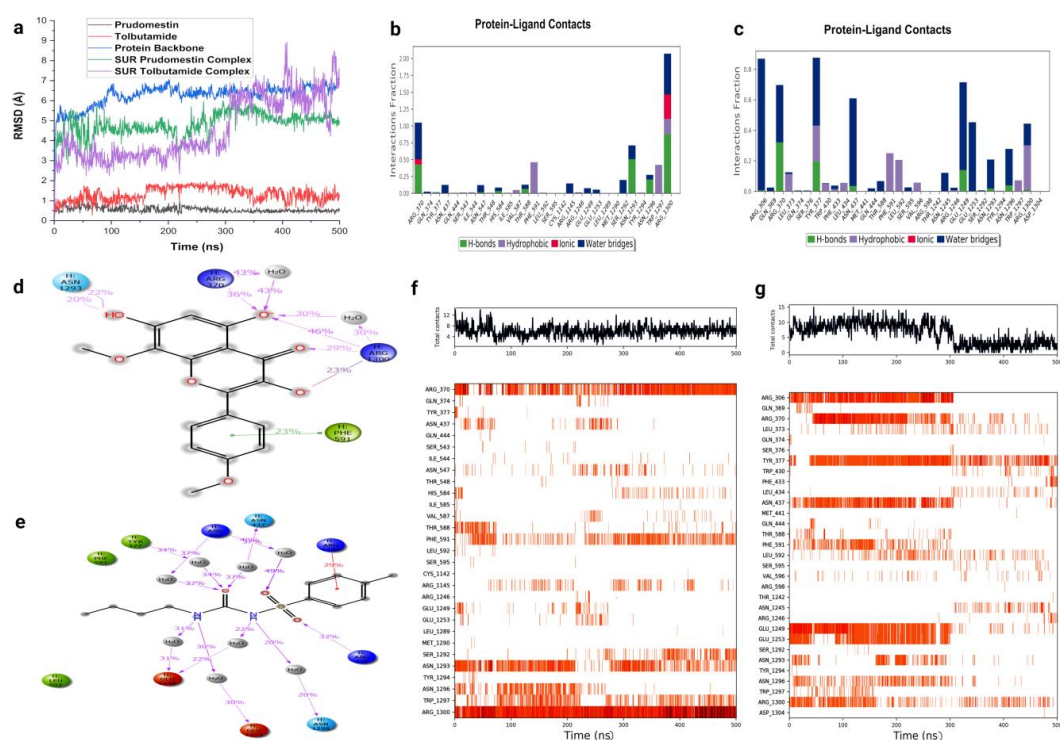


**Figure 56:** RMSD and molecular interaction analysis of MD simulation trajectory: (a) The RMSD plot of prudomestine and tolbutamide with SUR. Normalized stacked bar chart of SUR binding site residues interacting with (b) prudomestine and (c) tolbutamide via hydrogen bonds, hydrophobic and ionic interactions, and water bridges. Detailed schematic interaction of (d) prudomestine and (e) tolbutamide atoms with the binding site residues of SUR. Timeline representation of protein-ligand contact during whole trajectory (f) prudomestine (g) tolbutamide

The timeline charts also showed that at least two bonds in the SUR complex of prudomestine interacted significantly throughout the simulation. ARG1300 interacted via more or less uninterrupted bonding with prudomestine, while ARG370, PHE591, ASN1293, and TRP1297 interacted via partial bonding (**Figure 56 f**). Similarly, tolbutamide interacted via nearly partial bonding with ARG306, ARG370, TYR377, ASN437, GLU1249, GLU1253, and ARG1300 (**Figure 56 g**). Tolbutamide was found to have a discontinuous molecular interaction compared to prudomestine. It is therefore anticipated to be efficient in inhibiting SUR based on comparative stability and

interactions. This evidence substantiates the hypothesis that prDOMESTIN helps in insulin secretion.

**CHAPTER 4**  
**RESULTS AND DISCUSSION**

**PART TWO**

*Sarcococca coriacea* (Hook.F.) and *Sarcococca wallichii* Staph.

#### 4.11 *Sarcococca* species

Both species of *Sarcococca* were observed against the in-vitro antioxidant, antidiabetic, and anticancer activities. The potent biological applications of *Sarcococca coriacea* leaf (**Sc-A**), *Sarcococca coriacea* stem (**Sc-S**), and dichloromethane fraction of methanolic extract of *Sarcococca wallichii* (**Sw-D**), *Sarcococca coriacea* basic fraction (**Sc-B**) and *Sarcococca coriacea* neutral (**Sc-N**) concerning antioxidant, antidiabetic, and anticancer and antibacterial activities is discussed below.

##### 4.11.1 Bioactivities of *S. coriacea* and *S. wallichii*

##### 4.11.2 Antioxidant activity

DPPH free radical scavenging assay was performed to determine the antioxidant activity. Both **Sc-A** and **Sc-S** were found to significantly inhibit the DPPH free radical with IC<sub>50</sub> values of  $24.56 \pm 3.3 \mu\text{g/mL}$  and  $28.90 \pm 5.22 \mu\text{g/mL}$ , respectively. Comparatively, the other species' **Sw-D** fraction has IC<sub>50</sub> =  $53.79 \pm 2.50 \mu\text{g/mL}$ . Among all three extracts, **Sc-A** possesses stronger antioxidant potential. The antioxidant potential of standard quercetin was IC<sub>50</sub> =  $1.17 \pm 0.35 \mu\text{g/mL}$ .

##### 4.11.3 *In vitro* $\alpha$ -glucosidase and $\alpha$ -amylase inhibition activity

Both these digestive enzymes function differently.  $\alpha$ -amylase breaks down dietary carbohydrates to monosaccharides while glucosidase further breaks monosaccharides into absorbable glucose. For the *in vitro*  $\alpha$ -glucosidase and  $\alpha$ -amylase inhibition activity, samples were first screened at the concentration of 500  $\mu\text{g/mL}$ . Samples inhibiting >50% were further diluted to calculate their IC<sub>50</sub> value. The IC<sub>50</sub> was calculated using Graph Pad Prism 8 software. The **Sc-A** showed significant inhibition against both digestive enzymes;  $\alpha$ -glucosidase and  $\alpha$ -amylase, with an IC<sub>50</sub> of  $39.92 \pm 2.52 \mu\text{g/mL}$  and  $224.3 \pm 1.87 \mu\text{g/mL}$ , respectively. Likewise, **Sc-S** disclosed significant inhibition against  $\alpha$ -glucosidase with IC<sub>50</sub>  $20.97 \pm 2.37 \mu\text{g/mL}$ ; however, it showed <50% inhibition against the  $\alpha$ -amylase. Another species **Sw-D** significantly inhibits  $\alpha$ -amylase with an IC<sub>50</sub> =  $2.116 \pm 0.058 \mu\text{g/mL}$  than  $\alpha$ -glucosidase < 50% comparatively. Standard Acarbose's IC<sub>50</sub> against  $\alpha$ -glucosidase and  $\alpha$ -amylase were found to be  $5.66 \pm 0.8 \mu\text{g/mL}$  and  $6.18 \pm 0.97 \mu\text{g/mL}$ , respectively. This proves the stronger inhibition capacity of **Sw-D** than the standard acarbose used. The IC<sub>50</sub> of  $\alpha$ -glucosidase and  $\alpha$ -amylase inhibition activity of **Sc-A**, **Sc-S** and **Sw-D** compared to the standard acarbose is presented in **Table 29**.

**Table 29:** IC<sub>50</sub> values of antioxidant,  $\alpha$ -glucosidase, and  $\alpha$ -amylase inhibition activity of Sc-A, Sc-S and Sw-D

Sample	Antioxidant( $\mu\text{g}/\text{mL}$ )	$\alpha$ -Glucosidase( $\mu\text{g}/\text{mL}$ )	$\alpha$ -Amylase ( $\mu\text{g}/\text{mL}$ )
Sc-A	24.56 $\pm$ 3.3	39.92 $\pm$ 2.52	224.3 $\pm$ 1.87
Sc-S	28.90 $\pm$ 5.22	20.97 $\pm$ 2.37	<50%
Sw-D	53.79 $\pm$ 2.50	<50%	2.116 $\pm$ 0.058
Quercetin	1.17 $\pm$ 0.35	-	-
Acarbose	-	5.66 $\pm$ 0.8	6.18 $\pm$ 0.97

Values are expressed as average  $\pm$  standard deviation of three independent assays.

#### 4.11.4 Comparative studies on the antioxidant and antidiabetic activities

In-vitro potency of plant extract provides a rationale for diet and supplement in type II diabetes management. Synergetic effect of active phytochemicals such as alkaloids, tannins, phenols, saponins, terpenoids, flavonoids, steroids, and sterols contribute to the plant's medicinal properties (Mehrotra *et al.*, 2019). Due to the adverse effects of synthetic drugs, the efficacy of plant-based food profiles with potent inhibitors is in demand. Major hydrolyzing enzymes of carbohydrate metabolism are the  $\alpha$ -glucosidase and  $\alpha$ -amylase. Inhibiting these enzymes may result in controlling blood sugar (Nagmoti & Juvekar, 2013). This research reveals the unique in vitro antidiabetic potency of **Sc-A** and **Sc-S** as these both inhibited the digestive enzymes,  $\alpha$ -glucosidase and  $\alpha$ -amylase. The methanolic stem extract of the plant *S. coriacea* inhibited  $\alpha$ -glucosidase substantially more than its leaf extract whereas stem extract of the same at the concentration 500  $\mu\text{g}/\text{mL}$  could not inhibit the  $\alpha$ -amylase enzyme. Leaf extract **Sc-A** was found to inhibit the  $\alpha$ -amylase comparatively. Interestingly another species **Sw-D** is found to be one of the potent inhibitors of  $\alpha$ -amylase that could not inhibit the  $\alpha$ -glucosidase enzyme at the concentration 500 $\mu\text{g}/\text{mL}$ . **Sc-A** possesses higher phenolic and stronger antioxidant potential. However, the enzymatic inhibition was not correlated to antioxidant the total phenolic and flavonoid content in the plants. Enzyme inhibition activity of both methanolic extracts of **Sc-A**, **Sc-S**, and **Sc-D** accredit to the synergetic effect of phyto constituents present in it.

#### 4.11.5 Anticancer activities bioassay

#### 4.11.6 Anticancer activities of *S. wallichii*

*S. wallichii* did not possess any anticancer activities on the tested cell lines as observed through MTT assay in HeLa (cervical cancer cell line) and breast cancer cell lines (MCF-7).

#### 4.11.7 Anticancer activity of *S. coriacea* against breast cancer (MCF-7)

The chloroform fraction of *S. coriacea* extract both in basic condition (**Sc-B**) and neutral pH condition (**Sc-N**) was the potent sample studied against breast cancer (MCF-7) which activity against breast cancer at the highest tested concentration (400µg/ml) therefore the samples were further diluted for observing the impact at lower concentrations. *S. coriacea* basic fraction **Sc-B** possesses an IC<sub>50</sub> value of (11.50 ± 0.50 µg/mL) and its neutral fraction (**Sc-N**) possesses potent activity of IC<sub>50</sub> at (68.42 ± 5 µg/mL). Anticancer activity against the breast cancer cell line (MCF-7) of these samples with their inhibition values (IC<sub>50</sub>± S.D.) µg/mL is presented in **Table 30** below.

**Table 30:** IC<sub>50</sub> values of Sc-B and Sc-N against breast cancer cell line (MCF-7)

Sample	(IC <sub>50</sub> ± SD) µg/mL
Sc-B	11.50 ± 0.50
Sc-N	68.42 ± 5
N <sub>a</sub> -methylepipachysamine D	84 ± 3
Doxorubicin	0.9 0 ±.14

#### 4.11.8 Anticancer activity of *S. coriacea* against cervical cancer (HeLa)

Sc-B and Sc-N both revealed their activity against cervical cancer (HeLa). **Table 31** below depicts the activity of *S. coriacea* against the cervical (HeLa) cancer cell line.

**Table 31:** IC<sub>50</sub> values of Sc-B and Sc-N against cervical (HeLa) cell line

Sample	( IC <sub>50</sub> ± SD) µg/mL
Sc-B	36.33 ± 10
Sc-N	85.5 ± 5
Doxorubicin	0.9 ± 0.14

#### 4.11.9 Antibacterial activities of *S. coriacea*

Five different bacteria *Bacillus subtilis* ATCC23875, *Staphylococcus aureus* NCTC 6571, *Escherichia coli* ATCC 25922, *Pseudomonas aeruginosa* ATCC 10145, and *Salmonella typhi* ATCC 14028 were used for preliminary screening of the antibacterial activities of the extract. Antibacterial activities with 60 mg of *S. coriacea* basic (Sc-B) fraction at a final concentration of 3000 µg/ml were carried with standard drug ofloxacin at 100 µg/ml. Results showed *S. coriacea* showed good percentage inhibition against all strains of bacteria as [*Escherichia. coli* (65.42%) when std. (92.47%)], [*S. aureus* (64.27%) std.(90.89%)], [*B. subtilis* (65.65%) std. 90.23%], [*Pseudomonas*

*aeruginosa* (64.04%),std. 90.01%], [*Salmonella typhi* (69.31%) std.90.61%]. The MIC of the extract on *Staphylococcus aureus* (NCTC 13143) as 100µg/ml, *Staphylococcus aureus* (NCTC 6571) 100 µg/ml, *Escherichia coli* (ATCC25922) 1000 µg/ml, *Salmonella typhi* (ATCC 14028) 1110 µg/ml. The inhibition against these particular bacteria could be related to the major constituent with hydrophobicity in nature. Hydrophobicity makes them easy to partition with the lipids in the cell membrane of bacteria thus making it more permeable by disrupting the cell membrane leading to changes in cytoplasm, and leakage of critical molecules eventually causing the death of the bacterial cells (Chouhan *et al.*, 2017). **Table 32** below presents the details of bacterial strains used in the activities and their minimum inhibitory concentration values of the samples studied.

**Table 32:** MIC values of **Sc-B** on five different bacterial strains

Bacteria	MIC Values (µg/mL)
<i>Staphylococcus aureus</i> (NCTC 13143)	100
<i>Staphylococcus aureus</i> (NCTC 6571)	100
<i>Escherichia coli</i> (ATCC 25922)	1000
<i>Salmonella typhi</i> (ATCC 14028)	1110
<i>Pseudomonas aeruginosa</i> (ATCC 10145)	Inactive

## 4.12 Column chromatography

### 4.12.1 Column chromatography and compound isolation from *Sarcococca wallichii*

Hydromethanolic extract 80% of 450 g was defatted using hexane that yielded 50.0g coded as Sw-H. To obtain the neutral fraction aqueous layer was then re-extracted with dichloromethane that yielded 40 g coded as **Sw-D**. Some portion of this neutral fraction (**Sw-D**) *S. wallichii* 4 g were column chromatographed to obtain compound **8-11** at the first step under 10% acetone: hexane with a few drops of diethyl amine. And successively under neutral alumina using ethylacetate: hexane that also yields compound **8**. Different staining reagents such as sulphuric acid, Dragendroff reagent were used for locating the pure compound. The scheme of isolation of pure compound from *S. wallichii* is presented in **Figure 18** and **Figure 19**.

#### 4.12.2 Structure elucidation of the isolated compounds

Structure elucidation of the isolated compounds was carried out using spectroscopic tools such as mass, UV, 1D-NMR, and 2D NMR. The details of all four isolated compounds are presented below.

#### 4.12.3 Structure elucidation of N<sub>a</sub>-methylepipachysamine D (8)

This compound was obtained as a white amorphous solid from sub-fraction A2 of Fr 57-66 (**Figure 19**). The developed TLC was UV active and stained by Dragendroff reagent. Thus, the obtained white mass was re-crystallized using dichloromethane to obtain the colorless crystal structure. The EI MS showed the M<sup>+</sup> at  $m/z$  464, base peak at  $m/z$  72, and other fragment peaks at  $m/z$  105, and 136. The <sup>1</sup>H-NMR spectrum displayed the presence of two up-field singlets at  $\delta$  0.67 and 0.78 assigned for C-18 and C-19 angular methyl's, respectively. A doublet at  $\delta$  1.18 ( $J_{21,20} = 6.5$  Hz) was due to C-21 methyl protons. The NMe<sub>2</sub> protons have appeared at  $\delta$  2.26. Two broad multiplets at  $\delta$  3.43 and 4.43 were ascribed to H-20 and H-3 protons, respectively. The N-Me protons also appeared as a singlet at  $\delta$  2.58. The downfield signals between  $\delta$  7.24 - 7.36 were assigned to the aromatic protons. The <sup>13</sup>C-NMR spectra (broad-band decoupled) of the compound displayed resonances for 31 carbons. The compound structure **Figure 57** was further confirmed by using 2D-NMR (HMQC, COSY, HMBC single-crystal X-ray diffraction technique (ORTEP diagram is shown in **Figure 58**). The compound was finally identified as N<sub>a</sub>-Methylepipachysamine D a previously obtained compound from *Sarcococca saligna* (Atta-ur-Rahman *et al.*, 1997).

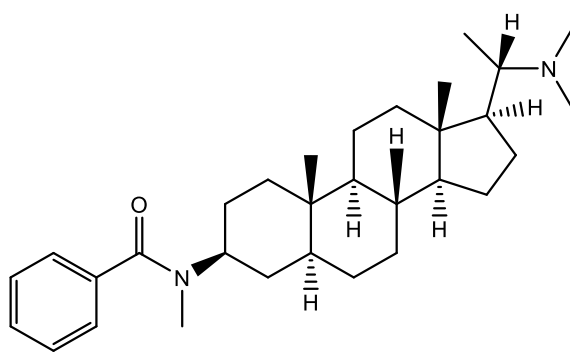


**Figure 57:** Structure of N<sub>a</sub>-methylepipachysamine D (8)

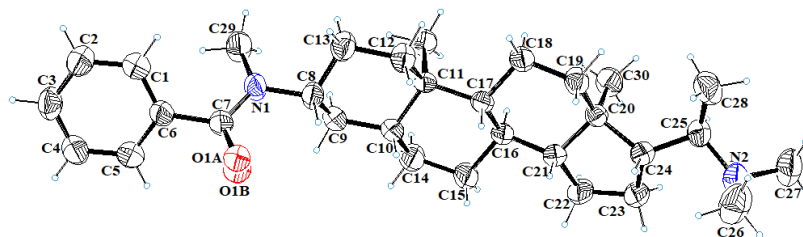


**Figure 58:** ORTEP diagram of  $N_{\alpha}$ -methylepipachysamine D (**8**)

#### 4.12.3.1 Anticancer activity against breast cancer cell line (MCF-7)

$N_{\alpha}$ -methylepipachysamine D possessed anticancer activity against the breast cancer cell line (MCF-7) with an inhibition ( $IC_{50} \pm SD$ ) value of  $84 \pm 3 \mu\text{g/mL}$ .

#### 4.12.4 Structure elucidation of taraxerol (**9**)

The compound was obtained as a white amorphous from the (Fr-26-35) obtained from *S. wallichii*, 3% of hexane, and acetone as eluent with the drop of diethylamine (**Figure 18**). This fraction was again column chromatographed to obtain white-colored fraction of the plant. The EIMS spectrum showed  $M^+$  at  $m/z$  426, and other fragment peaks at  $m/z$  411, 302, 287, 204, and 135. The  $^1\text{H-NMR}$  spectrum depicted a downfield signal at  $\delta$  5.51 dd ( $J= 8.0, 2.0$  Hz) was ascribed to H-15, and another broad multiplet at  $\delta$  3.16 was attributed to H-3. The  $^1\text{H-NMR}$  signal also displayed signals for eight angular methyl protons at 0.78, 0.80, 0.89, 0.91, 0.93, 0.95, 1.07, and 1.23. The position of the double bond at C-14/C-15 was determined from the HMBC correlation of methyl protons of C-26 and C-27 to C-14 (158.2). The structure was finalized using 2D-NMR techniques **Figure 59**. The key HMBC interactions of the compound are shown in **Figure 60**. All the spectral data were closely similar to the previously reported compound taraxerol. The details of the NMR of the compound are presented in **Table 33** below.

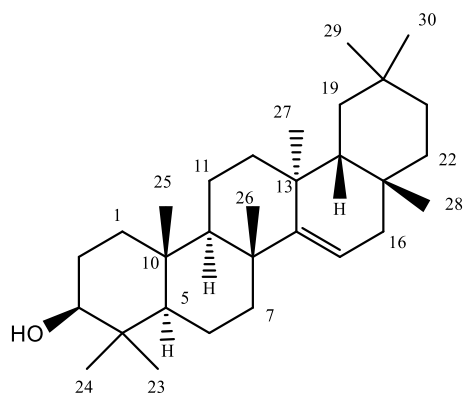


**Figure 59:** Structure of taraxerol (**9**)

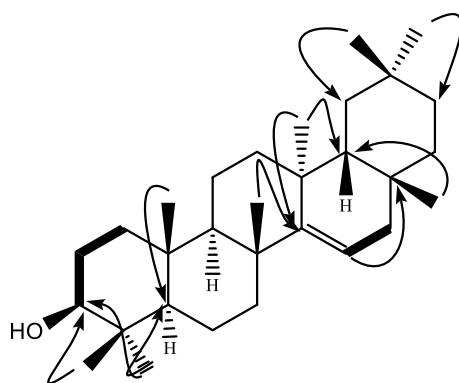


**Figure 60:** Key COSY (—) and HMBC (→) correlations in taraxerol (**9**)

**Table-33:**  $^{13}\text{C}$ - and  $^1\text{H}$ -NMR chemical shift values of taraxerol ( $\text{CDCl}_3$ , 100 and 400 MHz)

Carbon No	$^{13}\text{C}$ -NMR value	$\delta_{\text{H}}$ (J, Hz)
1	38.0	1.32, 1.58
2	27.1	1.29, 1.31
3	79.0	3.18 br m
4	39.0	-
5	55.5	0.76
6	18.9	0.71, 0.97
7	35.2	1.0, 1.34
8	39.0	-
9	49.2	0.96
10	37.7	-
11	17.5	1.01, 1.44
12	35.8	1.02, 1.36
13	37.7	-

14	158.2	
15	116.8	5.51 dd (8.0, 2.0)
16	38.5	1.61, 1.91
17	37.5	-
18	49.3	1.40
19	41.3	1.33, 2.01
20	28.8	-
21	33.7	1.22, 1.32
22	33.1	1.23, 1.34
23	28.0	0.96s
24	15.4	0.78 s
25	15.3	0.91 s
26	25.9	1.85 s
27	29.9	0.89 s
28	29.8	1.23
29	33.3	0.95
30	29.4	0.81

#### 4.12.5 Structure elucidation of $\beta$ -sitosterol (10)

The EI-MS spectrum of compounds displayed  $M^+$  at  $m/z$  414 and fragments peaks at  $m/z$  396, 255, 55. The  $^1\text{H-NMR}$  spectrum of the compound displayed a peak at  $\delta$  5.32 br s was assigned to H-6.

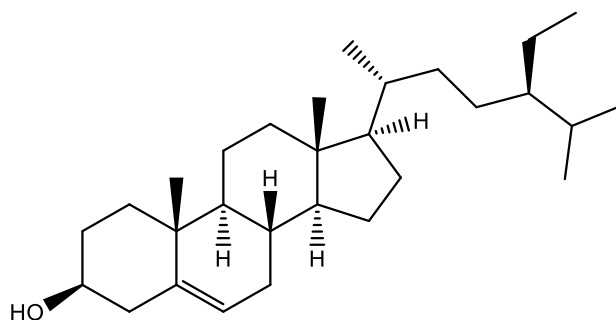


**Figure 61:** Structure of  $\beta$ -sitosterol (10)

A signal at  $\delta$  3.53 br m, was attributed to H-3. **Figure 61** represents the structure of the compound  $\beta$ -sitosterol. All the spectra of the compounds were closely similar to previously reported compound  $\beta$ -sitosterol (Patra *et al.*, 2010).

#### 4.12.6 Structure elucidation of oleanolic acid (11)

The compound was isolated as a white amorphous from the fraction 46-56. This was again chromatographed using silica gel using hexane: acetone with a drop of diethylamine yielded 25 mg of the compound.

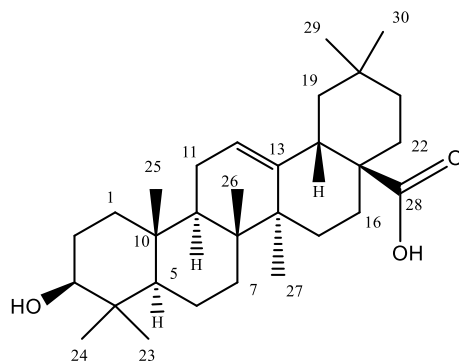


**Figure 62:** Structure of oleanolic acid (11)

The EIMS of the compound displayed an  $M^+$  peak at  $m/z$  456 and major fragments peak at  $m/z$  248 (96%) and 203 (100%), indicating the oleanolic acid-type skeleton. The  $^1\text{H-NMR}$  spectrum displayed a downfield peak at  $\delta$  5.28 t (5.5 Hz) was assigned to H-13, and another broad multiplet at  $\delta$  3.21 was attributed to H-3. The  $^1\text{H-NMR}$  spectrum also displayed signals for seven angular methyls at  $\delta$  0.72 s, 0.78 s, 0.90s, 0.93s, 0.97 s, 1.14 s, and 1.25 s. The structure of the compound was further confirmed using 2D-NMR techniques (HSQC, COSY, HMBC, and NOESY). The Key HMBC correlations in the compound is shown in **Figure 63** below.

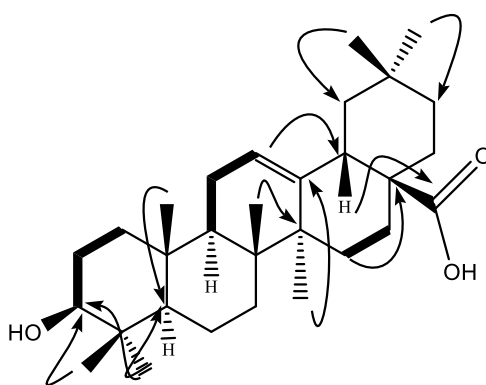


**Figure 63:** Key COSY (—) and HMBC (→) correlations of oleanolic acid (11)

## CHAPTER 5

### CONCLUSIONS AND RECOMMENDATION

#### 5.1 Conclusions

The bioprospecting studies of *Z. armatum*, *S. coriacea* and *S. wallichii* concerning their antioxidant, antidiabetic, and anticancer activities were the major objectives of this study. This evidence-based study was based on Indigenous practice and consumption of these particular floras. The preparation of extract using a suitable solvent can readily extract multiple phyto-constituents from the plants. Such phyto-constituents can serve as alternative medicines to replace synthetic drugs. One of the basic parameters is the proper use of solvent and extraction technique which can explore qualitative and quantitative variation of the constituents. Isolation of constituents from the extract varies depending on the gradient of various solvent systems and the constituent nature. The findings of present investigations led to the following conclusions:

- Extraction of *Z. armatum*: *Z. armatum* fruit pericarps extract yield and activity varies on the nature of solvent ethanol and methanol.
- Antioxidant properties of crude extract: The antioxidant properties of *Z. armatum* crude extract both methanoic and ethanoic were determined to be  $169.85 \pm 0.244$   $\mu\text{g/mL}$  and  $174 \pm 1.1$   $\mu\text{g/mL}$  respectively.
- *Z. armatum*'s fruit pericarp extract was fractionated for a bioassay-guided isolation.
- *Z. armatum* ethylacetate fraction: Ethylacetate fraction showed high antioxidant  $42.94 \pm 1.19$   $\mu\text{g/mL}$  and anti-inflammatory properties  $17.8 \pm 1.1$   $\mu\text{g/mL}$  compared to other fractions.
- Bioassay guided isolation using column chromatography was carried out on ethylacetate fraction which yielded 7 compounds.
- Both extracts methanolic and ethanolic of *Z. armatum*, its hexane fraction and cinnamic acid possess remarkable activity against breast cancer cell line (MCF-7) while the extract and hexane fraction was also active against cervical cancer cell line (HeLa).
- Compounds isolated were identified using spectroscopic tools such as Mass, 1D NMR, and 2 D NMR were tambulin (1), prudomestin (2), cinnamic acid (3), methyl cinnamate (4), isovanillic acid (5), isoquercetin (6) and ducoesterol (7).

- Antioxidant activities of tambulin (**1**) and prudomestin (**2**) differed due to the higher number of –OH moieties in prudomestin (**2**).
- The isolated flavonoids tambulin (**1**) and prudumestin (**2**) are remarkable insulin secretagogue that helps to lower body glucose.
- Isolated flavonoids tambulin (**1**) and prudumestin (**2**) possess stronger anti-inflammatory properties and both inhibited digestive enzyme  $\alpha$ -glucosidase.
- Computational studies on tambulin (**1**) and prudomestin (**2**) suggest these both compounds are suitable drug candidates and are free from any toxic impressions.
- **Essential oil**
- Sixty constituents were identified in the essential oil of *Z. armatum* with the dominance of fatty acid, terpenes, and their oxides.
- Twenty-five enantiomeric components were identified using chiral GC-MS among its sixty constituents.
- Enantiomerically linalool and limonene were in (+) dextrorotatory form while others were in levorotatory form.
- *Z. armatum* from the Myagdi district of Nepal possesses the highest amount of linalool.
- Comparative antimicrobial activities of the essential oil from Myagdi, Salyan, and Surkhet revealed that the oil extracted from fruit pericarp of Myagdi origin was significant.
- According to the deduction made above, the bioactivities of *Z. armatum* largely vary on various dimensions, particularly on the topography.
- **Hexane fraction of *Z. armatum***
- Using GC-MS spectra, twenty constituents were identified in the hexane fraction.
- GC-MS suggests a hexane fraction of *Z. armatum* DC with an abundance of fatty acids.
- The hexane fraction of *Z. armatum* stands out as a highly impactful bio-pesticide, demonstrating insecticidal, antimicrobial, and antifungal activities, and can be developed as a novel bio-pesticide for specific applications.
- Moreover, the hydrophobic nature of its constituents, such as polyunsaturated fatty acids, terpenes, and esters, suggest potentially potent anti-inflammatory effects comparable to ibuprofen.

- Hexane fraction possess remarkable activity against breast cancer (MCF-7) and cervical cancer (HeLa).
- **Extract toxicity and antidiabetic properties of *Z. armatum***
- Among two different animal species Adult Swiss Albino Mice and Long Evans Rats used for determining extract toxicity of *Z. armatum*'s through oral acute toxicity revealed no signs of toxicity and mortality in LER suggesting single oral dose feed of *Z. armatum* fruit extract up to 3200 mg/kg as safer.
- Toxic impact of extract observed in case of SAM at LD<sub>50</sub>=565.68 mg/kg concludes *Z. armatum* plant's toxicity varies based on the animal model, route of dosage administered, and change in body weight and also on the immunity level of the particular species.
- The histopathological studies suggest doses of 800 mg and higher doses are comparatively toxic in the case of SAM.
- Methanoic extract of *Z. armatum* fruits pericarp showed significant hypoglycemic activities at both doses in type II diabetic model rats.
- Methanoic extract helps to decrease atherogenic lipid profile, increasing liver enzymes (ALT & AST) in type II diabetic model rats.
- Methanoic extract of *Z. armatum* impacts glycogen storage in type 2 diabetic model rats.
- **Elemental toxicity** in *Z. armatum* fruit pericarp powder and its essential oil was determined using EDX. The EDX spectra showed that *Z. armatum* is free from toxic/hazardous elements.
- **Bioprospecting of *Sarcococca* species**
- Sc-A and Sc-S both inhibited digestive enzymes,  $\alpha$ -glucosidase and  $\alpha$ -amylase.
- Sw-D strongly inhibited  $\alpha$ -amylase stronger than the standard reflecting remarkable anti-diabetic potential.
- Sc-A, Sc-S, and Sw-D possess good to moderate antioxidant properties.
- The basic and neutral fraction of *S. coriacea*, Sc-B, and Sc-N possess anticancer activities against breast cancer (MCF-7) and (HeLa) cell line.
- Sc-B possesses remarkable antibacterial activities.
- The column chromatography of Sw-D yield four compounds N<sub>a</sub>-methylepipachysamine D (**8**), taraxerol (**9**),  $\beta$ -sitosterol (**10**), oleanolic acid (**11**).

## 5.2 Recommendation

“*Z. armatum* possesses antioxidant, anti-inflammatory, antidiabetic properties and anticancerous activities, while *Sarcococca* species also demonstrate antibacterial properties. Among both the extract of *Z. armatum*'s methanolic extract possesses effective properties in animal models. The following recommendations are suggested for application and future research:”

- Future research can conduct in-depth bioactivity studies to explore the mechanism behind the action of bioactive compounds of these plants.
- Investigation on how seasonal and geographical variations affect the concentration and bioactivity of compounds in the particular species.
- Future researchers can explore the dimension of commercialization and application prospective. Working on commercial product based on the research findings such as preparation of bio-pesticides using *Z. armatum* can be extremely efficient, economical, and environmentally favorable.
- Modifying compound isolation techniques for natural plant extracts to focus on particular functional groups of interest may prove to be promising field of future research.
- Interdisciplinary collaboration on the interaction of particular compounds' their involvement in certain pathways may enhance the existing knowledge.
- Focusing on optimizing the solvent system ratio can improve the isolation process in column chromatography.
- Employing environmentally friendly extraction methods using green chemistry approaches to reduce the use of harmful solvents is a promising avenue for future research.

## CHAPTER 6

### SUMMARY

The sedentary and sophisticated lifestyle of people in this 21<sup>st</sup> century is the leading cause of different diseases. Synthetic drugs cause undesirable side effects. Global concern for nature-based alternative sources of medicine and treatment is increasing. However, the huge biodiversity in its various topography in a country like Nepal needs to be researched for the overall benefit of humankind. Such studies promote optimum benefits in the medicinal sector as well as encourage farmers for the economic benefits. Such economic aspects of particular plants could support in preservation, conservation, and protection of the habitat of such flora that possess an impact on human health.

There are six chapters in this thesis. The following lists the important points of each chapter.

**Chapter 1** describes the context of this study and provides a detailed research background for this study. The impacts of natural resources and increasing demand on emerging diseases with background have been discussed. The importance and application of natural plants and natural-based compounds are discussed. This chapter also briefly describes some phyto-constituents and their impacts. The research objectives and rationale of the study are highlighted.

**Chapter 2** presents a summary of the literature review on natural products. A literature review concerning *Z. armatum* and *Sarcococca* species revealed *Z. armatum* can be a cost-effective source for the preparation of anti-inflammatory and antioxidant drugs while the plants *S. coriacea*, and *S. wallichii* are promising plants to explore bioactivities.

**Chapter 3** covers the materials and methods. It describes the experimental procedure for preparing animal models used for extract toxicity studies and antidiabetic model animal preparation, experimental procedure of feeding, and extract preparation. Extraction, fractionation, and isolation of compounds using various solvent systems of *Z. armatum*, *S. coriacea*, and *S. wallichii* and bioactivities performed. It discusses the chemicals, solvents, and related parameters used in the experimental procedure along with the spectroscopic tools used in the experiment and structure elucidation of compounds.

**Chapter 4** refers to the results and discussion containing the antioxidant, anti-inflammatory, antidiabetic, and anticancerous properties of *Z. armatum*, *S. coriacea* and *S. wallichii* with the probable reason based on previous studies. It presents the details of compounds isolated, GC-MS of hexane fraction of *Z. armatum*. GC-MS and chiral GC-MS of the essential oil extracted from the fruit pericarp of *Z. armatum* and bioactivities results with their discussion. Chapter 4 also discusses the bio-applications *S. coriacea* and *S. wallichii*. and the structure elucidation of the isolated compounds from *S. wallichii*.

**Chapter 5** alludes to overall conclusions drawn from the findings of this research work and finishes with recommendations for upcoming research.

**Chapter 6** presents the summary of this thesis and ends with the references cited.

Based on the results and discussions, the studied plants *Z. armatum*, its ethylacetate fraction, and isolated flavonoids can be regarded as effective, economical, antioxidant sources possessing anti-inflammatory properties while the *S. wallichii* and *S. coriacea* possess further anticancerous and antibacterial properties.

## REFERENCES

- Abbasi, A. M., Khan, M. A., & Zafar, M. (2013). Ethno-Medicinal Assessment of Some Selected Wild Edible Fruits and Vegetables of Lesser-Himalayas, Pakistan. *Pakistan Journal of Botany*, **45** (SPL.ISS): 215–222. Retrieved from: [https://www.pakbs.org/pjbot/PDFs/45\(S1\)/29.pdf](https://www.pakbs.org/pjbot/PDFs/45(S1)/29.pdf) Accessed on: (20/12/2019)
- Abdul, D., Abbas, H., & Hadi, N. (2009). Effects of Subchronic Exposure to Meloxicam on Some Hematological, Biochemical and Liver Histopathological Parameters in Rats. *Iraqi Journal of Veterinary Sciences*, **23**: 249–254. Retrieved from: <https://www.cabidigitallibrary.org/doi/full/10.5555/20103085511> Accessed on(12/12/2020)
- Adhikari, K., Owens, P. R., Ashworth, A. J., Sauer, T. J., Libohova, Z., Richter, J. L., & Miller, D. M., (2018) .Topographic Controls on Soil Nutrient Variations in a Silvopasture System. *Agrosystems, Geosciences and Environment*. **1**(1): 1–15. doi: 10.2134/age2018.04.0008
- Adhikari, A. (2009). *Bioprospecting Studies on Sarcococca coriacea (Hook. F.) of Nepalese Origin* (Unpublished doctoral dissertation).University of Karachi. Karachi, Pakistan. Retrieved from: <http://103.69.125.248:8080/xmlui/handle/123456789/227> Accessed on (12/01/2021)
- Adhikari, A., Vohra, M. I., Jabeen, A., Dastagir, N., & Choudhary, M. I. (2015). Anti-inflammatory Steroidal Alkaloids from *Sarcococca wallichii* of Nepalese Origin. *Natural Product Communications*, **10**(9): 13–16. doi: 10.1177/1934578X1501000911
- Ahmed, E., Arshad, M., Ahmad, M., Saeed, Ishaque, M., (2004). Ethnopharmacological Survey of Some Medicinally Important Plants of Galliyat Areas of NWFP, Pakistan. *Asian Journal of Plant Sciences*, **3**(4): 410-415. Retrieved from: <https://www.cabidigitallibrary.org/doi/full/10.5555/20> Accessed on (02/09/2020)
- Alam, F., & us Saqib, Q. N. (2017). Evaluation of *Zanthoxylum armatum* Roxb for In Vitro Biological Activities. *Journal of Traditional and Complementary*

*Medicine*, **7**(4): 515–518. doi: 10.1016/j.jtcme.2017.01.006

- Alam, F., Mohammad, K., Rasheed, R., Sadiq, A., Saeed, M., Mehmood, A., & Khan, A. (2020). Phytochemical Investigation, Anti-inflammatory, Antipyretic and Antinociceptive Activities of *Zanthoxylum armatum* DC Extracts In Vivo and In Vitro Experiments. *Heliyon*, **6**: e05571. doi: 10.1016/j.heliyon.2020.e05571
- Alam, F., us Saqib, Q. N., & Ashraf, M. (2018). *Zanthoxylum armatum* DC Extracts from Fruit, Bark and Leaf Induce Hypolipidemic and Hypoglycemic Effects in Mice In Vivo and In Vitro Study. *BMC Complementary and Alternative Medicine*, **18**(1): 1–9. doi: 10.1186/s12906-018-2138-4
- Ames, B. N., Shigenaga, M. K., & Hagen, T. M., (1993). Oxidants , Antioxidants , and the Degenerative Diseases of Aging. *Proceedings of the National Academy of Sciences of the United States of America*. National Academy of Sciences. **90**(17): 7915–7922. doi: 10.1073/pnas.90.17.7915
- Amin, A., Gali-Muhtasib, H., Ocker, M., & Schneider-Stock, R. (2009). Overview of Major Classes of Plant Derived Anticancer Drugs. *International Journal of Biomedical Science*, **5**(1): 1–11. Retrieved from: <https://www.ncbi.nlm.nih.gov/pmc/articles/PMC36147> Accessed on (01/05/2020)
- Anand, U., Jacobo-Herrera, N., Altemimi, A., & Lakhssassi, N. (2019). A Comprehensive Review on Medicinal Plants as Antimicrobial Therapeutics: Potential Avenues of Biocompatible Drug Discovery. *Metabolites*, **9**(11): 1–13. doi: 10.3390/metabo9110258
- Aparna, V., Dileep, K. V, Mandal, P. K., Karthe, P., Sadasivan, C., & Haridas, M. (2012). Anti-Inflammatory Property of n-Hexadecanoic Acid: Structural Evidence and Kinetic Assessment. *Chemical Biology and Drug Design*, **80**: 434–439. doi: 10.1111/j.1747-0285.2012.01418.x.
- Arora, A., Byrem, T. M., Nair, M. G., & Strasburg, G. M. (2000). Modulation of Liposomal Membrane Fluidity by Flavonoids and Isoflavonoids. *Archives of biochemistry and biophysics*. **373**(1): 102–109. doi: 10.1006/abbi.1999.1525
- Astudillo, A. M., Meana, C., Guijas, C., Pereira, L., Lebrero, P., Balboa, M. A., & Balsinde, J. (2018). Occurrence and Biological Activity of Palmitoleic Acid

- Isomers in Phagocytic Cells. *Journal of Lipid Research*, **59**(2): 237–249. doi: 10.1194/jlr.M079145
- ATT Bioquest, (2024). Quest Calculate Phosphate Buffer (pH 5.8 to 7.4) Preparation and Recipe. ATT Retrieved from: <https://www.aatbio.com/resources/buffer-preparation> Accessed on (04/08/2021)
- Atta-ur-Rahman, Choudhary, M. I., & Thomsen, W. J.(2001). Bioassay techniques for drug development. Amsterdam: Harwood Academic Publishers. 67-68. doi: 10.3109/9780203304
- Ayatollahi, A. M., Ghanadian, M., Afsharypuor,S., Siddiq, S. & Pour-Hosseini, S. M. (2010). Biological screening of *Euphorbia aellenii*. *Iranian Journal of Pharmaceutical Research*, **9**(4): 429. Retrieved from: <https://www.ncbi.nlm.nih.gov/pmc/articles/PMC3870068/>. Accessed on (07/09//2021)
- Balunas, M. J., & Kinghorn, A. D. (2005). Drug Discovery from Medicinal Plants. *Life Sciences*, **78**(5): 431–441. doi: 10.1016/j.lfs.2005.09.012
- Baral, J., Satyal, P., & Adhikari,A.,(2024). Sapital Variation in Constituents of Essential Oils From Fruit Pericarp of *Zanthoxylum armatum* DC of Nepali Origin and their Antibacterial Activities. *Journal of Essential Oil Bearing Plants*, **27**. doi: 10.1080/0972060X.2023.2296549
- Baral, J., Shrestha, D., & Adhikari, A. (2022).  $\alpha$ -Glucosidase and  $\alpha$ -Amylase Inhibition Activities of *Sarcococca coriacea* Hook . And *Sarcococca wallichii* Staph . of Nepalese Origin. *Journal of Nepal Chemical Society*, **43**(1): 135–140. doi: 10.3126/jncs.v43i1.46950
- Baral, J., Shrestha, D., Devkota, H. P., & Adhikari ,A. (2023). Potent ROS Inhibitors from *Zanthoxylum armatum* DC of Nepali Origin. *Natural Product Research*. doi: 10.1080/14786419.2023.2261608
- Barham, D., & Trinder, P. (1972). An Improved Colour Reagent for the Determination of Blood Glucose by the Oxidase System. *The Analyst*, **97**(1151): 142–145. doi: 10.1039/an9729700142
- Barkatullah, M. I., Muhammad, N., Rauf, A., Nasruddin, Khan, H., & Ali, J., (2015). Evaluation of *Zanthoxylum armatum* its Toxic Metal Contents and Proximate

- Analysis. *The Journal of Phytopharmacology*, **4**(43): 157–163. doi: 10.31254/phyot.2015.4306
- Basnet, R. (2020). Cultivation Technology of *Zanthoxylum armatum* DC. *Plant Research Center Jumla*. Retrieved from: [https://www.researchgate.net/publication/342301331\\_Cultivation\\_Technology\\_of\\_Zanthoxylum\\_armatum\\_DC\\_in\\_Nepali\\_Language](https://www.researchgate.net/publication/342301331_Cultivation_Technology_of_Zanthoxylum_armatum_DC_in_Nepali_Language) Accessed on (02/05/2021)
- Batool, F., Sabir, M., S., Rocha, J. B. T., Shah, A. H., Saify, Z. S., & Ahmed, S. D. (2010). Evaluation of Antioxidant and Free Radical Scavenging Activities of Fruit Extract from *Zanthoxylum alatum*: a Commonly Used Spice from Pakistan. *Pakistan Journal of Botany*, **42**(6): 4299–4311. Retrieved from: [http://www.pakbs.org/pjbot/PDFs/42\(6\)/PJB42\(6\)4299.pdf](http://www.pakbs.org/pjbot/PDFs/42(6)/PJB42(6)4299.pdf) Accessed on (2/2/2018)
- Bhakuni, G. S., Bedi, O., Bariwal, J., Deshmukh, R., & Kumar, P. (2016). Animal Models of Hepatotoxicity. *Inflammation Research*, **65**(1): 13–24. doi: 10.1007/s00011-015-0883-0
- Bhalla, Y., Gupta, V. K., & Jaitak, V. (2013). Anticancer Activity of Essential Oils: A Review. *Journal of the Science of Food and Agriculture*, **93**(15): 3643–3653. doi: 10.1002/jsfa.6267
- Bhatt N, & Upadhyaya K. (2010) . Anti-inflammatory Activity of Ethanolic Extract of Bark of *Zanthoxylum aramatum* D.C. *Pharmacology online*. **2**:123–132. Retrieved from: <https://d1wqtxts1xzle7.cloudfront.net/8290> Accessed on (12/12/2020)
- Bisht, M., Mishra, D., Sah, M., Joshi, S., & Mishra, S. (2014). Biological Activities of the Essential Oil of *Zanthoxylum armatum* DC. Leaves. *The Natural Products Journal*. **4**(3):229–232. doi: 10.2174/2210315504666141111231606
- Boedeker, W., Watts, M., Clausing, P., & Marquez, E. (2020). The Global Distribution of Acute Unintentional Pesticide Poisoning : Estimations Based on a Systematic Review. *BMC Public Health*. **20**(1): 1–19. doi: 10.1186/s12889-020-09939-0
- Bonner-Weir, S., Trent, D. F., Honey, R. N., & Weir, G. C. (1981). Responses of Neonatal Rat Islets to Streptozotocin Limited  $\beta$ -cell regeneration and

- hyperglycemia. *Diabetes*, **30**(1): 64–69. doi: 10.2337/diab.30.1.64
- Bottero, J. (1985). The Cuisine of Ancient Mesopotamia. *The Biblical Archeologist*, **48**(1): 36-47. doi: 10.2307/3209946
- Bowers, K. J., Chow, E., Xu, H., Dror, R. O., Eastwood, M. P., Gregersen B. A., Klepeis, J. L., Kolossary, I., Moraes, M. A., Sacerdoti, F. D., & Salmon, J. K., (2006). Scalable Algorithms for Molecular Dynamics Simulations on Commodity Clusters. *SC 06: Proceedings of the 2006 ACM-IEEE Conference on Supercomputing*, USA, 43-43, doi:10.1109/SC.2006.54
- Brand-Williams, W., Cuvelier, M. E., & Berset, C. L. W T.(1995). Use of a Free Radical Method to Evaluate Antioxidant Activity. *LWT-Food Science and Technology*, **28** (1): 25–30. doi: 10.1016/S0023-6438(95)80008-5
- Buchbauer, G., Jäger, W., Jirovetz, L., Ilmberger, J., & Dietrich, H. (1993). *Therapeutic Properties of Essential Oils and Fragrances*. doi: 10.1021/bk-1993-0525.ch012
- Burt, S. (2004). Essential Oils: Their Antibacterial Properties and Potential Applications in Foods - A review. *International Journal of Food Microbiology*, **94**(3): 223–253. doi: 10.1016/j.ijfoodmicro.2004.03.022
- Chang, C. C., Yang, M. H., Wen, H. M., & Chern, J. C. (2002). Estimation of Total Flavonoid Content in Propolis by Two Complementary Colometric Methods. *Journal of food and drug analysis*, **10**(3): 3. doi: 10.38212/2224-6614.2748
- Chatzigeorgiou, A., Halapas, A., Kalafatakis, K., & Kamper, E. F. (2009). The Use of Animal Models in the Study of Diabetes Mellitus. *In Vivo*, **23** (2): 245–258. Retrieved from: <https://pubmed.ncbi.nlm.nih.gov/19414410/> Accessed on (19/09/2019)
- Che, E., Gao, Y., Wan, L., Zhang, Y., Han, N., Bai, J., Li, J., Sha, Z., & Wang, S. (2015). Paclitaxel/Gelatin Coated Magnetic Mesoporous Silica Nanoparticles: Preparation and Antitumor Efficacy in Vivo. *Microporous and Mesoporous Materials*, **204**: 226–234. doi: 10.1016/j.micromeso.2014.11.013
- Cheng, J., Hou, X., Cui, Q., Shen, G., Li, S., Lou, Q., Zhou, M., Chen, H., & Zhang, Z., (2023). Separation and Purification of Hydroxyl- $\alpha$ -Sanshool from *Zanthoxylum armatum* DC. by Silica Gel Column Chromatography. *International Journal of Molecular Sciences*. **24**(4): 3156. doi:

10.3390/ijms24043156

- Chopra, R. N., & Nayar, S. L.(1956). *Glossary of Indian Medicinal Plants*. Council of Scientific and Industrial Research. Retrieved from: <http://hdl.handle.net/123456789/1023> Accessed on (18/4/2020)
- Choudhary, M. I., Adhikari, A., Samreen, & Rahaman, A. (2010). Antileishmanial Steroidal Alkaloids from Roots of *Sarcococca coriacea*. *Journal of Chemical Society of Pakistan*, **32**(6): 799–802. Retrieved from: <http://142.54.178.187:9060/xmlui/handle/123456789/19764> Accessed on (12/12/2021)
- Choudhary, M. I., Devkota, K. P., Nawaz, S. A., & Ranjit, R.(2005). Cholinesterase Inhibitory Pregnane-Type Steroidal Alkaloids from *Sarcococca hookeriana*. *Steroids*, **70** (4): 295–303. doi: 10.1016/j.steroids.2004.11.007
- Chouhan, S., Sharma, K., & Guleria, S. (2017). Antimicrobial Activity of Some Essential Oils Present Status and Future Prespectives. *Medicines*, **4**(3): 58. doi: 10.3390/medicines4030058
- Cicchetti, E., Duroure, L., Perez, M., Sizaire, L. & Vasseur, C.(2017). Characterization of Odour Active Compounds in Timur ( *Zanthoxylum armatum* DC.) Fruits from Nepal. *Flavor and Fragrance Journal*, **32** (5):317–329. doi: 10.1002/ffj.3381
- Commenges, D., Scotet, V., Renaud, S., Jacqmin-Gadda, H., Barberger-Gateau, P., & Dartigues, J. F. (2000). Intake of Flavonoids and Risk of Dementia. *European Journal of Epidemiology*, **16**: 357–363. doi:10.1023/a:1007614613771
- Cornblatt, B. S., Ye, L., Dinkova-Kostova, A. T., Erb, M., Fahey, J. W., Singh, N. K., Chen, M. S. A., Stierer, T., Garrett-Mayer, E., Argani, P., Davidson, N. E., Talalay, P., Kensler, T. W., & Visvanathan, K. (2007). Preclinical and Clinical Evaluation of Sulforaphane for Chemoprevention in the Breast. *Carcinogenesis*, **28** (7):1485–1490. doi: 10.1093/carcin/bgm049
- Cragg, G. M., & Newman, D. J. (2001). Natural Product Drug Discovery in the Next Millennium.*PharmaceuticalBiology*,**39**(1):8–17. doi:10.1076/phbi.39.s1.8.0009
- Cragg, G. M., & Newman, D. J. (2005). Plants as a Source of Anticancer Agents.

- Journal of Ethnopharmacology*, **100**(1–2):72–79. doi: 10.1016/j.jep.2005.05.011
- Cragg, G. M., & Newman, D. J. (2013). Natural Products: A Continuing Source of Novel Drug Leads. *Biochimica et Biophysica Acta - General Subjects*, **1830** (6).
- Daina A, Michielin O, & Zoete V. (2017). Swiss ADME: A Free Web Tool to Evaluate Pharmacokinetics, Druglikeness and Medicinal Chemistry Friendliness of Small Molecules. *Scientific Reports*. **7**: 1–13. Retrieved from : <https://www.nature.com/articles/srep42717> Accessed on (9/7/2022)
- Das, U. N. (2006). Essential Fatty Acids A Review. *Current Pharmaceutical Biotechnology*, **7**, 467–482. doi: 10.2174/138920106779116856
- De Cássia Da Silveira E Sá, R., Andrade, L. N., & De Sousa, D. P. (2013). A review on Anti-inflammatory Activity of Monoterpenes. *Molecules*, **18** (1):1227–1254.
- Decsi, T., Boehm, G., Tjoonk, H. M. R., Molnár, S., Dijck-Brouwer, D. A. J., Hadders-Algra, M., Martini, I. A., Muskiet, F. A. J., & Boersma, E. R. (2002). Trans Isomeric Octadecenoic Acids are Related Inversely to Arachidonic Acid and DHA and Positively Related to Mead Acid in Umbilical Vessel Wall Lipids. *Lipids*, **37**: 959-965. doi: 10.1007/s11745-006-0987-y
- Devkota, K. P., Lenta, B. N., Choudhary, M. I., Naz, Q., Fekam, F. B., Rosenthal, P. J., & Sewald, N. (2007). Cholinesterase Inhibiting and Antiplasmodial Steroidal Alkaloids from *Sarcococca hookeriana*. *Chemical and Pharmaceutical Bulletin*, **55** (9):1397–1401. doi: 10.1248/cbp.55.1397
- Devkota, K., Choudhary, I., Ranjit, R., Samreen, & Sewald, N. (2007). Structure Activity Relationship Studies on Antileishmanial Steroidal Alkaloids from *Sarcococca hookeriana*. *Natural Product Research: Formerly Natural Product Letters*, **21** (4):292–297. doi: 10.1080/1478610701192736
- Devkota, K. P., Wilson, J., Henrich, J. C., McMahon, B. J., Reilly, K. M., & Beutler, J. A., (2012). Isobutylhydroxyamides from the pericarp of Nepalese *Zanthoxylum armatum* Inhibit *NFI*-Defective Tumor Cell Line Growth, *Journal of Natural Products*, **76**(1): 59-63. doi: 10.1021/np300696gl
- Koul, O., Walia, S., & Dhaliwal, G. S. (2008). Essential Oils as Green Pesticides : Potential and Constraints. *Biopesticides International*, **4** (1): 63–84. doi:0973-483X/08/63-84©2008 (KRF)

- Dhami, A., Singh, A., Palariya, D., Kumar, R., Prakash, O., Rawat, D. S., & Pant, A. K. (2019).  $\alpha$ -Pinene Rich Bark Essential Oils of *Zanthoxylum armatum* DC. from Three Different Altitudes of Uttarakhand, India and their Antioxidant, In Vitro Anti-inflammatory and Antibacterial Activity. *Journal of Essential Oil-Bearing Plants*, **22** (3): 660–674. doi: 10.1080/0972060X.2019.1630015
- International Diabetes Federation. (2021). Diabetes Facts & Figures. Retrieved from. <https://www.idf.org/aboutdiabetes/what-is-diabetes/facts-figures.html>  
Accessed on (11/25/2022)
- Dietschy, L. A. woollett and J. M. (1994). Effect of Long-Chain Fatty Acids on Low-Density Lipoprotein Cholesterol Metabolism<sup>14</sup>. *The American Journal of Clinical Nutrition*, **60** (6): 991S-996S. doi: 10.1093/ajcn/60.6.991S
- Ding, D., Wang, M., Wu, J. X., Kang, Y., & Chen, L. (2019). The Structural Basis for the Binding of Repaglinide to the Pancreatic KATP Channel. *Cell reports*, **27** (6): 1848-1857. doi:10.1016/j.celrep.2019.04.050
- Doyle, G., Jayawardena, S., & Ashraf, E., (2010). The Journal of Clinical Efficacy and Tolerability of Nonprescription Ibuprofen versus Celecoxib for Dental Pain. *The Journal of Clinical Pharmacology*. **42**(8): 912–919. doi: 10.1177/009127002401102830
- Egan, W.J., Merz, K. M., & Baldwin, J. J., (2000). Prediction of Drug Absorption using Multivariate Statistics. *Journal of Medicinal Chemistry*. **43** (21):3867–3877. doi: 10.1021/jm000292e
- Einarson, T. R., Acs, A., Ludwig, C., & Panton, U. H. (2018). Prevalence of Cardiovascular Disease in Type 2 Diabetes: A Systematic Literature Review of Scientific Evidence from Across the World in 2007-2017. *Cardiovascular Diabetology*. **17** (1): 1-19. doi: 10.1186/s12933-018-0728-6.
- Elisabetsky, E. (2002). Traditional Medicines and the New Paradigm of Psychotropic Drug Action. *Advances in Phytomedicine*, **1**: 133-144. doi: 10.1016/S1572-557X(02)80020-4
- Erharuyi, O., Adhikari, A., Falodun, A., Jabeen, A., Imad, R., Ammad, M., Choudhary, M. I., & Goren, N., (2017). Cytotoxic, Anti-inflammatory and Leishmanicidal Activities of Diterpenes Isolated from the Roots of *Caesalpinia pulcherrima*.

*Planta Medica*. **83** (01/02): 104-110. doi: 10.1055/s-0042-110407

- Fabricant, D. S., & Farnsworth, N. R. (2001). The Value of Plants used in Traditional Medicine for Drug Discovery. *Environmental Health Perspectives*, **109** (1): 69–75. doi: 10.1289/ehp.01109s169
- Farnsworth, Norman R., & Soejarto D. D. (1991). Global Importance of Medicinal Plants. *The Conservation of Medicinal Plants*, **26**: 25–51. doi: 10.1017/CBO9780511753312.005
- Ferlay, J., Colombet, M., Soerjomataram, I., Parkin, D. M., Piñeros, M., Znaor, A., & Bray, F. (2021). Cancer Statistics for the Year 2020: An Overview. *International Journal of Cancer*, **149** (4):778–789. doi: 10.1002/ijc.33588
- Ferrero-Miliani, L., Nielsen, O. H., Andersen, P. S., & Girardin, S. E. (2007). Chronic Inflammation: Importance of NOD2 and NALP3 in Interleukin-1 $\beta$  Generation. *Clinical and Experimental Immunology*, **147** (2):227–235. doi: 10.1111/j.1365-2249.2006.03261.x
- Finkel, T., (2011). Signal Transduction by Reactive Oxygen Species. *Journal of Cell Biology*, **194** (1):7–15. doi: 10.1083/jcb.201102095
- Fouotsa, H., Meli, A., Djama, C., Rasheed, S., Marasini, B. P., Ali, Z., Prasad, K., Ephrem, A., Shaheen, F., Iqbal, M., & Sewald, N. (2012). Xanthones Inhibitors of a  $\alpha$ -Glucosidase and Glycation from *Garcinia nobilis*. *Phytochemistry Letters*, **5** (2):236–239. doi: 10.1016/j.phytol.2012.01.002
- Friedewald, W. T., Levy, R. I., & Fredrickson, D. S. (1972). Estimation of the Concentration of Low Density Lipoprotein Cholesterol in Plasma, Without Use of the Preparative Ultracentrifuge. *Clinical Chemistry*, **18** (6): 499–502. doi: 10.1093/clinchem/18.6.499
- Fürst, R., & Zündorf, I., (2014). Plant-derived anti-inflammatory compounds : hopes and disappointments regarding the translation of preclinical knowledge into clinical progress. *Mediators of Inflammation*, **2014**. doi: 10.1155/2014/146832
- Gagliardino, J. J., Martella, A., Etchegoyen, G. S., Caporale, J. E., Guidi, M. L., Olivera, E. M., & González, C. (2004). Hospitalization and Re-hospitalization of People With and Without Diabetes in La Plata, Argentina: Comparison of Their Clinical Characteristics and Costs. *Diabetes Research and Clinical*

*Practice*, **65** (1): 51–59. doi: 10.1016/j.diabres.2023.11.011

- Gautam, R., & Jachak, S. M.(2009). Recent Developments in Anti-inflammatory Natural Products. *Medicinal Research Reviews*. **29** (5): 767–820. doi: 10.1002/med.20156
- Ghose, A. K., Viswanadhan, V. N.,& Wendoloski, J. J.(1999). A Knowledge-Based Approach in Designing Combinatorial or Medicinal Chemistry Libraries For Drug Discovery. 1. A Qualitative and Quantitative Characterization of Known Drug Databases. *Journal of Combinatorial Chemistry*. **1** (1): 55–68. doi: 10.1021/cc9800071
- Musharraf, S. G., Goher, M., Ali, A., Adhikari, A., & Choudhary, M. I. (2012). Rapid Characterization and Identification of Steroidal Alkaloids in *Sarcococca coriacea* Using Liquid Chromatography Coupled With Electrospray Ionization Quadropole Time-of-Flight Mass Spectrometry. *Steroids*, **77**(1–2):138–148. doi: 10.1016/j.steroids.2011.11.001
- Goodnight Jr, S. H., Harris, W. S., Connor, W. E., & Illingworth, D. R. (1982). Polyunsaturated Fatty Acids, Hyperlipidemia, and Thrombosis. *Atherosclerosis: An official Journal of the American Heart Association*, **2**(2): 87–113. doi: 10.1161/01.ATV.2.2.87
- Gorrini, C., Harris, I. S., & Mak, T. W. (2013). Modulation of Oxidative Stress as an Anticancer Strategy. *Nature Reviews Drug Discovery*,**12** (12): 931–947. doi: 10.1038/nrd4002
- Government of Nepal. (2013). *Value Chain Designing of Timur of Panchase Protected Forest Area*. Ecosystem Based Adaptation in Mountain Ecosystem in Nepal Retrieved from [https://www.adaption-undp.org/sites/default/files/resources/2013\\_dept\\_of\\_forests\\_undp\\_timur\\_value\\_chain\\_study.pdf](https://www.adaption-undp.org/sites/default/files/resources/2013_dept_of_forests_undp_timur_value_chain_study.pdf) Accessed on (25/5/2023)
- Grace, S. C, & Logan, B. A. (2000). Energy Dissipation and Radical Scavenging by the Plant Phenylpropanoid Pathway. *Philosophical Transactions of the Royal Society of London Series B: Biological Sciences*, **355** (1402): 1499–1510. doi: 10.1098/rstb.2000.0710
- Groppo, M., Pirani, J. R., Salatino, M. L. F., Blanco, S. R., & Kalunki, J. A. (2008).

- Phylogeny of Rutaceae Based on Two Noncoding Regions From cpDNA. *American Journal of Botany*, **95**(8): 985–1005. doi: 10.3732/ajb.2007313
- Guardia, T., Rotelli, A. E., Juarez, A. O., & Pelzer, L. E. (2001). Anti-inflammatory Properties of Plant Flavonoids. Effects of Rutin, Quercetin and Hesperidin on Adjuvant Arthritis in Rat. *II Farmaco*, **56**(9): 683–687. doi: 10.1016/s0014-827X(01)01111-9
- Hafizur, R. M., Hameed, A., Shukrana, M., Raza, S. A., Chisti, S., Kabir, N., & Shiddiqui, R. A.,(2015). Cinnamic Acid Exerts Anti-diabetic Activity by Improving Glucose Tolerance In Vivo and by Stimulating Insulin Secretion In Vitro. *Phytomedicine*, **22** (2): 297-300. doi:10.1016/j.phymed.2015.01.003
- Hakkola, J., Hukkanen, J., Turpeinen, M., Pelkonen, O.,(2020). Inhibition and Induction of CYP Enzymes in Humans: An Update. *Archives of Toxicology* **94**(11): 3671–3722. doi: 10.1007/s00204-020-02936-7
- Halliwell, B., & Gutteridge, J. M. C. (2015). *Free Radicals in Biology and Medicine*. Oxford University Press. Retrieved from: <https://doi.org/10.1093/acprof:oso/97801987174778.001.0001> Accessed on (24/9/2022)
- Halliwell, B. (2012). Free Radicals and Antioxidants: Updating a Personal View. *Nutrition reviews*, **70**(5): 257–265. Doi: 10.1111/j.1753-4887.2012.00476.x
- Hameed, A., Raza, S. A., Israr Khan, M., Baral, J., Adhikari, A., Nur-e-Alam, M., Ahmed, S., Al-Rehaily, A. J., Ashraf, S., Ul-Haq, Z., & Hafizur, R. M. (2019). Tambulin From *Zanthoxylum armatum* Acutely Potentiates the Glucose-Induced Insulin Secretion Via KATP-Independent Ca<sup>2+</sup>-Dependent Amplifying Pathway. *Biomedicine and Pharmacotherapy*, **120**, 109348. doi: 10.1016/j.biopha.2019.109348
- Hara, H., Chater, A. O. & Williams, L. H. J. (1982). *An enumeration of the flowering plants of Nepal*. **3**. British Museum, Mansell Books Binders Limited. Retrieved from: [https://An+enumeration+of+the+flowering+plants+of+Nepal.+3.+Manse ll+Books+Binders+Limited.&oq=Hara+H%2C+Chater%2C+A.+O.+%26+Wi lliams%2C+L.+H.+J.+\(1982\)](https://An+enumeration+of+the+flowering+plants+of+Nepal.+3.+Manse ll+Books+Binders+Limited.&oq=Hara+H%2C+Chater%2C+A.+O.+%26+Wi lliams%2C+L.+H.+J.+(1982)) Accessed on (22/12/2020)
- Hassan tusher, M. M., Asrafuzzaman, M., & Hafizur, M. (2021). Antidiabetic Effect of

- Grape Seed ( OPC 95 %) Powder on nSTZ-Induced Type 2 Diabetic Model Rats. *African Journal of Pharmacy and Pharmacology*, **15** (6): 109–117. doi: 10.5897/AJPP2021.5247
- Hassid, W. Z., & Abraham, S. (1957). Chemical Procedures For Analysis of Polysaccharides. *Methods in Enzymology*, **3**: 34–50. doi: 10.1016/S0076-6879(57)03345-5. doi: 10.1016/S0076-6879957003345-5
- Hawkins, P. C., Skillman, A. G., Warren, G. L., Ellingson, B. A., & Stahl, M. T. (2010). Conformer Generation with OMEGA: Algorithm and Validation Using High Quality Structures from the Protein Databank and the Cambridge Structural Database. *Journal of chemical information and modeling*, **50** (4): 572-584. doi: 1110.1021/ci100031x
- Hden, W. H., & Wiersum, K. F. (2000). Timur (*Zanthoxylum armatum*) Production in Nepal. *Mountain Research and Development*, **20** (2):136–145. doi: 10.1659/0276-47419(2000)020[0136:TZAPIN]2.0.CO;2
- Helfand, S. L., Werkmeister, J., & Roder, J. C. (1982). Chemiluminescence Response of Human Natural Killer Cells: I. The Relationship Between Target Cell Binding, Chemiluminescence, and Cytolysis. *The Journal of Experimental Medicine*, **156** (2): 492–505. doi: 10.1084/jem.156.2.492
- Hodge, W. H. (1958). Glossary of Indian Medicinal Plants. In *The Quarterly Review of Biology* **33**(2): 156-156. doi:10.1086/402350
- Hofbauer, R., Speiser, W., & Kapiotis, S. (1998). Ibuprofen Inhibits Leukocyte Migration Through Endothelial Cell Monolayers. *Life Sciences*, **62** (19): 1775–1781. doi: 10.1016/S0024-3205(98)00139-8
- Horie, T., Ohtsuru, Y., Shibata, K., Yamashita, K., Tsukayama, M., & Kawamura, Y. (1998). <sup>13</sup>C NMR spectral assignment of the A-ring of polyoxygenated flavones. *Phytochemistry*, **47**(5): 865-874. doi: 10.1016/S0031-9422(97)00629-8
- Hüsni, K., Başer, C., & Demirci, F. (2007). Chemistry of essential oils. In *Flavours and Fragrances: Chemistry, Bioprocessing and Sustainability*. Springer, Berlin, Heidelberg: Springer Berlin Heidelberg: 43-86. doi: 10.1007/978-3-540-49339-6\_4
- Hussain, T., Tan, B., Yin, Y., Blachier, F., Tossou, M. C. B., & Rahu, N., (2016).

- Oxidative Stress and Inflammation: What Polyphenols Can Do for Us? *Oxidative Medicine and Cellular Longevity*, **2016**. doi: 10.1155/2016/7432797
- Iannaccone, P. M., & Jacob, H. J. (2009). Rats! *Disease Models and Mechanisms*, **2** (5–6): 206–210. doi:10.1242/dmm.002733
- IBMnc. (2007). *Statistical Package for Social Sciences(SPSS) Inc. Released 2007. SPSS for Windows, Version 12.0. Chicago, SPSS Inc:12.*
- In Kwon, Y., Apostolidis, E., & Shetty, K. (2006). Evaluation of Pepper (*Capsicum Annuum*) for Management of Diabetes and Hypertension. *Journal of Food Biochemistry*, **31** (2007): 370–385. doi:10.1111/j.1745-4514.2007.00120.x
- Irshad, A., Naveed, M., Ullah, I., & Khan, M. F. (2021). Antibacterial and Antioxidant Effects of *Zanthoxylum armatum* DC Extracts. *Bangladesh Journal of Botany*, **50**(1), 159–164. doi:10.3329/bjb.v50i1.52683
- J. A. Depree, T. M. Howard, G. P. S. (1999). Flavour and pharmaceutical properties of the volatile sulphur compounds of Wasabi (*Wasabia japonica*). *Food Research International*, **31**(5) :329–337. doi: 10.1016/s0963-9969(98)00105-7
- Vane, J. R., & Botting, R. M. (1998). Mechanism of Action of Nonsteroidal Anti-inflammatory Drugs. *The American Journal of medicine*, **104** (3S1): 2S-8S. doi:10.1016/s0002-9343(97)00203-9
- Johnston, S. A., & Fox, S. M.(1997).Mechanisms of Action of Anti-inflammatory Medications Used for the Treatment of Osteoarthritis. *Journal of the American Veterinary Medical Association*, **210** (10): 1486–1492.Retrieved from [www.europepmc.org/article/med/9154203](http://www.europepmc.org/article/med/9154203) Accessed on (20/01/2022)
- Jones, P. A., & Baylin, S. B. (2007). The Epigenomics of Cancer. *Cell*, **128** (4): 683–692. doi: 10.1016/j.cell.2007.01.029
- Jordan, M. A., & Wilson, L. (2004). Microtubules as a Target for Anticancer Drugs *Nature Reviews Cancer*, **4** (4): 253–265. doi: 10.1038/nrc1317
- Jun, H., Lee, J. H., Kim, J., Jia, Y., Kim, K. H., Hwang, K. Y., Yun, E. J., Do, K. R., & Lee, S. (2014). Linalool is a PPAR  $\alpha$ -Ligand That Reduces Plasma TG Levels and Rewires the Hepatic Transcriptome and Plasma Metabolome. *Journal Lipid Research*, **55** (6): 1098–1110. doi: 10.1194/jlr.M045807

- Kalauni, S. K., Choudhary, M. I., Khalid, A., Manandhar, M. D., Shaheen, F., Atta-ur-Rahman, & Gewali, M. B. (2002). New Cholinesterase Inhibiting Steroidal Alkaloids From the Leaves of *Sarcococca coriacea* of Nepalese Origin. *Chemical and Pharmaceutical Bulletin*, **50** (11): 1423–1426. doi: 10.1248/cpb.50.1423
- Kalia, N. K., Singh, B., & Sood, R. P.(1999). A New Amide from *Zanthoxylum armatum*. *Journal of Natural Products*. **62** (2): 322-312. doi: 10.1021/np980224j
- Kamatou, G. P. P., & Viljoen, A. M. (2008). Linalool - A Review of a Biologically Active Compound of Commercial Importance. *Natural Product Communications*, **3** (7) :1183–1192. doi:10.1177/1934578X0800300727
- Kamboj, V. P.(2000). Herbal Medicine. *Current Science Association*. **78** (1): 35–39. Retrieved from: <https://www.jstor.org/stable/24103844> Accessed on (23/03/2020)
- Kanwal, R., Arshad, M., Bibi, Y., Asif, S., & Chaudhari, S. K. (2015). Evaluation of Ethnopharmacological and Antioxidant Potential of *Zanthoxylum armatum* DC. *Journal of Chemistry*, **2015**. doi: 10.1155/2015/925654
- Karki, H., Upadhayay, K., Pal, H., & Singh, R. (2014). Antidiabetic Potential of *Zanthoxylum armatum* Bark Extract on Streptozotocin Induced Diabetic Rats. *International Journal of Green Pharmacy*, **8**(2): 77–83. doi: 10.4103/0973-8258.129568
- Kayat, H. P., Gautam, S. D., & Jha, R. N. (2016). GC-MS Analysis of Hexane Extract of *Zanthoxylum armatum* DC Fruits. *Journal of Pharmacognosy and Phytochemistry*, **5** (2): 58–62. Retrieved from:<https://www.phytojournal.com/archives/2016.v5.i2.758>. Accessed on (12/04/2022)
- Kazeem, M. I., Adamson, J. O., & Ogunwande, I. A. (2013). Modes of Inhibition of  $\alpha$ -Amylase and  $\alpha$ -Glucosidase by Aqueous Extract of *Morinda lucida* Benth Leaf. *Biomed Research International*. **2013**. doi: 10.1155/2013/527570
- Kazi, A. A. & L., & Blonde, L. (2001). Classification of Diabetes Mellitus. *Clinics in Laboratory Medicine*, **21** (1):1–13.Retrieved from:

<https://www.ncbi.nlm.nih.gov/11321930> Accessed on (09/03/ 2022)

- Khadayat, K., Marasini, B. P., Gautam, H., Ghaju, S., & Parajuli, N. (2020). Evaluation of the Alpha-Amylase Inhibitory Activity of Nepalese Medicinal Plants Used in the Treatment of Diabetes Mellitus. *Clinical Phytoscience* 2020, **6** (1): 1–8. doi:10.1186/s40816-020-00179-8
- Khatri, D., Chhetri, S. B. B., Poudel, P., & Devkota, H. P. (2023). *Zanthoxylum armatum* DC. *Himalayan Fruits and Berries*. Academic Press. 479-490. doi: 10.1016/B978-0-323-85591-4.00039
- Kilkenny, C., Browne, W., Cuthill, I., Emerson, M., & Altman, D. (2010). Improving Bioscience Research Reporting: The ARRIVE Guidelines for Reporting Animal Research. *Journal of Pharmacology and Pharmacotherapeutics*, **1** (2): 94. doi: 10.4103/0976-500x.72351
- Koek, M. M., Jellema, R. H., van der Greef, J., Tas, A. C., & Hankemeier, T. (2011). Quantitative Metabolomics Based on Gas chromatography Mass Spectrometry: Status and Perspectives. *Metabolomics*, **7**(3): 307–328. doi: 10.1007/s11306-010-0254-3
- Kumar, A., & Somasundaram, S. T. (2014). Gas Chromatography-Mass Spectrum ( GC-MS ) Analysis of Bioactive Components of the Methanol Extract of Halophyte, *Sesuvium portulacastrum* L . *International Journal of Advances in Pharmacy, Biology and Chemistry*, **3** (3): 766–772. Retrieved from: <http://www.ijapbc.com/files/39-3396.pdf> . Accessed on (3/03/2021)
- Kumar, A., Chandra, S. S., Dobhlal, S. M., S, K., D, S., U, B., & G, K. (2015). Chemical and Potential Biological Perspectives of Genus *Sarcococca* (Buxaceae). *The Natural Products Journal*, **5**: 28–49.  
doi: 10.2174/2210315505666150219233014
- Kumhálová, J., Matějková, Š., Fifernová, M., Lipavský, J., & Kumhála, F. (2008). Topography Impact on Nutrition Content in Soil and Yield. *Plant, Soil and Environment*, **54** (6): 255–261. doi: 10.17221/257-pse
- Lawson, S. K., Satyal, P., & Setzer, W. N. (2021). Phytochemical Analysis of the Essential Oils From Aerial Parts of Four *Scutellaria* “skullcap” Species Cultivated in South Alabama: *Scutellaria baicalensis* Georgi, *S. Barbata* D.

- Don, S. *Incana* Biehler, and S. *Lateriflora* L. *Natural Product Communications*, **16** (8): 1–12. doi: 10.1177/1934578X211025930
- Li, T., Chen, M., Ren, G., Hua, G., Mi, J., Jiang, D., & Liu, C. (2021). Antifungal Activity of Essential Oil From *Zanthoxylum armatum* DC. on *Aspergillus flavus* and *Aflatoxins* in Stored Platycladi Semen. *Frontiers in Microbiology*, **12**: 1–8. doi: 10.3389/fmicb.2021.633714
- Li, P-L., Zhai, X-X., Wang, J., Zhu, X., Zhao, L., You, S., Sang, C.-Y., & J.-L. (2023). Two Ferulic Acid Derivatives Inhibit Neuroinflammatory Response in Human HMC3 Microglial Cells via NF-kB Signaling Pathway. *Molecules*, **28**,2080. doi: 10.3390/molecules28052080
- Liaqat, I., Riaz, N., Saleem, Q. U. A., Tahir, H. M., Arshad, M., & Arshad, N. (2018). Toxicological Evaluation of Essential Oils From Some Plants of Rutaceae Family. *Evidence-Based Complementary and Alternative Medicine*, **2018**. doi: 10.1155/2018/4394687
- Lim G. P., Yang, F., Chu, T., Chen, P., Beech, W., Teter, B., Tran, T., Ubeda, O., Ashe, K. H., Frautschy, S. A., & Cole, G. M. (2000). Ibuprofen Suppresses Plaque Pathology and Inflammation in a Mouse Model for Alzheimer's Disease. *Journal of Neuroscience*, **20** (15): 5709–5714. doi: 10.1523/JNEUROSCI.20-15-05709.2000
- Lima, L. A. R. D. S., Johann, S., Cisalpino, P. S., Pimenta, L. P. S., & Boaventura, M. A. D. (2011). In Vitro Antifungal Activity of Fatty Acid Methyl Esters of the Seeds of *Annona cornifolia* A.St.-Hil. (Annonaceae) Against Pathogenic Fungus *Paracoccidioides brasiliensis*. *Revista da Sociedade Brasileira de Medicina Tropical*, **44**: 777–780. Doi: 10.1590/S0037-86822011000600024
- Lipinski, C. A., Lombardo, F., Dominy, B. W., & Feeney, P. J. (2012). Experimental and Computational Approaches to Estimate Solubility and Permeability in Drug Discovery and Development Settings. *Advanced drug delivery reviews*, **64**: 4-17. Doi: 10.1016/j.addr.2012.09.019
- Lopes-Virella, M. F., Stone, P., Ellis, S., & Colwell, J. A. (1977). Cholesterol Determination in High Density Lipoproteins Separated by Three Different Methods. *Clinical Chemistry*, **23** (5): 882–884. Doi: 10.1093/clinchem/23.5.882

- Lorke, D. (1983). A New Approach to Practical Acute Toxicity Testing. *Archives of Toxicology*, **54** (4): 275–287. doi: 10.1007/BF01234480
- Lu, X., Ross, C. F., Powers, J. R., Aston, D.E., & Rasco, B. A. (2011). Determination of Total Phenolic Content and Antioxidant Activity of Garlic (*Allium sativum*) and Elephant Garlic (*Allium ampeloprasum*) by Attenuated Total Reflectance - Fourier Transformed Infrared Spectroscopy. *Journal of agricultural and food chemistry*, **59** (10): 5215–5221. doi: 10.1021/jf201254f
- Talluri, M. R., Gummadi, V. P., Battu, G. R., & Killari, K. N. (2019). Evaluation of Hepatoprotective Activity of *Zanthoxylum armatum* on Paracetamol Induced Liver Toxicity in Rats. *Indian Journal of Pharmaceutical Sciences*, **81** (2018): 138–145. doi: 10.4172/pharmaceutical-sciences.1000489
- Malik, N. P., Naz, M., Ashiq, U., Jamal, R. A., Gul, S., Saleem, F., & Yousuf, S. (2021). Oxamide Derivatives as Potent  $\alpha$ -Glucosidase Inhibitors: Design, Synthesis, in Silico Docking Studies. *Chemistry Select*, **6** (28), 7188-7201. doi: 10.1002/slct.202101709
- Malla, B., Gauchan, P. D., & Chhetri, R. B. (2014). Medico Ethnobotanical Investigations in Parbat District of Western Nepal. *Journal of Medicinal Plants Research*, **8** (2): 95–108. doi: 10.5897/jmpr2013.5228
- Mccue, P., Kwon, Y. I., & Shetty, K. (2005). Anti-Amylase, Anti- Glucosidase and Anti-Angiotensin I-Converting Enzyme Potential of Selected Foods. *Journal of Food Biochemistry*, **29** (3): 278–294. doi: 10.1111/j.1745-4514.2005.00020.x
- McGann, M. (2011). FRED Pose Prediction and Virtual Screening Accuracy. *Journal of chemical information and modeling*, **51** (1): 578-596. doi: 10.1021/ci00436p
- Mehrotra, N., Jadhav, K., Rawalgaonkar, S., Khan, S. A., & Parekh, B. (2019). In vitro Evaluation of Selected Indian Spices for  $\alpha$ -Amylase and  $\alpha$ -Glucosidase Inhibitory Activities and their Spice-Drug Interactions. *Annals of Phytomedicine: An International Journal*, **8** (2): 43-54. doi: 10.21276/ap.2019.8.2.5
- Mensor, L. L., Menezes, F. S., Leitaõ, G. G., Reis, A. S., Santos, T. C. D., Coube, C. S., & Leitao, S. G. (2001). Screening of Brazilian Plant Extracts for Antioxidant Activity by the Use of DPPH Free Radical Method. *Phytotherapy Research*, **15**

(2):127–130. doi: 10.1002/ptr.687

- Mesripour, A., Shahnooshi, S., Hajhashemi, V. (2019). Celecoxib, Ibuprofen, and Indomethacin Alleviate Depression Like Behavior Induced by Interferon- $\alpha$  in Mice. *Journal of Complementary and Integrative Medicine*, **17** (1): 20190016. doi: 10.1515/jcim-2019-0016
- Michael, B., Yano, B., Sellers, R. S., Perry, R., Morton, D., Roome, N., Johnson, J. K., Schafer, K., & Pitsch, S. (2007). Evaluation of Organ Weights for Rodent and Non-Rodent Toxicity Studies: A Review of Regulatory Guidelines and a Survey of Current Practices. *Toxicologic pathology*, **35** (5): 742–750. doi: 10.1080/01926230701595292
- Mittal, M., Siddiqui, M. R., Tran, K., Reddy, S. P., & Malik, A. B. (2014). Reactive Oxygen Species in Inflammation and Tissue Injury. *Antioxidants & Redox Signaling*, **20** (7): 1126- 1167. doi: 10.1089/ars.2012.5149
- Muegge, I., Heald, S. L., Brittelli, D. (2001). Simple Selection Criteria for Drug-Like Chemical Matter. *Journal of medicinal chemistry*, **44** (12): 1841- 846. doi: 10.1021/jm015507e
- Mukhija, M., Dhar, K. L., & Kalia, A. N. (2014). Bioactive Lignans from *Zanthoxylum alatum* Roxb. Stem Bark With Cytotoxic Potential. *Journal of ethnopharmacology*, **152** (1):106–112. doi: 10.1016/j.jep.2013.12.039
- Mushtaq, M. N., Ghimire, S., Akhtar, M. S., Adhikari, A., Auger, C., & Schini-Kerth, V. B. (2019). Tambulin is a Major Active Compound of a Methanolic Extract of Fruits of *Zanthoxylum armatum* DC Causing Endothelium-Independent Relaxations in Porcine Coronary Artery Rings via the Cyclic AMP and Cyclic GMP Relaxing Pathways. *Phytomedicine*, **53**: 163–170. doi: 10.1016/j.phymed.2018.09.020
- Nagajyoti, P. C., Lee, K. D., & Sreekanth, T. V. M. (2010). Heavy Metals, Occurrence and Toxicity for Plants: A Review. *Environmental chemistry letters*, **8**: 199–216. doi: 10.1007/s10311-010-0297-8
- Nagmoti, D. M., & Juvekar, A. R. (2013). In vitro inhibitory effects of *Pithecellobium dulce* (Roxb.) Benth. Seeds on Intestinal  $\alpha$ -Glucosidase and Pancreatic  $\alpha$ -Amylase. *Journal of Biochemical Technology*, **4**: 616- 621. Retrieved from :

<https://jbiochemtech.com/storage/models/article/Fn5ULAyH4rUL4G2kIOxKo y8HwHj2agATPxrHRCKXsAcwVAHdi7eVsujXMW1d/in-vitro-inhibitory-effects-of-pithecellobium-dulce-roxb-benth-seeds-on-intestinal-i-glucosidase-a.pdf> . Accessed on (2/04/2020)

- Nair, S. S., Kavrekar, V., & Mishra, A. (2013). In vitro Studies on Alpha Amylase and Alpha Glucosidase Inhibitory Activities of Selected Plant Extracts. *European Journal of Experimental Biology*, **3** (1): 128- 132. Retrieved from : [www.pelagiaresearchlibrary.com](http://www.pelagiaresearchlibrary.com) Accessed on (2/2/2019)
- Nefzi, A., Aydi, B. A. R., Jabnoun, H., Saidana, S., & Haouala, R. (2016). Antifungal Activity of Aqueous and Organic Extracts from *Withania somnifera* L. Against *Fusarium oxysporium* f. sp. *Radicis-lycopersici*. *Journal of microbial & biochemical technology*, **8**: 144-150.doi: 10.4172/1948-5948.1000277
- Negi, J. S., Bisht, V. K., Bhandari, A. K., Bisht, R., & Negi, S. K. (2012). Major Constituents, Antioxidant and Antibacterial Activities of *Zanthoxylum armatum* DC. Essential Oil. *Iranian Journal of Pharmacology & Therapeutics*, **11** (2): 68- 72. Retrieved from: <http://ijpt.iums.ac.ir> Accessed on (3/03/2019)
- Negi, J. S., Bisht, V. K., Bhandari, A. K., Singh, P., & Sundriyal, R. C. (2011). Chemical Constituents and Biological Activities of the Genus *Zanthoxylum*: A Review. *African Journal of Pure and Applied Chemistry*, **5** (12): 412-416. Retrieved from: <http://www.academicjournals.org/AJPAC> Accessed on (1/01/2019)
- Nepal, G.(2013). Value Chain Designing of Timur of Panchase Protected Forest Area. *Ecosystem Based Adaptation in Mountain in Nepal*. (Issue December).1-12. Retrieved from: [https://www.adaptation-undp.org/sites/default/files/resources/2013\\_dept\\_of\\_forests\\_undp\\_timur\\_value\\_chain\\_study.pdf](https://www.adaptation-undp.org/sites/default/files/resources/2013_dept_of_forests_undp_timur_value_chain_study.pdf) Accessed on (12/22/2023)
- Neupane, B., Gautam, N., Miya, M. S., Upadhyaya, A., Timilsina, Y. P., Gautam, D., Kandel, S., & Dhimi, B. (2023). Socio-Economic Contribution of *Zanthoxylum armatum* (Timur) in the Rural Household Income of Myagdi District, Nepal. *Environment and Natural Resources Journal*, **21**(1): 58- 66. doi: 10.32526/enrj/21/202200175
- Newman, D. J., & Cragg, G. M. (2012). Natural Products as Sources of New Drugs

- Over the 30 Years from 1981 to 2010. *Journal of Natural Products*, **75** (3), 311-335. doi: 10.1021/np200906s
- Newman, D. J., & Cragg, G. M. (2016). Natural Products as Sources of New Drugs from 1981 to 2014. *Journal of Natural Products*, **79** (3): 629- 661. doi: 10.1021/acs.jnatprod.5b01055
- Newman, D. J., & Cragg, G. M. (2020). Natural Products as Sources of New Drugs from 1981 to 2019. *Journal of Natural Products*, **83** (3): 770-803. doi: 10.1021/acs.jnatprod.9b01285
- Tagoe, D. N. A., & Amo-Kodieh, P. (2013). Type 2 Diabetes Mellitus Influences Lipid Profiles of Diabetic Patients. *Annals of Biological Research*, **4** (6): 88- 92. Retrieved from: [scholarsresearchlibrary.com/archive.html](http://scholarsresearchlibrary.com/archive.html) Accessed on (12/12/2022)
- Niu, H., & Zhou, Y. (2021). Nonlinear Relationship Between AST-to-ALT Ratio and the Incidence of Type 2 Diabetes Mellitus : A Follow-Up Study. *International Journal of General Medicine*, **14**: 8373- 8382. doi: 10.2147/IJGM.S341790
- Nooreen, Z., Singh, S., Singh, D. K., Tandon, S., Ahmad, A., & Luqman, S. (2017). Characterization and Evaluation of Bioactive Polyphenolic Constituents from *Zanthoxylum armatum* DC., a Traditionally Used Plant. *Biomedicine & Pharmacotherapy*. **89**: 366- 375. doi: 10.1016/j.biopha.2017.02.040
- Nooreen, Z., Kumar, A., Bawankule, D. U., Tandon, S., Ali, M., Xuan, T. D., & Ahmad, A. (2019). New Chemical Constituents From the Fruits of *Zanthoxylum armatum* and its In Vitro Anti-inflammatory Profile. *Natural Product Research*, **33**(5): 665- 672. doi: 10.1080/14786419.2017.1405404
- Odeyemi, O. O., Yakubu, M. T., Masika, P. J., & Afolayan, A. J. (2009). Toxicological Evaluation of the Essential Oil From *Mentha longifolia* l. Subsp. Capensis Leaves in Rats. *Journal of Medicinal Food*, **12**(3): 669- 674. Doi: 10.1089/jmf.2008.0136
- Olson, H., Betton, G., Robinson, D., Thomas, K., Monro, A., Kolaja, G., Lilly, P., Sanders, J., Sipes, G., Bracken, W., Dorato, M., Van Deun, K., Smith, P., Berger, B., & Heller, A. (2000). Concordance of the Toxicity of Pharmaceuticals in Humans and in Animals. *Regulatory toxicology and pharmacology*, **32** (1):

56- 67. doi: 10.1006/rtp.2000.1399

- World Health Organization.(2022). *WHO Global Centre for Traditional Medicine*. Retrieved from: <https://www.who.int/initiatives/who-global-centre-for-traditional-medicine> Accessed on (2/07/2022)
- Orhan, I. E., Deniz, F. S. S. (2021). Natural Products and Extracts as Xantine Oxidase Inhibitors – A Hope for Gout Disease? *Current Pharmaceutical Design*. **27**(2): 143-158. doi: 10.2174/1381612826666200728144605
- Paduch, R., Kandefor-Szerszeń, M., Trytek, M., & Fiedurek, J. (2007). Terpenes: Substances Useful in Human Healthcare. *Archivum Immunologiae Et Therapiae Experimentalis*, **55**(5): 315- 327. Doi: 10.1007/s00005-007-0039-1
- Pandey, T., Sammi, S. R., Nooreen, Z., Mishra, A., Ahmad, A., Bhatta, R. S., & Pandey R. (2019). Anti- Ageing and Anti-Parkinsonian Effects of Natural Flavonol, Tambulin from *Zanthoxylum armatum* Promotes Longevity in *Caenorhabditis elegans*. *Experimental Gerontology*. **120**: 50- 61. doi: 10.1016/j.exger.2019.02.016
- Peana, A. T., D' Aquila, P. S., Panin, F., Serra, G., Pippia, P., & Moretti, M. D. L. (2002). Anti-inflammatory Activity of Linalool and Linalyl Acetate Constituents of Essential Oils. *Phytomedicine*, **9**(8): 721-726. Doi: 10.1078/094471102321621322
- Pereira, I., Severino, P., Santos, A. C., Silva, A. M., & Souto, E. B. (2018). Linalool Bioactive Properties and Potential Applicability in Drug Delivery Systems. *Colloids and Surfaces B: Biointerfaces*, **171**: 566- 578. doi: 10.1016/j.colsurfb.2018.08.001
- Phuyal, N., Jha, P. K., Raturi, P. P., & Rajbhandary, S. (2019). *Zanthoxylum armatum* DC.: Current Knowledge, Gaps and Opportunities in Nepal. *Journal of Ethnopharmacology*, **229**: 326- 341. doi: 10.1016/j.jep.2018.08.010
- Phuyal, N., Jha, P. K., Raturi, P. P., & Rajbhandary, S. (2020). Comparison Between Essential Oil Compositions of *Zanthoxylum armatum* DC. Fruits Grown at Different Altitudes and Populations in Nepal. *International Journal of Food Properties*, **23** (1): 1971-1978. doi: 10.1080/10942912.2020.1833032
- Phuyal, N., Jha, P. K., Raturi, P. P., & Rajbhandary, S. (2020). Total Phenolic,

- Flavonoid Contents, and Antioxidant Activities of Fruit, Seed, and Bark Extracts of *Zanthoxylum armatum* DC. *The Scientific World Journal*, **2020**. doi: 10.1155/2020/8780704
- Pires, D. E., Blundell, T. L., & Ascher, D.B., (2015). pkCSM: Predicting Small-Molecule Pharmacokinetic and Toxicity Properties Using Graph-Based Signatures. *Journal of Medicinal Chemistry*, **58** (9): 4066- 4072. doi: 10.1021/acs.jmedchem.5b00104
- Pledgie-Tracy, A., Sobolewski, M. D., & Davidson, N. E. (2007). Sulforaphane Induces Cell Type-Specific Apoptosis in Human Breast Cancer Cell Lines. *Molecular Cancer Therapeutics*, **6**(3): 1013- 1021. doi: 10.1158/1535-7163.MCT-06-0494
- Poledne, R. (2013). A New Atherogenic Effect of Saturated Fatty Acids. *Physiological Research*, **62** (2): 139- 143. doi: 10.33549/physiolres.932443
- Singh, T. P., & Singh, O. M. (2011). Phytochemical and Pharmacological Profile of *Zanthoxylum armatum* DC. An Overview. *Indian Journal of Natural Products and Resources*, **2**(3): 275-285. Retrieved from: [https://nopr.niscpr.res.in/bitstream/123456789/12730/1/IJNPR%202\(3\)%20275-285.pdf](https://nopr.niscpr.res.in/bitstream/123456789/12730/1/IJNPR%202(3)%20275-285.pdf) Accessed on (2/02/2019)
- Product datasheet trans-9-Methyl Hexadecenoate, Monounsaturated Fatty Acid Methyl Ester* ab143885:1–2. Retrieved form: <https://www.abcam.com/products/biochemicals/trans-9-methyl-hexadecenoate-monounsaturated-fatty-acid-methyl-ester-ab143885.html> Accessed on (12/04/2022)
- Rai, N. P., Adhikari, B. B., Paudel, A., & Masuda, K. Mckelvey, R. D., & Manandhar, M. D. (2006). Phytochemical Constituents of the Flowers of *Sarcococca coriacea* of Nepalese Origin . *Journal of Nepal Chemical Society*, **21**: 1- 7. doi: 10.3126/jncs.v2i0.214
- Ramaiah, S. K. (2007). A Toxicologist Guide to the Diagnostic Interpretation of Hepatic Biochemical Parameters. *Food and Chemical Toxicology*, **45**(9):1551-1557. doi: 10.1016/j.fct.2007.06.007
- Nooreen, Z., Bushra, U., Bawankule, D. U., Shanker, K., Ahmad, A., & Tandon, S. (2019). Standardization and Xanthine Oxidase Inhibitory Potential of

- Zanthoxylum armatum* Fruits. *Journal of Ethnopharmacology*, **230**:1–8.doi: 10.1016/j.jep.2018.10.018
- Ríos, J., Francini, F., & Schinella, G. (2015). Natural Products for the Treatment of Type 2 Diabetes Mellitus. *Planta Medica*, **81**(12/13): 975- 994.doi: 10.1055/s-0035-1546131
- Ruwizhi, N., & Aderibigbe, B. A. (2020). Cinnamic Acid Derivatives and Their Biological Efficacy. *International Journal of Molecular Sciences*, **21**(16): 5712. doi: 10.3390/ijms21165712
- Rynjah, C. V., Devi, N. N., Khongthaw, N., Syiem, D., & Majaw, S. (2018). Evaluation of the Antidiabetic Property of Aqueous Leaves Extract of *Zanthoxylum armatum* DC. Using In Vivo and In Vitro Approaches. *Journal of Traditional and Complementary Medicine*, **8**(1): 134- 140.doi: 10.1016/j.jtcme.2017.04.007
- Sarwar, N., Gao, P., Kondapally Seshasai, S. R., Gobin, R., Kaptoge, S., Di Angelantonio, E., Ingelsson, E., Lawlor, D. A., Selvin, E., Stampfer, M., Stehouwer, C. D. A., Lewington, S., Pennells, L., Thompson, A., Sattar, N., White, I. R., Ray, K. K., Danesh, J., Tipping, R. W.& Wormser, D. (2010). Diabetes Mellitus, Fasting Blood Glucose Concentration, and Risk of Vascular Disease: A Collaborative Meta-Analysis of 102 Prospective Studies. *The Lancet*, **375** (9733): 2215- 2222.doi: 10.1016/S0140-6736(10)60484-9
- Savelev, S., Okello, E., Perry, N. S. L. L., Wilkins, R. M., & Perry, E. K. (2003). Synergistic and Antagonistic Interactions of Anticholinesterase Terpenoids in *Salvia lavandulaefolia* Essential Oil. *Pharmacology Biochemistry and Behavior*, **75** (3): 661- 668. doi: 10.1016/S0091-3057(03)00125-4
- Schieber, M., & Chandel, N. S. (2014). ROS Function in Redox Signaling and Oxidative Stress. *Current Biology*, **24** (10): R453- R462. doi: 10.1016/j.cub.2014.03.034
- Schrodinger Release 2023-2: Mastero, Schrodinger, LLC, New York, NY, 2023
- Shah, U., Shah, R., Acharya, S., & Acharya, N. (2013). Novel Anticancer Agents From Plant Sources. *Chinese Journal of Natural Medicines*, **11** (1): 16- 23. doi: 10.1016/S1875-5364(13)60002-3
- Shahidi, F., Janitha, P. K., & Wanasundara, P. D. (1992). Phenolic Antioxidants.

- Critical Reviews in Food Science and Nutrition*, **32** (1): 67- 103.doi: 10.1080/10408399209527581
- Sies, H. (2015). Oxidative Stress: A Concept in Redox Biology and Medicine. *Redox Biology*, **4**: 180- 183. doi: 10.1016/j.redox.2015.01.002
- Sies, H. (2017). Hydrogen Peroxide as a Central Redox Signaling Molecule in Physiological Oxidative Stress: Oxidative Eustress. *Redox Biology*, **11**: 613–619. doi: 10.1016/j.redox.2016.12.035
- Sigdel, S. R., Rokaya, M. B., & Timsina, B. (2013). Plant Inventory and Ethnobotanical Study of Khimti Hydropower Project, Central Nepal. *Scientific World*, **11**(11): 105- 112. doi: 10.3126/sw.v11i11.8563
- Smith, A., Hara, H., Steam, W. T., & Williams, L. H. J. (1979). An Enumeration of the Flowering Plants of Nepal, *Kew Bulletin*, **34** (1), 198. doi: 10.2307/4117986
- Solowey, E., Lichtenstein, M., Sallon, S., Paavilainen, H., Solowey, E., & Lorberboum-Galski, H. (2014). Evaluating Medicinal Plants for Anticancer Activity. *The Scientific World Journal*, **2014**. doi: 10.1155/2014/721402
- Son, I. H., Chung, I. M., Lee, S. I., Yang, H. D., & Moon, H. I. (2007). Pomiferin, Histone Deacetylase Inhibitor Isolated From the Fruits of *Maclura pomifera*. *Bioorganic & Medicinal Chemistry Letters*, **17**(17): 4753-4755.doi: 10.1016/j.bmcl.2007.06.060
- Soobrattee, M. A., Neergheen, V. S., & Luximon-ramma, A. (2005). Phenolics as Potential Antioxidant Therapeutic Agents : Mechanism and Actions. *Mutation Research/Fundamental and Molecular Mechanisms of Mutagenesis*, **579** (1-2): 200- 213. doi: 10.1016/j.mrfmmm.2005.03.023
- Spruce 1.5.1.1: OpenEye Scientific Software,Santa Fe, NM. Retrieved from: <http://www.Eyesopen.com> Accessed on (9/10/2023)
- Stephen, S. E. (2014). NIST Standard Reference Database 1A. In *Standard Reference Data NIST*. U. S. Department of Commerce. Retrieved from: <https://www.nist.gov/srd/nist-standard-reference-database-1a>. Accessed on (1/01/2022)
- Tenscher, A., & Richterich, P. (1971). Enzymatic Colorimetric End Point Method With GOD POD (GOD: Glucose oxidase, POD: Peroxidase). *Schweiz Med. Wschr*,

101: 345- 390.

- Tietz, N. W. (1990). Clinical Guide to Laboratory Tests. *In Clinical Guide to Laboratory Tests* (2nd ed.). W. B. Saunders Company. Retrieved from: <https://pesquisa.bvsalud.org/portal/resource/pt/biblio-1069218> Accessed on (11/02/2019)
- Tiwary, M., Naik, S. N., Tewary, D. K., Mittal, P. K., & Yadav, S. (2007). Chemical Composition and Larvicidal Activities of the Essential Oil of *Zanthoxylum armatum* DC (Rutaceae) Against Three Mosquito Vectors. *Journal of Vector Borne Diseases*, **44**: 198- 204. Retrieved from: <https://pubmed.ncbi.nlm.nih.gov/17896622/> Accessed on (9/05/2022)
- Trott, O., & Olson, A. J. 2010. AutoDock Vina: Improving the Speed and Accuracy of Docking With a New Scoring Function, Efficient Optimization and Multithreading. *Journal of Computational Chemistry*. **31** (2): 455- 461. doi: 10.1002/jcc.21334
- Twaij, H. A., Kery, A., & Al-Khazraji, N. K. (1983). Some Pharmacological, Toxicological and Phytochemical Investigations on *Centaurea phyllocephala*. *Journal of Ethnopharmacology*, **9** (2-3): 299-314. doi: 10.1016/0378-8741(83)90037-5
- Ugwah-Oguejiofor, C. J., Okoli, C. O., Ugwah, M. O., Umaru, M. L., Ogbulie, C. S., Mshelia, H. E., Umar, M., & Njan, A. A. (2019). Acute and Sub-Acute Toxicity of Aqueous Extract of Aerial Parts of *Caralluma dalzielii* NE Brown in Mice and Rats. *Heliyon*, **5**(1) : e01179. doi: 10.1016/j.heliyon.2019.e01179
- Valko, M., Leibfritz, D., Moncol, J., Cronin, M. T., Mazur, M., & Telser, J. (2007). Free Radicals and Antioxidants in Normal Physiological Functions and Human Disease. *The International Journal of Biochemistry & Cell Biology*, **39** (1): 44-84. doi: 10.1016/j.biocel.2006.07.00
- Van Hoorn, D. E., Nijveldt, R. J., Van Leeuwen, P. A., Hofman, Z., M'Rabet, L., De Bont, D. B., & Van Norren, K. (2002). Accurate Prediction of Xanthine Oxidase Inhibition Based on the Structure of Flavonoids. *European Journal of Pharmacology*. **451** (2): 111- 118. doi: 10.1016/S0014-2999(02)02192-1
- Veber, D. F., Johnson, S.R., Cheng, H. Y., Smith, B. R., Ward, K. W., & Kopple, K.

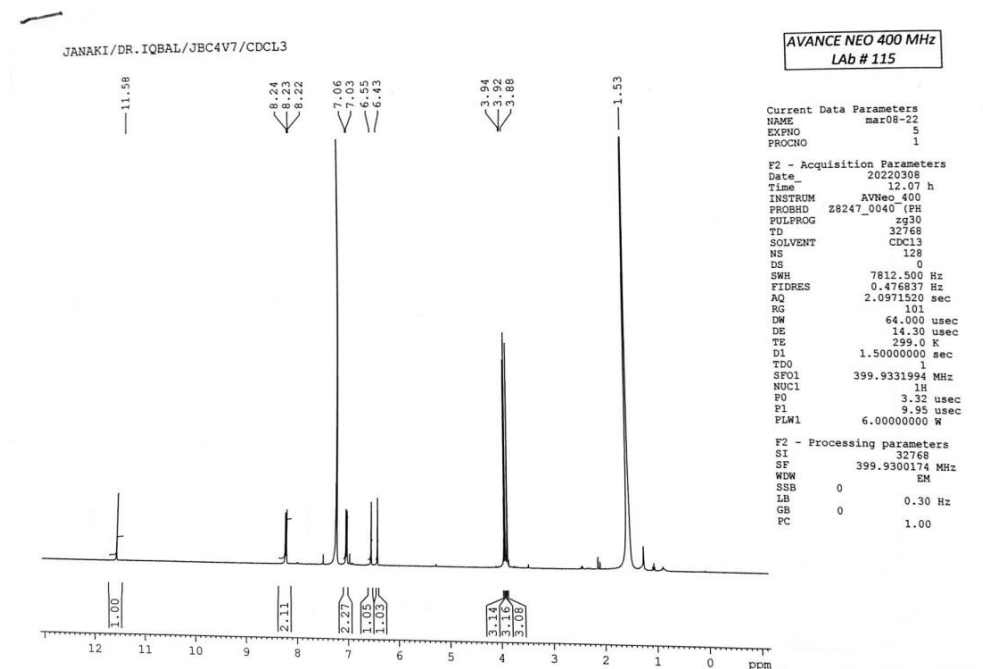
- D. (2002). Molecular Properties that Influence the Oral Bioavailability of Drug Candidates. *Journal of Medicinal Chemistry*, **45** (12): 2615- 2623. doi: 10.1021/jm020017n
- Waheed, A., Mahmud, S., Akhtar, M., & Nazir, T. (2011). Studies on the Components of Essential Oil of *Zanthoxylum armatum* by GC-MS. *American Journal of Analytical Chemistry*, **2** (2): 258-261. doi: 10.4236/ajac.2011.22031
- Walia, S., Saha, S., Tripathi, V., & Sharma, K. K. (2017). Phytochemical Biopesticides : Some Recent Developments. *Phytochemistry Reviews*. **16** (5): 989-1007. doi: 10.1007/s11101-017-9512-6
- Wang, Y., Xing, J., Xu, Y., Zhou, N., Peng, J., Xiong, Z., Liu, X., Luo, X., Luo, C., Chen, K., & Jiang, H. (2015). In Silico ADME/T Modelling for Rational Drug Design. *Quarterly Reviews of Biophysics*, **48**(4): 488-515. doi: 10.1017/S0033583515000190
- Wassall, S. R., & Stillwell, W. (2009). Polyunsaturated Fatty Acid – Cholesterol Interactions: Domain Formation in Membranes. *Biochimica et Biophysica Acta (BBA)- Biomembranes*, **1788** (1): 24- 32. doi: 10.1016/j.bbamem.2008.10.011
- Weiss Edward A. (2002). *Spice Crops*. Wallingford, London, UK, CABI. doi: 10.1079/9780851996059.0000
- Beynen, A. C., & Katan, M. B. (1985). Why do polyunsaturated fatty acids lower serum cholesterol? (1985). *The American Journal of Clinical Nutrition*, **42** (3), 560-563. doi: 10.1093/ajcn/42.3.560
- Woollett, L. A., & Dietschy, J. M. (1994). Effect of Long-Chain Fatty Acids on Low-Density-Lipoprotein- Cholesterol Metabolism. *The American Journal of Clinical Nutrition*, **60** (6): 991S- 996S. doi: 10.1093/ajcn/60.6.991S
- Wright, G. D. (2017). Opportunities for natural products in 21st century antibiotic discovery. *Natural product reports*, **34**(7): 694- 701. doi: 10.1039/C7NP00019G
- Yahfoufi, N., Alsadi, N., Jambi, M., & Matar, C. (2018). The Immunomodulatory and Anti-inflammatory Role of Polyphenols. *Nutrients*, **10** (11): 1618. doi: 10.3390/nu10111618
- Yang, C. W. H., Cheng, M. J., Lee, S. J., Yang, C. W. H., Chang, H. S., & Chen, I. S.

- (2009). Secondary Metabolites and Cytotoxic Activities From the Stem Bark of *Zanthoxylum nitidum*. *Chemistry and Biodiversity*, **6** (6): 846- 857. doi: 10.1002/cbdv.200800107
- Ye, Q. N., Wang, C. B., Chai, T., Wang, J., Meng, X. H., Shi, X. F., & Yang, J. L., (2023). Alkylamides From *Zanthoxylum armatum* DC. and Their Neuroprotective Activity. *Phytochemistry*, **211**, 113704. doi: 10.1016/j.phytochem.2023.113704
- Zuliani, G., Galvani, M., Leitersdorf, E., Volpato, S., Cavalieri, M., & Fellin, R. (2009). The Role of Polyunsaturated Fatty Acids (PUFA) in the Treatment of Dyslipidemias. *Current Pharmaceutical Design*, **15** (36): 4087- 4093. doi: 10.2174/138161209789909773
- Zhai, X. X., Meng, W. H., Wang, C. B., Zhao, Y. M., & Yang, J. L., (2022). Anti-Hypoxic Active Constituents From the Twigs of *Zanthoxylum armatum* DC. and their Chemotaxonomic Significance. *Biochemical Systematics and Ecology*, **104**;104480. doi: 10.1016/j.bse.2022.104480

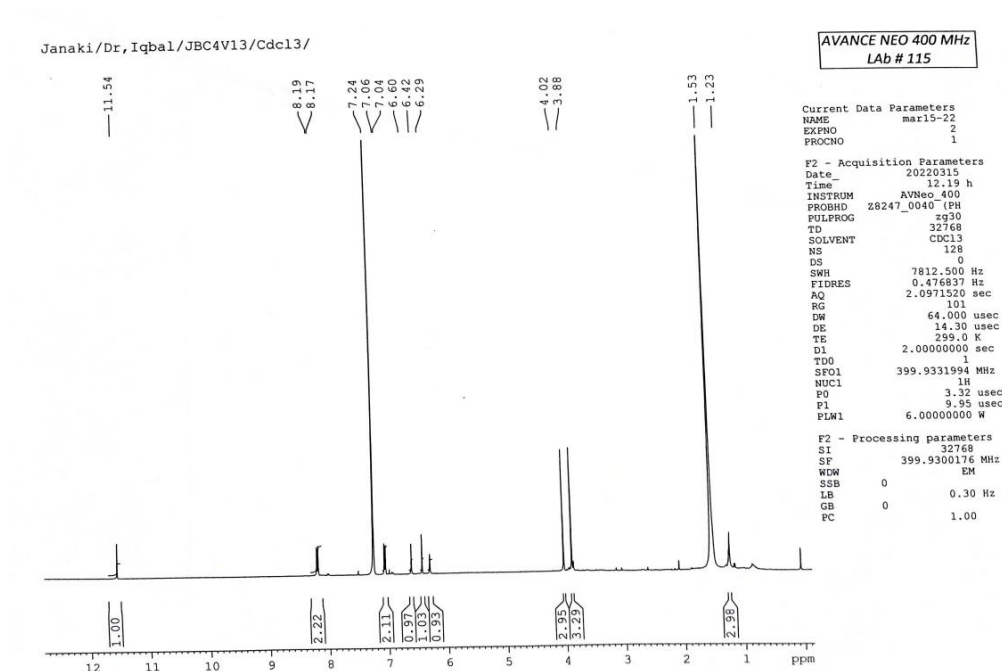
# APPENDICES

## Appendix I

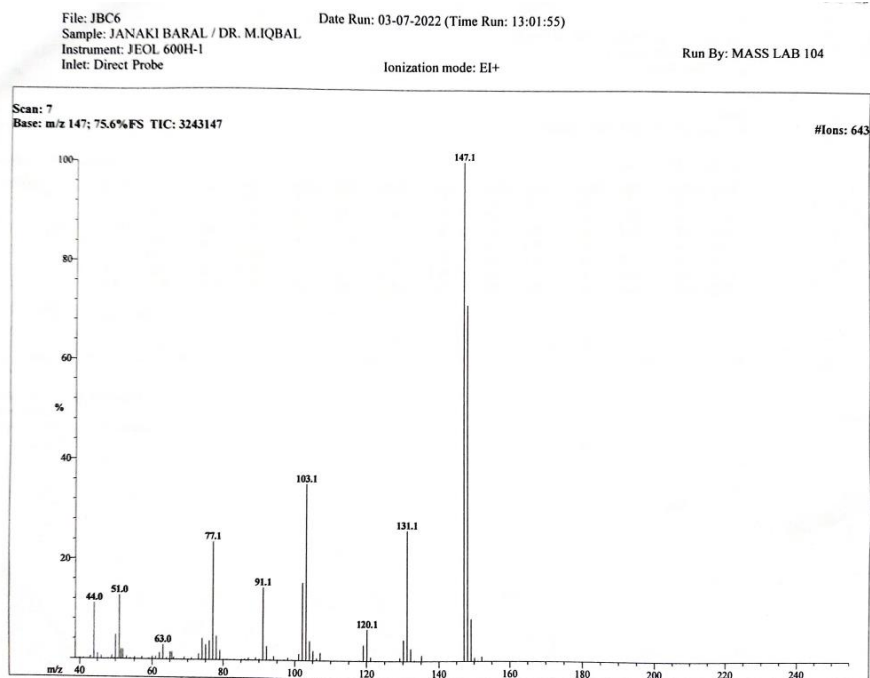
### Appendix A: <sup>1</sup>H NMR spectra of tambulin (1)



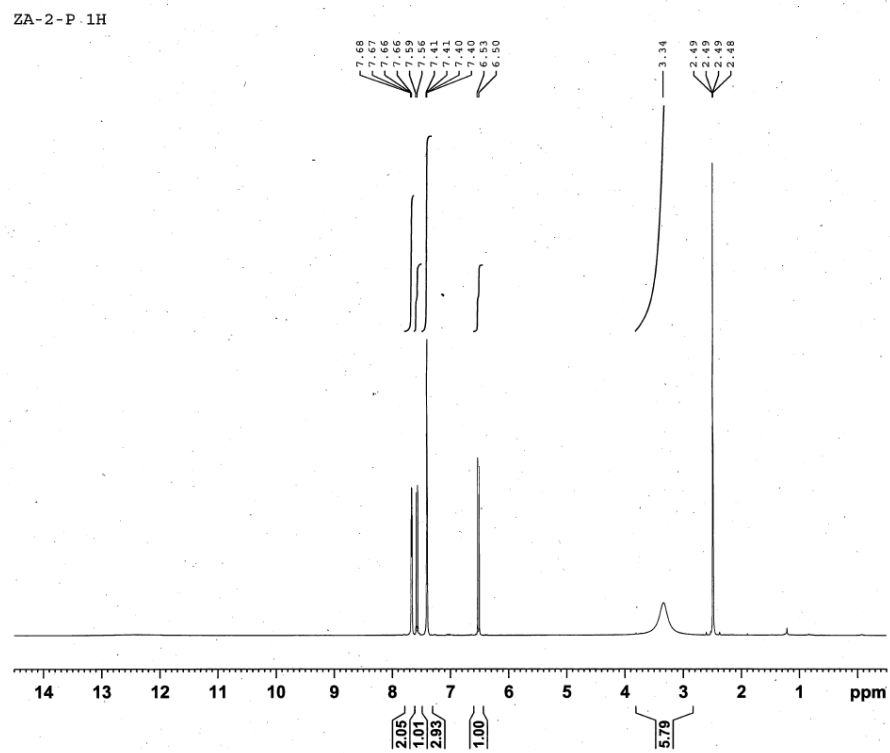
### Appendix B: <sup>1</sup>H NMR Spectra of Prudomestin (2)



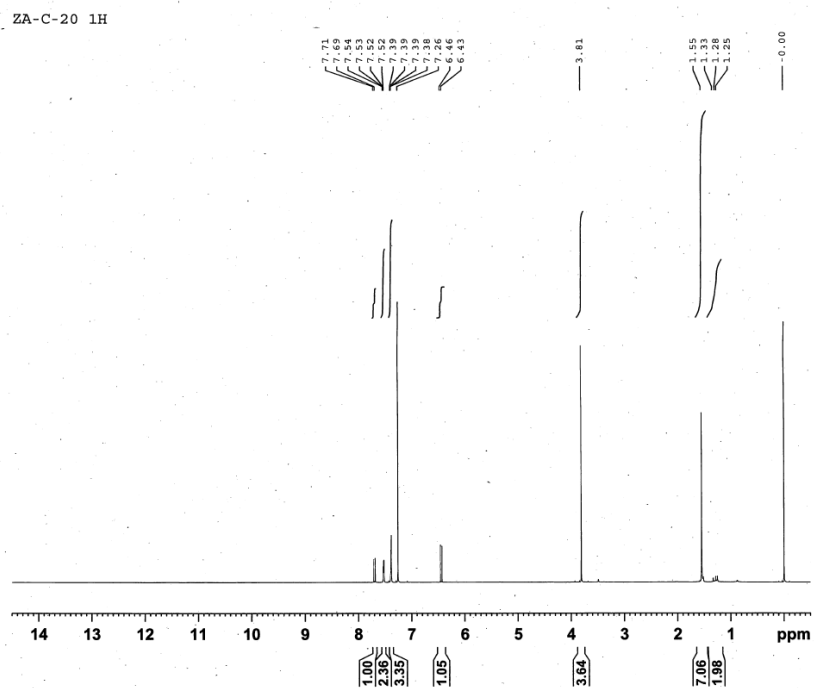
## Appendix C: Mass spectra of cinnamic acid (3)



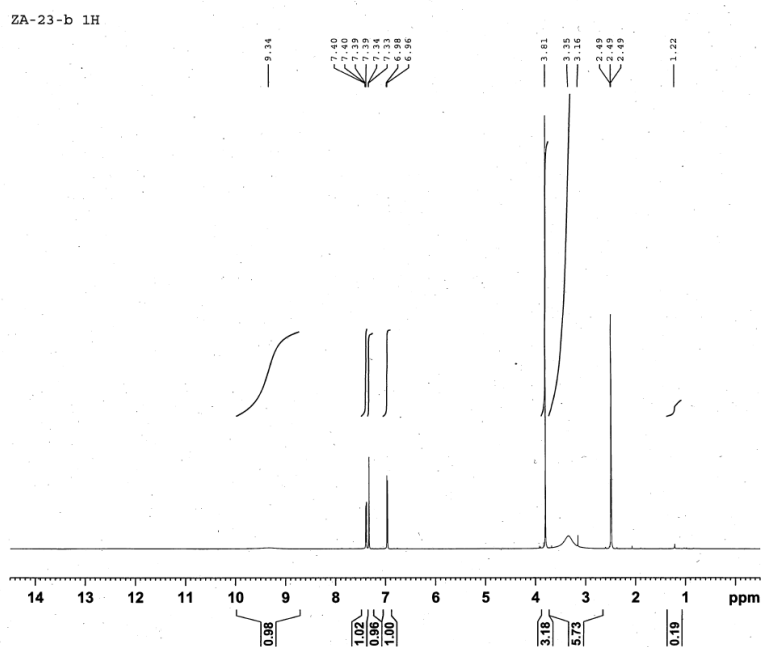
## Appendix C1: $^1\text{H}$ NMR spectra of Cinnamic acid (3)



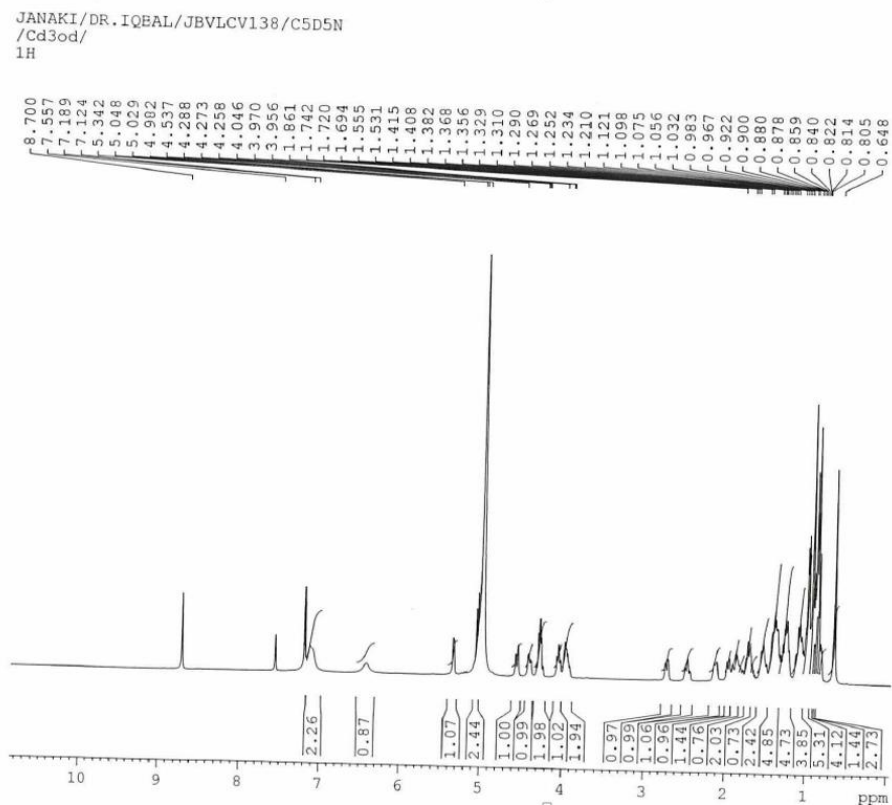
## Appendix D: $^1\text{H}$ NMR spectra of cinnamic ester (4)



## Appendix E: $^1\text{H}$ NMR spectra of isovanillic acid (5)

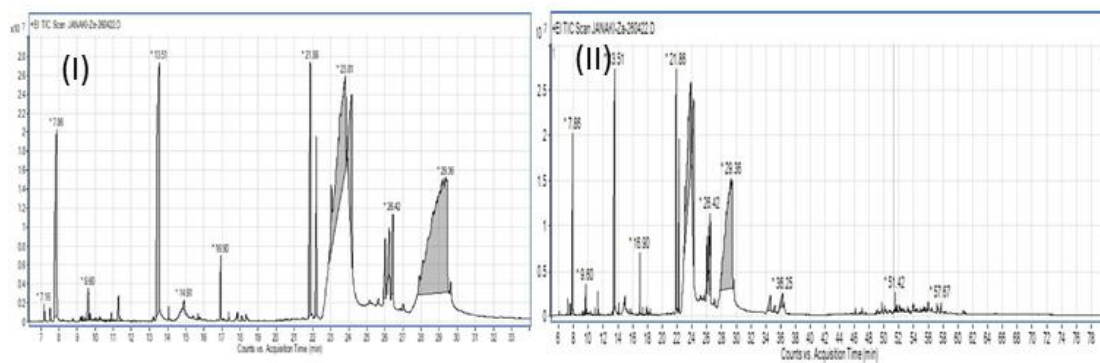


## Appendix F: <sup>1</sup>H NMR spectra of ducosterol (7)



## Appendix II

## Appendix G: GCMS chromatogram of hexane fraction of *Z. armatum*



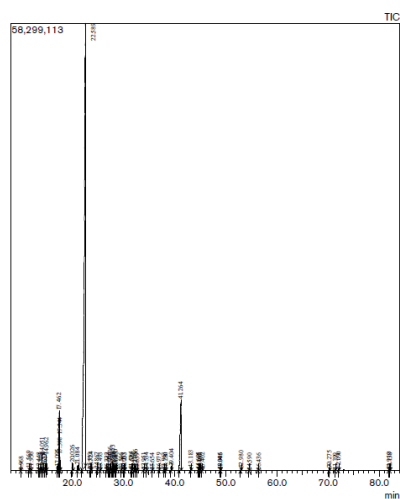
## Appendix III (Oil)

## Appendix H: GCMS of ZaM



### Sample Information

Analyzed by : Dr. Prabodh Satyal  
 Analyzed : 1/8/2022 1:29:30 AM  
 Sample Type : Essential Oil  
 Sample Name : Zanthoxylum  
 Lot# : 220106D  
 Injection Volume : 0.30



R Time	Name	Area%
9.988	Styrene	0.01
11.560	alpha-Thujene	0.05
11.956	alpha-Phene	0.04
13.448	Borneadihyde	0.03
13.713	Unidentified	0.01
14.051	Sabinene	0.53
14.530	beta-Pinene	0.04
14.676	6-Methyl-5-hepten-2-one	0.01
14.962	Myrcene	0.51
17.095	para-Cymene	0.17
17.462	Limonene	3.85
17.544	beta-Phellandrene	1.23
17.699	1,8-Cineole	0.38
20.026	cis-Linalool oxide (luranoid)	0.50
21.084	trans-Linalool oxide (luranoid)	0.50
22.990	Linalool	80.37
23.553	trans-para-Menth-2,8-dien-1-ol	0.01
23.724	cis-para-Menth-2-en-1-ol	0.04
24.987	trans-para-Menth-2-en-1-ol	0.04
25.493	Citronellal	0.03
26.722	cis-Linalool oxide (pyranoid)	0.05
27.093	trans-Linalool oxide (pyranoid)	0.03
27.296	para-1,8-Menthadien-4-ol	0.01
27.456	Terpinen-4-ol	0.25
27.959	Cryptone	0.26
27.988	3-cis-Hexenyl butyrate	0.10
28.157	Methyl salicylate	0.01
28.430	alpha-Terpenol	0.18
28.603	Methyl chavicol	0.03
29.846	Linalool formate	0.01
30.063	trans-Carveol	0.01
30.233	Unidentified	0.01
31.874	Cumin aldehyde	0.03
31.689	Carvone	0.02
32.116	Linalyl acetate	0.01
32.266	Piperitone	0.17
32.639	Methyl citronellate	0.01
33.051	Phellandral	0.04
34.534	alpha-Terpinen-7-ol	0.01
35.054	cis-Methyl cinnamate	0.01
36.070	4-Hydroxy cryptone	0.01
37.963	trans-para-menth-1-en-7-ol	0.02
38.280	Unidentified	0.01
39.404	Terpenediol	0.23
41.264	trans-Methyl cinnamate	0.55
43.183	beta-Caryophyllene	0.14
44.695	Unidentified	0.03
44.845	Unidentified	0.02
45.036	Methyl palmistate	0.02
45.402	alpha-Humulene	0.03
48.845	gamma-Cadinene	0.01
49.006	Unidentified	0.01
52.980	Caryophyllene oxide	0.12
54.500	Humulene epoxide II	0.01
56.458	alpha-Murolol	0.12
70.275	Methyl palmistate	0.12
71.309	Methyl-palmitate	0.03
72.070	Cyclohexadecanoid	0.06
81.410	Unidentified	0.01
82.138	Unidentified	0.01
		100.00

## Appendix H1: Chiral GCMS of ZaM

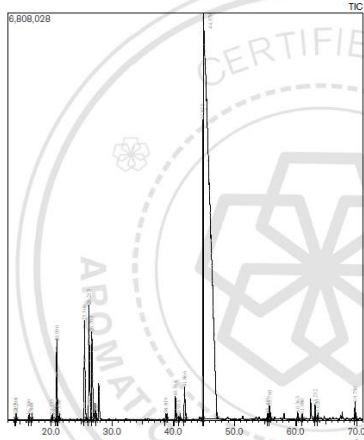
### Chiral GCMS Analysis Report

#### Sample Information

Analyzed by : Dr. Prabodh Satyal  
 Analyzed : 1/7/2022 8:12:43 PM  
 Sample Type : Essential Oil  
 Sample Name : Zanthoxylum  
 Lot# : 220106D  
 Injection Volume : 0.30

#### Peak Report TIC

R Time	Name	Area%
14.203	alpha-Thujene	0.01
14.298	alpha-Thujene	0.10
16.990	alpha-Phene	0.08
18.948	alpha-Phene	0.02
20.155	Sabinene	0.10
20.280	beta-Pinene	0.01
20.990	Sabinene	1.01
21.334	beta-Pinene	0.09
26.960	Limonene	2.81
28.215	Limonene	3.89
29.905	beta-Phellandrene	2.84
27.440	beta-Phellandrene	0.01
38.910	cis-Linalool oxide (luranoid)	0.17
40.384	cis-Linalool oxide (luranoid)	0.84
40.935	trans-Linalool oxide (luranoid)	0.09
41.988	trans-Linalool oxide (luranoid)	1.05
44.935	Linalool	5.99
44.970	Linalool	79.93
55.451	Terpinen-4-ol	0.15
55.760	Terpinen-4-ol	0.38
60.365	alpha-Terpenol	0.16
61.096	alpha-Terpenol	0.12
63.232	Piperitone	0.28
63.820	Piperitone	0.06
69.790	beta-Caryophyllene	0.31
		100.00



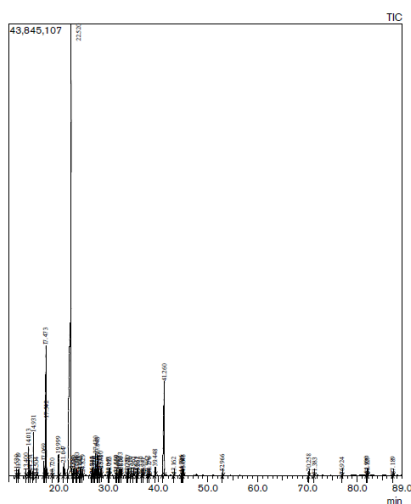
Compound	Standard (S1)	Sample (S2)	Retention Time (min)	Area	Area%
alpha-Phene	NA	NA	14.203	0.01	0.01
alpha-Phene	NA	NA	14.298	0.10	0.10
alpha-Phene	NA	NA	16.990	0.08	0.08
alpha-Phene	NA	NA	18.948	0.02	0.02
beta-Pinene	NA	NA	20.155	0.10	0.10
beta-Pinene	NA	NA	20.280	0.01	0.01
Sabinene	NA	NA	20.990	1.01	1.01
Sabinene	NA	NA	21.334	0.09	0.09
Limonene	NA	NA	26.960	2.81	2.81
Limonene	NA	NA	28.215	3.89	3.89
beta-Phellandrene	NA	NA	29.905	2.84	2.84
beta-Phellandrene	NA	NA	27.440	0.01	0.01
cis-Linalool oxide (luranoid)	NA	NA	38.910	0.17	0.17
cis-Linalool oxide (luranoid)	NA	NA	40.384	0.84	0.84
trans-Linalool oxide (luranoid)	NA	NA	40.935	0.09	0.09
trans-Linalool oxide (luranoid)	NA	NA	41.988	1.05	1.05
Linalool	NA	NA	44.935	5.99	5.99
Linalool	NA	NA	44.970	79.93	79.93
Terpinen-4-ol	NA	NA	55.451	0.15	0.15
Terpinen-4-ol	NA	NA	55.760	0.38	0.38
alpha-Terpenol	NA	NA	60.365	0.16	0.16
alpha-Terpenol	NA	NA	61.096	0.12	0.12
Piperitone	NA	NA	63.232	0.28	0.28
Piperitone	NA	NA	63.820	0.06	0.06
beta-Caryophyllene	NA	NA	69.790	0.31	0.31
					100.00

# Appendix I: GCMS of ZaSur



## Sample Information

Analyzed by : Dr. Prabodh Satyal  
 Analyzed : 1/7/2022 9:37:57 PM  
 Sample Type : Essential Oil  
 Sample Name : Zanthoxylum  
 Lot# : 220106B  
 Injection Volume : 0.30



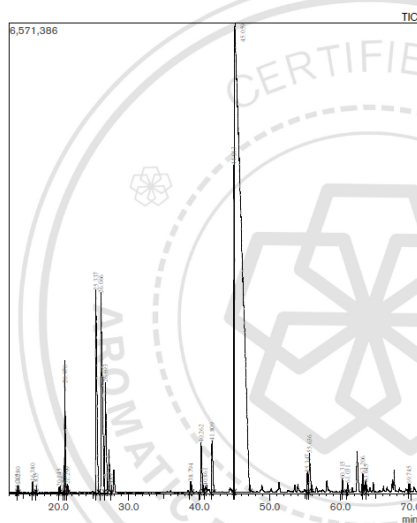
RTime	Name	Area%
11.530	alpha-Thujone	0.11
11.919	alpha-Pinene	0.19
13.400	Benzaldehyde	0.18
14.013	Sabinene	1.04
14.291	beta-Pinene	0.17
14.531	Myrcene	1.54
15.504	delta-2-Carene	0.04
17.069	para-Cymene	0.74
17.473	Limonene	11.20
17.542	beta-Phellandrene	1.51
18.720	2,6-Dimethyl-2,6-octadiene	0.01
19.959	cis-Linalool oxide (furanoid)	1.37
21.947	trans-Linalool oxide (furanoid)	1.16
22.520	Linalool	58.45
22.886	Linalool derivative	0.10
23.026	endo-Fenchol	0.04
23.504	trans-para-Mentha-2,8-dien-1-ol	0.06
23.880	cis-para-Mentha-2-en-1-ol	0.21
24.191	cis-Limonene oxide	0.07
24.440	cis-para-Mentha-2,8-dien-1-ol	0.10
24.829	trans-para-Mentha-2-en-1-ol	0.14
26.713	cis-Linalool oxide (granatoid)	0.09
26.845	Octanoic acid	0.04
27.101	trans-Isocitral	0.15
27.275	para-1,8-Menthadien-4-ol	0.04
27.430	Terpinen-4-ol	1.09
27.848	Cryptone	1.05
27.955	3-cis-Hexenyl butyrate	0.38
28.410	alpha-Terpinol	0.38
28.578	Methyl chavicol	0.08
30.047	trans-Carveol	0.04
30.223	Unidentified	0.06
31.550	Cumin aldehyde	0.11
31.605	Carvone	0.11
32.092	Linalyl acetate	0.04
32.333	Piperitone	0.28
32.614	Methyl citronellate	0.02
33.796	trans-Ascaridol glycol	0.09
33.927	Phellandral	0.18
34.510	alpha-Terpinen-7-ol	0.08
34.961	para-Cymen-7-ol	0.15
35.631	cis-Methyl cinnamate	0.03
35.862	neo-Dihydro carveol acetate	0.04
36.739	Limonene hydroperoxide	0.04
36.981	4-Hydroxy cryptone	0.05
37.942	3-Chloro-para-menth-1-en-7-ol	0.07
38.076	Unidentified	0.05
39.448	Terpenediol	0.53
41.280	trans-Methyl cinnamate	14.61
43.182	beta-Caryophyllene	0.05
44.706	Unidentified	0.16
44.841	Unidentified	0.15
45.045	Unidentified	0.17
52.966	Caryophyllene oxide	0.18
70.258	Methyl palmitoleate	0.22
71.383	Methyl palmitate	0.36
76.924	Unidentified	0.06
81.900	Unidentified	0.09
82.127	Unidentified	0.04
87.169	cis-9-Tocosene	0.05
		100.00

# Appendix II: Chiral GCMS of ZaSur

## Chiral GCMS Analysis Report

### Sample Information

Analyzed by : Dr. Prabodh Satyal  
 Analyzed : 1/7/2022 4:08:35 PM  
 Sample Type : Essential Oil  
 Sample Name : Zanthoxylum  
 Lot# : 220106B  
 Injection Volume : 0.30



RTime	Name	Area%
14.028	alpha-Thujone	0.01
14.280	alpha-Thujone	0.10
16.380	alpha-Pinene	0.17
16.835	alpha-Pinene	0.03
20.145	Sabinene	0.09
20.820	beta-Pinene	0.01
20.970	Sabinene	1.59
21.209	beta-Pinene	0.18
25.337	Limonene	5.89
26.066	Limonene	7.18
26.889	beta-Phellandrene	3.09
27.489	beta-Phellandrene	0.01
38.794	cis-Linalool oxide (furanoid)	0.24
40.262	cis-Linalool oxide (furanoid)	1.25
40.661	trans-Linalool oxide (furanoid)	0.16
41.809	trans-Linalool oxide (furanoid)	1.44
44.013	Linalool	5.28
45.098	Linalool	71.28
55.347	Terpinen-4-ol	0.42
55.636	Terpinen-4-ol	1.08
60.515	alpha-Terpinol	0.23
61.031	alpha-Terpinol	0.16
63.206	Piperitone	0.30
63.645	Piperitone	0.08
66.740	beta-Caryophyllene	0.11
		100.00

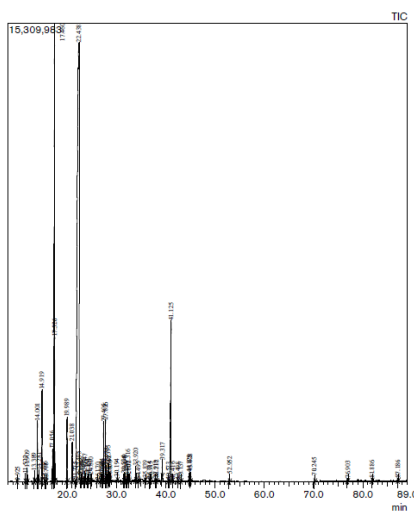
Chromatogram	Method to Match	Min. S to Max. L	Content	Chromatogram
Chromatogram	Min to Max	Min. S to Max. L	Content	Chromatogram
alpha-Thujone	N/A	14.2735 - 14.2827	N/A	
beta-Pinene	N/A	16.8354 - 16.8428	N/A	
Sabinene	N/A	16.3778 - 16.3827	N/A	
alpha-Pinene	N/A	14.0281 - 14.0351	N/A	
Limonene	N/A	14.0281 - 14.0351	N/A	
beta-Phellandrene	N/A	26.8891 - 26.8969	N/A	
cis-Linalool oxide (furanoid)	N/A	40.2621 - 40.2691	N/A	
trans-Linalool oxide (furanoid)	N/A	40.6611 - 40.6689	N/A	
Linalool	N/A	44.0131 - 44.0199	N/A	
Terpinen-4-ol	N/A	55.3471 - 55.3539	N/A	
alpha-Terpinol	N/A	61.0311 - 61.0379	N/A	
Piperitone	N/A	63.2061 - 63.2129	N/A	
beta-Caryophyllene	N/A	66.7401 - 66.7469	N/A	

## Appendix J: GCMS of ZaSal



### Sample Information

Analyzed by : Dr. Prabodh Satyal  
 Analyzed : 1/7/2022 5:20:52 AM  
 Sample Type : Essential Oil  
 Sample Name : Zanthoxylum  
 Lot# : 220105A  
 Injection Volume : 0.30



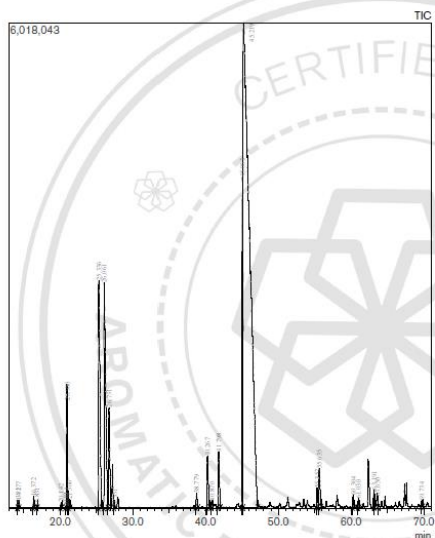
RTime	Name	Area%
9.925	Styrene	0.01
11.522	alpha-Thujene	0.12
11.909	alpha-Pinene	0.20
13.389	Benzaldehyde	0.16
14.001	Sabinene	0.09
14.281	beta-Pinene	0.19
14.919	Myrcene	1.53
15.496	delta-2-Carene	0.05
15.779	para-Mentha-1(7),8-diene	0.03
17.056	para-Cymene	0.73
17.460	Limonene	16.67
17.826	beta-Phellandrene	1.71
19.980	cis-Linalool oxide (furanoid)	1.66
21.038	trans-Linalool oxide (furanoid)	1.42
21.775	Perillene	0.03
22.438	Linalool	58.31
22.495	Hotrienol	0.01
22.846	Linalool derivative	0.12
22.980	endo-Fenchol	0.05
23.468	trans-para-Mentha-2,8-dien-1-ol	0.09
23.647	cis-para-Mentha-2-en-1-ol	0.21
24.161	cis-Limonene oxide	0.09
24.425	cis-para-Mentha-2,8-dien-1-ol	0.12
24.810	trans-para-Mentha-2-en-1-ol	0.15
25.170	Lavandulol	0.02
26.894	Unidentified	0.03
27.084	trans-linalool	0.11
27.263	para-1,8-Menthadien-4-ol	0.09
27.405	Terpinen-4-ol	1.34
27.826	Cryptone	1.40
27.979	9-cis-Hexanyl butyrate	0.45
28.305	alpha-Terpinol	0.44
28.562	Methyl chavicol	0.10
28.670	Dihydro carveol	0.05
30.194	Unidentified	0.07
31.534	Cumin aldehyde	0.15
31.640	Camphor	0.19
32.078	Linalyl acetate	0.04
32.316	Piperitone	0.33
32.602	Methyl citronellate	0.03
33.920	Phellandriol	0.32
34.405	alpha-Terpinen-7-ol	0.04
35.839	neo-Dihydro carveol acetate	0.06
36.714	Limonene hydroperoxide 1	0.09
36.915	4-Hydroxy cryptone	0.03
37.918	3-Oxo-para-menth-1-en-7-ol	0.07
38.212	Unidentified	0.06
39.317	Terpenediol	0.47
40.573	Limonene hydroperoxide 2	0.04
41.123	trans-Methyl cinnamate	8.22
41.416	Unidentified	0.03
42.498	Unidentified	0.03
43.137	beta-Caryophyllene	0.06
44.623	Unidentified	0.17
45.028	Unidentified	0.25
52.552	Caryophyllene oxide	0.20
70.245	Methyl pantoiclate	0.44
76.903	Unidentified	0.09
81.886	Unidentified	0.06
87.166	cis-D-Troscene	100.00

## Appendix J1: Chiral GCMS of ZaSal

### Chiral GCMS Analysis Report

#### Sample Information

Analyzed by : Dr. Prabodh Satyal  
 Analyzed : 1/7/2022 2:08:19 PM  
 Sample Type : Essential Oil  
 Sample Name : Zanthoxylum  
 Lot# : 220105A  
 Injection Volume : 0.30

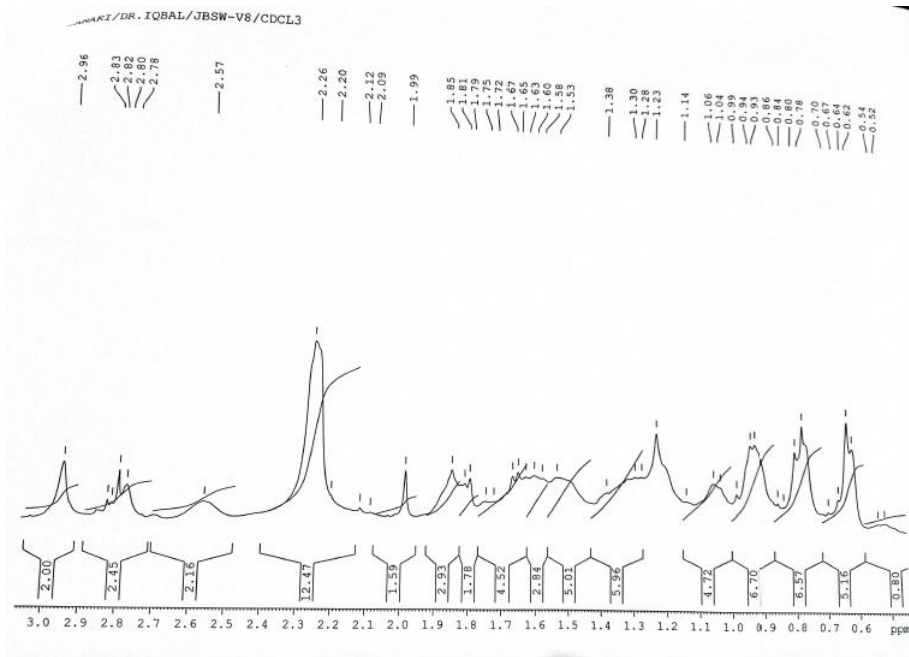


RTime	Name	Area%
14.191	alpha-Thujene	0.01
14.277	alpha-Thujene	0.11
16.372	alpha-Pinene	0.17
16.851	alpha-Pinene	0.03
20.142	Sabinene	0.09
20.814	beta-Pinene	0.01
20.980	Sabinene	1.02
21.306	beta-Pinene	0.18
25.936	Limonene	6.66
26.081	Limonene	8.70
26.791	beta-Phellandrene	2.67
27.531	beta-Phellandrene	0.01
38.779	cis-Linalool oxide (furanoid)	0.32
40.287	cis-Linalool oxide (furanoid)	1.29
40.870	trans-Linalool oxide (furanoid)	0.16
41.798	trans-Linalool oxide (furanoid)	1.55
45.083	Linalool	5.53
45.219	Linalool	68.11
55.382	Terpinen-4-ol	0.40
55.835	Terpinen-4-ol	1.08
60.804	alpha-Terpinol	0.22
61.039	alpha-Terpinol	0.16
63.191	Piperitone	0.31
63.850	Piperitone	0.09
69.734	beta-Caryophyllene	0.10
		100.00

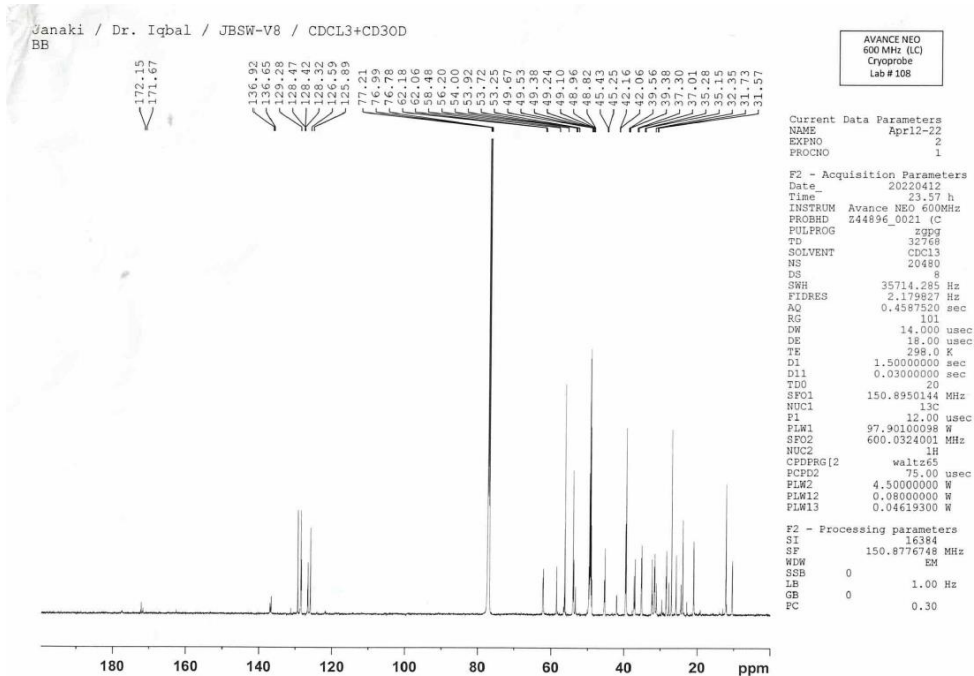
Component	Expected (E/F)	Found	Comments
Caryophyllene	Min: 61.15, Max: 61.15	61.15	N/A
alpha-Thujene	Min: 13.28, Max: 13.28	13.28	N/A
alpha-Pinene	Min: 16.18, Max: 16.18	16.18	N/A
Sabinene	Min: 17.23, Max: 17.23	17.23	N/A
beta-Pinene	Min: 19.25, Max: 19.25	19.25	N/A
Limonene	Min: 24.22, Max: 24.22	24.22	N/A
beta-Phellandrene	Min: 26.25, Max: 26.25	26.25	N/A
cis-Linalool oxide (furanoid)	Min: 31.76, Max: 31.76	31.76	N/A
trans-Linalool oxide (furanoid)	Min: 34.26, Max: 34.26	34.26	N/A
Linalool	Min: 39.25, Max: 39.25	39.25	N/A
Terpinen-4-ol	Min: 47.15, Max: 47.15	47.15	N/A
alpha-Terpinol	Min: 59.24, Max: 59.24	59.24	N/A
Piperitone	Min: 61.15, Max: 61.15	61.15	N/A
beta-Caryophyllene	Min: 61.15, Max: 61.15	61.15	N/A

## Appendix V (Sarcococca)

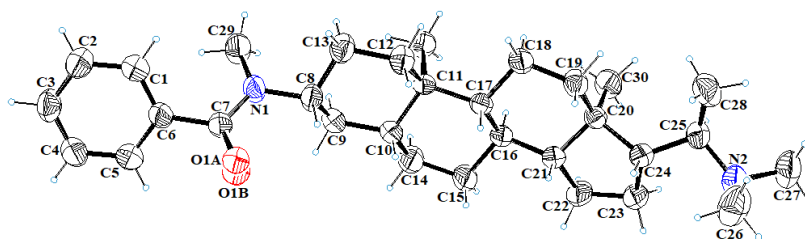
### Appendix A1: <sup>1</sup>H NMR Spectra of Methylepipachysamine D (8)



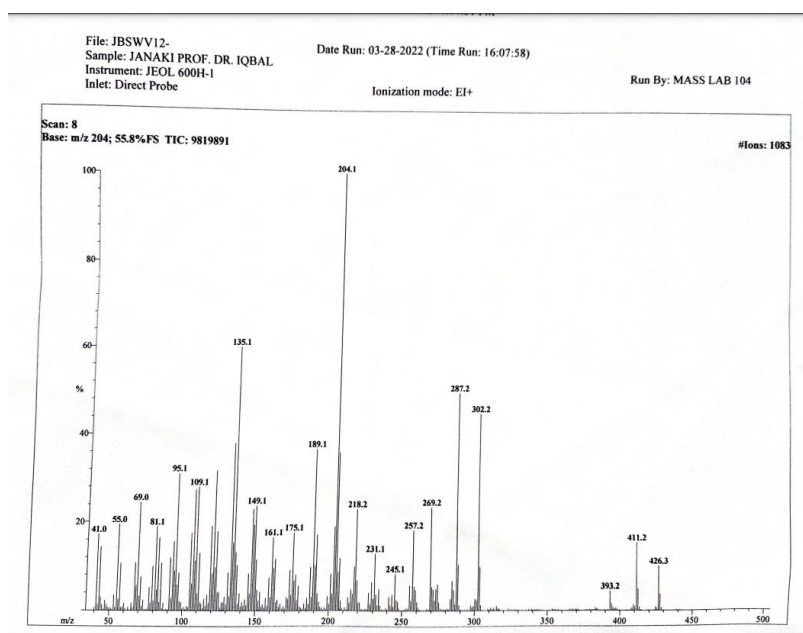
### Appendix A4: <sup>13</sup>C Spectra of Methylepipachysamine 8



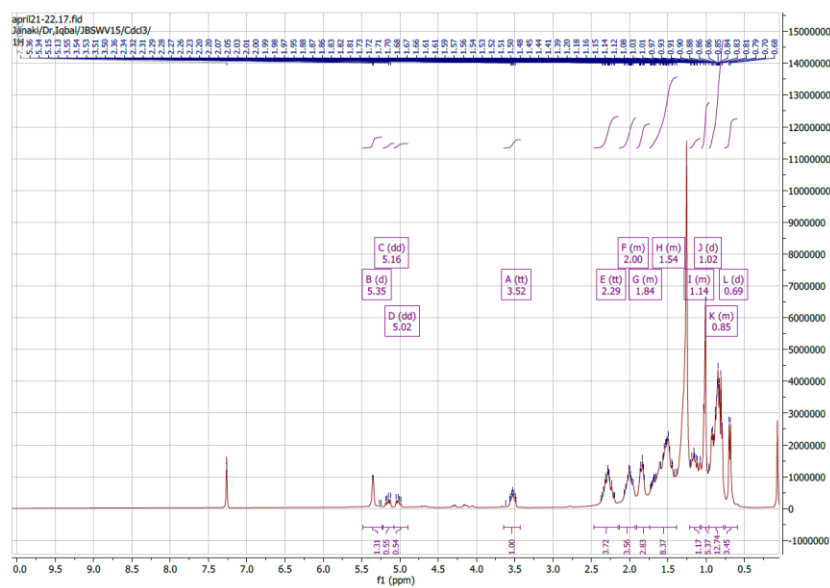
## Appendix A5: ORTEP diagram of Methylepipachysamine D (8)



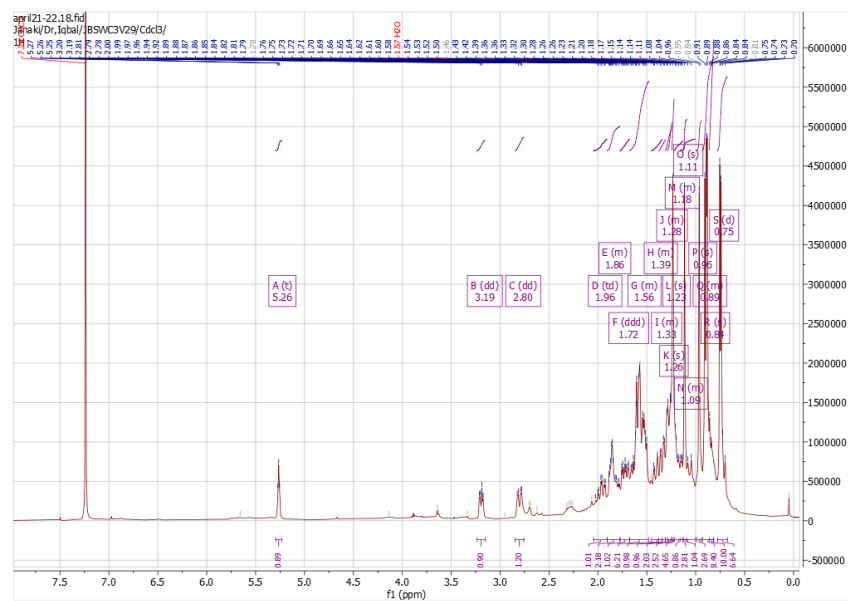
## Appendix B: Mass spectra of taraxerol (9)



## Appendix C1: <sup>1</sup>H NMR Spectra of beta-sitosterol (10)



## Appendix D: <sup>1</sup>H Spectra of oleanolic acid (12)



## APPENDIX

### Scientific Publications

#### Publications:

1. **Baral, J.**, Satyal, P., & Adhikari, A. (2024). Sapital variation in constituents of essential oils from fruit pericarp of *Zanthoxylum armatum* DC of Nepali origin and their antibacterial activity, *Journal of Essential Oil Bearing Plants*, <https://doi.org/10.1080/0972060X.2023.2296549>
2. **Baral, J.**, Shrestha, D., Devkota, H. P., & Adhikari, A. (2023). Potent ROS inhibitors from *Zanthoxylum armatum* of Nepali origin. *Natural Product Research*, 1-9. <https://doi.org/10.1080/14786419.2023.2261608>
3. **Baral, J.**, Shrestha, D., Adhikari, A., (2022).  $\alpha$ -Glucosidase and  $\alpha$ -Amylase Inhibition Activities of *Sarcococca coriacea* Hook. and *Sarcococca wallichii* Staph. of Nepalese Origin *Journal of Nepal Chemical Society*, **43**(1):135-140. <https://doi.org/10.3126/jncs.v43i1.46950>
4. **Baral, J.**, & Adhikari, A., (2024). Bio-pesticidal, antimicrobial, and antiinflammatory potentials of n-hexane fraction of *Zanthoxylum armatum* DC and its chemical profiling. *Journal of Nepal Chemical Society*. **44**(1): 41-51. <https://doi.org/10.3126/jncs.v44i1.62679>
5. Hameed, A., Raza, S. A., Khan, M. I., **Baral, J.**, Adhikari, A., Nur-e-Alam, M. & Hafizur, R. M. (2019). Tambulin from *Zanthoxylum armatum* acutely potentiates the glucose-induced insulin secretion via KATP-independent Ca<sup>2+</sup>-dependent amplifying pathway. *Biomedicine & Pharmacotherapy*, *120*, 109348. <https://doi.org/10.1016/j.biopha.2019.109348>

## **Participation in International conferences**

1. Presenter at “**4<sup>th</sup> Edition of International Conference on Traditional Medicine, Ethnomedicine and Natural Therapies (ICTM 2022)**” Online Conference on September 1-2, 2022 (Oral Presentation)
2. Presented a **poster on 15<sup>th</sup> International Symposium on Natural Product Chemistry (ISNPC-15)** on February 21-24, 2022, University of Karachi, Karachi, Pakistan
3. Participated in the **15<sup>th</sup> International Symposium on Natural Product Chemistry (ISNPC-15)** on February 21-24, 2022, University of Karachi, Karachi, Pakistan
4. Participated in the **COMSTECH International Workshop and Exhibition on “Research Commercialization: Challenges and Opportunities”** June 14<sup>th</sup> -15<sup>th</sup>, 2022. Virtual Participation
5. Participated in Kathmandu Humboldt-Kolleg 2022 **Interdisciplinary Collaboration for Strengthening Science and Culture** October 16-19 2022, Kathmandu, Nepal
6. Participated in **International Chemical Congress (ICC-2023) held in Park Village Hotel, Kathmandu, Nepal** during May 25-27, 2023 (Oral presentation).
7. Participated in **Ph.D Festival 2023, University Campus, Kritipur, Institute of Science & Technology, Tribhuvan University, 9-10 October, 2023)**

### **Fellowship and training**

- Research **Fellowship in Natural Product Chemistry** (17Feb2022 -18 May2022) Supervisor Prof. Dr. M. Iqbal Choudhary at the H.E.J. Research Institute of Chemistry, International Center for Chemical and Biological Sciences (ICCBS), University of Karachi, Karachi-75270, Pakistan
- **Fellowship Program at Asian Network of Research on Antidiabetic Plants**, Bangladesh University of Health Sciences (Dec-March 2018-2019) Supervisor Prof. Dr. Begum Rokeya, Darussalam, Mirpur, Dhaka, Bangladesh
- **Training on LC/MS/MS on Waters UPLC/ Acquity TQD system** at Nepal Academy of Science and Technology, Lalitpur, Nepal Duration: 1-5<sup>th</sup> July, 2019
- **Participated in 3<sup>rd</sup> International Flow Cytometry Workshop, Nepal, October 2023**

**Awards:**

- International Foundation of Science, **IFS grantees 2020** for PhD
- University Grant Commission, **PhD fellowship awardee 2074/75**



Tribhuvan University  
Institute of Science and Technology  
Dean's Office

### SEMESTER EXAMINATION 2075

Name of Student: Janaki Baral

Exam Roll No.: 100013

Level: Ph.D.

Ph.D. Enrolment No.: 75/047

Department: Central Dept. of Chemistry

T.U. Regd. No.: 5-2-48-33-2003

Semester: I

### Grade Sheet

Code No.	Course Title	Cr. Hrs.	Grade Point	Grade
PHS 911	Philosophy of Science	3	3.7	A-
RM 912	Research Methodology	3	3.7	A-
Sem 913	Seminar	3	3.3	B+

SGPA: 3.6

Verified By: *Indu*

Date: *oct. 9, 2018*



*Haragon*  
Asst. Dean



**Tribhuvan University  
Institute of Science and Technology  
Dean's Office**

### **SEMESTER EXAMINATION-2075**

**Name of Student:** Janaki Baral

**Exam Roll No.:** 200013

**Level:** Ph.D.

**Ph.D. Enrolment No.:** 75/074

**Department:** Central Dept. of Chemistry

**T.U. Regd. No.:** 5-2-48-33-2003

**Semester:** 2

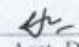
#### **Grade Sheet**

<b>Code No.</b>	<b>Course Title</b>	<b>Cr. Hrs.</b>	<b>Grade Point</b>	<b>Grade</b>
CHE 951	Advanced Research Methodology	3	4	A
CHE 953	Natural Products Chemistry	3	4	A
CHE 952	Seminar	3	4	A

SGPA: 4.00

Verified By: 

Date: Sept. 16, 2019

  
Asst. Dean



বাংলাদেশ ইউনিভার্সিটি অব হেলথ সায়েন্সেস  
**BANGLADESH UNIVERSITY OF HEALTH SCIENCES**

Memo No: BUHS/BIO/EA/19/162/1  
Date: 02.01.2019

To  
Janaki Baral  
Assistant Professor/PhD Scholar  
Central Department of Chemistry  
Tribhuvan University,  
Nepal

**Subject: Ethical Clearance**

The Ethical Review Committee (ERC) of the Bangladesh University of Health Science (BUHS) has the pleasure to accord ethical clearance to your Protocol “**Determination of Antidiabetic activity of Zanthoxylum armatum fruits & Artemesia dubia bark methanolic extract on nSTZ induced type-2 diabetic model rats**” subject to the condition that the guidelines overleaf must be followed carefully.



(Prof MA Hafez)

(Prof MA Hafez)  
Chairman  
Ethical Review Committee



## 15<sup>th</sup> International Symposium on Natural Product Chemistry

Organized by

H.E.J. Research Institute of Chemistry, International Center for Chemical and Biological Sciences (ICCBS)  
University of Karachi, Karachi-75270 Pakistan

In collaboration with

Standing Committee on Scientific and Technological Cooperation of the OIC (COMSTECH)  
Commission on Science and Technology for Sustainable Development in the South (COMSATS) &  
The United Nations Educational, Scientific and Cultural Organization (UNESCO)

February 21-24, 2022, Karachi, Pakistan

*It is certified that*

**Janaki Baral**

has participated in the "15<sup>th</sup> International Symposium on Natural Product Chemistry", held during 21-24 February, 2022.  
His/Her active participation has contributed to the overall success of the event. He/She has presented a poster in this international event.

Prof. Dr. M. Iqbal Choudhary *Mustafa (PBUH) Prize Laureate, H.I., S.I., T.I.*  
Director/Organizing Secretary

Prof. Dr. Atta-ur-Rahman, *FRS, N.I., H.I., S.I., T.I.*  
Patron-in-chief



## 15<sup>th</sup> International Symposium on Natural Product Chemistry

Organized by

H.E.J. Research Institute of Chemistry, International Center for Chemical and Biological Sciences (ICCBS)  
University of Karachi, Karachi-75270 Pakistan

In collaboration with

Standing Committee on Scientific and Technological Cooperation of the OIC (COMSTECH)  
Commission on Science and Technology for Sustainable Development in the South (COMSATS) &  
The United Nations Educational, Scientific and Cultural Organization (UNESCO)

February 21-24, 2022, Karachi, Pakistan

*It is certified that*

**Janaki Baral**

has participated in the "15<sup>th</sup> International Symposium on Natural Product Chemistry", held during 21-24 February, 2022. His/Her active participation has contributed to the overall success of the event.

Prof. Dr. M. Iqbal Choudhary *Mustafa (PBUH) Prize Laureate, H.I., S.I., T.I.*  
Director/Organizing Secretary

Prof. Dr. Atta-ur-Rahman, *FRS, N.I., H.I., S.I., T.I.*  
Patron-in-chief



# CERTIFICATE OF RECOGNITION

*Magnus Group Conferences and Organizing Committee wish to thank*

*Prof/Dr/Mr/Ms. **Janaki Baral***  
*Tribhuvan University, Nepal*

*for phenomenal and worthy Oral presentation  
at the "4th Edition of International Conference on Traditional Medicine, Ethnomedicine and  
Natural Therapies (ICTM 2022)"  
Online Conference held on September 01-02, 2022*

*Wendelin Niederberger*

**Wendelin Niederberger**  
Visionary Success Academy, Switzerland



**Asian Network of Research on  
Antidiabetic Plants (ANRAP)**

**05 March, 2019**

This is to certify that **Janaki Baral**, PhD student of Central Department of Chemistry, Institute of Science and Technology, Tribhuvan University, Nepal has successfully completed her three months ANRAP (Asian Network of Research on Antidiabetic Plants) Fellowship Program from December 2018 to March 2019. Her Host was the Bangladesh University of Health Sciences (BUHS), Darussalam, Mirpur, Dhaka. During her stay in Bangladesh she worked with "Quest of Antidiabetic effect of *Artemisia vulgaris* and *Zanthoxylum armatum* which she brought from Nepal", under the supervision of Prof Begum Rokcya.

**(Prof Begum Rokeya)**  
General Secretary  
ANRAP

**(Prof M Mosihuzzaman)**  
Chairman  
ANRAP



## CERTIFICATE OF COMPLETION

This certifies that

**Mrs. Janaki Baral**

has Successfully Completed Research Fellowship in

**NATURAL PRODUCT CHEMISTRY**

February 17, 2022– May 18, 2022

(Supervisor Prof. Dr. M. Iqbal Choudhary *H.I., B.I., T.I.*)

at the H. E. J. Research Institute of Chemistry,  
International Center for Chemical and Biological  
Sciences (ICCBS), University of Karachi,  
Karachi-75270, Pakistan

Director ICCBS



## Certificate of Participation

OIC Ministerial Standing Committee on Scientific and Technological Cooperation  
(COMSTECH)

awards this certificate to

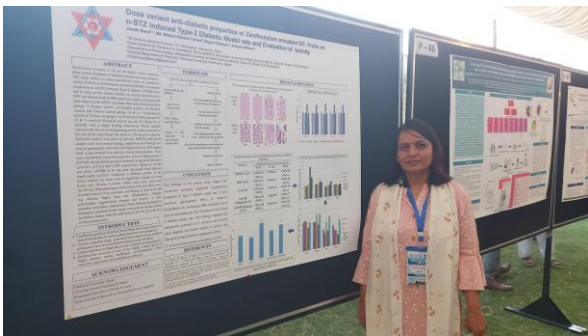
**Janaki Baral**

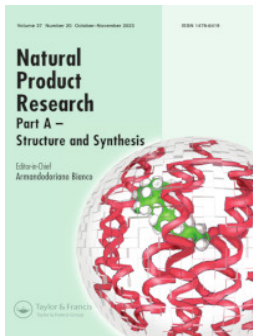
For virtual participation in the COMSTECH International Workshop and Exhibition on  
“Research Commercialization: Challenges and Opportunities”

Organized by COMSTECH  
June 14<sup>th</sup> – 15<sup>th</sup>, 2022

Prof. Dr. M. Iqbal Choudhary *H.I., S.I., T.I.*  
Coordinator General, COMSTECH  
Islamabad, Pakistan







# Natural Product Research

Formerly Natural Product Letters

ISSN: (Print) (Online) Journal homepage: <https://www.tandfonline.com/loi/gnpl20>


## Potent ROS inhibitors from *Zanthoxylum armatum* DC of Nepali origin

Janaki Baral, Dipesh Shrestha, Hari Prasad Devkota & Achyut Adhikari

To cite this article: Janaki Baral, Dipesh Shrestha, Hari Prasad Devkota & Achyut Adhikari (03 Oct 2023): Potent ROS inhibitors from *Zanthoxylum armatum* DC of Nepali origin, Natural Product Research, DOI: [10.1080/14786419.2023.2261608](https://doi.org/10.1080/14786419.2023.2261608)

To link to this article: <https://doi.org/10.1080/14786419.2023.2261608>

 View supplementary material [↗](#)

 Published online: 03 Oct 2023.

 Submit your article to this journal [↗](#)

 View related articles [↗](#)

 View Crossmark data [↗](#)



## Potent ROS inhibitors from *Zanthoxylum armatum* DC of Nepali origin

Janaki Baral<sup>a,b</sup>, Dipesh Shrestha<sup>b</sup>, Hari Prasad Devkota<sup>c</sup> and Achyut Adhikari<sup>a</sup>

<sup>a</sup>Central Department of Chemistry, Tribhuvan University, Kathmandu, Nepal; <sup>b</sup>Department of Chemistry, Tri-Chandra Multiple Campus, Tribhuvan University, Kathmandu, Nepal; <sup>c</sup>Graduate School of Pharmaceutical Sciences, Kumamoto University, Kumamoto, Japan

### ABSTRACT

A bioassay-guided isolation on the plant *Zanthoxylum armatum* DC yielded compounds tambulin (**1**), and prudomestin (**2**), from ethyl acetate fraction which showed the highest ROS inhibiting activity ( $IC_{50} = 17.8 \pm 1.1 \mu\text{g/mL}$ ). Structure elucidation of pure compounds was done using mass and NMR spectroscopic techniques. Compounds **1** and **2** revealed potent ROS inhibition with  $IC_{50} = 7.5 \pm 0.3$  and  $1.5 \pm 0.3 \mu\text{g/mL}$ , respectively, as compared to standard ibuprofen ( $IC_{50} = 11.2 \pm 1.9 \mu\text{g/mL}$ ). Likewise, both compounds **1** and **2** showed potent antioxidant activity with  $IC_{50} = 32.65 \pm 0.31$  and  $26.96 \pm 0.19 \mu\text{g/mL}$ , respectively. *In vitro* studies were supported by molecular docking and drug-likeness properties. *In silico* studies of **1** and **2** with cyclooxygenase-2 (COX-2) showed perfect binding affinity with binding energies of  $-8.4$  and  $-8.6 \text{ kcal/mol}$ , respectively, comparable to standard ibuprofen ( $-7.7 \text{ kcal/mol}$ ). Drug likeness and ADMET showed higher gastrointestinal absorption of **1** and **2** and no toxic impact.

### ARTICLE HISTORY


Received 6 June 2023  
Accepted 16 September 2023

### KEYWORDS

Anti-inflammatory;  
antioxidant; flavonoids;  
molecular docking;  
reactive oxygen species;  
*Zanthoxylum armatum* DC



**CONTACT** Achyut Adhikari  [achyutraj05@gmail.com](mailto:achyutraj05@gmail.com)

 Supplemental data for this article can be accessed online at <https://doi.org/10.1080/14786419.2023.2261608>.

© 2023 Informa UK Limited, trading as Taylor & Francis Group

## 1. Introduction

Reactive oxygen species (ROS) belong to a group of chemically reactive molecules generated during aerobic respiration as a natural byproduct of normal cellular metabolism that plays a vital role in cell signaling and immune response (Valko et al. 2007; Finkel 2011; Halliwell and Gutteridge 2015; Sies 2017). ROS are necessary for cell stability and kill pathogens but excessive production leads to tissue damage through various mechanisms of oxidative stress. The imbalance between the production and elimination of ROS results in oxidative stress (Mittal et al. 2014) that damages cells, proteins, lipids, and DNA hence causing various neurodegenerative disorders, cardiovascular diseases, and early ageing (Valko et al. 2007). Excess intracellular ROS triggers disorders and inflammation in old age (Hussain et al. 2016). Neutralizing these ROS to less harmful substances or scavenging to prevent oxidative damage requires antioxidants (Gorrini et al. 2013). Thus, the balance between ROS, stress, inflammation, and antioxidants is necessary to maintain good health. Increased level of ROS amplifies and deteriorates oxidative stress hence aggravating inflammation (Gautam and Jachak 2009; Mittal et al. 2014). Antioxidants have both endogenous and exogenous defenses in scavenging ROS and its effects. Endogenous deficiency primarily needs enzymatic supplements (Sies 2015) and antioxidants (Halliwell 2012) which is inaccessible as exogenous sources such as food and vegetables with polyphenols and flavonoids possessing strong immunity regulator, improving inflammation, neurodegeneration, cardiovascular disease and diabetes (Guardia et al. 2001; Yahfoufi et al. 2018). Since flavonoids are non-enzymatic antioxidants and strong XO inhibitors these crucially inhibit the production of ROS functionally (Valko et al. 2007; Orhan and Deniz 2021). Additionally, polyphenols inhibit enzymes related to pro-inflammation and decrease the risk of dementia (Hussain et al. 2016). Thus, the increased antioxidant supplements through diet activity are quite remarkable (Gorrini et al. 2013).

*Zanthoxylum armatum* DC, of the Rutaceae family, is commonly called 'Timur', and is widely distributed in forests and glades at 1000–2500m elevation in Nepal (Hertog Hden and Wiersum 2000) and also in India, Bhutan, Malaysia, China, the Philippines, Japan, and Pakistan (Singh and Singh 2011). Phenolic compounds of *Z. armatum* inhibit the production of pro-inflammatory cytokines (Nooreen et al. 2019) while tambulin, prudomestin, and ombuin are anti-proliferative, scavenge nitric oxide (Nooreen et al. 2017), prevent ageing, and Parkinson's disease (Pandey et al. 2019), help in secreting insulin (Hameed et al. 2019) and are significant vasorelaxants (Mushtaq et al. 2019). Such polyphenolics possess efficacy in memory loss, immunomodulatory, and osteoporosis (Kamboj 2000). Owing to such potent activities of *Z. armatum*, it triggered interest in the unexplored one of Nepali origin from a higher altitude as soil nutrients and topography affect qualitative and quantitative content (Kumhálová et al. 2008; Adhikari et al. 2018). This investigation thus focuses on the effect of *Z. armatum* on anti-inflammatory and antioxidant properties *via in vitro* and *in silico* studies.

## 2. Result and Discussion

### 2.1. Structure elucidation of compounds

Tambulin (**1**) was obtained as a yellow powder. Its molecular formula was determined to be  $C_{18}H_{16}O_7$  through various spectroscopic techniques. The EI-MS spectrum showed a molecular ion  $[M^+]$  at  $m/z$  344 with a base peak at  $m/z$  329. The HREI-MS spectrum also confirmed the  $[M^+]$  ion at  $m/z$  344.0906 (344.0896 for  $C_{18}H_{16}O_7$ ). The BB and DEPT spectra supported the molecular formula of  $C_{18}H_{16}O_7$ . In the IR spectrum, characteristic absorption peaks were observed at 3327, 1651, and  $1556\text{ cm}^{-1}$ , corresponding to the functionality's hydroxyl, aromatic, and olefinic. Similarly, in the UV spectrum, absorption peaks were detected at 367, 325, and 273 nm, respectively.

The  $^1\text{H-NMR}$  spectra displayed three singlets at  $\delta$  3.88, 3.9, and 3.97, which were assigned to the protons of the methoxy groups connected to C-4', C-7, and C-8, respectively. The H-6 proton was identified as a downfield singlet at  $\delta$  6.51. Two of the downfield linked ortho doublets were observed at  $\delta$  7.13 (d,  $J_{3',2'/5',6'}=9.0\text{ Hz}$ ) and 8.27 (d,  $J_{2',3'/6',5'}=9.0\text{ Hz}$ ), and were assigned to H-3'/H-5' and H-2'/H-6', respectively. The presence of two protons at  $\delta$  11.58 and 6.55 was due to protons linked with hydroxyl to C-5 and C-3, respectively. The HMBC relationships of protons and carbons at  $\delta$  3.87 and  $\delta$  162.2 (C-4'), 3.92 and  $\delta$  130.3 (C-8), and 3.94 and 159.6 (C-7) specified the location of compounds methoxy groups. All the spectra were matched with the previously reported compound tambulin from the same plant (Mushtaq et al. 2019). Major HMBC correlations in compound **1** are shown in Figure S1 (Supplementary material).

Prudomestin (**2**) was also obtained as a yellow powder. The EI-MS spectra of compound **2** revealed an  $[M^+]$  ion at  $m/z$  330 with a base peak at  $m/z$  315. HREI-MS spectra further confirmed the molecular formula as  $C_{17}H_{14}O_7$  with  $[M^+]$  at  $m/z$  330.0746. The infra-red spectrum showed absorptions at 3327, 1651, and  $1556\text{ cm}^{-1}$ , corresponding to OH, aromatic, and olefinic functionalities. Similarly, the UV spectrum displayed absorptions at 367, 325, and 373 nm. The  $^1\text{H-}$  and  $^{13}\text{C-NMR}$  spectra of compound **2** were closely similar to compound **1**, with only the difference in the presence of the hydroxy group instead of the methoxy group in compound **1**. Significant HMBC correlations in compound **2** are shown in Figure S1.

### 2.2. Antioxidant activities by DPPH method

The antioxidant values of the extract, fractions, and pure compounds were determined using the DPPH radical scavenging assay method. All samples were initially screened at various concentrations and samples inhibiting  $\geq 50\%$  at this concentration were further diluted for the calculation of the  $IC_{50}$  value. The antioxidant values of crude ethanoic extract ( $IC_{50} = 174 \pm 1.01\ \mu\text{g/mL}$ ), ethyl acetate fraction ( $42.94 \pm 1.19\ \mu\text{g/mL}$ ), tambulin ( $32.65 \pm 0.31\ \mu\text{g/mL}$ ), and prudomestin ( $26.96 \pm 0.19\ \mu\text{g/mL}$ ) were observed. At the same time, the standard compound quercetin showed an  $IC_{50}$  value of  $1.17 \pm 0.015\ \mu\text{g/mL}$ . This reveals stronger antioxidant properties of compounds among

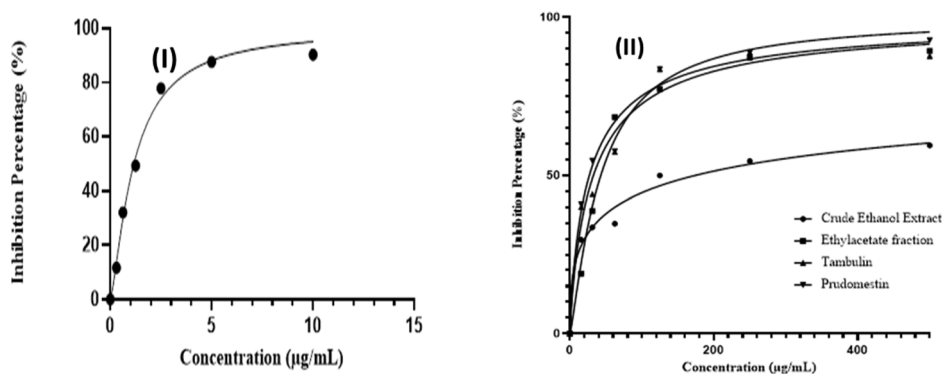


**Figure 1.** (I, II): Graphical representation of antioxidant activities of standard quercetin (I) and samples (II).

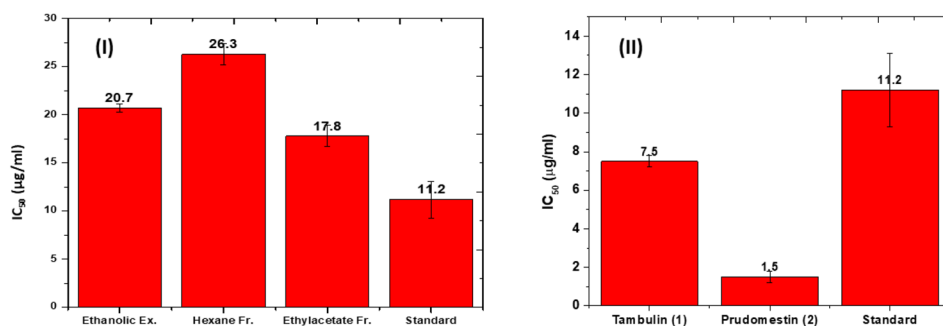


**Figure 2.** (I, II): Graphical representation of  $IC_{50} \pm$  standard error of the mean (SEM) values of ROS inhibition activities of sample versus standard of three independent tests of each sample.

the tested samples. Antioxidant activities observed are prudumestin > tambulin > ethyl acetate fraction > ethanoic extract in decreasing order. The flavonoids **1** and **2** possess higher activity than ethyl acetate fraction. A higher potential of **2** accounts for more replaceable –OH moieties. A graphical representation of antioxidant activities of standard comparable to all tested samples is presented below as inhibition percentages versus concentration ( $\mu\text{g/ml}$ ) in Figure 1(1, 2).

### 2.3. ROS inhibiting activity

The effect of *Z. armatum* constituents on myeloperoxidase-dependent ROS produced by human whole-body phagocytes was observed at various levels. Macrophages releases ROS, cyclooxygenase-2, and other to combat inflammation. Crude extract and fractions possessing potent inhibition percentages on screening were diluted further for the calculation of  $IC_{50}$  as described previously (Erharuyi et al. 2017). Anti-inflammatory activities of samples resulted in a crude ethanoic extract revealing  $IC_{50} = 20.7 \pm 0.4 \mu\text{g/mL}$ , hexane fraction as  $26.3 \pm 1.1 \mu\text{g/mL}$ . The ethyl acetate fraction possessing higher inhibition of  $17.8 \pm 1.1 \mu\text{g/mL}$  was column chromatographed to

obtain various compounds, among which the flavonoids **1** and **2** were significant ROS inhibitors with an  $IC_{50}$  value of  $7.5 \pm 0.3$  and  $1.5 \pm 0.3 \mu\text{g/mL}$ , respectively, while standard drug ibuprofen revealed  $11.2 \pm 1.9 \mu\text{g/mL}$ . The graphical representation of  $IC_{50}$  values of all samples with the standard is presented in [Figure 2\(1, 2\)](#) with data on top, and the bar showing the standard error of the mean of three independent assays of all samples.

#### 2.4. Molecular docking

The Autodock vina was used to perform molecular docking. The protocol was validated by redocking the extracted compound (SC-558) from 1CX2 to its same position. The overlay of the conformer of the SC-558 before and after docking is pictured in [Figure S2](#), and its RMSD value was found to be  $< 2 \text{ \AA}$ . Compounds **1** and **2** and the standard anti-inflammatory ibuprofen were docked into the binding cavity of COX-2. Compound **1** reported perfect binding to the active site of COX-2 with a binding affinity of  $-8.4 \text{ kcal/mol}$  as compared to the standard ibuprofen's affinity of  $-7.7 \text{ kcal/mol}$ . The binding was supported by the hydrogen bonding between HIS388 and ASN382 to the oxygen atom of the compound **1**. Some pi-interactions further assisted the binding with LEU390, ALA199, LEU391, HIS214, HIS386 and HIS207. [Figure S3\(a\)](#) depicts the 2D diagram of the interaction of **1** and amino acid residues. The binding affinity for **2** was found to be  $-8.6 \text{ kcal/mol}$ , as compared to the ibuprofen's affinity of  $-7.7 \text{ kcal/mol}$ . HIS388, ASN382, and TYR385 form hydrogen bonds with oxygen and hydrogen atoms of the **2**. At the same time, a couple of pi-interactions were observed with HIS386, HIS 207, ALA 199, and LEU 390. The 2D and 3D representation of the binding interaction of enzyme (1CX2) with **1**, **2**, and ibuprofen is shown in [Figure S3](#).

#### 2.5. Drug-likeness and ADMET analysis

The isolated compounds **1** and **2** have molecular weights of 344.32 and 330.29 g/mol, respectively, and a topological polar surface area (TPSA) of 98.36 and  $109.36 \text{ \AA}^2$ , which is an acceptable criterion for being a drug candidate as suggested by Lipinski's rule of five. Both compounds did not violate any rules for drug-likeness, as suggested by Lipinski, Ghose, Veber, Egan, and Muegge, with both compounds having a bioavailability score of 0.55. Inhibition of these cytochromes enzymes is the main mechanism that causes pharmacokinetic drug-drug interactions (Wang et al. 2015; Hakkola et al. 2020). As the Swiss ADME web server predicted, **1** and **2** were foreseen to inhibit enzymes CYP1A2, CYP2C9, CYP2D6, and CYP3A4. In addition, it also indicated that both compounds are non-inhibitors of the enzyme CYP2C19. Both compounds have high gastrointestinal absorption. Compounds **1** and **2** tested for no blood-brain barrier penetration levels, which means both compounds would not have CNS negative effects. Moreover, compounds are necessary to test for toxicity. Both **1** and **2** were also found to have no AMES toxicity, skin sensitization, and hepatotoxicity, as predicted by the pkCSM web server. The ADMET properties of compounds **1** and **2** are presented in [supplementary data in Table S1](#), and the mol-inspiration enzyme inhibition score in

**Table S2.** This table displays activities with a specific focus on enzyme inhibition by compounds **1** and **2** since the *in silico* studies were carried out after the compounds' potent activities were observed in *in vitro*. Both studies contribute differently to a comprehensive understanding of compounds and their properties in designing a drug candidate.

## 2.6. Discussion

*Zanthoxylum armatum* possesses promising biological properties on ROS inhibition and antioxidant activities as observed *in vitro*. The synergetic effect of phytoconstituents was reflected in both activities of the ethyl acetate fraction that inherits polyphenolic abundance. Flavonoids can chelate due to –OH functionality assisting in scavenging free radicals and transition metals. More –OCH<sub>3</sub> substituents of **1** justify its lower antioxidant potential than **2** possessing more –OH moieties (Arora et al. 2000). Hexane fraction due to non-polar compounds, fatty acids, and their oxides possess lower value. The present work is in accordance with previous possessing potent ethyl acetate fraction (Hertog Hden and Wiersum 2000), ethanoic extract (Bhatt and Upadhyaya 2010), and its essential oil possessing anti-inflammatory activity (Dhami et al. 2019). Moreover, the anti-inflammatory properties of the plant can be associated with the indigenous practice of using twigs of the plant to cure inflamed gums during toothache (Ahmed et al. 2004; Abbasi et al. 2013; Kanwal et al. 2015). Consuming plants possessing antioxidant properties lowers the risk of many life-threatening inflammatory diseases (Ames et al. 1993) also structurally planar flavonoids are proven as potent Xanthane oxidase inhibitors (Van Hoorn et al. 2002) and previous studies report **1** and **2** as potential Xanthane oxidase inhibitors (Ranjana et al. 2019). These compounds probably inhibit and reduce the production of ROS in the body by inhibiting the activity of XO at the same time (Ranjana et al. 2019) in protecting cells from oxidative damage and inflammation. Both compounds qualify criteria of drug likeliness suggested by Lipinki's rule of five. Compounds like these resembling NSAIDS that relieve pain without gastrointestinal toxicities are in demand (Johnston and Fox 1997). *In silico* studies of these compounds show higher COX-2 binding energy, lesser side effects non-toxic, and higher gastrointestinal absorption such drugs possessing anti-inflammatory and higher COX-2 activities are more favourable drugs with lesser side effects (Vane and Botting 1998). Hence, compounds **1** and **2** are stronger anti-inflammatory units possessing higher COX-2 activity and hence are possible drug candidates. These compounds with inhibitory potential in XO (Ranjana et al. 2019) and ROS serve in regulating hyperuricaemia and inflammation could be due to their drug-likeness nature.

## 3. Experimental (see supplementary material)

### 3.1. Supporting information

Instrumentation, plant collection extraction and isolation, DPPH antioxidant assay, oxidative burst inhibition assay, molecular docking and ADMET analysis along with Figures S1–S3, and tabulated data Tables S1 and S2.

## 4. Conclusion

Bioassay-guided isolation of the hydro-ethanoic extract of *Z. armatum* was performed and ethyl acetate fraction was column chromatographed yielding compounds tambulin (1) and prudomestin (2). Extracts, fractions and compounds all possess remarkable antioxidant and ROS inhibiting activities. Both compounds are found to be more potent than standard ibuprofen, supporting traditional uses of this plant to cure gum pain.

## Acknowledgments

The authors would like to acknowledge Prof. Dr. Mohammad Iqbal Choudhary and Dr. Almas Jabeen of H. E.J. Research Institute of Chemistry and the Dr. Panjwani Center for Molecular Medicine and Drug Research, ICCBS, University of Karachi, Pakistan, for providing laboratory facilities.

## Disclosure statement

The authors have no conflict of interest.

## Funding

This research was carried out with funding support partially from the University Grants Commission 10.13039/501100001501, Nepal, (Award No: PhD-74/75-S & T-6) and the International Foundation of Sciences grant I-1-F-6437-1 to Janaki Baral.

## References

- Abbasi AM, Khan MA, Zafar M. 2013. Ethno-medicinal assessment of some selected wild edible fruits and vegetables of Lesser-Himalayas, Pakistan. *Pak J Bot.* 45(51):215–222.
- Adhikari K, Owens PR, Ashworth AJ, Sauer TJ, Libohova Z, Richter JL, Miller DM. 2018. Topographic Controls on Soil Nutrient Variations in a Silvopasture System. *Agrosyst Geosci Environ.* 1(1):1–15. doi:10.2134/age2018.04.0008.
- Ahmed E, Arshad M, Ahmad M, Saeed M, Ishaque M. 2004. Ethnopharmacological survey of some medicinally important plants of Galliyat Areas of NWFP, Pakistan. *Asian J Plant Sci.* 3(4):410–415. doi:10.3923/ajps.2004.410.415.
- Ames BN, Shigenaga MK, Hagen TM. 1993. Oxidants, antioxidants, and the degenerative diseases of aging. *Proc Natl Acad Sci U S A.* 90(17):7915–7922. doi:10.1073/pnas.90.17.7915.
- Arora A, Byrem TM, Nair MG, Strasburg GM. 2000. Modulation of liposomal membrane fluidity by flavonoids and isoflavonoids. *Arch Biochem Biophys.* 373(1):102–109. doi:10.1006/abbi.1999.1525.
- Bhatt N, Upadhyaya K. 2010. Anti-inflammatory activity of ethanolic extract of bark of *Zanthoxylum armatum* D.C. *Pharmacol Online.* 2:123–132.
- Dhami A, Singh A, Palariya D, Kumar R, Prakash O, Rawat DS, Pant AK. 2019.  $\alpha$ -Pinene Rich Bark Essential Oils of *Zanthoxylum armatum* DC. from three different altitudes of Uttarakhand, India and their antioxidant, in vitro anti-inflammatory and antibacterial activity. *J Essent Oil-Bearing Plants.* 22(3):660–674. doi:10.1080/0972060X.2019.1630015.
- Erharuyi O, Adhikari A, Falodun A, Jabeen A, Imad R, Ammad M, Choudhary MI, Goren N. 2017. Cytotoxic, antiinflammatory and leishmanicidal activities of diterpenes isolated from the roots of *Caesalpinia pulcherrima*. *Planta Med.* 83(1-02):104–110. doi:10.1055/s-0042-110407.

- Finkel T. 2011. Signal transduction by reactive oxygen species. *J Cell Biol.* 194(1):7–15. doi:10.1083/jcb.201102095.
- Gautam R, Jachak MS. 2009. Recent Developments in anti-inflammatory natural products. *Med Res Rev.* 29(5):767–820. doi:10.1002/med.20156.
- Gorrini C, Harris IS, Mak TW. 2013. Modulation of oxidative stress as an anticancer strategy. *Nat Rev Drug Discov.* 12(12):931–947. doi:10.1038/nrd4002.
- Guardia T, Rotelli AE, Juarez AO, Pelzer LE. 2001. Anti-inflammatory properties of plant flavonoids. effects of rutin, quercetin and hesperidin on adjuvant arthritis in rat. *Farmacol.* 56(9):683–687. doi:10.1016/S0014-827X(01)01111-9.
- Hakkola J, Hukkanen J, Turpeinen M, Pelkonen O. 2020. Inhibition and induction of CYP enzymes in humans: an update. *Arch Toxicol.* 94(11):3671–3722. doi:10.1007/S00204-020-02936-7.
- Halliwell B. 2012. Free radicals and antioxidants: updating a personal view. *Nutr Rev.* 70(5):257–265. doi:10.1111/j.1753-4887.2012.00476.x.
- Halliwell B, Gutteridge JMC. 2015. *Free radicals in biology and medicine.* 5th ed. New York: Oxford University Press. doi:10.1093/acprof:oso/98701987178.001.0001.
- Hameed A, Raza SA, Israr Khan M, Baral J, Adhikari A, Nur-E-Alam M, Ahmed S, Al-Rehaily AJ, Ashraf S, Ul-Haq Z, et al. 2019. Tambulin from *Zanthoxylum armatum* acutely potentiates the glucose-induced insulin secretion via KATP-independent Ca<sup>2+</sup>-dependent amplifying pathway. *Biomed Pharmacother.* 120:109348. doi:10.1016/j.biopha.2019.109348.
- Hertog Hden W, Wiersum FK. 2000. Timur (*Zanthoxylum armatum*) Production in Nepal. *Mt Res Dev.* 20:136–145. doi:10.1659/0276-47419(2000)020[0136:TZAPIN]2.CO;2.2.0.CO;2]
- Hussain T, Tan B, Yin Y, Blachier F, Tossou MCB, Rahu N. 2016. Oxidative stress and inflammation: what polyphenols can do for us? *Oxid Med Cell Longev.* 2016:7432797. doi:10.1155/2016/7432797.
- Johnston SA, Fox SM. 1997. Mechanisms of action of anti-inflammatory medications used for the treatment of osteoarthritis. *J Am Vet Med Assoc.* 210(10):1486–1492.
- Kamboj VP. 2000. Herbal medicine. *Curr Sci Assoc.* 78(1):35–39. <https://www.jstor.org/stable/24103844>.
- Kanwal R, Arshad M, Bibi Y, Asif S, Chaudhari SK. 2015. Evaluation of ethnopharmacological and antioxidant potential of evaluation of ethnopharmacological and antioxidant potential of *Zanthoxylum armatum* DC. *Journal of Chemiatry.* 2015:1–8. doi:10.1155/2015/925654.
- Kumhálová J, Matějková Š, Fiferňová M, Lipavský J, Kumhála F. 2008. Topography impact on nutrition content in soil and yield. *Plant Soil Environ.* 54(6):255–261. doi:10.17221/257-PSE.
- Mittal M, Siddiqui MR, Tran K, Reddy SP, Malik AB. 2014. Reactive oxygen species in inflammation and tissue injury. *Antioxid Redox Signal.* 20(7):1126–1167. doi:10.1089/ars.2012.5149.
- Mushtaq MN, Ghimire S, Alamgeer , Akhtar MS, Adhikari A, Auger C, Schini-Kerth VB. 2019. Tambulin is a major active compound of a methanolic extract of fruits of *Zanthoxylum armatum* DC causing endothelium-independent relaxations in porcine coronary artery rings via the cyclic AMP and cyclic GMP relaxing pathways. *Phytomedicine.* 53:163–170. doi:10.1016/j.phymed.2018.09.020.
- Nooreen Z, Kumar A, Bawankule DU, Tandon S, Ali M, Xuan TD, Ahmad A. 2019. New chemical constituents from the fruits of *Zanthoxylum armatum* and its in vitro anti-inflammatory profile. *Nat Prod Res.* 33(5):665–672. doi:10.1080/14786419.2017.1405404.
- Nooreen Z, Singh S, Singh DK, Tandon S, Ahmad A, Luqman S. 2017. Characterization and evaluation of bioactive polyphenolic constituents from *Zanthoxylum armatum* DC., a traditionally used plant. *Biomed Pharmacother.* 89:366–375. doi:10.1016/j.biopha.2017.02.040.
- Orhan IE, Deniz FSS. 2021. Natural products and extracts as xantine oxidase inhibitors - a hope for gout disease? *Curr Pharm Des.* 27(2):143–158. doi:10.2174/1381612826666200728144605.
- Pandey T, Sammi SR, Nooreen Z, Mishra A, Ahmad A, Bhatta RS, Pandey R. 2019. Anti-ageing and anti-Parkinsonian effects of natural flavonol, tambulin from *Zanthoxylum aramatum* promotes longevity in *Caenorhabditis elegans*. *Exp Gerontol.* 120:50–61. doi:10.1016/j.exger.2019.02.016.
- Ranjana , Nooreen Z, Bushra U, Jyotshna , Bawankule DU, Shanker K, Ahmad A, Tandon S. 2019. Standardization and xanthine oxidase inhibitory potential of *Zanthoxylum armatum* fruits. *J Ethnopharmacol.* 230:1–8. doi:10.1016/j.jep.2018.10.018.

- Sies H. 2015. Oxidative stress: a concept in redox biology and medicine. *Redox Biol.* 4:180–183. doi:[10.1016/j.redox.2015.01.002](https://doi.org/10.1016/j.redox.2015.01.002).
- Sies H. 2017. Hydrogen peroxide as a central redox signaling molecule in physiological oxidative stress: oxidative eustress. *Redox Biol.* 11:613–619. doi:[10.1016/j.redox.2016.12.035](https://doi.org/10.1016/j.redox.2016.12.035).
- Singh TP, Singh OM. 2011. Phytochemical and pharmacological profile of *Zanthoxylum armatum* DC. - An overview. *Indian J Nat Prod Resour.* 2(3):275–285. doi:[10.17812/blj2015.32.18](https://doi.org/10.17812/blj2015.32.18).
- Valko M, Leibfritz D, Moncol J, Cronin MTD, Mazur M, Telser J. 2007. Free radicals and antioxidants in normal physiological functions and human disease. *Int J Biochem Cell Biol.* 39(1):44–84. doi:[10.1016/j.biocel.2006.07.001](https://doi.org/10.1016/j.biocel.2006.07.001).
- Van Hoorn DEC, Nijveldt RJ, Leeuwen PAM, Van Hofman Z, Rabet LM, De Bont DBA, Van Norren, K. 2002. Accurate prediction of xanthine oxidase inhibition based on the structure of flavonoids. *Eur J Pharmacol.* 451(2):111–118. doi:[10.1016/s0014-2999\(02\)02192-1](https://doi.org/10.1016/s0014-2999(02)02192-1).
- Vane JR, Botting RM. 1998. Mechanism of action of nonsteroidal anti-inflammatory drugs. *Am J Med.* 104(3A):2S–8S. doi:[10.1016/s0002-9343\(97\)00203-9](https://doi.org/10.1016/s0002-9343(97)00203-9).
- Wang Y, Xing J, Xu Y, Zhou N, Peng J, Xiong Z, Liu X, Luo X, Luo C, Chen K, et al. 2015. In silico ADME/T modelling for rational drug design. *Q Rev Biophys.* 48(4):488–515. doi:[10.1017/S0033583515000190](https://doi.org/10.1017/S0033583515000190).
- Yahfoufi N, Alsadi N, Jambi M, Matar C. 2018. The immunomodulatory and anti-inflammatory role of polyphenols. *Nutrients.* 10(11):1–23. doi:[10.3390/nu10111618](https://doi.org/10.3390/nu10111618).

## **SUPPLEMENTARY MATERIAL**

### **Potent ROS Inhibitors from *Zanthoxylum armatum* DC of Nepali Origin**

*Janaki Baral*<sup>1,2</sup>, *Dipesh Shrestha*<sup>2</sup>, *Hari Prasad Devkota*<sup>3</sup>, *Achyut Adhikari*<sup>1\*</sup>

<sup>1</sup>*Central Department of Chemistry, Tribhuvan University, Kathmandu 44618, Nepal*

<sup>2</sup>*Department of Chemistry, Tri-Chandra Multiple Campus, Tribhuvan University, Kathmandu, 44605, Nepal*

<sup>3</sup>*Graduate School of Pharmaceutical Sciences, Kumamoto University, Kumamoto, Japan*

*\*Corresponding email: [achyutraj05@gmail.com](mailto:achyutraj05@gmail.com)*

Janaki Baral, E-mail: [knock2janaki@gmail.com](mailto:knock2janaki@gmail.com)

ORCID: 0000-0002-5208-6817

Dipesh Shrestha, E-mail: [dpesstha@gmail.com](mailto:dpesstha@gmail.com)

ORCID: 0000-0003-4613-199X

Hari Prasad Devkota, E-mail: [devkotah@kumamoto-u.ac.jp](mailto:devkotah@kumamoto-u.ac.jp)

Achyut Adhikari, E-mail: [achyutraj05@gmail.com](mailto:achyutraj05@gmail.com)

ORCID id: 0000-0002-1065-5727

*\*Corresponding address: Central Department of Chemistry, Tribhuvan University, Kathmandu 44618, Nepal, Email: [achyutraj05@gmail.com](mailto:achyutraj05@gmail.com)*

**ABSTRACT:** A bioassay-guided isolation on the plant *Zanthoxylum armatum* DC yielded compounds tambulin (**1**), and prudomestin (**2**), from ethyl acetate fraction which showed the highest ROS inhibiting activity ( $IC_{50} = 17.8 \pm 1.1 \mu\text{g/mL}$ ). Structure elucidation of pure compounds was done using mass and NMR spectroscopic techniques. Compounds **1** and **2** revealed potent ROS inhibition with  $IC_{50} = 7.5 \pm 0.3 \mu\text{g/ml}$  and  $1.5 \pm 0.3 \mu\text{g/ml}$ , respectively as compared to standard ibuprofen ( $IC_{50} = 11.2 \pm 1.9 \mu\text{g/mL}$ ). Likewise, both compounds **1** and **2** showed potent antioxidant activity with  $C_{50} = 32.65 \pm 0.31 \mu\text{g/mL}$ , and  $26.96 \pm 0.19 \mu\text{g/mL}$  respectively. *In vitro* studies were supported by molecular docking and drug-likeness properties. In silico studies of **1** and **2** with *cyclooxygenase-2* (COX-2), the enzyme explored the perfect binding affinity with binding energies of  $-8.4 \text{ kcal/mol}$  and  $-8.6 \text{ kcal/mol}$  respectively, comparable to standard ibuprofen ( $-7.7 \text{ kcal/mol}$ ). Drug likeness and ADMET showed higher gastrointestinal absorption of **1** and **2** and no toxic impact.

**Key Words:** Anti-inflammatory, Antioxidant, Flavonoids, Molecular docking, Reactive Oxygen Species, *Zanthoxylum armatum* DC

### 3. Experimental

#### 3.1. Instrumentation

The ethanolic extract was concentrated in a rotatory evaporator IKA (Werke GmbH & Co. KG, Germany) at  $40^{\circ}\text{C}$  and freeze dried. Column chromatography was performed using (230-400 mesh size, E. Merck, Darmstadt). The EI-MS spectra were obtained on EI (LR) JEOL MS ROUTE 600H-1, (JEOL, Ltd, Tokyo, Japan). The NMR spectra were acquired on AV-400 instruments (Bruker, Switzerland).

#### 3.2. Plant Collection

Matured fruits of *Z. armatum* DC were collected from the Pyuthan district at an altitude of 2200 meters above sea level in Nepal in October 2017. Deposition of a voucher specimen (TUCH:

201016) of the herbarium was done after authentication at the Tribhuvan University Central Herbarium, Kritipur.

### 3.3. Extraction and Isolation

Five kilograms of mature fruit pericarp, *Z. armatum* DC, were used for extraction using 80% ethanol/water (20 L). 600 g of concentrated extract yield 150.0 g of hexane fraction. 145 g of ethylacetate fraction (Za-B) obtained was column chromatographed on silica gel using different gradients of hexanes and dichloromethane, resulting in 10 sub-fractions. Eluents were collected based on the TLC results (ZaBA–ZaBJ). 20 grams of ZaBE further purified that yield compounds 1 and 2 quantitatively 70 mg and 30 mg, respectively.

### 3.4. DPPH Antioxidant Assay

Antioxidant activities of the extract, fraction, and compound of *Z. armatum* were determined by free radical scavenging assay following the previously described method with minor modifications (Mensor et al. 2001). For antioxidant determination, 2,2-diphenyl-1-picrylhydrazyl radical (DPPH, Sigma-Aldrich). Triplicates of the sample (100 $\mu$ L), 1mg/ml prepared in 50% DMSO and serially diluted, with (100 $\mu$ L) DPPH of concentration 0.1 mM each were pipetted in 96 well plates. After recording the initial absorbance at 517 nm (Epoch 2, BioTek, Instruments, Inc., USA), the sample was placed in the dark for half an hour. Percentage inhibition was calculated using formula below. After final absorbance the half maximum inhibitory concentration (IC<sub>50</sub>) was calculated.

$$\% \text{ inhibition} = \left( \frac{A_{\text{control}} - A_{\text{sample}}}{A_{\text{control}}} \right) \times 100$$

Where  $A_{\text{control}}$  is the absorbance of the control and  $A_{\text{sample}}$  is the absorbance of the sample.

### 3.5. Oxidative Burst Inhibition Assay

Investigation were carried after an approval from an independent ethics committee was for anti-inflammatory studies on cells from human blood at, ICCBS, UoK, No: ICCBS/IEC-008-BC-2015/Protocol/1.0. The anti-inflammatory activity was determined using a luminol-enhanced chemiluminescence test a predetermined protocol (Helfand et al. 1982). For the effects of samples of *Z. armatum* on reactive oxygen species produced by human whole blood phagocytes

briefly, 25  $\mu$ L of diluted whole blood HBSS++ (Hanks Balanced Salt Solution, containing calcium chloride and magnesium chloride) [Sigma, St. Louis, USA] was added to 25  $\mu$ L of the sample at three different concentrations, all in triplicate, and were incubated. HBSS++, and in the control wells, only cells were added. The experiment was carried out in a white half-area 96-well plate [Costar, NY, USA], which was incubated for 15 minutes at 37°C in the thermostat chamber of a luminometer [Labsystems, Helsinki, Finland]. After incubation, 25  $\mu$ L of serum opsonized zymosan (SOZ) [Fluka, Buchs, Switzerland] and 25  $\mu$ L of luminol [Research Organics, Cleveland, OH, USA], an intracellular ROS detecting probe, were added to each well except blank wells (containing just HBSS++). Relative light units (RLU) luminometer was used to record the wells ROS level and % inhibition calculated using formula as below. Standard Ibuprofen is preferred over others due to wide availability over the counter as a generic medication, cost-effective, an anti-inflammatory for humans (Hofbauer et al. 1998) that delays Alzheimers' disease associated with chronic inflammation (Lim et al. 2000), effective analgesic(Doyle et al. 2010) and a better antidepressant (Mesripour et al. 2020).

$$\text{Percentage inhibition} = \text{averageRLU} \left( \frac{\text{Control} - \text{Sample}}{\text{Control}} \right) \times 100$$

### **3.6. Molecular Docking and ADMET Analysis**

#### **3.7. Preparation of Protein and Ligands**

The three-dimensional structure of Cyclooxygenase-2 (prostaglandin synthase-2) complexed with a selective inhibitor SC-558 (PDBID: 1CX2) was retrieved from the protein data bank (PDB) (<https://www.rcsb.org/>) in .pdb format. The protein was prepared using ChimeraX and AutoDockTools-1.5.6. All the co-crystallized ligands, non-standard residues, and water molecules were removed from the protein. In addition, the polar hydrogens and Kollman charges were added to it saved in .pdbqt format for molecular docking. The ligands were prepared using Avogadro and AutoDockTools-1.5.6. The 3D structures of **1** and **2** and the standard ibuprofen were downloaded from PubChem (<https://pubchem.ncbi.nlm.nih.gov/>) in .sdf format. The downloaded ligands in .sdf format were first converted to .pdb format using Avogadro after optimizing geometry. Then, they were converted into .pdbqt format.

### **3.8. Protein Active Site Prediction and Molecular Docking**

The active binding site of the downloaded protein was predicted using Biovia Discovery Studio. After determining the perfect binding site of the enzyme, a grid box was set to  $20 \times 20 \times 20$  with spacing  $0.375\text{\AA}$  and the center set to  $x = 25.720$ ,  $y = 28.054$ , and  $z = 7.827$ . All the target proteins, ligands, and grid box center data were saved as a configuration.txt file. Lastly, molecular docking was performed using autodock vina (Trott and Olson 2010). In the context of bioactive compounds, the conformation of the ligand with the lowest affinity was considered as the most stable conformation. Biovia Discovery Studio was used to analyze the result.

### **3.9. Validation of Molecular Docking**

The molecular docking protocol was validated by isolating the SC-558 ligand from the protein (1CX2) and redocking in the same position. The lowest energy pose on redocking was chosen to superimpose the previous bind position of the ligand, and its root mean square deviation (RMSD) was calculated.

### **3.10. Drug Likeness and ADMET Analysis**

The compounds were subjected to the drug-likeness test. Lipinski's rule of 5 (RO5), Ghose, Veber, Egan, and Muegge's rules were applied to test the drug-likeness of the compounds (Lipinski et al.; Ghose et al. 1999; Egan et al. 2000; Muegge et al. 2001; Veber et al. 2002). The drug-likeness was tested using SwissADME, and pkCSM web server (Pires et al. 2015; Daina et al. 2017). Additionally, Molinspiration webserver was used to determine the enzyme inhibitor mol inspiration bioactivity score.

## Supplementary data of anti-inflammatory and antioxidant activities

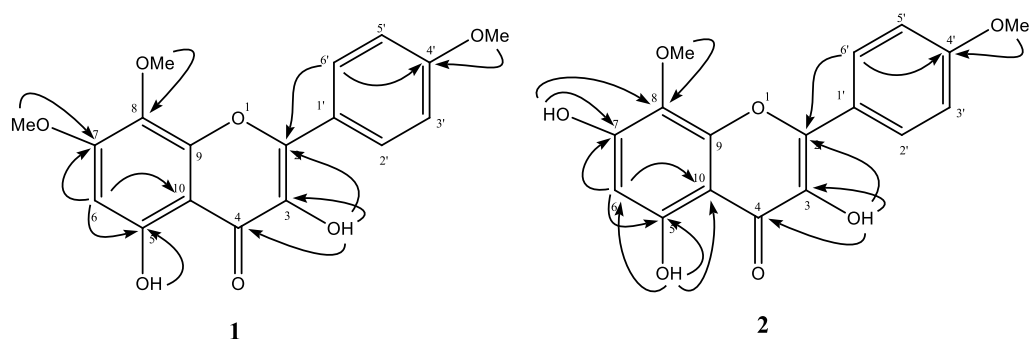


Fig-S1: Key HMBC correlations of **1** and **2**

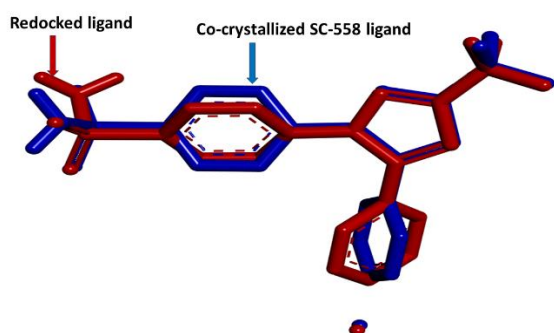


Fig. S2: Superimposition of co-crystallized SC-558 ligand (blue) and redocked ligand (red)

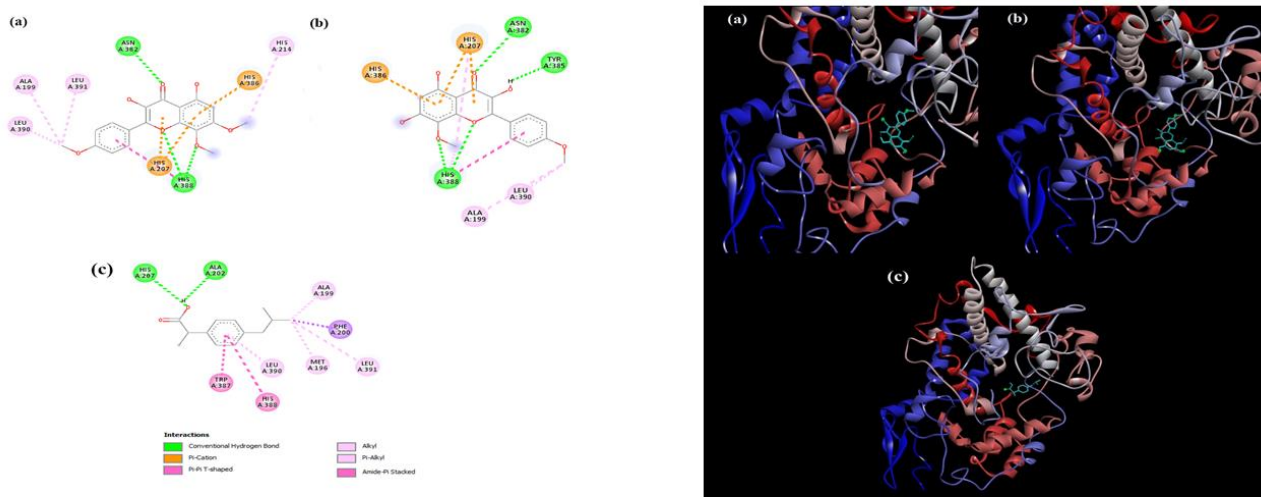


Fig. S3: 2D & 3D interaction of enzyme (1CX2) with a) compound **1** and b) **2** c) Ibuprofen

**Table S1:** ADMET parameters of compounds **1** and **2**.

Properties	Tambulin (1)	Prudomestin (2)
Molecular Weight (g/mol)	344.32	330.29
Topological Polar Surface Area (TPSA)	98.36 Å <sup>2</sup>	109.36 Å <sup>2</sup>
Water Solubility	Moderately Soluble	Moderately Soluble
Gastrointestinal (GI) absorption	High	High
BBB permeant	No	No
CYP1A2 inhibitor	Yes	Yes
CYP2C19 inhibitor	No	No
CYP2C9 inhibitor	Yes	Yes
CYP2D6 inhibitor	Yes	Yes
CYP3A4 inhibitor	Yes	Yes
AMES toxicity	No	No

---

Hepatotoxicity	No	No
Skin sensitization	No	No
Drug-likeness	Yes	Yes

(Lipinski, Ghose, Veer, Egan,  
Muegge)

---

**Table S2:** Molinspiration bioactivity score of compounds:

---

Compounds	Enzyme inhibitor (molinspiration bioactivity score)
<b>1</b>	0.17
<b>2</b>	0.20

---

## References:

- Daina A, Michielin O, Zoete V. 2017. SwissADME: A free web tool to evaluate pharmacokinetics, drug-likeness and medicinal chemistry friendliness of small molecules. *Scientific Reports*.7:1–13. doi:10.1038/srep42717.
- Doyle G, Jayawardena S, Ashraf E. 2010. The Journal of Clinical Efficacy and Tolerability of Nonprescription Ibuprofen versus Celecoxib for Dental Pain. *The Journal of Clinical Pharmacology*. 42(8): 912–919. doi:10.1177/009127002401102830
- Egan WJ, Merz KM, Baldwin JJ. 2000. Prediction of drug absorption using multivariate statistics. *J Med Chem*. 43(21):3867–3877. doi:10.1021/jm000292e.
- Ghose AK, Viswanadhan VN, Wendoloski JJ. 1999. A knowledge-based approach in designing combinatorial or medicinal chemistry libraries for drug discovery. 1. A qualitative and quantitative characterization of known drug databases. *J Comb Chem*. 1(1):55–68. doi:10.1021/CC9800071.
- Helfand SL, Werkmeister J, Roder JC. 1982. Chemiluminescence response of human natural killer cells: I. the relationship between target cell binding, chemiluminescence, and cytolysis. *J Exp Med*. 156(2):492–505. doi:10.1084/jem.156.2.492.
- Hofbauer R, Speiser W, Kapiotis S. 1998. Ibuprofen Inhibits Leukocyte Migration Through Endothelial Cell Monolayers. *Life Sci*. 62(19):1775–1781. doi: 10.1016/S0024-3205(98)00139-8
- Lim GP, Yang F, Chu T, Chen P, Beech W, Teter B, Tran T, Ubeda O, Ashe KH, Frautschy SA, Cole GM.. 2000. Ibuprofen Suppresses Plaque Pathology and Inflammation in a Mouse Model for Alzheimer ' s Disease. *Journal of Neuroscience*. 20(15):5709–5714. doi:10.1523/JNEUROSCI.20-15-05709.2000
- Lipinski CA, Lombardo F, Dominy BW, Feeney PJ.(2012). Experimental and computational approaches to estimate solubility and permeability in drug discovery and development settings. *Advanced drug delivery reviews*, 64,4-17. doi:10.1016/j.addr.2012.09.019
- Mensor LL, Menezes FS, Leitaõ GG, Reis AS, Dos TCS. 2001. Screening of Brazilian plant extracts for antioxidant activity by the use of DPPH free radical method . *Phytother Res*,15(2) :127–130. doi:10.1002/ptr.687

Mesripour A, Shahnooshi S, Hajhashemi V. 2020. Celecoxib, ibuprofen, and indomethacin alleviate depression-like behavior induced by interferon-alfa in mice. *J Complement Integr Med.* 17(1):1–9. doi:10.1515/jcim-2019-0016.

Muegge I, Heald SL, Brittelli D. 2001. Simple selection criteria for drug-like chemical matter. *J Med Chem.* 44(12):1841–1846. doi:10.1021/jm015507e.

Pires DE V, Blundell TL, Ascher DB, 1ga UK. 2015. pkCSM: Predicting Small-Molecule Pharmacokinetic and Toxicity Properties Using Graph-Based Signatures. doi:10.1021/acs.jmedchem.5b00104.

Trott O, Olson AJ. 2010. AutoDock Vina: improving the speed and accuracy of docking with a new scoring function, efficient optimization and multithreading. *J Comput Chem.* 31(2):455. doi:10.1002/JCC.21334.

Veber DF, Johnson SR, Cheng HY, Smith BR, Ward KW, Kopple KD. 2002. Molecular properties that influence the oral bioavailability of drug candidates. *J Med Chem.* 45(12):2615–2623. doi:10.1021/jm020017n.

## Bio-pesticidal, Antimicrobial, and Anti-inflammatory Potentials of n-Hexane Fraction of *Zanthoxylum armatum* DC and Its Chemical Profiling

Janaki Baral<sup>1,2</sup> & Achyut Adhikari<sup>1\*</sup>

<sup>1</sup>Central Department of Chemistry, Tribhuvan University, Kathmandu 44618, Nepal

<sup>2</sup>Department of Chemistry, Tri-Chandra Multiple Campus, Tribhuvan University, Kathmandu, 44605, Nepal

\*Corresponding email: [achyutraj05@gmail.com](mailto:achyutraj05@gmail.com)

Submitted: 06/23/2023, revised, 01/08/2024, accepted: 01/15/2024

### Abstract:

*Zanthoxylum armatum* DC, commonly known as toothache tree, is utilized for treating inflamed gums. The plant's volatile constituent possesses a robust fragrance and contributes to its tangy taste. This study investigates the bioactivities, including bio-pesticidal, antimicrobial, and anti-inflammatory properties as well as the chemical profiling of the n-hexane fraction based on GC-MS analysis. The evaluated activities involve contact toxicity, microplate alamar blue assay, against three different insects, five bacteria, and seven fungi, and oxidative burst assay. The NIST library serves as a standard reference database for constituent identification. Remarkable insecticidal activities comparable to the standard drug permethrin were observed, particularly against *Rhyzopertha dominica* (100%), *Tribolium castaneum* (60%), and *Sitophilus oryzae* (50%). The fraction exhibited significant antifungal activity against *Fusarium lini* (85%) and notable inhibition against *B. subtilis* (67.27%) and *S. aureus* (65.25%). Potent anti-inflammatory effects were noted with an IC<sub>50</sub> value of 11.2±1.9 µg/ml, equivalent to standard ibuprofen at various concentrations. GC-MS analysis identified twenty compounds, with major ones including trans-13-Octadecenoic acid (36.08%), Cis-9 hexadecenoic acid (18.66%), and 2-propenoic acid 3 phenyl methyl ester (11.08%). The diverse bioactivities observed may be attributed to the varied nature of compounds such as polyunsaturated fatty acids and their oxides. This research revealed the potential of *Z. armatum* as a potential bio-pesticide, anti-inflammatory, and antimicrobial agent.

**Keywords:** Anti-inflammatory, Bio-pesticide, GC-MS, Insecticidal, *Zanthoxylum armatum* DC

### Introduction

Synthetic pesticides have adverse effects on all consumers in the food chain, impacting the entire ecosystem [1]. Pathogens such as insects, fungi, and bacteria contribute to significant losses in productivity and yield in agriculture. To combat these challenges, farmers often resort to the excessive use of chemical

pesticides, resulting in acute pesticide poisoning, particularly in developing nations [2]. The concern for unintentional acute pesticide poisoning poses a major health challenge, with Southern Asia reporting the highest number of cases [3]. Embracing traditional practices, such as using specific plants for food storage by indigenous communities, presents an

alternative approach to preserving food and managing pests. Natural resources like plants, animals, bacteria, and minerals can serve as bio-pesticide due to their insecticidal, antibacterial, or antifungal properties. The use of various natural resources such as plants, animals, bacteria, and minerals can serve as bio-pesticides in controlling pests, insects, weeds, and various diseases due to their insecticidal, antibacterial, or antifungal properties, offering a more sustainable and eco-friendly means of pest control [2]. The adaptation of eco-friendly pesticides can have long-term positive impacts on overall plant and animal species with numerous modern medications being derived from conventional practices [4].

*Zanthoxylum armatum*, locally known as Timur in Nepal, is an economically valued medicinal plant belonging to the Rutaceae family. Widely distributed in Nepal ranging from 1000-2500m in uncluttered places. Besides this plant is also distributed in India, Bhutan, China, Taiwan, the Philippines, Malaysia, Pakistan, and Japan, at an altitudes ranging from 1000-1500m [5], [6]. Renowned as a toothache tree, it contains various phytochemicals, including alkaloids, sterols, flavonoids, saponins, coumarins, glycosides, benzoids fatty acids, alkenes acids, and amino acids [7], [8]. Studies have demonstrated the antioxidant, anti-inflammatory, cytotoxic, and hepato-protective activities of phytochemicals found in different parts of the plant [9]. The alkaloids in *Z. armatum* exhibit diverse biological and pharmacological properties including larvicidal, antinociceptive, antioxidant, antibiotic, hepatoprotective, antiplasmodial, cytotoxic, antiproliferative, anthelmintic, antiviral, antifungal, and anti-inflammatory activities [10]. Locals use crude extracts for their purported anti-helminthic, stomachic, and carminative properties to treat bacterial infections [11]. Additionally, the essential oil

from leaves and fruits, rich in fatty acids and esters, adds to the plant's economic value.

This study specifically focuses on investigating the bioactivities on the n-hexane fraction of *Zanthoxylum armatum* DC and its constituents through GC-MS. The synergistic effects of natural compounds may reveal various biological benefits and provide essential dietary supplements. The hydrophobic nature of hexane as a solvent makes it adept at extracting volatile compounds like fatty acids and their derivatives, underscoring the potential significance of the identified constituents.

## Material and Methods

### I) Collection of plant materials and partitioning

Matured fruit pericarp of *Zanthoxylum armatum* DC were collected in October 2018 from higher altitude (>2200 m above sea level) Pyuthan district of Nepal. Authentication of the herbarium of *Zanthoxylum armatum* was done at the Central Department of Botany, Tribhuvan University Central Herbarium, Kirtipur. Specimen voucher no TUCH (201016) was deposited in the same department. The powdered form of the extract five kilograms was soaked in 80% EtOH/H<sub>2</sub>O, one kilogram in four litres. It was shaken manually for homogeneous distribution. This procedure was repeated thrice. The clear filtrate was taken and concentrated in rotatory evaporator IKA (Werke GmbH & Co. KG, Germany) at 40 °C and dried in the freeze drier (HETOSICC, Heto Lab Equipment, Denmark) at 55 °C. The concentrated ethanolic extract (600 g) was then fractionated to obtain a lower polarity hexane fraction of 150 g.

### II) Characterization of hexane fraction of *Zanthoxylum armatum*

The Agilent technologies 7000 GC/MS triple quadrupole acquisition method was used to characterize the hexane fraction (MS-7000, GC 7890A). The ZEBRONZB-5HT column was used at 400 °C: 30m×320µm × 0.25 µm, In Front SS inlet He and Out Vacuum. The oven was equilibrated for 5 minutes before running for 72 minutes at 60°C (8°C/min to 240 °C for 20 minutes and 15 °C/min to 300 °C for 5 minutes). The injected sample volume was 1.5 µL. The spectra were computer-matched using the NIST Mass Spectrometry Data Center and the WILEY 7.0 library, and the retention times of known species injected in the chromatographic column were used to identify the peaks.

### III) Identification of Components

Each of the mass spectra in GC-MS was identified by comparing the mass spectral fragmentation patterns head to tail of each constituent with those in the National Institute of Standards and Technology's (NIST) Mass Spectral Libraries version 2.2 database [12].

### IV) Microplate Alamar Blue Assay (MABA)

Microplate alamar blue assay test used five different bacteria: *Bacillus subtilis* ATCC23875, *Staphylococcus aureus* NCTC 6571, *Escherichia coli* ATCC 25922, *Pseudomonas aeruginosa* ATCC 10145, and *Salmonella typhi* ATCC 14028. MABA was performed on hexane fraction at the concentration of 3000 µg/ml whereas the concentration of standard ofloxacin used was 100 µg/ml.

### V) Insecticidal activity by contact toxicity method

For insecticidal activity by contact toxicity method, three major insects were used namely *Tribolium*

*castaneum*, *Sitophilus oryzae*, *Rhyzopertha dominica*. The hexane fraction used for the activity was 2038.20 µg/cm<sup>2</sup> whereas the standard Permethrin used was 239.5 µg/cm<sup>2</sup>.

### VI) Antifungal activities

*In vitro* antifungal bioassay was performed with a concentration of sample as 3000 µg/mL of DMSO with an incubation time of 7 days at a temperature of 27 °C. Seven different fungi; *Trichophyton rubrum*, *Candida albicans*, *Aspergillus niger*, *Microsporumcanis*, *Fusarium lini*, *Candida glabarata* and *Aspergillus fumigatus* were used for the antifungal activities.

### VII) Oxidative Burst Assay using Chemiluminescence Technique

The anti-inflammatory activity was determined using a luminol-enhanced chemiluminescence test, based on a predetermined protocol [13]. In brief, 25 µL of diluted whole blood HBSS++ (Hanks Balanced Salt Solution, containing calcium chloride and magnesium chloride) [Sigma, St. Louis, USA] was added to 25 µL of the hexane fraction in triplicate at three different concentrations (10, 50 and 250µg/ml) and incubated. HBSS++, cells were added to the control wells only. The experiment was carried out in a white half-area 96-well plate [Costar, NY, USA], which was incubated for 15 minutes at 37 °C in a luminometer's thermostat chamber [Labsystems, Helsinki, Finland]. Following incubation, 25 µL of serum opsonized zymosan (SOZ) [Fluka, Buchs, Switzerland] and 25 µL of an intracellular reactive oxygen species detecting probe, luminol [Research Organics, Cleveland, OH, USA] were added into each well beside the blank wells containing HB++. Ibuprofen was used as a standard. A luminometer was used to

calculate the amount of ROS in terms of relative light units (RLU).

## Result and Discussion

The result section consists mainly of two parts chemical and biological.

### A) Chemical part

This portion consists of the analysis of the GC-MS portion, the structure of major compounds, and the mass spectra of major compounds as follows.

### I) GC-MS Analysis

Gas Chromatography coupled with mass spectrometry is a direct and quick analytical approach. It operates with high separation efficiency flexibility and

selectivity with mass sensitivity in detection [14]. Identification of volatile matters generally includes long and short-chain polyunsaturated fatty acids, hydrocarbons, esters, alcohols, etc. The GC chromatograms of the hexane fraction indicating total ion concentration are shown in Fig1 and Fig. 2 below. Table 1 consists of the compounds identified from each constituent's mass spectral fragmentation pattern from head to tail. The sample mainly consists of hydrocarbons, polyunsaturated fatty acids, long and short-chain hydrocarbons, terpenoids, and esters. The aromatic flavor of the fruit was found to be a mixture of esters and various compounds.

SN	t <sub>R</sub> (min.)	Compound	Compound nature	Peak area
1	5.96	Bicyclo[3.1.1]hept-3-en-2-one, 4,6,6-trimethyl-	2-Pinen-4-one	0.04
2	7.16	2Furanmethanol,5ethanyltetrahydro- $\alpha,\alpha,5$ -trimethyl-cis-	<i>cis</i> -Linaool Oxide	0.16
3	7.49	$\alpha$ -methyl- $\alpha$ [4-methyl-3pentrnyl]oxiranemethanol		0.16
4	7.86	1,6-Octadien-3-ol,3,7,dimethyl-	$\beta$ -Linalool	6.77
5	9.4	3-Cyclohexen-1-ol, 4-methyl-1-(methylethyl)-	<i>p</i> -Menth-1-en-4-ol	0.03
6	9.6	3,7-octadione-2,6-diol,2,6-dimethyl	1,5-Octadiene-3,7-diol,3,7-dimethyl-	1.72
7	13.51	2-propenoic acid,3 phenylmethylester	Methyl cinnamate	11.08
8	14.06	Bicyclo[7.2.0]undec-4-ene,4,11,11-trimethyl-8-methylene-[IR-(1R*,4Z,9S*)]	1.4,11,11-Trimethyl-8-methylenebicyclo[7.2.0]undec-4-ene	0.12
9	14.89	2-Propenic acid, 3-phenyl	Cinnamic acid	0.22
10	16.9	Caryophyllene oxide	$\beta$ -Caryophyllene oxide	0.61
11	21.85	Methylhexadec-9-enoate		5.58
12	22.2	Hexadecanoic acid, methylester	Palmitic acid, methyl ester	2.77
13	23.8	<i>Cis</i> -9 hexadecenoicacid	Palmitoleic acid	18.66
14	24.2	n-hexadecanoic acid	Palmitic acid	7.5
15	26	9-octadecenoicacid(Z)-methylester	Oleic acid, methyl ester	2.93
16	27.85-29.46	9,12-Octadecadienoic acid (Z, Z)-	Linoleic acid	1.78
17	29.36	Trans-13-Octadecenoic acid		36.08
18	29.63-36.25	Icosapent	$\omega$ -3 Marine Triglycerides	3.28
19	51.42	Isopulegol acetate	Isopulegyl acetate	0.37
20	57.67	$\beta$ -Amyrin	Olean-12-en-3-ol, (3 $\beta$ )-	0.14

Table 1: Phytoconstituent identified in the hexane fraction of *Zanthoxylum armatum* DC.

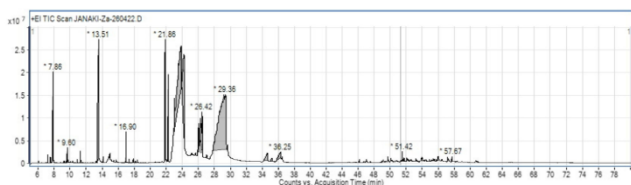


Fig 1 GC Chromatogram showing tR between 6.0 and 68 min

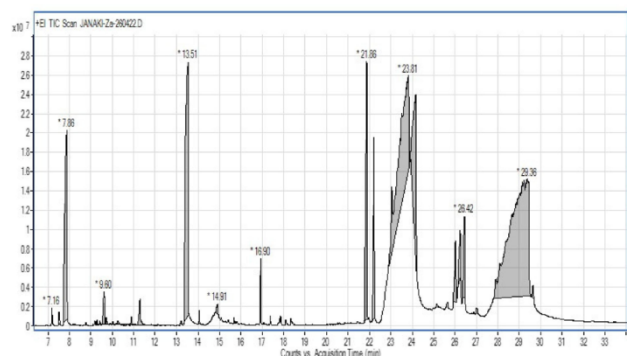
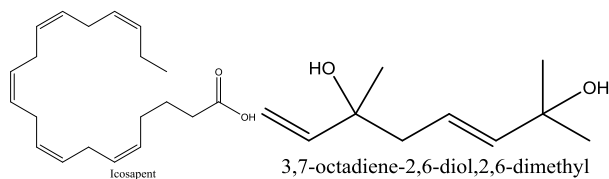
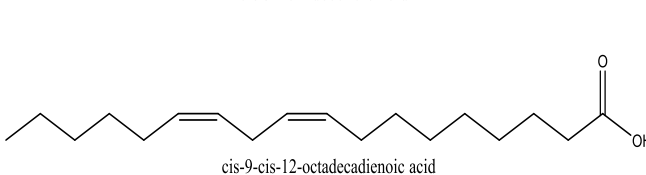
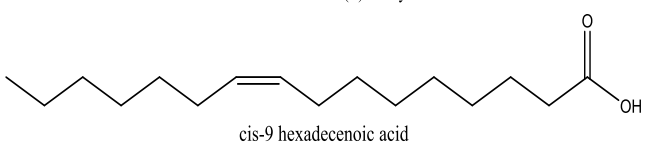
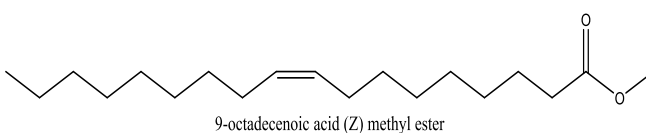
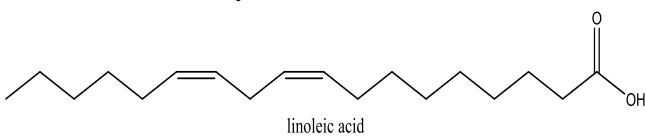
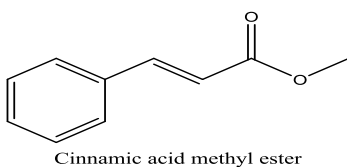
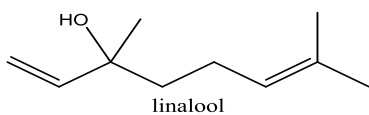


Fig 2 GC Chromatogram showing tR between 7.0 and 31 min

## II) Structures of major compounds

The structure of some compounds of hexane fraction *Zanthoxylum armatum* is presented below.



## III) Bioactive constituents

Among the twenty compounds identified from the hexane fraction, some compounds with remarkable activities reported are listed below. Compound linalool is one of the major constituents reported with diverse activities along with palmitic acid, cinnamic acid methyl ester, methyl oleate, trans-13 – octadecenoic acid, palmitoleic acid, and methyl palmitoleate. Studies show these compounds as anticancer, antibacterial, and anti-inflammatory along with diverse applications as mentioned in Table 2.

Table 2. Phytoconstituents with reported activities

Compound	Activities	Citation
Linalool	Anti-inflammatory,	[15]
	anticancer, anti	[16]
	hyperlipedemic,	[17]
	antimicrobial, antinoceptive,	
	analgesic, anxiolytic,	
	antidepressive,	
	neuroprotective,	
	anticonvulsant	
Palmitic acid	Anti-inflammatory	[18]
Cinnamic acid	Anticancer, Antibacterial,	[19]
methyl ester	Anti-fungal, Neurological	
	disorders	
Methyl oleate	Antifungal	[20]
Trans-13-	Human metabolite	
octadecenoic		
acid		
Palmitoleic acid	Anti-inflammatory	[21]

#### IV) Major compounds of hexane fraction of *Zanthoxylum armatum* DC

Predominant compounds with area percentages above 10% are presented in Table 3 below with their name/nature, molecular weight, molecular formula, and NIST matching as observed from GC-MS.

Table 3: List of major compounds from hexane fraction of *Zanthoxylum armatum* DC.

Peak no	Retention time	Area %	Compound name/nature	MF/Mwt	NIST matching
7	13.51	11.08	2-propenoic acid, 3-phenylmethyl ester (Methyl cinnamate)	C <sub>10</sub> H <sub>10</sub> O <sub>2</sub> 162	229225
13	23.81	18.66	Cis-9-hexadecenoic acid (Palmitoleic acid)	C <sub>16</sub> H <sub>30</sub> O <sub>2</sub> 254	333195
18	29.36	36.08	Trans-13-Octadecenoic acid	C <sub>18</sub> H <sub>34</sub> O <sub>2</sub> 282	333615

NB: MF: Molecular Formula, Mwt: Molecular weight

#### B) Biological Activities

##### I) MABA Bioassay

The preliminary screening of antibacterial assay of hexane fraction revealed good percentage inhibition against *S. aureus* (65.25%) and *B. subtilis* (67.27%) only but no activity against *Escherichia coli* ATCC 25922, *Pseudomonas aeruginosa* ATCC 10145, and *Salmonella typhi* ATCC 14028. The standard drug ofloxacin possesses 91.23%. The inhibition against particular bacteria could be related to the major constituents of hexane fraction possessing a hydrophobic nature which makes it easier during partition with the lipids in the cell membrane of bacteria thus making it more permeable by disrupting the cell membrane leading to changes in cytoplasm, and leakage of critical molecules eventually causing the death of the bacterial cells [23].

#### II) Insecticidal activity

The insecticidal activity was observed using the contact toxicity method in three types of insects namely *Tribolium castaneum*, *Sitophilus oryzae*, *Rhyzopertha dominica*. The hexane fraction used for the activity was 2038.20 µg/cm<sup>2</sup> whereas the standard insecticidal drug Permethrin used was 239.5 µg/cm<sup>2</sup>. Insecticidal activity revealed hexane fractions as highly active. The percentage mortality of these insects observed was 100% against *Rhyzopertha dominica* and moderately active against *Tribolium castaneum* at 60% and *Sitophilus oryzae* at 50%. The hexane fraction of *Zanthoxylum armatum* was active against *Tribolium castaneum* and *Sitophilus oryzae*. The highest activity, comparable to the standard drug, was found to be against *Rhyzopertha dominica*. Fig. 3 illustrates the efficacy of hexane fraction equivalent to the standard drug in the case of *Rhyzopertha dominica* along with other insects used during insecticidal activity by contact toxicity method.

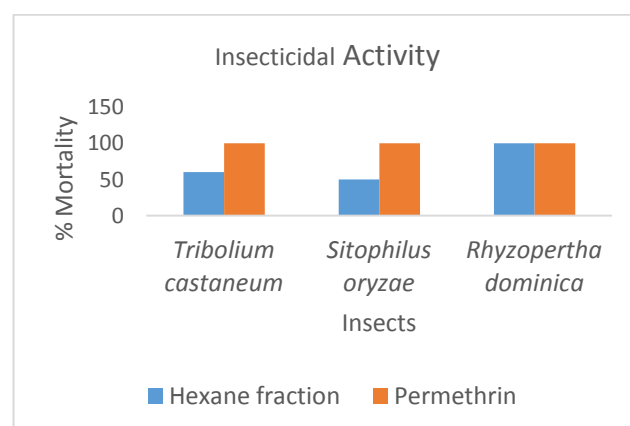


Fig: 3 Graphical representation of percentage mortality of various insects due to hexane fraction of *Z. armatum* and standard drug Permethrin

### III) Antifungal activity

*In vitro* antifungal bioassay was performed with a concentration of sample as 3000 µg/ml of DMSO with an incubation time of 7 days and temperature of 27 °C. Among seven different fungus; *Trichophyton rubrum*, *Candida albicans*, *Aspergillus niger*, *Microsporumcanis*, *Fusarium lini*, *Candida glabarata* and *Aspergillus fumigatus*. The hexane fraction was significant on only *Fusarium lini*. Hexane fraction of *Zanthoxylum armatum* showed highly significant activity against *F. lini* with linear growth of 15 mm and inhibition of 85%. Standard drug Miconazole possesses 73.25 µg/mL as its minimum inhibitory concentration. Particular antifungal properties of *F. lini* might be due to terpenes in this fraction [24].

### IV) Anti-inflammatory activity

Inflammation is a non-specific immune response that occurs after physical injury with primary symptoms as changes in blood flow, cellular metabolism, and related. This disorder in some conditions leads to chronic inflammatory disease [25] amplifying stress in chronic condition cases disturbing the quality and productivity of life with huge financial loss [26]. For the anti-inflammatory activity determination, 1 mg of hexane fraction was used with the standard Ibuprofen. The percentage inhibition of Ibuprofen at 25 µg/mL was (73.2± 1.4) % with the inhibitory capacity  $IC_{50}=11.2\pm 1.9\mu\text{g/mL}$ . Likewise, the hexane fraction at 10µg/ml concentration inhibited 79.4% revealing potency  $IC_{50} = 11.2\pm 1.9\mu\text{g/mL}$ . The potency of this fraction against reactive oxygen species (ROS) might be due to the well-known anti-inflammatory compounds such as terpenes and sesquiterpenes. Studies show the use of terpenes as a skin penetration booster medium in the case of various inflammatory diseases probably supports the potency of hexane

fraction [24]. Fig 4. Represents the anti-inflammatory activities of hexane fraction at various concentrations and standard drug ibuprofen used.

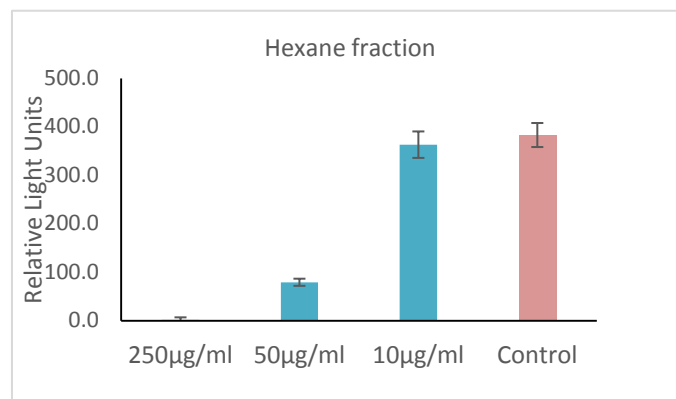


Fig: 4 ROS inhibition activity ( $IC_{50}$  value) of hexane fraction and standard drug ibuprofen

### Discussions

This investigation of non-polar constituents through GC-MS revealed the polyunsaturated fatty acids and their oxygenated derivatives and terpenes as the majority. GC-MS quantitatively identified 20 phytoconstituents some of which are potent bioactive. The major bioactive compounds identified were 2-propenoic acid, and 3-phenylmethyl ester consisting of 11.08 percent of the area. Similarly, Cis-9-Hexadecenoic acid (18.66 %), and trans-13-octadecenoic acid (36.08 %) were found as major constituents. Studies show the essential oil from the fruit pericarp of *Z. armatum* possesses remarkable antibacterial activities with the majority of constituents as linalool, methyl trans-cinnamate, and limonene as revealed through GC-MS [27]. These degradable, environmentally friendly, non-toxic bioactive compounds are responsible for insecticidal and antimicrobial characteristics overall possessing the qualities of bio-pesticides [28]. Studies also suggest flavonoids isolated from the plants such as tambulin and prudomestine possess remarkable anti-inflammatory properties and hence are suitable drug

candidates [29]. The present study revealed higher mortality of some insects by the n-hexane fraction of the plant may be due to the presence of the mono-terpenoids. The presence of various esters with a mixture of aromatic compounds is responsible for the strong odor of fruits. The potent bioactive properties of its volatile oil are also due to compounds like linalool, limonene, and lignin [27], [6]. Studies through GC-MS of hexane extract obtained through hot Soxhlet revealed 36 phytoconstituents in GC-MS with 2-hydroxy cyclopentadecanone as a major constituent [30]. Compounds like unsaturated fatty acids play an important role from an early stage of neurodevelopment [31], [32]. Polyunsaturated fatty acids due to their flexibility and conformational states are more significant than corresponding saturated fatty acids as the liver prefers to convert them to ketone bodies rather than to other atherogenic lipoproteins [33], [34]. Nutrition with polyunsaturated fatty acids has been employed to treat and fight against atherosclerosis as well as to inhibit thrombosis [35] thus dietary supplement of this highly valued *Zanthoxylum armatum* is quite relatable to the practical impacts. Together polyunsaturated fatty acids with hyperlipidemia and statin medication aid in lowering triglyceride levels [36]. Dietary saturated fatty acids influence inducing inflammation, in addition to their indirect role of raising low-density lipoprotein (LDL) cholesterol levels [37]. Such fatty acids affect the rate of LDL cholesterol synthesis and elimination besides preserving the steady state of LDL content of cholesterol in plasma. Hence dietary intake of polyunsaturated fatty acids obtained from plant *Zanthoxylum armatum* is of high importance in

improving lipid profile as the length of the fatty acid chains of their cis/trans isomers also has drastic variation in cholesterol metabolism [38]. Potent insecticidal activity against *Rhyzopertha dominica* revealed the possible use of a hexane fraction of *Z. armatum* as a potential bio-pesticide.

## Conclusions

The hexane fraction of *Zanthoxylum armatum* DC was found to be abundant in unsaturated fatty acids which may be beneficial for human health and can be developed as a biopesticide against *Rhyzopertha dominica*.

## Funding

Financial support in this research was done by University Grants Commissions (UGC), Nepal to Mrs. Janaki Baral through Ph. D. Fellowship and Research Support (Award No. PhD/074-075/S&T-6) and International Foundation of Sciences (IFS) Sweden for the grant (Grant name: I-1-F-6437-1).

## Acknowledgments

We would like to acknowledge Prof. Dr. Mohammad Iqbal Choudhary, Prof. Atia Tul Wahab, and Dr. Almas Jabeen of H. E.J Research Institute of Chemistry and Dr Panjwani Center for Molecular Medicine and Drug Research, International Center for Chemical and Biological Sciences, University of Karachi, Karachi, 75270, Pakistan for providing a laboratory for the research work.

## Conflict of Interest

The authors declare that there is no conflict of interest.

## References:

- [1] S. Walia, S. Shah, V. Tripathi, and K. K. Sharma, Phytochemical bio-pesticides, Some recent

- developments, *Phytochemistry Reviews*, 2017, 16, 989-1007.
- [2] O. Koul, S. Walia, and G. S. Dhaliwal, Essential Oils as Green Pesticides: Potential and Constraints, *Biopesticides International*, 2008, 4, 1, 63-84.
- [3] W. Boedeker, M. Watts, P. Clausing, and E. Marquez, The global distribution of acute unintentional pesticide poisoning: estimations based on a systematic review, *BMC public health*, 2020, 20, 1, 1–19.
- [4] G. M. Cragg, and D. J. Newman, Natural Product Drug Discovery in the Next Millennium, *Pharmaceutical biology*, 2001, 39, 1, 8–17.
- [5] W. H. Hertog, and K.F. Wiersum, Timur (*Zanthoxylum armatum*) Production in Nepal. *Mountain Research and Development*, 2000, 20, 2, 136–145.
- [6] T. P. Singh, and O. M. Singh. Phytochemical and pharmacological profile of *Zanthoxylum armatum* DC. an overview. *Indian Journal of Natural Products Resources*, 2011, 2, 3, 275–285.
- [7] R.N. Chopra, S. L. Nayar, and I. C. Chopra. Glossary of Indian Medicinal Plants, *The Quarterly Review of Biology*, 1958, 33, 2.
- [8] H. Karki, K. Upadhyay, H. Pal, and R. Singh. Antidiabetic potential of *Zanthoxylum armatum* bark extract on streptozotocin-induced diabetic rats. *International Journal of Green Pharmacy*, 2014, 8, 2.
- [9] N. Phuyal, P. K. Jha, P. P. Raturi and S. Rajbhandary, *Zanthoxylum armatum* DC.: Current knowledge, gaps and opportunities in Nepal, *Journal of Ethnopharmacology*. 2019, 229, 326–341.
- [10] J. S. Negi, V. K. Bisht, A. K. Bhandari, P. Singh, and R. C. Sundriyal. Chemical constituents and biological activities of the genus *Zanthoxylum*: A review. *African Journal of Pure and Applied Chemistry*, 2011, 5, 12, 412-6.
- [11] N. Phuyal, P. K. Jha, P. P. Raturi, and S. Rajbhandary. Total phenolic, flavonoid contents, and antioxidant activities of fruit, seed, and bark extracts of *Zanthoxylum armatum* DC, *The Scientific World Journal*, 2020, 2020.
- [12] S. E. Stephen, *NIST Standard reference database 1A*. Standard Reference Data, NIST, Gaithersburg, MD, USA, 2014, 1-72.
- [13] S. L. Helfand, J. E. Werkmeister, and J. C. Roder. Chemiluminescence response of human natural killer cells: I. the relationship between target cell binding, chemiluminescence, and cytolysis, *The Journal of experimental medicine*, 1982, 156, 2, 492–505.
- [14] M. M. Koek, R. H. Jellema, J. van der Greef, A. C. Tas, and T. Hankemeier, Quantitative metabolomics based on gas chromatography mass spectrometry: Status and perspectives. *Metabolomics*, 2011, 7, 307–328.
- [15] I. Pereira, P. Severino, A. C. Santos, A. M. Silva, and E. B. Souto, Linalool Bioactive Properties and

- Potential Applicability in Drug Delivery Systems. *Colloids Surfaces B: Biointerfaces*, 2018, 171, 566–578.
- [16] A. T. Peana, P. S. D'Aquila, F. Panin, G. Serra, P. Pippia, and M. D. Moretti, Anti-inflammatory activity of linalool and linalyl acetate constituents of essential oils. *Phytomedicine*, 2002, 9, 8, 721–726.
- [17] E. Elisabetsky, Traditional medicines and the new paradigm of psychotropic drug action. *In Advances in Phytomedicine*, 2002, 1, 133-144.
- [18] V. Aparna, K. V. Dileep, P. K. Mandal, P. Karthe, C. Sadasivan, and M. Haridas, Anti-Inflammatory property of n-hexadecanoic acid: structural evidence and kinetic assessment, *Chemical Biology & Drug Design*, 2012, 80, 434–439.
- [19] N. Ruwizhi, and B. A. deribigbe, Cinnamic acid derivatives and their biological efficacy. *International Journal of Molecular Sciences*, 2020, 21, 16, 5712.
- [20] L. A. Lima, S. Johann, P. S. Cisalpino, L. P. Pimenta, and M. A. Boaventura, *In vitro* antifungal activity of fatty acid methyl esters of the seeds of *Annona cornifolia* A.St.-Hil. (Annonaceae) against pathogenic fungus *Paracoccidioides brasiliensis*. *Revista da Sociedade Brasileira de Medicina Tropical*, 2011, 44, 777–780.
- [21] A. M. Astudillo, C. Meana, C. Guijas, L. Pereira, P. Lebrero, M. A. Balboa, and J. Balsinde Occurrence and biological activity of palmitoleic acid isomers in phagocytic cells. *Journal of Lipid Research*, 2018, 59, 2, 237–249.
- [22] Abcam, Chemical. Product datasheet trans-9-Methyl hexadecenoate, Monounsaturated fatty acid methyl ester. 2024. ab143885, 1–2.
- [23] S. Chouhan, K. Sharma and S. Guleria, Antimicrobial activity of some essential oils- present status and future perspectives. *Medicines*, 2017, 4, 3, 58.
- [24] R. Paduch, M. K. Szerszeń, M. Trytek and J. Fiedurek, Terpenes: substances useful in human healthcare. *Archivum Immunologiae Therapiae Experimentalis*. 2007, 55, 315–327.
- [25] L. Ferrero-Miliani, O. H. Nielsen, P. S. Andersen and S. Girardin, Chronic inflammation: importance of NOD2 and NALP3 in interleukin-1 $\beta$  generation. *Clinical & Experimental Immunology*, 2007, 147, 2, 227–235.
- [26] R. da Silveira, L. N. Andrade, and D. P. Sousa, A review on anti-inflammatory activity of monoterpenes. *Molecules*, 2013, 18, 1, 1227–1254.
- [27] J. Baral, P. Satyal and A. Adhikari, Spatial variation in constituents of essential oils from fruit pericarp of *Zanthoxylum armatum* DC of Nepali origin and their antibacterial activity. *Journal of Essential Oil Bearing Plants*, 2024, 27.
- [28] A. Nefzi and R. A. Abdallah, Antifungal activity of aqueous and organic extracts from *Withania somnifera* L. against *Fusarium oxysporum* f. sp. *Radicis-lycopersici*. *Journal of Microbial & Biochemical*

*Technology*, 2016, 8, 3.

- [29] J. Baral, D. Shrestha, H. P. Devkota and A. Adhikari, Potent ROS inhibitors from *Zanthoxylum armatum* DC of Nepali origin, *Natural Product Research*, 2023, 1–9.
- [30] H. P. Kayat, S. D. Gautam and R. N. Jha, GC-MS analysis of hexane extract of *Zanthoxylum armatum* DC. fruits, *Journal of Pharmacognosy Phytochemistry*, 2016, 5, 2, 58–62.
- [31] U. N. Das, Essential fatty acids- A Review. *Current Pharmaceutical Biotechnology*. 2006, 7, 467–482.
- [32] T. Decsi, G. Boehm, H. M. Tjoonk, S. Molnar, D. A. Dijck- Brouwer, M. Hadders-Algra, I. A. Martini, F. A. Muskiet, and E. R. Boersma, Trans isomeric octadecenoic acids are related inversely to arachidonic acid and DHA and positively related to mead acid in umbilical vessel wall lipids. *Lipids*, 2002, 37, 959-965.
- [33] A. C. Beynen and M. B. Katan, Why do polyunsaturated fatty acids lower serum cholesterol? The *American Journal of Clinical Nutrition*, 1985, 42, 3, 560–563.
- [34] S. R. Wassall, and W. Stillwell, Polyunsaturated fatty acid – cholesterol interactions: domain formation in membranes. *Biochimica et Biophysica Acta (BBA)-Biomembranes*, 2009, 1788, 1, 24–32.
- [35] S. H. Goodnight, W. S. Harris, W. E. Connor, and D. R. Illingworth. Polyunsaturated fatty acids , hyperlipidemia , and thrombosis. *Arteriosclerosis. An official Journal of the American Heart Association, Inc.* 1982, 2, 2, 87–113.
- [36] G. Zuliani, M. Galvani, E. Leitersdorf, S. Volpato, M. Cavalieri and R. Fellin. The role of polyunsaturated fatty acids (PUFA) in the treatment of dyslipidemias. *Current Pharmaceutical Design*. 2009, 15, 36, 4087–4093.
- [37] R. Poledne, A new atherogenic effect of saturated fatty acids. *Physiological Research*. 2013, 62 ,139–143.
- [38] L. A. Woollett and J. M. Dietschy, Effect of long-chain fatty acids on low-density-lipoprotein- cholesterol metabolism. *American journal of clinical nutrition*, 1994. 60, 6, 991S - 996S.

# Spatial variation in constituents of essential oils from fruit pericarp of *Zanthoxylum armatum* DC of Nepali origin and their antibacterial activity

Janaki Baral, Prabodh Satyal & Achyut Adhikari

To cite this article: Janaki Baral, Prabodh Satyal & Achyut Adhikari (04 Jan 2024): Spatial variation in constituents of essential oils from fruit pericarp of *Zanthoxylum armatum* DC of Nepali origin and their antibacterial activity, Journal of Essential Oil Bearing Plants, DOI: [10.1080/0972060X.2023.2296549](https://doi.org/10.1080/0972060X.2023.2296549)

To link to this article: <https://doi.org/10.1080/0972060X.2023.2296549>



Published online: 04 Jan 2024.



Submit your article to this journal [↗](#)



View related articles [↗](#)



View Crossmark data [↗](#)

---

## Spatial variation in constituents of essential oils from fruit pericarp of *Zanthoxylum armatum* DC of Nepali origin and their antibacterial activity

Janaki Baral<sup>1,2</sup>, Prabodh Satyal<sup>3</sup> and Achyut Adhikari<sup>2\*</sup>

<sup>1</sup> Department of Chemistry, Tri-Chandra Multiple Campus, Tribhuvan University, Kathmandu, Nepal

<sup>2</sup> Central Department of Chemistry, Tribhuvan University, Kathmandu, Nepal

<sup>3</sup> Aromatic Plant Research Center, Lehi, UT 84043, United States

### \*Corresponding Author

Achyut Adhikari  
achyutraj05@gmail.com

**Received** 16 June 2023

**Revised** 11 December 2023

**Accepted** 11 December 2023

### Abstract

The fruit pericarp of *Zanthoxylum armatum* DC is used in spices and to manage different diseases like toothaches, inflamed gums, arthritis, swollen joints, insect bites, diarrhea, common flu, and respiratory difficulties by local people. In this study, the essential oil was extracted from the fruit pericarp of *Z. armatum* DC collected from different commercial sites in Nepal using the hydro-distillation method. The chiral gas chromatography-mass spectrometry (GC/MS) was used to identify the chemical compounds present in the essential oil with their stereochemistry. Major constituents identified in all samples included linalool, limonene, and methyl trans-cinnamate. Linalool, a monoterpene alcohol, exhibited the highest percentages in all three samples, recording 58.31%, 58.45%, and 80.37% in Salyan, Surkhet, and Myagdi respectively. Notably, twenty-five enantiomeric components were identified using chiral GC/MS among its sixty constituents. The enantiomeric component distribution of linalool and limonene was in their (+) dextrorotatory form, while others were dominant in the levorotatory form. This research underscores that *Z. armatum* from the Myagdi district of Nepal, is a prominent source of the medicinally and industrially important compound linalool, along with exhibiting higher antimicrobial activity. To the best of our knowledge, this represents the first report of a chiral GC/MS study conducted on this plant.

### Keywords

Antimicrobial activity, Chiral GC/MS, Essential oil, Linalool, *Zanthoxylum armatum* DC

## INTRODUCTION

*Zanthoxylum armatum* DC Synonym *Zanthoxylum alatum* Roxb<sup>1</sup> is an economically valuable plant of the Rutaceae family commonly called ‘Timur’ in Nepal. In Nepal, it is distributed from east to west at an altitude range of 1000-2500 m while in other countries such as India, Bhutan, Taiwan, Malaysia, China, the Philippines, and Japan it is found at 1300-1500 m above sea level<sup>3</sup>. For centuries, locals have used it as a spice and condiment, as well as in cooking. Besides it is used in the treatment of various ailments due to promising properties like toothache, anthelmintic, stomachic, and carminative<sup>4,5</sup>. Whole parts of the plants such as leaves, bark, fruit, and seed are used due to

their beneficial properties as hepatoprotective, cytotoxic, antioxidant, anti-inflammatory, dental pain, scabies and insect repellents<sup>6</sup>. Such diverse bioactive properties can be collectively attributed to the presence of various phytochemicals, including potent flavonoids<sup>7</sup>, alkaloids, sterols, phenolics, lignins, coumarins, terpenoids, glycosides, benzenoids fatty acids, alkanolic acids, and amino acids<sup>8</sup>. Tambulin from this plant acts as an insulin secretagogue<sup>9</sup> and active vasorelaxant<sup>10</sup>. With potent analgesic, antipyretic, and anti-inflammatory activities demonstrated in many *in vivo* and *in vitro* experiments, this plant is also used in the treatment of various illnesses, and disorders such as fever, pain, and inflammation<sup>11</sup>. Alkaloids from this plant possess

anti-plasmodial, antiviral, anti-helminthic, larvicidal, and anti-proliferative properties<sup>4</sup>. The methanolic extract of the plant, which contains crude saponins from the fruit, bark, and leaves possesses potent anticancer properties against human breast and colorectal cell lines<sup>12</sup>. The promising nature of the whole plant beneficially supports preliminary therapeutics in areas lacking easy access to medicine. Nature has been a boon to humankind for ages through its plethora of floral kingdoms storing mysterious medicinal properties that are explored at different times<sup>13</sup>. *Z. armatum* is one of such magical spices of medicinal importance that needs to be explored. Being an economically promising plant, its fruits and essential oils are exported by locals<sup>14</sup>. Studies on its constituents during harvesting season and topographic variation could result in different bioactivities.

Essential oils are the secondary metabolites produced by aromatic plants characterized by a mixture of natural substances volatile in nature that produce a strong odor<sup>15</sup>. Oil from aromatic plants vaporizes quickly on heating without any stain in filter paper unlike that of fixed oil that remains longer<sup>16</sup>. Aromatherapy of the volatile constituent in an essential oil employing inhalation helps to prevent and cure diseases<sup>17</sup>. The synergetic effect of various terpenes is responsible for exhibiting such therapeutic value<sup>18</sup>. Some remarkable constituents of the essential oil, such as linalool and its acetate, are potent anti-inflammatory agents<sup>19</sup>. Linalool alone possesses remarkable properties such as antimicrobial, anticancer, and antioxidant. It is also an eco-friendly pesticide besides being a fragrance creator<sup>20</sup>. Wider application of essential oil is as a food preservative<sup>21,22</sup>, flavoring<sup>23</sup>, and in cancer prevention<sup>24</sup>. Among 3000 essential oils reported 300 of them are industrially demanding. On an industrial scale, essential oil and their constituents hold good commercial space in perfumes and cosmetics, in preparing sanitary items, in dentistry, in preserving food, in agriculture, and many more<sup>23</sup>. Monoterpenes and sesquiterpenes are well-known anti-inflammatory compounds and are hence used as skin penetration booster

mediums in different inflammatory diseases<sup>25</sup>. The gas chromatography coupled with mass spectrometry explores probable bioactive constituents in medicinal plants<sup>26</sup>. Chirality in GC-MS plays a crucial role in aroma chemicals because two enantiomers of the same compound can have distinct sensory characteristics<sup>21</sup>. Many authors have reported the GC-MS analysis of the essential oils of *Z. armatum*, but analysis of the enantiomeric distribution of compounds using chiral GC-MS is still lacking. This research aims to reveal the enantiomeric distribution of the constituents of the essential oil of fruits of *Z. armatum* from the high altitude of Nepal like Salyan (ZaS), Surkhet (ZaSU) and Myagdi (ZaM) and their antibacterial properties.

## **MATERIALS AND METHODS**

### **Collection of fruits and extraction of essential oil**

The matured fruits of *Zanthoxylum armatum* DC were collected from the major commercial sites of Nepal, with the help of Botanist Dr. Baburam Nepali. A voucher specimen (TUCH: 201016) was deposited after authentication of the herbarium at the Tribhuvan University Central Herbarium, Kritipur. Quantitatively, 250 g of fruit pericarp from each site was used for oil extraction. The hydro-distillation procedure of the extraction of essential oils was done in a Clevenger apparatus for three hours.

### **Gas chromatography-flame ionization detection (GC-FID)**

Thus, obtained essential oils of the fruits of *Zanthoxylum armatum* were analyzed through Gas chromatography-flame ionization detection with the previously reported method<sup>27</sup>. Operating condition for GC-MS used Shimadzu GC 2010 with flame ionization detector and column ZB-5GC. Raw peak areas were used for the determination of percentage composition without standardization.

### **Chiral gas chromatography-mass spectrometry (GC-MS)**

Determination of chiral GC-MS was conducted to analyze the essential oil obtained from fruit pericarp of *Z. armatum*. The instrument used for

this analysis was a Shimadzu GCMS-QP2010S, operating in the electron impact (EI) mode with an electron energy of 70 eV. The scan range was set between 40 to 400 amu, with a scan rate of 3.0 scans per second.

The GC was equipped with a Restek B-Dex 325 capillary column, which had dimension of 30 meters in length, 0.25 mm internal diameter, and a 0.25  $\mu\text{m}$  film thickness. The temperature in the oven was programmed to start at 50°C that gradually increased to 120°C at a rate of 1.5°C per minute, followed by an increase to 200°C at 2°C per minute. It was maintained at 200°C for 5 minutes. Helium gas with a flow rate of 1.8 ml per minute was a carrier. Samples were diluted in dichloromethane in 3% w/v concentration which was injected 0.1  $\mu\text{L}$  in a split mode at a split ratio of 1:45. The enantiomers of monoterpene were identified by comparing their retention times with authentic samples acquired from Sigma-Aldrich in Milwaukee, WI, USA. The relative percentages of enantiomers were determined based on the areas of the chromatographic peaks.

#### Antimicrobial activity and microorganisms

Antibacterial activities were conducted using bacteria obtained from the American Type Culture Collection (ATCC). The bacterial cultures underwent sub-culturing and preservation in Muller Hinton Agar (MHA) media, maintained at a temperature of 4°C. The detailed list of the microorganisms employed in the experiment is presented in Table 1<sup>28</sup>.

#### Agar well diffusion assay

The agar well diffusion method was adopted to observe the antibacterial properties with slight modifications<sup>26</sup>. The bacteria used in the experiment were cultured in Muller Hinton Broth until their turbidity reached a level equivalent to 0.5 McFarland's standard, which corresponds

to a concentration of  $1.5 \times 10^8$  CFU/mL. Each sterile cork borer was used to create wells with a diameter of 6 mm. These wells were then loaded with 10  $\mu\text{L}$  of sample prepared in (1:1) DMSO, positive control ciprofloxacin (5  $\mu\text{g}$ ), and negative control DMSO and incubated for 24 hours at 37°C. The Zone of inhibition (ZOI) was measured in mm.

## RESULTS

### Essential oil yield

The essential oil thus obtained from the Clevenger apparatus was dried over sodium sulfate and their yield was recorded. Fruit of *Z. armatum* DC from various sites yields different quantities of essential oil ranging from 3.4 to 4%. The dry fruit mass was taken for extraction and the yield of these oils is presented in Table 2.

### Compositions

The GC-MS of *Z. armatum* Salyan origin (ZaS), *Z. armatum* of Surkhet (ZaSU), and *Z. armatum* of Myagdi (ZaM) all revealed 60 different constituents at various retention times. Composition-wise, the GC-MS of the essential oil from the fruits of *Z. armatum* revealed a predominant constituent of linalool; 58.32%, 58.45%, and 80.37% in ZaS, ZaSU, and ZaM respectively. Limonene consists of 16.67%, 11.2%, and 3.65% in ZaS, ZaSU, and ZaM respectively. A quantitatively remarkable difference was observed with oil from ZaM. *trans*-Methyl cinnamate occupies 8.22%, 14.61%, and 9.55% at ZaS, ZaSU, and ZaM respectively. A quantitatively higher amount was observed in ZaSU. Additionally, the content of  $\beta$ -phellenderene was found to be more consistent at 1.71%, 1.91%, and 1.23 % respectively. *Cis* and *trans* linalool oxide are relatively lower in the case of ZaM with only 0.5% whereas both these constituents are >1% in both ZaS and ZaSU

**Table 1.** The microorganisms employed for antimicrobial activities in the experiment

Bacteria	Gram Staining	ATCC Number
<i>Escherichia coli</i>	Gram-negative	25922
<i>Klebsiella pneumoniae</i>	Gram-negative	700603
<i>Staphylococcus aureus</i>	Gram-positive	25293

**Table 2.** Essential oil yields after hydro-distillation

Site of Collection	Dry fruit mass	Essential oil colour	Percent yield (v/w)
Salyan	250gm	Transparent	3.5
Surkhet	250gm	Transparent	3.4
Myagdi	250gm	Transparent	4

ZaS, ZaSU, and ZaM all were collected at the same period from their site of collection

respectively. The chemical compositions of the constituents are depicted in a compiled form in Table 3 with their Kovats index experimental ( $KI_{exp}$ ) and Kovats index based on literature ( $KI_{Lit}$ )<sup>29</sup>.

### Structures of major compounds

Structures of a few significant compounds present in the essential oil of *Z. armatum*, as observed in the GC-MS profile, are presented in Fig. 1.

### Monoterpenoid enantiomeric distribution

Among 25 chiral compounds identified, the chiral GC/MS revealed 13 compounds with their enantiomeric distribution as depicted in Table 4. Linalool in its d (+) form is the dominant constituent of essential oil from all three sites. Similar to limonene, (-)- $\beta$ -phellandrene and all other enantiomeric components were dominant in levorotatory forms in all the samples.

### Enantiomeric distribution

The (+)linalool seems to be the predominant constituent in all the samples along with limonene, in their dextrorotatory form. Enantiomeric distribution of the trace elements present as  $\alpha$ -thujene,  $\alpha$ -pinene,  $\beta$ -pinene, and sabinene revealed more of their distribution in the levorotatory ones. Among all the thirteen constituents in their various enantiomeric distributions,  $\beta$ -caryophyllene is the only constituent that is present in the levorotatory form with no dextrorotatory component.

### Elements detection

The elements detected in *Z. armatum* oil (EDX-8000) quantitatively revealed the presence of S (0.438%) and Cu (0.003%) only, with abundant hydrocarbons (99.559%). The presence of sulphur

in a mixture of volatile-natured compounds imparts its characteristic pungent order<sup>30</sup> in addition to dominant olfactory receptors<sup>31</sup>, ethyl *cis*-cinnamate, and methyl *trans*-cinnamate. The dominance of methyl *trans*-cinnamate possessing characteristic flavour imparts tartness in spices and condiments for pickles and vegetables.

### Antibacterial activity

The essential oil obtained from the fruit of *Z. armatum* was moderately active against the bacteria tested compared to ciprofloxacin. Fig. 2 shows the potency of antibacterial activity of the samples against the test organisms studied. All the experiments were done in triplicates and the results are expressed in mean $\pm$ SD mm. The highest zone of inhibition (ZOI) against *Escherichia coli* (22.1 $\pm$ 0.1 mm) was observed from the essential oils extracted from *Z. armatum* seeds of Myagdi (ZaM) and moderate in *Klebsiella pneumoniae* (19.37 $\pm$ 0.15 mm) while no activity was observed against the gram-positive test organism *Staphylococcus aureus* used. Likewise the activity of essential oil obtained from the fruit pericarp of salyan reflected its ZOI at 14.1 $\pm$ 0.1 mm against *E. coli* and 12.13 $\pm$ 0.15 mm against *K. pneumoniae* whereas essential oil based from Surkhet possessed its antibacterial activity against *E. coli* at 13.2 $\pm$ 0.1 mm and 13.10 $\pm$ 0.10 mm against *K. pneumoniae*. *Z. armatum* essential oils possess remarkable ZOI against gram-negative bacteria than the positive ones. Present research contradicts previous ones which reported an impact on gram-positive ones<sup>22</sup>. Due to these peculiar antimicrobial activities, indigenous people often use it for brushing teeth, toothaches, inflamed gums, wounds, and cuts as a natural healing herb.

**Table 3.** Chemical profiling of the constituents of the essential oil (% area) from the fruit pericarp of *Z. armatum* from different commercial sites in Nepal with actual and literature based KI values

Compound	ZaS	ZaSU	ZaM	KI <sub>exp</sub>	KI <sub>Lit</sub>
Styrene	0.01	-	-	890	-
$\alpha$ -Thujene	0.12	0.11	0.05	923	930
$\alpha$ -Pinene	0.2	0.18	0.04	931	939
Benzaldehyde	0.16	0.18	0.03	958	960
Sabinene	0.99	1.04	0.53	970	975
$\beta$ -Pinene	0.19	0.17	0.04	975	979
6-Methyl-5-hepten-2-one	-	-	0.01	-	-
Myrcene	1.53	1.64	0.51	987	990
$\delta$ -2-Carene	0.05	0.04	-	998	1002
para-Mentha-1(7),8-diene	0.03	-	-	1003	1004
para-Cymene	0.73	0.74	0.17	1023	1024
Limonene	16.67	11.2	3.65	1029	1029
$\beta$ -Phellandrene	1.71	1.91	1.23	1030	1029
<i>cis</i> -Linalool oxide (furanoid)	1.66	1.37	0.5	1069	1072
<i>trans</i> -Linalool oxide (furanoid)	1.42	1.16	0.5	1085	1086
Perillene	0.03	-	-	1097	1103
Linalool	58.31	58.45	80.37	1106	1096
Hotrienol	0.01	-	-	1107	993
Linalool derivative	0.12	0.1	-	1112	-
endo-Fenchol	0.05	0.04	-	1115	1116
<i>trans</i> -para-Mentha-2,8-dien-1-ol	0.09	0.06	0.01	1122	983
<i>cis</i> -para-Menth-2-en-1-ol	0.21	0.04	0.04	1124	1118
<i>cis</i> -Limonene oxide	0.09	0.07	-	1132	1136
<i>cis</i> -para-Mentha-2,8-dien-1-ol	0.12	0.1	-	1136	1137
<i>trans</i> -para-Menth-2-en-1-ol	0.15	0.14	0.04	1141	1140
Citronellal	-	-	0.03	-	1140
Lavandulol	0.02	-	-	1161	1169
Unidentified	0.03	-	-	1172	-
<i>trans</i> -Isocitral	0.11	0.15	-	1175	1180
para-1,8-Menthadien-4-ol	0.09	0.04	-	1177	-
Terpinen-4-ol	1.34	1.09	0.25	1179	1177
Cryptone	1.4	1.05	0.36	1185	1185
3- <i>cis</i> -Hexenyl butyrate	0.45	0.38	0.1	1188	1146
$\alpha$ -Terpineol	0.44	0.38	0.18	1194	1188
Methyl chavicol	0.1	0.08	0.03	1196	1196
Dihydrocarveol	0.05	-	-	1198	1194
Unidentified	0.07	0.06	-	1220	-
Cumin aldehyde	0.15	0.11	0.03	1240	1241
Carvone	0.19	0.11	0.02	1242	1263

**Table 3 cont.**

Compound	ZaS	ZaSU	ZaM	KI <sub>exp</sub>	KI <sub>Lit</sub>
Linalyl acetate	0.04	0.04	0.01	1248	-
Piperitone	0.33	-	0.17	1251	1252
Methyl citronellate	0.03	0.02	0.01	1256	1261
Phellandral	0.32	0.18	0.04	1275	-
$\alpha$ -Terpinen-7-al	0.04	0.03	0.01	1284	1285
<i>neo</i> -Dihydrocarveol acetate	0.06	0.04	-	1304	1307
Limonene hydroperoxide	0.06	0.04	-	1317	-
Hydroxycryptone	0.03	0.05	0.01	1320	1315
Oxo-para-menth-1-en-7-al	0.07	0.07	-	1336	-
Unidentified	0.06	0.05	-	1340	-
Terpenediol	0.47	0.53	0.23	1357	-
Limonene hydroperoxide	0.04	0.04	-	1376	-
Methyl <i>trans</i> -cinnamate	8.22	14.61	9.55	1385	1378
Unidentified	0.03	-	-	1389	-
Unidentified	0.03	-	-	1406	-
$\beta$ -Caryophyllene	0.06	0.05	0.14	1416	-
Unidentified	0.17	0.15	0.02	1443	-
Unidentified	0.25	0.17	0.2	1447	-
Caryophyllene oxide	0.2	0.18	0.12	1578	-
Humulene epoxide II	-	-	0.01	-	-
$\gamma$ -Cadinene	-	-	0.01	-	-
$\alpha$ -Muurolol	-	-	0.01	-	-
Methyl palmitoleate	0.14	0.22	0.12	1899	-
Methyl palmitate		0.06	0.03	-	-
Cyclhexadecanolide	-	-	0.06	-	-
Unidentified	0.09	0.09	0.03	2039	-
Unidentified	0.06	0.04	0.01	2148	-
<i>cis</i> -9-Tricosene	0.08	0.05	-	2270	-

KI<sub>exp</sub> represents experimental Kovats Index value based on chemical profiling of *Z. armatum* essential oil from various sites and KI<sub>Lit</sub> represents Kovats Index based on literature

## DISCUSSION

The components of the essential oil of *Z. armatum* from various sites as shown in Table 3 reflected the same qualitative content with slight differences in quantity and d (+) linalool being one of the abundant compounds in all samples. The essential oil yield from *Z. armatum* fruit was reported to reach up to 6% in some cases, with an average of 4-5%<sup>14</sup> while we observed 3.4-4% variation in yield. Many farmers in Myagdi

district sustain their livelihood economically with this plant as it is one of the major cash crop<sup>32</sup>. Nationally 90% of its essential oil is exported while only 10% holds the local market<sup>6</sup>. Our study reveal *Z. armatum* from Myagdi recorded its highest content of linalool (80.37%) breaking its previous record (74.12%)<sup>33</sup>. Constituent-wise such variation is observed depending upon the part of the plant and its topography. Previous research explored essential oil from the bark of *Z.*

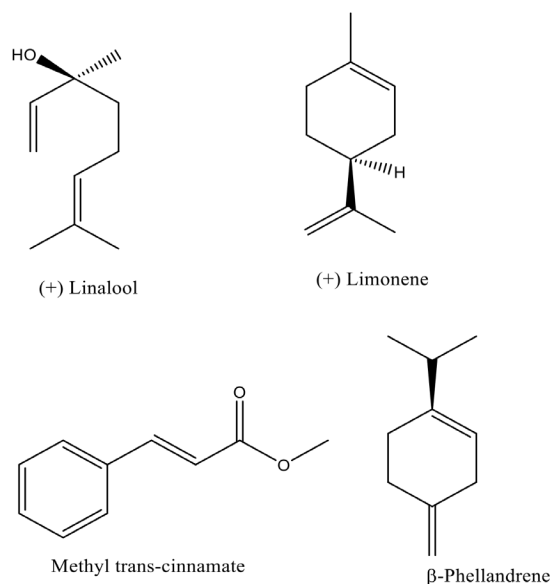


**Figure 1.** Structure of major compounds present in the essential oil of *Z. armatum*

*armatum* with  $\alpha$ -pinene in dominance<sup>34</sup>. Present study reveals the enantiomeric composition of chiral components of (-) nature with an almost racemic distribution of limonene whereas the essential oil of *Z. armatum* from Pakistan<sup>35</sup> did not possess limonene. Biologically potent activities of this oil constituent in synergy possess larvicidal activity against mosquito vectors<sup>36</sup>

whereas antibacterial potency and reduction of plasma triglyceride<sup>37</sup> of the oils of *Z. armatum* is particularly associated with the (+)linalool<sup>20</sup>. Topological variation in the oil constituent of its fruit is observed with an abundance of 3-borneol and iso bornyl acetate but not limonene<sup>34</sup> in plants of Pakistan origin whereas leaves extracted essential oil of *Z. armatum* belonging to India possess bornyl acetate abundantly with fewer percentages of limonene and linalool<sup>38</sup> likewise major constituents of its bark reveal  $\alpha$ -pinene and 2-undecanone<sup>34</sup>. The nature of constituent variation and the length of the fatty acid chain are detrimental to the biological properties. The olfactory response associated with *cis* and *trans* isomers of some constituents also possesses drastic variation in cholesterol metabolism<sup>39</sup>. Similarly, biologically potent activities of the essential oil reported in this plant are significant anti-inflammatory, analgesic<sup>40</sup> and antifungal<sup>41</sup> which is mainly due to its major volatile nature of constituents such as linalool and limonene. Essential oils particularly from plants of the Rutaceae family are claimed to possess qualitative improvement in lipid profile. Despite all remarkable studies few notable undesirable consequences of the essential oil of *Z. armatum* were observed as it raised the level

**Table 4.** Compounds with enantiomeric distribution [%(+):%(-)] in essential oil of *Zanthoxylum armatum*

Compounds	ZaS	ZaSU	ZaM
$\alpha$ -Thujene	5.38:94.62	7.13:92.87	4.87:95.13
$\alpha$ -Pinene	13.64:86.36	13.74:86.26	21.01:78.99
Sabinene	7.73:92.27	7.73:92.27	8.68:91.32
$\beta$ -Pinene	7.63:92.37	6.69:93.31	9.15:90.85
Limonene	56.62:43.38	54.92:45.08	56.74:43.26
$\beta$ -Phellandrene	0.29:99.71	0.31:99.69	0.2:99.8
<i>cis</i> -Linalool oxide	19.79:80.21	16.09:83.91	21.11:78.89
<i>trans</i> -Linalool oxide	9.34:90.66	10.14:89.86	7.88:92.12
Linalool	92.59:7.41	93.11:6.89	93.13:6.87
Terpinen-4-ol	27.13:72.87	28.16:71.84	28.08:71.92
$\alpha$ -Terpineol	41.96:58.04	40.87: 59.13	41.54:58.46
Piperitone	21.81:78.19	21.5:78.5	18.9:81.1
$\beta$ -Caryophyllene	0:100	0:100	0:100

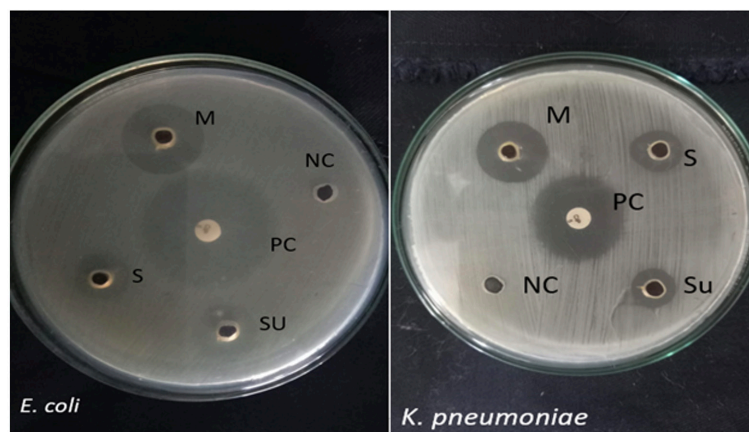


**Figure 2.** Antibacterial activity of Essential oil of *Zanthoxylum armatum* from three different sites. PC=positive control, NC=Negative control, Activity of EO. of *Z. armatum* fruits from M=Myagdi, S=Salyan, SU=Surkhet

of urea in animal models<sup>42</sup> similar to essential oil of *M. longifolia* which are toxic<sup>43</sup> in nature. Outweighing all the odds the uses of *Z. armatum* essential oil in asthma by the indigenous people is in accordance with broncho-relaxing and anti-asthmatic properties<sup>44</sup>. Value of essential oil can be maintained by appropriate monitoring techniques that can minimize the chances of commercial adulteration hence preserving qualitative properties<sup>45</sup>. Collectively, the wide-ranging properties of plants that possess essential oils outweigh their limitations. Therefore, continuous research to explore their potential from a broader perspective is a current necessity. This can add value to existing knowledge, belief, and indigenous practices. Since nature-based medications are associated with positive healing psychology, they are cost-effective and accessible to many people.

## CONCLUSIONS

Thus this study revealed variations of essential oil of *Z. armatum* from different topologies based on GC-MS and their enantiomeric composition. The essential oil extracted from the fruit pericarp of Myagdi was quantitatively higher. All oil consists of 60 different constituents from GC-MS and 13 form of various enantiomeric distribution. (+)Linalool and limonene were remarkably dominant in their dextrorotatory form. Antimicrobial activities of these essential

oils showed that oil extracted from fruit pericarp of Myagdi origin possesses potent activities. Since the dominance of a particular compound largely determines the bioactivity of the sample this could be attributed to a higher percentage of linalool comparatively. Likewise, the chiral GC-MS of these essential oils also revealed d(+) linalool in dominance.

## ACKNOWLEDGMENTS

The authors would like to acknowledge Mr. Tanner Beck and Mr. Sawyer Ashcroft for editing the English language of the manuscript. The authors are equally grateful to the University Grants Commissions, Nepal for the fellowship and research support of Mrs. Janaki Baral (Award No. PhD/074-075/S&T-6) and International Foundation of Sciences (IFS) Sweden for the grant (Grant name: I-1-F-6437-1).

## DECLARATION OF CONFLICTING INTERESTS

The authors declare no conflict of interest.

## REFERENCES

1. **Gabriele, G. and Enrico, B. (2012).** Notulae ad Plantas Advenas Longobardiae Spectantes : Page Botanique. 3: 141-208.
2. **Hertog, W.H. and Wiersum, F.K. (2000).** Timur (*Zanthoxylum armatum*) production in Nepal. Mountain Research and Development. 20: 136-145.

3. **Singh, T.P. and Singh, O.M. (2011).** Phytochemical and pharmacological profile of *Zanthoxylum armatum* DC. - An overview. Indian J. Nat. Prod. Resour. 2: 275-285.
4. **Negi, J.S., Bisht, V.K., Bhandari, A.K., Singh, P. and Sundriyal, R.C. (2011).** Chemical constituents and biological activities of the genus *Zanthoxylum*: A review. Afr. J. Pure and Appl. Chem. 5: 412-416.
5. **Phuyal, N., Jha, P.K., Prasad Raturi, P. and Rajbhandary, S. (2019).** *Zanthoxylum armatum* DC.: Current knowledge, gaps and opportunities in Nepal. J. Ethnopharmacol. 229: 326-341.
6. **Nepal, I.U.C.N. (2000).** National Register of Medicinal Plants. Kathmandu: IUCN Nepal.
7. **Baral, J., Shrestha, D., Devkota, H.P. and Adhikari, A. (2023).** Potent ROS inhibitors from *Zanthoxylum armatum* DC of Nepali origin. Nat. Prod. Res. 1-9.
8. **Karki, H., Upadhyay, K., Pal, H. and Singh, R. (2014).** Antidiabetic potential of *Zanthoxylum armatum* bark extract on streptozotocin-induced diabetic rats. Int. J. Green Pharm. 8: 77-83.
9. **Hameed, A., Raza, S.A., Khan, M.I., Baral, J., Adhikari, A., Nur-e-Alam, M., Sarfaraz Ahmed and Hafizur, R.M. (2019).** Tambulin from *Zanthoxylum armatum* acutely potentiates the glucose-induced insulin secretion via KATP-independent Ca<sup>2+</sup>-dependent amplifying pathway. Biomed. Pharmacother. 120: 109348.
10. **Mushtaq, M.N., Ghimire, S., Akhtar, M.S., Adhikari, A., Auger, C., SchiniKerth, V.B. (2019).** Tambulin is a major active compound of a methanolic extract of fruits of *Zanthoxylum armatum* DC causing endothelium-independent relaxations in porcine coronary artery rings via the cyclic AMP and cyclic GMP relaxing pathways. Phytomed. 53: 163-170.
11. **Alam, F., Din, K.M., Rasheed, R., Sadiq, A., Jan, M.S., Minhas, A.M. and Khan, A. (2020).** Phytochemical investigation, anti-inflammatory, antipyretic and anti-nociceptive activities of *Zanthoxylum armatum* DC extracts- *in vivo* and *in vitro* experiments. Heliyon. 6: e05571.
12. **Alam, F., Najum us Saqib, Q. and Waheed, A. (2017).** Cytotoxic activity of extracts and crude saponins from *Zanthoxylum armatum* DC. against human breast (MCF-7, MDA-MB-468) and colorectal (Caco-2) cancer cell lines. BMC Complement. Altern. Med. 17: 1-9.
13. **Cragg, G.M. and Newman, D.J. (2001).** Natural product drug discovery in the next millennium. Pharm. Biol. 39: 8-17.
14. **GoN. (2013).** Value chain designing of Timur of panchase protected forest area. Ecosystem based Adaptation. 1-12.
15. **De Cássia Da Silveira E Sá, R., Andrade, L. N. and De Sousa, D.P. (2013).** A review on anti-inflammatory activity of monoterpenes. Molecules. 18: 1227-1254.
16. **Bašer, K.H.C. and Demirci, F. (2007).** Chemistry of essential oils. Flavours and Fragrances: Chemistry, Bioprocessing and Sustainability, edited by Berger RG. New York: Springer. 43-86.
17. **Buchbauer, G., Jäger, W., Jirovetz, L., Ilmberger, J. and Dietrich, H. (1993).** Therapeutic properties of essential oils and fragrances. ACS Publications, 159-165.
18. **Savelev, S., Okello, E., Perry, N.S.L.L., Wilkins, R.M. and Perry, E.K. (2003).** Synergistic and antagonistic interactions of anticholinesterase terpenoids in *Salvia lavandulaefolia* essential oil. Pharmacol. Biochem. Behav. 75: 661-668.
19. **Peana, A.T., D' Aquilla, P.S., Panin, F., Serra, G.P. and Moretti, M.D.L. (2002).** Anti-inflammatory activity of linalool and linalyl acetate constituents of essential oils. Phytomed. 9: 721-726.
20. **Kamatou, G.P.P. and Viljoen, A.M. (2008).** Linalool - A review of a biologically active compound of commercial importance. Nat. Prod. Commun. 3: 1183-1192.
21. **Burt, S. (2004).** Essential oils: Their antibacterial properties and potential applications in foods - A review. Int. J. Food Microbiol. 94: 223-253.
22. **Chouhan, S., Sharma, K. and Guleria, S. (2017).** Antimicrobial activity of some essential oils- present status and future perspectives. Medicines. 4: 58.
23. **Bakkali, F., Averbeck, S., Averbeck, D. and Idaomar, M. (2008).** Biological effects of essential oils- A review. Food Chem. Toxicol. 46: 446-475.
24. **Bhalla, Y., Gupta, V.K. and Jaitak, V. (2013).** Anticancer activity of essential oils: A review. J. Sci. Food Agric. 93: 3643-3653.
25. **Paduch, R., Kandefer-Szerszeń, M., Trytek, M. and Fiedurek, J. (2007).** Terpenes: Substances useful in human healthcare. Arch. Immunol. Ther. Exp. (Warsz). 55: 315-327.
26. **Kumar, A. and Somasundaram, S. T. (2014).** Gas Chromatography-Mass Spectrum (GC-MS) Analysis of bioactive components of the methanol extract of halophyte, *Sesuvium portulacastrum* L. Int. J. Adv. Pharmacy, Biol. Chem. 3: 766-772.
27. **Lawson, S.K., Satyal, P. and Setzer, W. N.**

- (2021). Phytochemical analysis of the essential oils from aerial parts of four scutellaria "skullcap" species cultivated in South Alabama: *Scutellaria baicalensis* Georgi, *S. Barbata* D. Don, *S. Incana* Biehler, and *S. Lateriflora* L. Nat. Prod. Commun. 16: 1-12.
28. **Khanal, L.N., Sharma K.R., Paudyal, H., Parajuli, K., Dahal, B., Ganga, G.C., Pokheral, Y. R. and Kalauni, S.K. (2022).** Green synthesis of silver nanoparticles from root extracts of *Rubus ellipticus* Sm. and comparison of antioxidant and antibacterial activity. J. Nanomater. 2022: 1-11.
  29. **Robert, A.P. (2007).** Identification of essential oil components by gas chromatography/mass spectrometry. Allured Publishing Corporation. USA.
  30. **Depree, J.A., Howard, T.M. and Savage, G.P. (1998).** Flavour and pharmaceutical properties of the volatile sulphur compounds of Wasabi (*Wasabia japonica*). Food Res. Int. 31: 329-337.
  31. **Cicchetti, E., Droure, L., Perez, M., Sizaire, L. and Vasseur. (2017).** Characterization of odour-active compounds in Timur (*Zanthoxylum armatum* DC.) fruits from Nepal. Flavor Fragrance J. 32: 317-329.
  32. **Neupane, B., Gautam, N., Miya, M.S., Upadhaya, A., Timelsina, Y.P., Gautam, D., Kandel, S. and Dhama, B. (2023).** Socio-economic contribution of *Zanthoxylum armatum* (Timur) in the rural household income of Myagdi district, Nepal. Environ. Nat. Resour. J. 21: 58-66.
  33. **Phuyal, N., Jha, P.K., Raturi, P.P. and Rajbhandary, S. (2020).** Comparison between essential oil compositions of *Zanthoxylum armatum* DC. fruits grown at different altitudes and populations in Nepal. Int. J. Food Prop. 23: 1971-1978.
  34. **Dhama, A., Palariya, D., Kumar, R., Prakash, O., Rawat, D.S. and Pant, A. K. (2019).**  $\alpha$ -Pinene rich bark essential oils of *Zanthoxylum armatum* DC. from three different altitudes of Uttarakhand, India and their antioxidant, *in vitro* anti-inflammatory and antibacterial activity. J. Essent. Oil-Bearing Pl. 22: 660-674.
  35. **Waheed, A., Mahmud, S., Akhtar, M. and Nazir, T. (2011).** Studies on the components of essential oil of *Zanthoxylum armatum* by GC-MS. Am. J. Anal. Chem. 2011: 258-261.
  36. **Tiwary, M., Naik, S.N., Tewary, D.K., Mittal, P.K. and Yadav, S. (2007).** Chemical composition and larvicidal activities of the essential oil of *Zanthoxylum armatum* DC (Rutaceae) against three mosquito vectors. J. of Vector Borne Dis. 44: 198.
  37. **Jun, H.J., Lee, J.H., Kim, J., Jia, Y., Kim, K.H., Hwang, K.Y., Yun., E.J., Do, K.R. and Lee, S.J. (2014).** Linalool is a PPAR  $\alpha$ -ligand that reduces plasma TG levels and rewires the hepatic transcriptome and plasma metabolome. J. Lipid Res. 55: 1098-1110.
  38. **Negi, J.S., Bisht, V.K., Bhandari, A.K., Bisht, R. and Negi, S. (2012).** Major constituents, antioxidant and antibacterial activities of *Zanthoxylum armatum* DC. essential oil. Iran. J. Pharmacol. Ther. 11: 68-72.
  39. **Woollett, L.A. and Dietschy, J.M. (1994).** Effect of long-chain fatty acids on low-density-lipoprotein- cholesterol metabolism 14. Am. J. Clin. Nutr. 60: 991S-996S.
  40. **Bisht, M., Mishra, D., Sah, M., Joshi, S. and Mishra, S. (2014).** Biological activities of the essential oil of *Zanthoxylum armatum* DC. Leaves. J. Nat. Prod. 4: 229-232.
  41. **Li, T., Chen, M., Ren, G., Hua, G., Mi, J., Jiang, D. and Liu, C. (2021).** Antifungal activity of essential oil From *Zanthoxylum armatum* DC. on *Aspergillus flavus* and Aflatoxins in stored Platycladi Semen. Front. Microbiol. 12: 633714.
  42. **Liaqat, I., Riaz, N., Saleem, Q.U.A., Tahir, H.M., Arsal, M. and Arsal, N. (2018).** Toxicological evaluation of essential oils from some plants of rutaceae family. Evidence-based Complement. Altern. Med. 2018.
  43. **Odeyemi, O.O., Yakubu, M.T., Masika, P.J. and Afolayan, A.J. (2009).** Toxicological evaluation of the essential oil from *Mentha longifolia* L. subsp. *capensis* leaves in rats. J. Med. Food. 12: 669-674.
  44. **Sharma, S., Rasal, V.P., Joshi, R.K. and Patil, P.A. (2018).** *In vivo* evaluation of antiasthmatic activity of the essential oil of *Zanthoxylum armatum*. Indian J. Pharm. Sci. 80(2): 383-390.
  45. **Satyaj, P. (2015).** Development of GC-MS database of essential oil components by the analysis of natural essential oils and synthetic compounds and discovery of biologically active novel chemotypes in essential oils. University of Alabama in Huntsville. Dissertations/63.

## $\alpha$ -Glucosidase and $\alpha$ -Amylase Inhibition Activities of *Sarcococca coriacea* Hook. And *Sarcococca wallichii* Staph. of Nepalese Origin

Janaki Baral<sup>1,2</sup>, Dipesh Shrestha<sup>2</sup>, Achyut Adhikari<sup>1,\*</sup>

<sup>1</sup>Central Department of Chemistry, Tribhuvan University, Kathmandu 44618, Nepal

<sup>2</sup>Department of Chemistry, Tri-Chandra Multiple Campus, Tribhuvan University, Kathmandu 44605, Nepal

\*Corresponding email: [achyutraj05@gmail.com](mailto:achyutraj05@gmail.com)

Submitted : 17 June 2022, Revised 28 June 2022, Accepted 29 June 2022

### Abstract

Diabetes mellitus is being severe health problem globally with increasing patients every day. Due to lack of effective and non-toxic medicine to cure diabetes. Plants that are used in ethnomedicine may be a good source for antidiabetic drug discovery. Plants of the *Sarcococca* genus are medicinally important and are used by local people for managing many diseases including diabetes. In the course of our continuous search of antidiabetic plants and pure compounds, *in vitro*  $\alpha$ -glucosidase, and  $\alpha$ -amylase inhibition activity along with the antioxidant activity of methanolic extract of *Sarcococca coriacea* leaf (Sc-A), *Sarcococca coriacea* stem (Sc-B), and dichloromethane fraction of methanolic extract of *Sarcococca wallichii* (Sw-D) were carried out. The research revealed dichloromethane fraction of *S. wallichii* (Sw-D) with good inhibition of  $\alpha$ -amylase enzyme ( $IC_{50} = 53.79 \pm 2.50$ ), whereas Sc-B inhibits  $\alpha$ -glucosidase ( $20.97 \pm 2.37$ ) effectively. Similarly, Sc-A showed significant antioxidant activity with  $IC_{50} = 24.56 \pm 3.3$ . The total phenolic content on Sc-A and Sc-B was calculated as  $151.35 \pm 4.42$  mg GAE/g and  $86.22 \pm 1.59$  mg GAE/g whereas the total flavonoid content on Sc-A and Sc-B was found to be  $21.61 \pm 4.88$  mg QE/g and  $24.09 \pm 4.02$  mg QE/g respectively. Similarly, total phenolic and total flavonoid content on Sw-D were found to be  $85.26 \pm 3.16$  mg GAE/g and  $21.57 \pm 1.26$  mg QE/g. To the best of our knowledge, this is the first report of  $\alpha$ -glucosidase and  $\alpha$ -amylase inhibition activity in these plants. This research work has scientifically supported the use of these plants to manage diabetes by local people and has explored new plants for antidiabetic drug discovery research.

**Keywords:**  $\alpha$ -glucosidase inhibitor,  $\alpha$ -amylase inhibitor, antioxidant, *Sarcococca*

### Introduction

Diabetes mellitus, commonly called type 2 diabetes identified by hyperglycemia is caused due to various degrees of  $\beta$  cell dysfunction and insulin resistance. Patients with diabetes mellitus are increasing globally with an associated two-fold excess risk of cardiovascular, cerebrovascular, and peripheral artery disease [1], [2]. The search for potent antidiabetic secretagogue from plant origin is in high demand due to its low economic cost and lesser side effect. As the consumed food has a direct impact on the blood glucose level. The enzymatic digestion of complex

carbohydrates collectively by the role of  $\alpha$ -amylase and  $\alpha$ -glucosidase has been addressed as a potential means of controlling postprandial hyperglycemia by reducing the absorption of glucose from meals [3]. Inhibitors of these enzymes help by delaying in breaking mechanism of carbohydrates finally leading to a decrease in the postprandial glucose level in the blood [4]. Various researches targeting the plant-based inhibitors are on an increasing trend against these digestive enzymes  $\alpha$ -amylase and  $\alpha$ -glucosidase as natural supplement and diet plays a pivotal role in addressing the concern related to

synthetic drugs. Initiation of such research through *in vitro* antidiabetic property of plant extract is expressed by the inhibition of plant sample to the enzymes  $\alpha$ -amylase and  $\alpha$ -glucosidase[5]. Plants with the highest inhibitory activities against both of these digestive enzymes are rare. Very few natural plants are reported with a strong inhibiting capacity to both these enzymes concomitantly[6]. Plants belonging to Buxaceae family are reported to have potent to moderate inhibitory capacity in multiple diseases and need to be researched concerning antidiabetic properties.

The evergreen Buxaceae family have four species of *Sarcococca* reported from the various belt of Nepal, *S. coriacea*, *S. saligna*, *S. hookeriana* & *S. wallichii*[7]. These plants are rich in steroidal alkaloids. The nature of compound in plants are responsible for the impact of the result observed. The value of consumption of natural plant products as herbal remedies in treating certain ailments and disorders is a common practice in Nepal. Locally people use the bark of *Sarcococca coriacea* to get relief from swelling[8]. Similarly, leaves and shoots of *Sarcococca* plants have been used for the treatment of rheumatic fever in folk medicine[9]. Whole parts of this medicinally important plant roots, stem, leaves, bark, and flowers have been continuously under multidimensional intense research for years.

The importance of these genera is reflected in many types of research with biological activities ascribed to isolated steroidal alkaloids. The alkaloids are pregnane derivatives [10]. Potent biological activities include acetylcholinesterase and butyrylcholinesterase inhibition in various concentrations of compounds of class pregnane type steroidal alkaloids namely hookerianamide-D, hookerianamide-E, hookerianamide F and hookerianamide G isolated from *Sarcococca hookeriana* [11] in addition to the antileishmanial property [12]. Compounds of *Sarcococca hookeriana* as hookerianamide H, hookerianamide I, N-methylepipachysamine D, Sarcovagine C, and dictyophlebine possess both cholinesterase and antiplasmodial [13] properties with good inhibitory activities. Leaves of *Sarcococca coriacea* of Nepalese origin contains potent compounds

such as (-) vaganine D, (+) nepapakistamine A with cholinesterase inhibitory activities. Likewise other steroidal alkaloids isolated from leaves were epoxyakistanamine-A, epoxyarscovagenine D, Funtumafrine C, and N-methylfuntumine [14]. All these compounds except Funtumafrine C possess potent acetylcholinesterase and butyrylcholinesterase inhibition activity in a concentration-dependent pattern. Breakthrough in research was observed when fluorine containing secondary metabolite has been reported from a natural source for the first time from *Sarcococca coriacea*, a novel class of fluoropyrimidine substituted alkaloids along with many steroidal alkaloids with potent biological activities [15]. Others isolated compounds were alkaloid C, Na-methylepipachysamine D, Sarcovagenine, Sarcovagine D, N-methylpachysamine A, dictyophlebine, 5,6-dihydrosarconidine, terminaline and iso-N-formylchoenmorphine. Roots of *Sarcococca coriacea* possess anti-leishmanial activities which are also observed due to steroidal alkaloids such as iso-N-formylchonemorphine and alkaloid C [16]. Rare sugar alcohol, xylitol along with other sterols were reported from flowers of *Sarcococca coriacea* [17]. These all researches strongly add the medicinal value of the plant under this genera. Owing to the strong potency of all these species from Buxaceae family this investigation continues to the in-vitro application of antidiabetic property of *Sarcococca coriacea* leaf, *Sarcococca coriacea* stem and *Sarcococca wallichii* dichloromethane fractions as to the best of our knowledge the antidiabetic potential of these plants have not been reported till the date.

## Materials and Methods

### Plant Collection and Extract Preparation

*Sarcococca coriacea* plant was collected from Kathmandu district, Kritipur Municipality, Champadevi-4 [27.66 °N, 85.27 °E, 2229 m, 16 July, 2018, J. Baral & Y.B. Poudel, JB100 (KATH)]. The leaves and stems of the plants were separated air-dried and ground to powder. With occasional shaking, both leaves and stem powder were macerated in methanol for ten days. It was then filtered, and the filtrate was concentrated to obtain the crude extract in a rotary evaporator. Similarly, this section of

research on *Sarcococca wallichii* is in continuation of our previous research [18] where the aerial part of *Sarcococca wallichii* Staph. were collected from Dhampus (Kaski, Nepal) and identified by Prof. Krishna Kumar Shrestha, Central Department of Botany, Tribhuvan University, Kiritipur, Kathmandu, Nepal. A voucher specimen (No: SW-06) was deposited in the same department.

### Chemicals

2,2 Diphenyl 1 picrylhydrazyl (DPPH),  $\alpha$ -glucosidase from *Saccharomyces cerevisiae*,  $\alpha$ -amylase from porcine pancreases, 2-Chloro-4-nitrophenyl- $\alpha$ -D-Maltotriose (CNP3) and *p*-Nitrophenyl- $\alpha$ -D-glucopyranoside (PNPG) were purchased from Sigma-Aldrich.

### Total Phenolic Content (TPC)

Folin-ciocalteu's reagent was used for the estimation of total phenolic content [19]. In short, the plant samples (20 $\mu$ L) were mixed with Folin-Ciocalteu's reagent (100 $\mu$ L) and Na<sub>2</sub>CO<sub>3</sub> (80 $\mu$ L) and left in the dark for 15 minutes. Finally, absorbance was measured at 765nm in a microplate spectrophotometer

### Total Flavonoid Content (TFC)

The aluminium trichloride method was used to estimate the total flavonoid content [20]. Briefly, plant sample (20 $\mu$ L), distilled water (60 $\mu$ L), AlCl<sub>3</sub> (5 $\mu$ L), and CH<sub>3</sub>COOK (5 $\mu$ L) were mixed and kept for 30 minutes at room temperature. The absorbance was then measured at 415nm using a microplate spectrophotometer.

### Antioxidant Activity

The determination of antioxidant activity was done by following the previously described method with slight modification [21]. The plant sample (100 $\mu$ L) was mixed with DPPH (100 $\mu$ L) and kept in the dark for 30 minutes. Finally, the absorbance was taken at 517nm in a microplate spectrophotometer. The free radical scavenging activity was calculated using the following formula.

$$\% \text{ inhibition} = \left( \frac{A_{\text{control}} - A_{\text{sample}}}{A_{\text{control}}} \right) \times 100$$

Where A<sub>control</sub> is the absorbance of the control and A<sub>sample</sub> is the absorbance of the sample.

### In vitro $\alpha$ -Glucosidase Inhibition Activity

The *in vitro*  $\alpha$ -glucosidase inhibition assay was performed following the methods described previously with slight modifications[22]. Different concentrations of 20 $\mu$ L plant sample were mixed with 20 $\mu$ L of the enzyme (0.2U/mL) with 120 $\mu$ L of phosphate buffer solution and incubated at 37°C for 15 minutes. After that, PNPG (0.7mM) was added and again incubated for 15 minutes at 37°C. Finally, the absorbance was taken at 405nm in a microplate spectrophotometer. The inhibition percentage was calculated using the following formula.

$$\% \text{ inhibition} = \left( \frac{A_{\text{control}} - A_{\text{sample}}}{A_{\text{control}}} \right) \times 100$$

Where A<sub>control</sub> is the absorbance of the control (DMSO), and A<sub>sample</sub> is the absorbance of the sample.

### In vitro $\alpha$ -Amylase Inhibition Activity

Substrate-based  $\alpha$ -amylase inhibition assay was performed using CNPG3 as substrate[23] Different concentrations of 20 $\mu$ L plant sample were first mixed with 80 $\mu$ L of the enzyme (1.5U/mL) and incubated for 15 minutes at 37°C. After that, 100 $\mu$ L of CNPG3 (0.5mM) was added and incubated for 15 minutes at 37°C. Lastly, the absorbance was taken at 405nm in a microplate spectrophotometer. The inhibition percentage was calculated using the following formula.

$$\% \text{ inhibition} = \left( \frac{A_{\text{control}} - A_{\text{sample}}}{A_{\text{control}}} \right) \times 100$$

Where A<sub>control</sub> is the absorbance of the control (DMSO), and A<sub>sample</sub> is the absorbance of the sample.

## Results

### Total Phenolic and Flavonoid Content

The total phenolic and flavonoid content was expressed as mg GAE/g and mg QE/g, respectively. A calibration curve of gallic acid and quercetin was used to estimate TPC and TFC, respectively. The TPC and TFC of Sc-A were found to be 130.07 $\pm$ 5.74 mg GAE/g and 20.58 $\pm$ 3.82 mg QE/g, respectively.

Similarly, the TPC and TFC of Sc-B were  $68.34 \pm 2.57$  mg GAE/g and  $24.5 \pm 6.5$  mg QE/g, respectively. The total phenolic and total flavonoid content of Sw-D were found to be  $85.26 \pm 3.16$  mg GAE/g and  $21.57 \pm 1.26$  mg QE/g. The total phenolic content on all three extracts was higher than the corresponding flavonoid content.

### Antioxidant Activity

DPPH free radical scavenging assay was performed to determine the antioxidant activity. Both Sc-A and Sc-B were found to significantly inhibit the DPPH free radical with  $IC_{50}$  value  $24.56 \pm 3.3 \mu\text{g/mL}$  and  $28.90 \pm 5.22 \mu\text{g/mL}$ , respectively. Comparatively the other species, Sw-D fraction has  $IC_{50} = 53.79 \pm 2.50 \mu\text{g/mL}$ . Among all three extract Sc-A possess stronger antioxidant potential. The antioxidant potent of standard quercetin was  $IC_{50} = 1.17 \pm 0.35 \mu\text{g/mL}$ .

### In vitro $\alpha$ -glucosidase and $\alpha$ -amylase inhibition activities

For the *in vitro*  $\alpha$ -glucosidase and  $\alpha$ -amylase inhibition activity, samples were first screened at the concentration of  $500 \mu\text{g/mL}$ . Samples inhibiting  $>50\%$  were further diluted to calculate the  $IC_{50}$  value. The  $IC_{50}$  was calculated using GraphPad Prism 8 software. The Sc-A showed significant inhibition against both digestive enzymes;  $\alpha$ -glucosidase and  $\alpha$ -amylase, with an  $IC_{50} = 39.92 \pm 2.52 \mu\text{g/mL}$  and  $224.3 \pm 1.87 \mu\text{g/mL}$ , respectively. Likewise, Sc-B disclosed significant inhibition against  $\alpha$ -glucosidase with  $IC_{50} = 20.97 \pm 2.37 \mu\text{g/mL}$ ; however, it showed  $<50\%$  inhibition against the  $\alpha$ -amylase. Other species Sw-D significantly inhibits  $\alpha$ -amylase  $IC_{50}$   $2.116 \pm 0.058 \mu\text{g/mL}$  than  $\alpha$ -glucosidase  $< 50\%$  comparatively. Standard Acarbose's  $IC_{50}$  against  $\alpha$ -glucosidase and  $\alpha$ -amylase were found to be  $5.66 \pm 0.8 \mu\text{g/mL}$  and  $6.18 \pm 0.97 \mu\text{g/mL}$ , respectively. This proves the stronger inhibition capacity of Sw-D than standard acarbose used. The  $IC_{50}$  of  $\alpha$ -glucosidase and  $\alpha$ -amylase inhibition activity of Sc-A, Sc-B, and Sw-D compared to the standard acarbose is presented in table 1.

**Table 1:**  $IC_{50}$  values of antioxidant,  $\alpha$ -glucosidase and  $\alpha$ -amylase inhibition activities of plant's extract and fraction

Plant sample and standards	Antioxidant( $\mu\text{g/mL}$ )	$\alpha$ -Glucosidase ( $\mu\text{g/mL}$ )	$\alpha$ -Amylase ( $\mu\text{g/mL}$ )
Sc-A	$24.56 \pm 3.3$	$39.92 \pm 2.52$	$224.3 \pm 1.87$
Sc-B	$28.90 \pm 5.22$	$20.97 \pm 2.37$	NC
Sw-D	$53.79 \pm 2.50$	NC	$2.116 \pm 0.058$
Quercetin	$1.17 \pm 0.35$	-	-
Acarbose	-	$5.66 \pm 0.8$	$6.18 \pm 0.97$

Values are expressed as average  $\pm$  standard deviation of three independent assays. NC-not calculated

### Discussions

*In vitro* potency of plant's extract and fractions provides a platform for further research in the molecular label. Synergetic effect of active phytochemicals such as alkaloids, tannins, phenols, saponins, terpenoids, flavonoids, steroids, and sterols contribute to the plant's medicinal properties[24]. Due to the adverse effect of synthetic drugs the efficacy of plant-based food profiles with potent inhibitors is in demand. Major hydrolyzing enzymes of carbohydrate metabolism are the  $\alpha$ -glucosidase and  $\alpha$ -amylase. Inhibiting these enzymes may result in controlling blood sugar[25]. This research reveals the unique *in vitro* antidiabetic potency of Sc-A and Sc-B as these both inhibited the digestive enzymes,  $\alpha$ -glucosidase, and  $\alpha$ -amylase. The methanolic stem extract of the plant *Sarcococca coriacea* inhibited  $\alpha$ -glucosidase substantially more than its leaf extract whereas stem extract of the same at the concentration of  $500 \mu\text{g/mL}$  could not inhibit the  $\alpha$ -amylase enzyme. Leaf extract Sc-A was found to inhibit the  $\alpha$ -amylase comparatively. Interestingly another species Sw-D was found to be one of the potent inhibitors of  $\alpha$ -amylase that could not inhibit the  $\alpha$ -glucosidase enzyme at the concentration of  $500 \mu\text{g/mL}$ . Sc-A possesses higher phenolic and stronger antioxidant potential. Enzyme inhibition activity of both methanolic extract of Sc-A, Sc-B and Sc-D accredit to the synergetic effect of phytoconstituent present in it.

### Conclusions

Sc-A and Sc-B both inhibited digestive enzymes,  $\alpha$ -glucosidase, and  $\alpha$ -amylase. Sw-D strongly inhibited  $\alpha$ -amylase stronger than the standard reflecting remarkable anti-diabetic potential. All three extracts possess good to moderate antioxidant

properties. Our findings infer a strong biochemical rationale for further *in vivo* studies and as a dietary supplement of this plant-based product in type II diabetes management. Further researches are necessary on particular inhibiting compounds and biological pathways involved.

### Funding

This research is financially supported by University Grants Commissions (UGC), Nepal to Mrs. Janaki

Baral through Ph. D. Fellowship and Research Support (Award No. PhD/074-075/S&T-6).

### Acknowledgments

A. Adhikari would like to acknowledge HERP, Tribhuvan University, Nepal, for providing research support.

### Conflict of Interest

The authors declare that there is no conflict of interest.

### References:

- [1] World Health Organization. Classification of diabetes mellitus, 2019.
- [2] N. Sarwar *et al.*, Diabetes mellitus, fasting blood glucose concentration, and risk of vascular disease: A collaborative meta-analysis of 102 prospective studies, *Lancet*, 2010, **375** (9733). 2215–2222, doi: 10.1016/S0140-6736(10)60484-9.
- [3] P. Mccue, K. Young-In, and K. Shetty, Anti-amylase, anti-glucosidase and anti-angiotensin i- converting enzyme potential of selected foods, *Journal of Food Biochemistry*, 2005, **29**, 278–294, doi: 10.1111/j.1745-4514.2005.00020.x.
- [4] Y. In Kwon, E. Apostolidis, and K. Shetty, Evaluation of pepper (*Capsicum annuum*) for Management of Diabetes and Hypertension, *Journal of Food Biochemistry*, 2007, **31**, 370–385, doi: 10.1111/j.1745-4514.2007.00120.x.
- [5] S. S. Nair, V. Kavrekar, and A. Mishra, In vitro studies on alpha amylase and alpha glucosidase inhibitory activities of selected plant extracts, *European Journal of Experimental Biology*, 2013, **3** (1), 128–132.
- [6] M. I. Kazeem, J. O. Adamson, and I. A. Ogunwande, Modes of Inhibition of  $\alpha$ -Amylase and  $\alpha$ -Glucosidase by Aqueous Extract of *Morinda lucida* Benth Leaf, *BioMed Research international* 2013, **Vol 2013**, doi: 10.1155/2013/527570
- [7] W. L. H. J. Hara H, Chater A O, *An enumeration of the flowering plants of Nepal Vol 3*. London: Mansell Books Binders Limited, 1982.p.200.
- [8] S. R. Sigdel, M. B. Rokaya, and B. Timsina, Plant Inventory and Ethnobotanical Study of Khimti Hydropower Project, Central Nepal, *Scientific World*, 2013, **11** (11), 105–112, doi: 10.3126/sw.v11i11.8563.
- [9] A. Kumar, S. C. Sati, M. D. Sati, S. Kumar, D. Singh, U. Bhatt, and G. Kaur Chemical and Potential Biological Prespectives of Genus *Sarcococca* (Buxaceae), *The Natural Products Journal.*, 2015, **5**, 28–49, doi:10.2174/2210315505666150219233014
- [10] S. Ghulam, M. Goher, A. Ali, A. Adhikari, and M. I. Choudhary, Rapid characterization and identification of steroidal alkaloids in *Sarcococca coriacea* using liquid chromatography coupled with electrospray ionization quadropole time-of-flight mass spectrometry, *Steroids*, 2012, **77** (1-2), 138–148, doi: 10.1016/j.steroids.2011.11.001.
- [11] M. I. Choudhary, K. Prasad, S. Ahmad, R. Ranjit, and A.- Rahman, Cholinesterase inhibitory pregnane-type steroidal alkaloids from *Sarcococca hookeriana*, *Steroids*, 2005, **70**, 295–303, doi: 10.1016/j.

- [12] K. Devkota, I. Choudhary, R. Ranjit, Samreen, and N. Sewald, Structure activity relationship studies on antileishmanial steroidal alkaloids from *Sarcococca hookeriana*, *Natural Products Research, Former. Nat. Prod. Lett.*, 2007, **21** (4), 292–297, doi:10.1080/14786410701192736.
- [13] K. P. Devkota, B. N. Lenta, M. I. Choudhary, Q. Naz, F. B. Fekam, P. J. Rosenthal, N. Sewald, Cholinesterase inhibiting and antiplasmodial steroidal alkaloids from *Sarcococca hookeriana*, *Chemical and Pharmaceutical Bulletin*, 2007, **55** (9) 1397–1401, doi: 10.1248/cpb.55.1397.
- [14] S. K. Kalauni, M. I. Choudhary, A. Khalid, M. D. Manandhar, F. Shaheen, and M. B. Gewali. New cholinesterase inhibiting steroidal alkaloids from the leaves of *Sarcococca coriacea* of Nepalese origin, *Chemical and Pharmaceutical Bulletin*, 2002, **50** (11), 1423–1426, doi: 10.1248/cpb.50.1423.
- [15] A. Adhikari, Bioprospecting Studies on *Sarcococca coriacea* (Hook. F.) of Nepalese Origin, [Doctoral Dissertation]. University of Karachi, 2009. Available: <http://103.69.125.248:8080/xmlui/handle/123456789/227>
- [16] M. I. Choudhary, A. Adhikari, Samreen, and A. Rahaman, Antileishmanial Steroidal Alkaloids from Roots of *Sarcococca coriacea*, *Journal of Chemical Society of Pakistan*, 2010, **32**( 6), 799-802.
- [17] N. P. Rai, B. B. Adhikari, A. Paudel, and K. Masuda, Phytochemical constituents of the flowers of *Sarcococca coriacea* of Nepalese origin, *Journal of Nepal Chemical Society*, 2006, **21**,1–7
- [18] A. Adhikari, M. I. Vohra, A. Jabeen, N. Dastagir, and M. I. Choudhary, Anti-inflammatory Steroidal Alkaloids from *Sarcococca wallichii* of Nepalese Origin, *Natural Products Communication*, 2015, **10** (9), 13–16, doi: 10.1177/1934578X1501000911.
- [19] X. Lu, C. F. Ross, J. R. Powers, D. Eric Aston, and B. A. Rasco, Determination of Total Phenolic Content and Antioxidant Activity of Garlic (*Allium sativum*) and Elephant Garlic (*Allium ampeloprasum*) by Attenuated Total Reflectance–Fourier Transformed Infrared Spectroscopy, *Journal of Agricultural and Food Chemistry*, 2011, **59**(10), 5215–5221, doi: 10.1021/jf201254f.
- [20] C.-C. Chang, M.-H. Yang, H.-M. Wen, and J.-C. Chern, Estimation of total flavonoid content in propolis by two complementary colorimetric methods, *Journal of Food and Drug Analysis*, 2020, **10** (3), 3, doi: 10.38212/2224-6614.2748.
- [21] L. L. Mensor, F. S. Menezes, G. G. Leita~o, A. S. Reis, and T. C. S. Dos, Screening of Brazilian plant extracts for antioxidant activity by the use of DPPH free radical method, *Phytherapy Research*, 2001, **130**, 127–130.
- [22] H. Fouotsa, A. M. Lannang, C. D. Mbazoa, S., Rasheed, B. P. Marasini, Z. Ali, K. P. Devkota, A. E. Kengfack, F. Shaheen, M. I. Choudhary, N. Sewald, Xanthonic inhibitors of  $\alpha$ -glucosidase and glycation from *Garcinia nobilis*. *Phytochemistry letters*, 2012 **5**(2), 236-239., doi: 10.1016/j.phytol.2012.01.002.
- [23] K. Khadayat, B. P. Marasini, H. Gautam, S. Ghaju, and N. Parajuli, “Evaluation of the alpha-amylase inhibitory activity of Nepalese medicinal plants used in the treatment of diabetes mellitus,” *Clinical Phytoscience*, 2020, **6**, (1), 1–8, doi: 10.1186/S40816-020-00179-8.
- [24] N. Mehrotra, K. Jadhav, S. Rawalgaonkar, S. A. Khan, and B. Parekh, In vitro evaluation of selected Indian spices for  $\alpha$ -amylase and  $\alpha$ -glucosidase inhibitory activities and their spice-drug interactions, *Annals of Phytomedicine An International Journal*, 2019, **8**(2), doi: 10.21276/ap.2019.8.2.5.ISSN:0974-2328
- [25] D. M. Nagmoti and A. R. Juvekar, In vitro inhibitory effects of *Pithecellobium dulce* ( Roxb .) Benth . seeds on intestinal  $\alpha$ -glucosidase and pancreatic  $\alpha$ -amylase, *J. Biochemical Technology*, 2013, **4**, 616–621.